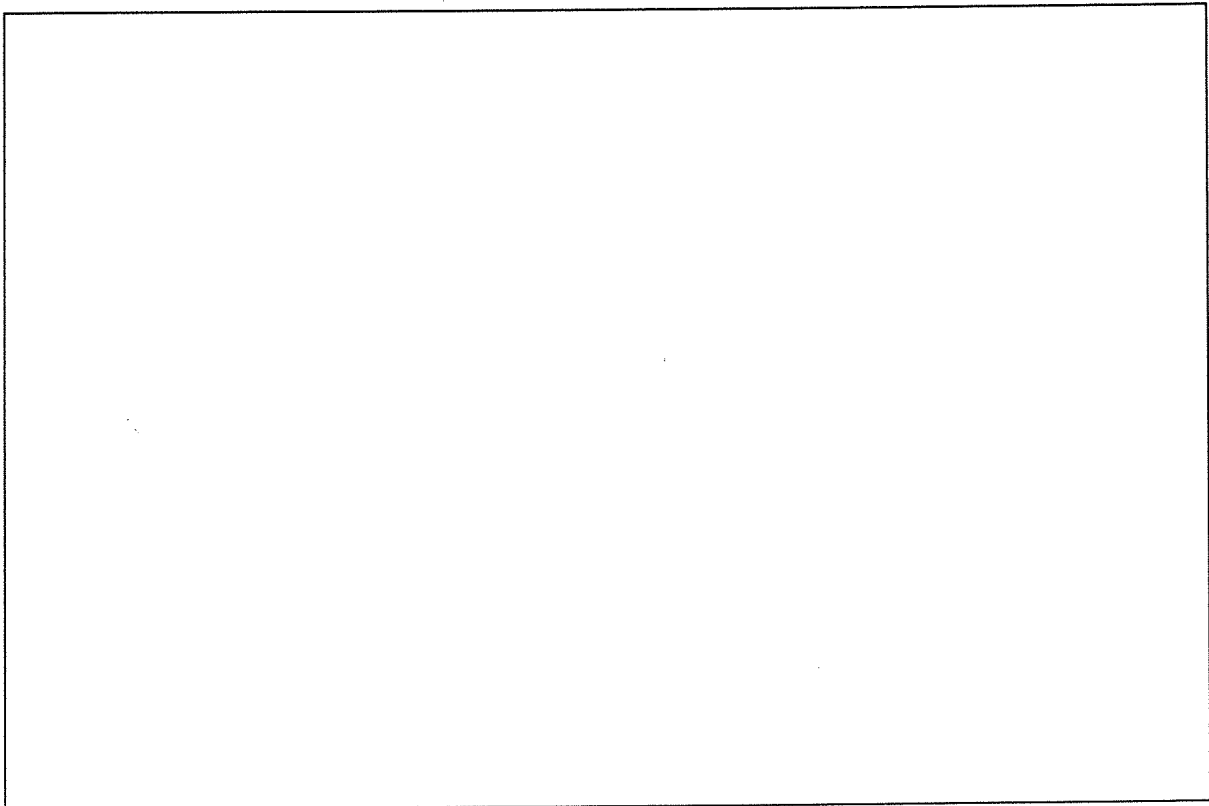


Wave Energy Conversion

- * Theory of Wave Energy Conversion**
- * Wave Energy Converters, the State of the Art**
- * Design of a Wave Power Converting Breakwater for the Port of Bilbao, North Spain**

MSc. Thesis by Herald Vervoorn
March 1997



Delft University of Technology
Faculty of Civil Engineering
Hydraulic and Geotechnical Engineering Division
Hydraulic Engineering Group



Preface and Acknowledgements

This study has been carried out as MSc. thesis of Delft University of Technology, Faculty of Civil Engineering, Hydraulic and Geotechnical Engineering Division, Hydraulic Engineering Group. It deals with the state of the art of wave energy converters, the theory of wave energy conversion and a design of a wave power converting breakwater for the Port of Bilbao, North Spain.

In the last decades, considerable research in wave energy conversion has been performed. Several concepts have been investigated and tested. As yet, it is unknown which type of wave energy device is useful to employ in which circumstances. In particular the working principle of wave energy converting breakwaters is insufficient understood.

The Hydraulic Engineering Group is interested in the state of the art of wave energy conversion and the prospects. Wave energy converters had to be investigated on theoretical as well as practical properties. Particularly, the combination of a breakwater with wave power converting devices attracted the attention.

For this final report and the appendixes, an extensive literature study has been carried out. The objective is to describe the different types of wave energy devices and the combination with a breakwater. For the Port of Bilbao, North Spain, a wave power converting breakwater has been designed, consisting of caissons on a rubble mound foundation.

I would like to thank prof. ir. K. d'Angremond, ir. J. van Duivendijk and ir. T. van der Meulen for giving the opportunity for this thesis, their recommendations and the time they spent in reading this report and the accompanying appendixes.

Pijnacker, the Netherlands
March 1997
Herald Vervoorn

Summary

Introduction

Since the awareness that the conventional energy sources will run short, the use of various renewable energy sources has been investigated, these are solar, wind, ocean and geothermal energy. Quite some countries are interested in wave energy conversion. In several countries some full-scale wave energy converting pilot plants have been tested. Some of these are still operating.

Several types of wave energy converting devices exist. There are some methods to classify these converters. According to their size and orientation three types can be distinguished: (1) point absorbers, devices which are small compared to a typical wave length, (2) terminators, wide structures perpendicular to the incident waves and (3) attenuators, long structures parallel to the wave propagation.

It is expected that in future, a number of point absorbers, installed some kilometres offshore will be used as large wave power plants. The advantage of these point absorbers is that they can capture wave energy from a larger width than the width of the structure.

At present, an useful power plant is the in Norway developed tapered channel, TAPCHAN. The waves are converted by a rising channel into potential energy and subsequently by a turbine into electricity. Also the combination of a breakwater with wave energy conversion converting devices is expected to have good prospects. This study deals with the design of wave power converting breakwaters.

Wave power converting breakwaters

Three types of wave energy converting devices have been investigated for the combination with a breakwater. Potential energy converting devices, flap type devices and oscillating water column devices. Oscillating water column devices have a good performance, while they are able to convert large wave power values and they are not sensitive to damage. It is concluded that these devices are most suitable for combination with a breakwater.

Two types of oscillating water column (= OWC) devices can be discerned: (1) devices with a single air chamber above a column and consequently one particular resonance frequency or (2) devices with in front of the chamber a 'harbour' such that the devices become multi-resonant. In Japan, Sakata Port, a wave power converting caisson with only an air chamber has been constructed. The British inventors expect that a breakwater with 'harbour' type devices has the best prospects. These devices are placed at intervals in the breakwater and operate as point absorbers.

In this study the 'harbour' type devices have been investigated. Several theories (mainly numerical methods) exist to model the hydrodynamic characteristics of 'harbour' type devices. Most theories show roughly the same results. Comparison of the results of the different theories and several designs of 'harbour' type devices has been made possible by dimensionless presentation of design parameters. In that way, general applicable design rules have been derived. With these rules, the dimensions of a 'harbour' type device can be determined without the help of complicated numerical methods.

Design of a Wave Power Converting Breakwater for the Port of Bilbao

With the derived design rules, a wave power converting breakwater has been designed for the Port of Bilbao, North Spain. Two design conditions are investigated, namely (1) the ultimate limit state (U.L.S.) required for the stability and strength of the breakwater and (2) the serviceability limit state (S.L.S.), for functioning of the breakwater for sheltering Bilbao Harbour and for wave power conversion.

For the U.L.S. the maximum wave height and the corresponding wave length have been determined. For the S.L.S. the wave height, length and direction and their accompanying probability of occurrence are discussed. The wave steepness, a relation between wave length and height, is derived to estimate the wave power, corresponding to a particular wave length or height.

The 2280 m long designed breakwater consists of 38 caissons. In the middle of each caisson a 'harbour' type OWC device is situated.

The stability of the caissons has been calculated by the theory of Goda, with some modifications. For the sections with device, the impulsive pressure is assumed to be zero. For the sections without device modification for the sloping top have been used. The stability of a total caisson is calculated by the average stability of the caisson sections, proportional to the part of the caisson that is occupied by the device.

When the caissons have a sloping top and a length of 39 m, a width of 60 m and a crest height of + 17 C.D., they are sufficiently stable against sliding and overturning. Also the average maximum and minimum rubble mound stresses are not exceeded. The width of a device is 13.75 m and in each device a tandem type Wells turbine of 1 MW is installed. This means that the total installed capacity of the breakwater is 38 MW.

During winter periods the operating performance of the devices is considerably better than during summer periods. Yearly, about 80 GWh of electricity is generated (2.2 GWh per device). This study shows that it is possible to make a design of a wave power converting breakwater, by using the derived design recommendations. Even for locations with very rough sea conditions, like Bilbao, this type of breakwater is feasible.

For Spain, the costs of the generated electricity are probably too high, but for locations with relatively high electricity costs and no large electricity demand, this type of breakwater can be successfully employed as commercial power plant.

At present a wave power converting breakwater with an installed capacity of 38 MW would be the largest wave energy converting power plant of the world. The construction of such a breakwater, followed by operation with a good performance, will result into more confidence in wave energy conversion.

Contents

Preface and Acknowledgements	iii
Summary	iv
List of Definitions	ix
1 Introduction	
1.1 Background to the Study	1-1
1.2 Scope and Objective of the Study	1-1
1.3 Structure of the Report.....	1-1
2 Energy Supply and Demand	
2.1 Introduction.....	2-1
2.2 World Energy Consumption	2-1
2.3 Energy Situation in The Netherlands	2-2
2.4 Energy Sources.....	2-2
2.4.1 Introduction.....	2-2
2.4.2 Oil- and Coal-fired Generation	2-2
2.4.3 Gas-fired Generation.....	2-3
2.4.4 Nuclear Generation	2-3
2.4.5 Hydro energy.....	2-3
2.5 Renewable Energy Sources.....	2-4
2.5.1 Solar Energy.....	2-4
2.5.2 Wind Energy	2-4
2.5.3 Ocean Energy	2-4
2.5.4 Geothermal Energy	2-4
2.6 Ocean Energy Conversion.....	2-4
2.6.1 Tidal Energy.....	2-5
2.6.2 Wave Energy.....	2-5
2.6.3 Energy from Ocean Currents	2-5
2.6.4 Thermal Energy	2-6
2.6.5 Energy from Salinity Differences	2-6
2.6.6 Energy from Marine Biomass.....	2-6
2.7 Conclusions.....	2-7
2.8 References and Literature	2-7
3 Wave Energy Conversion.	
3.1 Introduction.....	3-1
3.2 General Principles of Wave Energy Conversion	3-1
3.2.1 Wave Climate and Energy	3-1
3.2.2 Wave Energy Conversion	3-3
3.2.3 Theory for Wave Energy Conversion.....	3-4
3.3 Classification of Wave Energy Converters.....	3-4
3.3.1 Location	3-4
3.3.2 Point absorbers, Attenuators and Terminators.....	3-5
3.3.3 Types of converted Energy or Energy Use	3-6
3.3.4 The Nine Basic Types.....	3-7
3.4 Research Activity around the World.....	3-10
3.5 Evaluation of Wave Energy Converters.....	3-14
3.5.1 Evaluation Criteria.....	3-14
3.5.2 Results of the Evaluation	3-16
3.6 Wave Energy Conversion in Combination with a Breakwater	3-18
3.7 Conclusions.....	3-19
3.8 References and Literature	3-20

4 Wave Energy Devices for Combination with a Breakwater	
4.1 Introduction	4-1
4.2 Potential Energy Converting Devices	4-1
4.2.1 Russell's Rectifier	4-1
4.2.2 Converging Channel	4-2
4.2.3 Other Concepts	4-3
4.3 Flap Type Devices	4-4
4.3.1 Introduction to Flap Type Devices	4-4
4.3.2 Power Machine with Free Floating Vertical Plates	4-4
4.3.3 Tandem Flap Wave Power Device	4-6
4.3.4 The Pendulor	4-7
4.4 Oscillating Water Column Devices	4-9
4.4.1 Introduction to Oscillating Water Column Devices	4-9
4.4.2 Japanese Wave Power Converting Caisson	4-13
4.4.3 Kværner Harbour Type OWC	4-15
4.4.4 NEL Breakwater	4-16
4.4.5 The Q.U.B. Multi-Resonant Converter	4-19
4.5 Selection of the Device for Combination with a Breakwater	4-20
4.6 Conclusions	4-23
4.7 References	4-24
5 Design of the 'Harbour' Type OWC in a Breakwater	
5.1 Introduction	5-1
5.2 Shape of the Oscillating Water Column Device	5-1
5.2.1 Reflecting Back Wall	5-1
5.2.2 Rectangular or Circular Chamber Area	5-1
5.2.3 Optimal Shape of a Rectangular OWC Device	5-2
5.2.4 Comparison with the 'Harbour' Type OWC	5-3
5.2.5 Shape of the 'Harbour'	5-4
5.2.6 Pilot Plant Design for Ennore	5-4
5.2.7 Conclusions about the Shape of 'Harbour' Type OWC Device	5-5
5.3 Theory of the 'Harbour' Type Device in a Reflecting Wall	5-5
5.3.1 Development of the Theory	5-5
5.3.2 Vertical Caisson Breakwater instead of a Rubble Mound Breakwater	5-6
5.4 Design Parameters of the 'Harbour' Type Device	5-6
5.4.1 Method of Determining the Design Parameters	5-6
5.4.2 Dimensionless Presentation of Various Design Parameters	5-7
5.4.3 Length of the Chamber and 'Harbour'	5-8
5.4.4 Width of the Chamber and 'Harbour'	5-11
5.4.5 Immersion Depth of the Front Barrier	5-12
5.4.6 Height of the chamber	5-14
5.4.7 Crest Height of the breakwater	5-15
5.4.8 Turbine characteristic and damping level	5-16
5.4.9 Spacing between the devices in the breakwater	5-16
5.4.10 Reflection of the breakwater	5-17
5.5 Theory for Caisson Breakwaters	5-17
5.6 Conclusions	5-17
5.7 References	5-18

6 Location of the Breakwater and Design Conditions	
6.1 Introduction	6-1
6.2 Selection of the Location	6-1
6.2.1 Selection Criteria	6-1
6.2.2 Possible Locations	6-2
6.2.3 Description of the Location	6-3
6.3 Water Level and Wave Climate	6-4
6.3.1 Water Level.....	6-4
6.3.2 Wave Climate.....	6-6
6.4 Design conditions.....	6-13
6.4.1 U.L.S. Ultimate Limit State	6-13
6.4.2 S.L.S. Serviceability Limit State	6-19
6.5 Conclusions	6-25
6.6 References	6-25
7 Design of the Wave Power Converting Breakwater	
7.1 Introduction	7-1
7.2 Design Method.....	7-1
7.3 Global Design of the Caissons with a Device.....	7-3
7.4 Dimensions of the Device	7-5
7.5 Dimensions of the Caisson with a Device	7-11
7.6 Final Design	7-15
7.6.1 Information for Stability Calculation.....	7-15
7.6.2 Stability Calculation of the Caissons	7-17
7.7 Conclusions	7-20
7.8 References	7-21
8 Wave Power Conversion into Electricity	
8.1 Introduction	8-1
8.2 Turbine Room Equipment.....	8-1
8.2.1 Turbine Generator.....	8-1
8.2.2 Air Regulating Valves.....	8-4
8.2.3 Layout of the Turbine Room.....	8-4
8.3 Wave Power Conversion.....	8-4
8.3.1 Introduction.....	8-4
8.3.2 Incoming Wave Power.....	8-5
8.3.3 Wave Power Conversion.....	8-5
8.3.4 Generated Electricity	8-7
8.4 Economic Aspects	8-7
8.5 Conclusions	8-8
8.6 References	8-9
9 Construction Method and Dimensions of the Caisson	
9.1 Introduction	9-1
9.2 Construction Method	9-1
9.3 Stability and Strength during Transport.....	9-2
9.3.1 Stability and Wave Response of the Caisson.....	9-2
9.3.2 Strength of the Caisson during Transport	9-3
9.4 Stability of the Caisson during and after Sinking	9-4
9.5 Dimensions of Concrete Walls	9-4
9.6 Conclusions	9-6
9.7 References and Literature	9-7
10 Conclusions and Recommendations	

List of Definitions

angle of incidence	: angle between a line perpendicular to the width of a device and the wave propagation direction (angle of incidence between 0 and 90°)
bandwidth	: the efficiency of a device can have a broad or small bandwidth, what means that the efficiency has respectively high or low values for non-resonant conditions, see for instance Figure 5.1
capture	: the first phase of wave power conversion, wave power can be captured by a device, converted into another form of power, subsequently further conversion phases can take place
capture efficiency	: the efficiency of the first phase of wave power conversion
capture width	: width of a 2-dimensional wave crest having the same mean power as the captured power by the device, in 3-dimensional conditions a device can capture wave power from a width even larger than its own width
capture width ratio	: capture width divided by the device width
chamber	: oscillating water column devices have an air chamber above the column, in which air pressure can oscillate
diffracted waves	: the incoming waves that are not captured, i.e. reflected, transmitted and diffracted ¹ waves
extract	: other term for capture
'harbour'	: basin in front of a device in which 'harbour' (i.e. roughly quarter-wave) resonance occurs
incident	: incoming waves to device are incident waves
length of a device	: dimension of the device parallel to the (normally incident) wave propagation
length of a caisson	: dimension of the caisson parallel to the (normally incident) wave propagation
normally	: normally incident waves, waves with a propagation perpendicular to a device (angle of incidence is zero)
obliquely	: obliquely incident waves, waves which attack with a certain angle of incidence
OWC	: oscillating water column
radiation damping	: damping of a device related to the production of radiation waves
radiation waves	: waves, produced by the oscillation of a body (or water column) in the absence of incident waves
reflected waves	: incoming waves that are reflected by an obstacle, travelling back in the direction of the incoming waves
scattered waves	: same as diffracted waves
S.L.S.	: serviceability limit state
U.L.S.	: ultimate limit state
WEC	: wave energy converter
width of a device	: dimension of a device perpendicular to the (normally incident) wave propagation
width of a caisson	: dimension of a caisson perpendicular to the (normally incident) wave propagation

¹ In general the term diffraction is used for waves that bend around an obstacle, for instance a breakwater.

1 Introduction

1.1 Background to the Study

This report has been written as MSc. thesis report at Delft University of Technology, Faculty of Civil Engineering, Hydraulic and Geotechnical Engineering Division, Hydraulic Engineering Group. It deals with the state of the art of wave energy converters, the theory of wave energy conversion and a design of a wave power converting breakwater for the Port of Bilbao, North Spain.

At present, many countries are interested in renewable energy sources. Wave energy is one of these sources. Since the early 1970s, wave energy conversion has been investigated. Several devices have been developed and tested, most of them as scaled models, however also some full-scale devices have been constructed and are still operating. Until now, no large wave energy converting power plants have been constructed.

In Japan a full-scale wave power converting caisson has been constructed in the summer of 1989, at Sakata Port. Wave power is converted into air power in an air chamber and subsequently by a turbine into electricity. The operation, started in the winter of 1989, is successful. The caisson has survived some severe storms and the wave power is converted into electricity with sufficient efficiency.

It is for these reasons, that the Hydraulic Engineering Group is interested in the state of the art of wave energy conversion and its prospects. Theoretical as well as practical properties of wave energy converters have to be investigated. Particularly, the combination of a breakwater with wave power converting devices has attracted the attention.

1.2 Scope and Objective of the Study

Problem Description

In the last decades, considerable research in wave energy conversion has been performed. Several concepts have been investigated and tested. As yet, it is unknown which type of wave energy device is useful to employ, depending on local circumstances. In particular the working principle of wave energy converting breakwaters is insufficiently understood.

Objective

In this study, the different types of wave energy devices will be described. The combination of a breakwater with wave energy converting devices will be investigated. A location for a breakwater will be selected to design a wave power converting breakwater. Finally, an estimation of the yearly generated electricity will be calculated.

1.3 Structure of the Report

The structure of this report is as follows. In the next chapter the present energy situation is discussed. Different renewable energy sources exist. The subject of this study is focussed on wave energy.

In Chapter 3, the general principles of wave energy conversion is explained. The state of the art of energy devices is described, followed by some evaluation criteria and the prospects of several types of devices. In this chapter, also the prospects of a breakwater in combination with wave energy devices is given.

In Figure 1.1 the structure of the report for Chapter 1 to 3 is schematically shown.

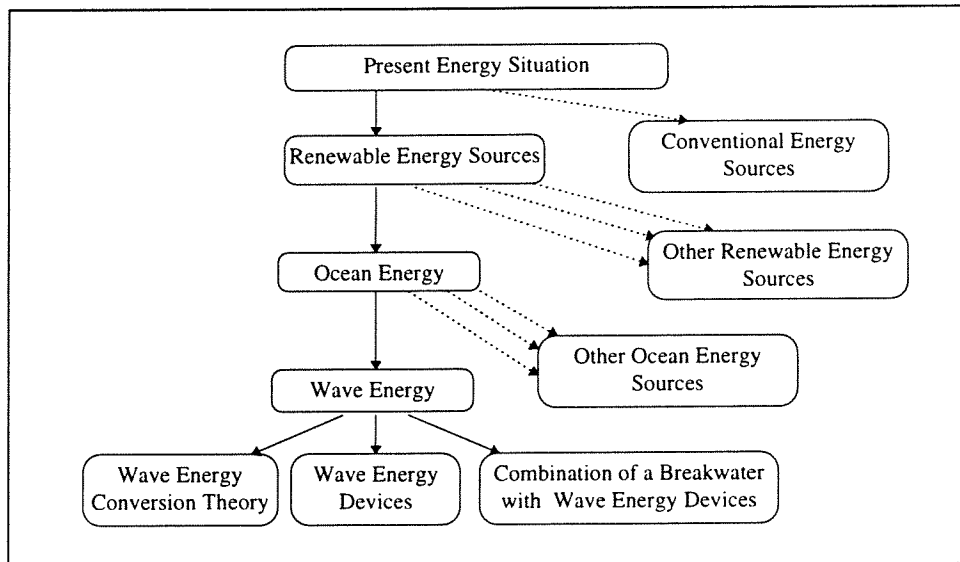


Figure 1.1 Structure of the report, Chapter 1 to 3, schematically

The devices which seem to be suitable for combination with a breakwater are investigated in Chapter 4. It turns out that the 'harbour' type oscillating water column device is the best for combination with a breakwater.

In Chapter 5, the principle of this type of device is explained and the influence of different design parameters is investigated. The results of theories of different authors and the dimensions of some designs are compared. This is possible by presenting the different design parameters dimensionless. The result of this comparison consists of figures and design recommendations to make a design of a device for a certain location.

In Figure 1.2 the structure of the report for Chapter 4 to 5 is schematically shown.

In Chapter 6, a location is selected for which a wave power converting breakwater will be designed.

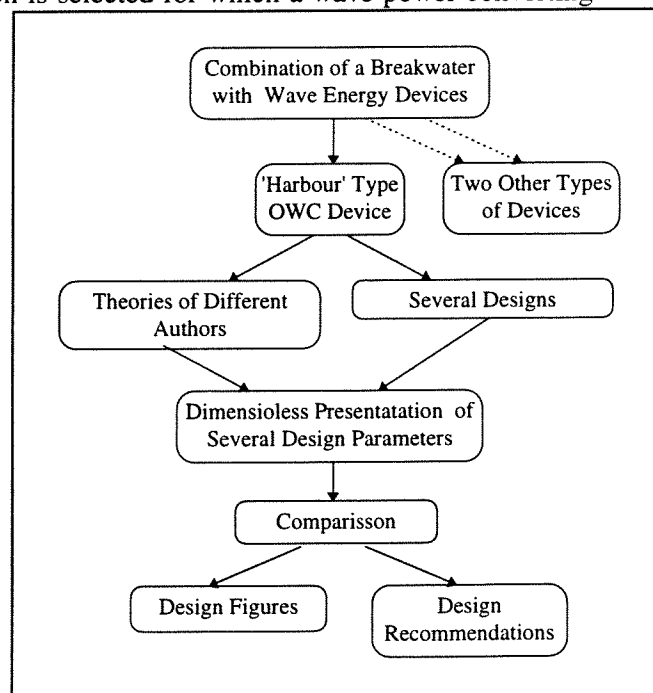


Figure 1.2 Structure of the report, Chapter 4 to 5, schematically

In this chapter two design conditions are investigated, namely the ultimate limit state (U.L.S.) and the

serviceability limit state (S.L.S.). The U.L.S is required for the stability and strength of the breakwater, the S.L.S. for functioning of the breakwater for sheltering Bilbao Harbour and for wave power conversion.

For the U.L.S. the maximum wave height and the corresponding wave length have been determined. For the S.L.S. the wave height, length and direction and their accompanying probability of occurrence are discussed. The wave steepness, a relation between wave length and height, is derived to estimate the wave power, corresponding to a particular wave length or height.

The structure of Chapter 6 is shown in Figure 1.3 schematically.

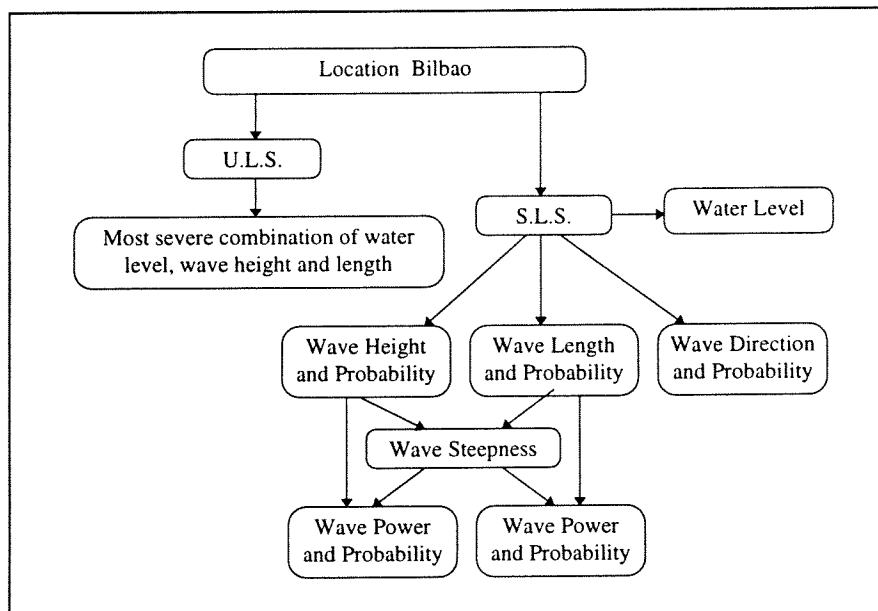


Figure 1.3 Structure of Chapter 6, schematically

The wave power converting caissons of the breakwater of Bilbao are designed in Chapter 7. The caissons are designed for stability and strength as well as for wave power conversion. For stability calculations, the Goda theory is used with some modifications. For the design concerning the wave power conversion, the results (i.e. the design figures and recommendations) of Chapter 5 are used.

In Chapter 8, the required equipment of the turbine room is discussed and the electricity generation is estimated for winter and summer periods. Some economic aspects are also described. A construction method is proposed in Chapter 9, the stability of the caissons is checked for different phases of the construction. In this chapter also some concrete dimensions are determined.

Finally, the conclusions of the study are drawn and some recommendations are given in Chapter 10.

2 Energy Supply and Demand

2.1 Introduction

In this chapter the energy demand and the different sources of energy are described. In Section 2.2, the world energy consumption and the future development of energy demand are discussed. Population growth and a raising standard of living, will lead to a further increase in the consumption of energy. In the following section, information about the energy situation in the Netherlands is given.

Subsequently, the present conventional energy sources such as coal, oil, gas, nuclear and hydro energy are described in Section 2.4. In the following section (2.5) the importance of renewable energy is explained and several sources are described. The state of the art of using the source 'ocean energy' is given in Section 2.6. Several techniques of energy generation exist like utilisation of tides, waves, ocean currents, thermal and salinity differences and biomass. Finally, some conclusions are given in the section 2.7 and the references in 2.8.

2.2 World Energy Consumption

World energy consumption has increased significantly since 1950 and the extra demand has been provided primarily by fossil fuels, as shown in figure 2.1(a) [Shaw; 1982]. In the years 1950 to 1975 this increased demand was satisfied by an almost sixfold increase in the use of oil and natural gas.

By the early 1970s however, an awareness that these sources would be seriously depleted within two or three decades, caused considerable concern. As a result of the abrupt increase in oil prices in 1973, especially the industrialised nations became interested in the possibilities of exploiting new energy sources.

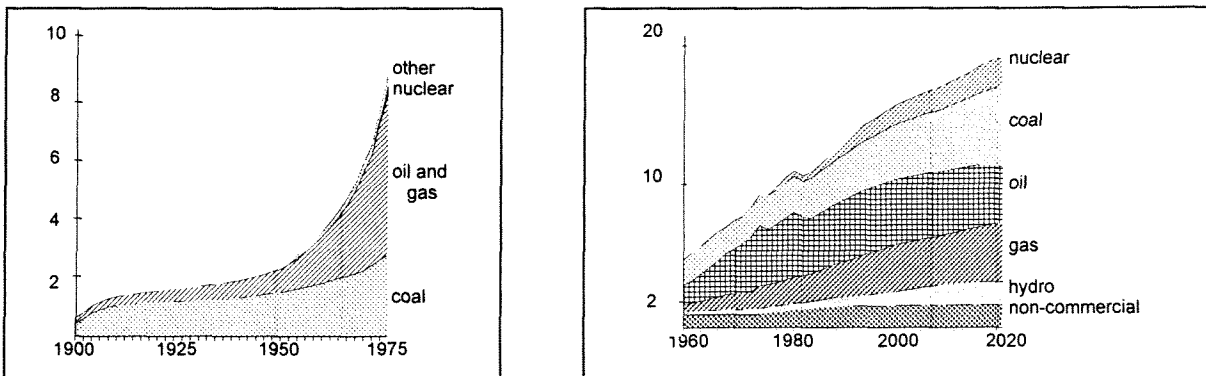


Figure 2.1 (a) World energy consumption 1900-1975; (b) World energy consumption 1960-2020
Energy consumption in milliard tonnes of coal equivalent per year

National consumption obviously varies with the number of inhabitants, but also depends on the standard of living and the level of industrialisation. Population growth of the world, the necessary raising of the standard of living of a very large fraction of the population, particularly in the Third World, will lead to a further increase in the consumption of energy.

Various energy advisory groups have attempted to identify possible future energy demands and supplies, in order to formulate the necessary strategies for the remainder of this century and the early part of the next. Figure 2.1(b) shows a prediction of the energy consumption to the year 2020. These different but plausible forecasts are based on many assumptions and must be revised continuously.

2.3 Energy Situation in The Netherlands

The new principles of the third 'Energienota' of 1995 are twofold, namely more renewable energy (see Section 2.5) and more competition on the energy market. The renewable energy has to increase from 1% to 17%, with the goal of 10% in the year 2020. The European Commission has the electricity companies already summoned to liberalisation. When this liberalisation goes on, the companies in the Netherlands have to expect also competition from some surrounding countries. Under the influence of this increasing competition, the electricity prices in Europe will decrease. However, by lower electricity prices, the use of renewable energy comes in a more difficult position, because of the fact that until now, the electricity prices are exclusive of costs of the environment. Therefore, special rules have to be made to promote the use of renewable energy sources. [Commandeur et al.;1996]

2.4 Energy Sources

2.4.1 Introduction

An important consideration in the application of energy sources concerns the form in which the energy is eventually consumed. The energy may ultimately be utilised as 'high grade' electrical energy or as 'low grade' thermal energy. The conversion of thermal energy to mechanical and subsequent electrical energy, involves the restriction of the Carnot cycle efficiency (Second Law of Thermodynamics). Therefore, it is common practice to refer to thermal energy as 'low grade' energy and mechanical and hence electrical energy as 'high grade' energy. Electricity is a form of energy which can be used for heating, light and motion. It is easy transportable, convertible and, as such, environmental friendly.

In all thermal power stations, the chemical energy of fossil fuels or the nuclear energy of fissile fuels is first released as thermal energy, before being converted in an engine by means of a thermodynamic cycle to mechanical and eventually electrical energy. This conversion into electricity can only be carried out by a thermal efficiency in the region of 40%, the maximum ideal efficiency would be about 63% [Shaw;1982].

In the following sections some sources, which are in widespread use around the world, are described.

2.4.2 Oil- and Coal-fired Generation

Oil and coal are the most common sources of electrical power generation in the world. This generation is usually firstly used to satisfy the customer demand.

A very large part of the oil is transported by ships. A much smaller quantity is carried by underwater pipelines, consisting almost entirely of connections between the fields at sea and land. Coal is the subject of a trade which is, at the present time, increasing rapidly because the consumer countries (Western Europe and Japan) are located at distance of the producing countries (USA, Australia, South Africa). Compared to oil transport, it is nevertheless only a modest traffic. Substantial quantities of fuel are stored at the power stations, so generally the output should be sustainable for several weeks even if no further fuel deliveries are possible.

Spectacular accidents with grave consequences for the environment, have made public opinion sensitive to the production and transport of oil. Pollution by oil often occurs near the coast in zones, which are generally highly productive in biological terms. The effect on the environment of using coal should not be overlooked. The sulphur content of the coal oxidises producing, in combination with water, acid rain. This rain has harmful effects on crops, forests and buildings.

Oil and coal, fossil fuels, are not renewable at present rates of consumption and hence limited in the extent of the source. However, coal sources are much larger than oil sources. Figure 2.1(b) also shows the probable decline in the use of gas and oil after the turn of the century, but coal can be an important source for two or three centuries.

2.4.3 Gas-fired Generation

Gas turbine generators were initially installed in power systems as quick start spare capacity. However, operating costs of aero type gas turbines are high, because of the required high grade fuel and the inherent low efficiency. More recently industrial grade gas turbines have been used, generally fired by natural gas. Their efficiency can reach a value higher than 50%. [Pope;1992]. The use of gas, however, is limited.

2.4.4 Nuclear Generation

Nuclear stations make a significant contribution to some power systems, for instance in France. Although these plants are generally capable of some regulation of output, economic pressures mean that they are classed as 'must run' plants, of which the output cannot be regulated. Nuclear plants have to cope with technical complexity, very high safety costs and high capital costs. Radioactive waste products from nuclear power stations present problems which are very difficult to solve. If the present research into controlled nuclear fusion would be successful, probably an unlimited energy source will be discovered.

2.4.5 Hydro Electricity Generation

Hydro energy is one of the oldest sources of energy known by man. Today, where suitable geographical conditions exist, it can provide an ideal source of electrical energy. Capital costs are generally high because of extensive civil engineering works and because of the frequent need for long electricity transmission lines, while the storage reservoir may cover a large land area. Although virtually free from emissions, hydro electricity nevertheless often comes in for environmental criticism because of its effect on river flow regimes and on the area to be flooded. Running costs are very low and there may be other benefits originally from flood control and irrigation or other purposes satisfied by the storage reservoir.

Hydro-electric power plants at their simplest, are of the 'run of river' type, without a reservoir for storing water. The power output depends on the flow in the river, operation occurs twenty-four hours a day, with the power output changing slowly according to the river flow. At their most complicated, hydro-electric power plants are able to store water (and thus energy) in a reservoir, on a seasonal basis. Consequently, they are able to generate electricity at any time of the day. The only constraint is that the water level behind the dam, must stay within prescribed limits, so the energy source is not unlimited and depends on the seasons and weather.

The effective out coming capacity of a hydro-electric power plant is:

$$P_G = \rho \cdot g \cdot Q \cdot H_N \cdot \eta_T \cdot \eta_G \quad (2.1)$$

with	P_G	= capacity at generator [W]	
	ρ	= density of water [kg/m^3]	$\approx 1000 \text{ kg/m}^3$
	g	= gravitational acceleration [m/s^2]	$\approx 9.81 \text{ m/s}^2$
	Q	= discharge [m^3/s]	
	H_N	= net head [m]	
	η_T	= efficiency of turbine [-]	≈ 0.88
	η_G	= efficiency of generator [-]	≈ 0.96

It can be concluded that the overall efficiency is about 80% [van Duivendijk;1993].

2.5 Renewable Energy Sources

The energy consumption will increase in future, as explained in Section 2.2. The conventional sources of energy may become unavailable, over-expensive or unacceptable and fear exists of radioactive emissions from nuclear power plants. Consequently, the larger the choice for different types of energy the more the energy supply is guaranteed.

The foregoing comments justify attention to energy sources which do not run short: solar, wind, ocean and geothermal energy. These are the so-called renewable energy sources.

2.5.1 Solar Energy

Solar radiation causes the hydrological cycle, which provides the potential energy of water. This potential energy can be converted into hydro electricity. This form of electricity can increase in future. The sun can also provide a considerable energy saving in the heating of water and space. The generation of electricity by photovoltaic conversion is not a serious contender, because of the low efficiency of about 11%. [Shaw;1982]. Biofuels, fuels from crops and organic wastes, can be an useful energy source, but their application as a mean of producing electricity will be on a small scale.

2.5.2 Wind Energy

Wind energy, also resulting from differences in solar radiation over the earth's surface, is a promising source. The technology is being used for both small, one-off installations feeding isolated systems or the local electricity distribution systems, and for large wind farms supplying energy to the grid. Proposals have been made for the construction of offshore installed turbines. Theoretical considerations show that the aerodynamic efficiency of a wind turbine cannot exceed a limit of about 50% [Brin;1979]. A good practical efficiency would be 30% [Shaw;1982].

2.5.3 Ocean Energy

The ocean, occupying most of the world surface, and the atmosphere above it intercept most of the energy from the sun. This energy appears in a variety of forms: as wind; as waves, generated by the wind blowing over the surface; and as currents, driven principally by the wind but also caused by density differences. An other source of energy is the gravitational system of sun, earth and moon resulting in tidal waves.

Different types of technologies have been developed to convert these forms of energy from the ocean. These technologies will be described in Section 2.6.

2.5.4 Geothermal Energy

Geothermal energy conversion is viable, especially for those parts of the world where geological faults occur in the earth's crust. Boreholes to tap the steam generated in such areas and the associated steam turbine power plant call only on established technology and many geothermal power stations exist, for instance in Japan [Hashimoto et al.;1993].

2.6 Ocean Energy Conversion

This section gives the state of the art of the existing technologies to extract energy from the ocean. Some methods have already achieved a significant level of development, others are only in an initial stage.

2.6.1 Tidal Energy

The use of tidal energy is very old, the first tide mills have appeared on the coast of England and France in the eleventh century. It is easy to forecast the size of a tide, so energy production can be determined in advance.

The simplest tidal unit is a basin separated from the sea by a dam. It is filled during flood and during ebb water flows back under a head through a turbine. This simplest system operates with one basin and one cycle. If the turbine can operate both on filling and on emptying, it is possible to fill the empty basin during flood and empty it during ebb (one basin, two cycles). By using two basins, one filled during flood, the other emptied during ebb, it is possible to generate more continuous power. Flow from the one basin to the other can then take place at any stage of the tide. [Warnock et al.;1992] [van Duivendijk;1993] The different systems are shown in Figure 2.2.

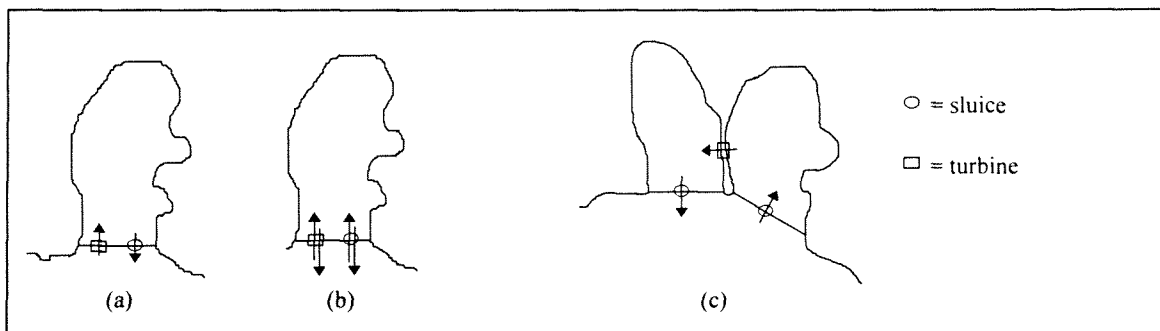


Figure 2.2 Different types of tidal energy systems: (a) single basin, single effect; (b) single basin, double effect; (c) double basin, single effect

The capacity and efficiency calculation is the same as for hydro electricity (see, equation 2.1).

A famous tidal power plant is La Rance in France, with an installed capacity of 240 MW, of which the operation started in 1966. Some other well known projects are: Kislaya Guba, USSR, 0.4 MW, 1968; Annapolis, Bay of Fundy in Canada, 18MW, 1985; and Severn Estuary, United Kingdom. Also many other countries, like Australia, India, Korea, and China are interested in tidal power development.

2.6.2 Wave Energy

Wave energy is the energy of the ocean which has aroused most interest by inventors. Many patents have been taken out on devices which convert the wave energy. An operating device was constructed in the early twentieth century in France. In this system, the rise and the fall of the water surface in a special chamber, communicating with the ocean, provided compressed air to drive a turbo-generator [McCormick;1981]. A number of processes have been the object of, sometimes costly, tests.

The magnitude of the source justifies this activity. The power dissipated by the waves over all the coasts has been evaluated at 2000 GW, corresponding to an average 'linear' power of 10 kW/m of coastline. This power varies according to the geographical position, from 3 kW/m in the Mediterranean to 90 kW/m in the North Atlantic Ocean [Brin;1979].

Wave energy conversion is subject of this study, so the general principles of wave energy conversion and the different devices will be described in the next chapter.

2.6.3 Energy from Ocean Currents

The Gulf Stream and the Kuroshio Current of Japan are well recognised examples of ocean currents. Interpretations of measurements leads to estimated flow rates of 80 million m³/s for the Gulf Stream and 55 million m³/s for the Kuroshio. Speeds are as high as 2.5 m/s in limited zones [Brin;1979].

To convert this energy, it would be necessary to use large turbines. The turbine generator would, like a wind turbine generator, have its efficiency limited to a value slightly higher than 50%. The generation of large amounts of power needs gigantic machines on, or anchored, to the sea bed [Brin;1979].

In the USA, a project existed to convert a part of the energy of the Florida Stream. This resulted in the design of a very large (91m) turbine of unconventional design. The machine, called Coriolis, is intended to be moored at a depth below the keels of ships. An other proposed technology is the use of open turbines. An example is the Kinetic Hydro Energy Conversion System (KHECS), under development by New York University and the Power Authority. The prototype design is rated at 30 kW and expected to produce an overall efficiency of 35% [Seymour;1992].

2.6.4 Thermal Energy

The principle of Ocean Thermal Energy Conversion (OTEC) is the utilisation of the temperature difference between warm surface and cold deep ocean water, to drive a heat engine. However, because of the small differences in these temperatures, the Carnot efficiency is low (under the most favourable conditions about 8%) [Brin;1979]. The quantities of water to be utilised would therefore be very considerable. OTEC plants can be land-based or in the open sea. Potential sites are Hawaii and many other islands in the Indian and Pacific Ocean.

Two techniques exist to generate electric power. The first idea of the year 1881, was that of the closed cycle. In the closed-cycle process, the warm-water flow provides and the cold-water flow extracts heat energy from a chemical working fluid. The vapour of that fluid, generates mechanical energy in a turbine. A new concept, developed in the year 1929 was the open or Claude cycle. Heat transfer from warm water could be achieved by vapourising a fraction of that flow in a partial vacuum. The steam so produced could be used as the working fluid. This technique can also produce fresh water.

2.6.5 Energy from Salinity Differences

Salinity power refers to a large unexploited energy source, which exists at the interface between water bodies with different salinities. Specifically, the salinity potential between the oceans and fresh water in rivers is equivalent to a hydrostatic head of 240 m high [Seymour;1992]. The potential difference where low salinity waters mixes with saturated brines in terminal lakes, can easily be 10-20 times as large. In theory, any strategy that can be used for desalination could be reversed to generate power. Various methods of harnessing salinity power have been proposed. Some of these have a chance to become economically attractive [Seymour;1992].

2.6.6 Energy from Marine Biomass

The concept of extracting energy from marine biomass is culturing fast-growing macroalgae in the ocean as a feedstock for methane production. In 1976, the Gas Research Institute sponsored a research and development program aimed at a system for culturing giant kelp off the Southern California coast. The system produced on-shore methane with ocean disposal of the residue of the extraction process. This program was abandoned in 1983 and the emphasis for biomass returned to harvesting on land [Seymour;1992].

2.7 Conclusions

World energy consumption has increased significantly since 1950. Population growth and a raising standard of living, will lead to a further increase in the consumption of energy. The use of oil and gas for the generation of electricity is limited to some decades and the use of coal to two or three centuries. Hydro energy is environmental friendly, but depend on geographical and climate conditions. The awareness that the conventional sources will be depleted has given interest in new sources.

Important sources are those which do not run short: solar, wind, ocean and geothermal energy. This is the so-called renewable energy. Many types of ocean energy conversion exist. The use of tidal energy is already very old, the USA has projects to convert energy from ocean currents and other principles are to make use of the differences in temperature or salinity of sea water.

Wave energy conversion has aroused most interest by inventors and is the subject of this study. Many patents have been taken out on devices for conversion this energy and a number of processes have been tested. In the next chapter, the general principles of wave energy conversion and some devices will be described.

2.8 References and Literature

- Brin, A.(1979); *Energy and the Oceans*; Westbury House, Great Britain
- Commandeur, P., Junne, G., Roscam Abbing, M.(16-2-1996); *Schone energie wordt prooi van Europese markt (in Dutch)*; De Volkskrant, the Netherlands
- Duivendijk, J.van(1993); *Energiewaterbouwkunde (in Dutch)*; Delft University of Technology, the Netherlands
- Hashimoto, S., Abe, K.(1993); *Geothermal Power Generation, The case of the Tohoku electric power co., inc.*; Civil Engineering in Japan, Vol.32, pp. 135-151
- McCormick, M.E.(1981); *Ocean Wave Energy Conversion*; U.S. Naval Academy, Annapolis, Maryland, Willey-Interscience Publication, USA
- Pope, I.(1992); *Fascilating Technology for Electric Power Generation*; Ocean Energy Recovery, The state of the Art; Scripps Institution of Oceanography, University of California at San Diego; Offshore Technology Research Center, Texas A&M University, USA
- Salverda, K.(13-1-1996); *Jan Terlouw wil met ECN de markt op (in Dutch)*; Nieuwe Noord-Hollandse Courant, the Netherlands
- Seymour, R.J. (1992); *State of the Art in Other Ocean Energy Sources*; Ocean Energy Recovery, The state of the Art; Scripps Institution of Oceanography, University of California at San Diego; Offshore Technology Research Center, Texas A&M University, USA
- Shaw, R.(1982); *Wave Energy, a design challenge*; University of Liverpool, England
- Simeons, C. (1980); *Hydro Power, The Use of Water as an Alternative Source of Energy*; Pergamon Press
- Warnock, J.G., Clark, R.H.; *The State of the Art in Tidal Power Recovery*; Ocean Energy Recovery, The state of the Art; Scripps Institution of Oceanography, University of California at San Diego; Offshore Technology Research Center, Texas A&M University, USA

3 Wave Energy Conversion

3.1 Introduction

The possibility of wave energy conversion has intrigued mankind for centuries, but it is only in the past two decades that technically suitable devices have been proposed. In general these devices have few environmental drawbacks. Some devices are believed to become economically attractive, especially in areas of the world with high wave energy and in locations where the electricity generation costs are high.

In the next section, the general principles of wave energy conversion will be explained. Subsequently, a classification of energy converters is given in Section 3.3. As said, many devices have been patented, but only some more advanced types of devices are described. The research activities and the results in some countries are discussed in Section 3.4.

After describing the devices, an evaluation can be made and the most promising systems can be selected. This evaluation and selection is described in Section 3.5. Some types of energy converters can be combined with breakwater protection. This combination is investigated in Section 3.6. Finally, some conclusions are drawn in Section 3.7 and the references are given in the last section.

3.2 General Principles of Wave Energy Conversion

3.2.1 Wave Climate and Energy

When the winds blow across the oceans, waves are generated. The energy in these waves provides a convenient and natural concentration of the wind energy. Once created, waves are attenuated only over considerable distances.

The two measurable properties of waves are the height and period. With the help of these values and the 'linear wave theory' the energy of waves can be calculated. See for more information about this linear wave theory, **Appendix A**. The most important equations concerning the energy of waves are given already in this section.

The total mean wave energy in the surface is:

$$E = \frac{\rho \cdot g \cdot H^2}{8} = \frac{\rho \cdot g \cdot A^2}{2} \quad (3.1)$$

with E = total energy per square metre of surface [J/m^2]
 ρ = water density [kg/m^3] $\approx 1000-1040 \text{ kg/m}^3$
 g = gravitational acceleration [m/s^2] $\approx 9.81 \text{ m/s}^2$
 H = wave height [m]
 A = wave amplitude = $1/2 \cdot H$

Total energy per metre wave crest:

$$E_T = \frac{\rho \cdot g \cdot H^2 \cdot \lambda}{8} = \frac{\rho \cdot g \cdot A^2 \cdot \lambda}{2} \quad (3.2)$$

with E_T = total energy per metre of crest length [J/m]
 λ = wave length [m]

The total energy in deep water waves is equally composed of potential energy and kinetic energy. The potential energy is exhibited by the wave height H , whereas the kinetic energy is dependent on the motions of the particles.

$$E_T = E_p + E_k \quad (3.3)$$

$$E_p = E_k = \frac{\rho \cdot g \cdot H^2 \cdot \lambda}{16} \quad (3.4)$$

with E_p = potential energy per metre of crest length [J/m]
 E_k = kinetic energy per metre of crest length [J/m]

The transfer of wave energy from point to point in the direction of the wave travel is characterised by the 'energy flux' or 'wave power'.

$$P_w = \frac{\rho \cdot g \cdot H^2 \cdot c_g}{8} = \frac{\rho \cdot g \cdot A^2 \cdot c_g}{2} = E \cdot n \cdot c \quad (3.5)$$

with P_w = wave power or energy flux [W/m]
 A = amplitude of wave = $\frac{1}{2} H$ [m]
 c_g = group velocity [m/s]
 $= n \cdot c$
 c = wave celerity [m/s]

See **Appendix A** for more information.

Figure 3.1 shows the estimated wave power around the world [Atlas of the Oceans]. The largest sources are found in the region receiving rather constant wind due to the climate conditions. For example the north east Atlantic is subjected to the air stream of the Gulf of Mexico, which consequently generates a substantial wave climate at the European Atlantic coast. The estimates shown are average wave power values in kW per metre of wave crest in deep water.

Along the coasts, in the North Atlantic 50 kW per metre is typical and around Japan 10 kW per metre is more usual [Duckers;1991]. Energy is lost as waves run into shallower water and so shore mounted devices are subjected to smaller wave power. Nevertheless, the total energy content of the world's waves is substantial and harnessing a small fraction of this energy would significantly contribute to mankind's energy demand. The total European source is estimated to be 110 GW what means about 85% of present European Community's electric demand. The total world wide wave energy source at any one time is in the order of 2000 GW [Duckers;1991].

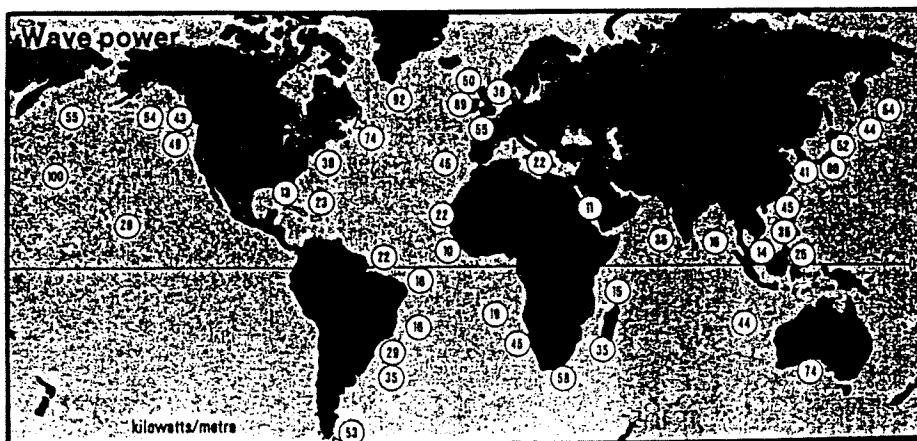


Figure 3.1 Average wave power in kW per metre in deep water

3.2.2 Wave Energy Conversion

In order to convert the energy from sea waves, it is necessary to intercept these waves by using a structure which can respond in an appropriate manner to the forces applied to it by the waves. If the structure is fixed to the sea bed or sea shore, wave energy can be converted into mechanical energy by a part of the structure that moves with respect to the fixed structure.

Floating structures can also be employed, but then a stable frame of reference must be established in the way that the 'active' part of the device moves relative to the main structure. This can be achieved by the application of inertia or by making the structure so large that it spans several wave crests and hence is reasonably stable in most sea states. In the next figure, a typical wave energy conversion system is shown [Count;1979].

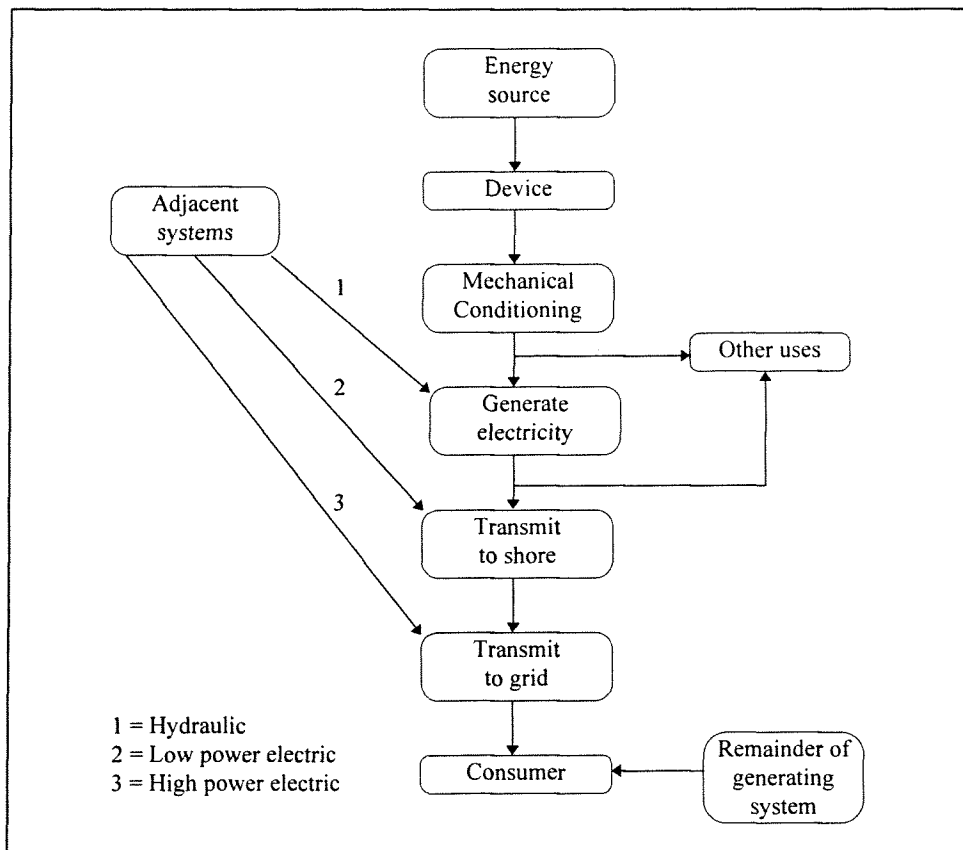


Figure 3.2 The main elements of a system converting wave energy into electricity

Any technique that can effectively create waves, can also be used to convert wave energy. A number of experimental naval architects and ocean engineers have suggested to use hinged vertical wave boards, moving bulkheads, plungers and pneumatic chambers as wave energy converters (WECs), since these devices are effective in creating waves.

Summarising, energy can be generated by an oscillating body or by an oscillating water column (OWC) in a chamber having an opening to the sea. It is also possible to enclose the water by blocking the chamber opening with an elastic or flexible membrane, which can oscillate under wave action. In this last case, it is not necessary to have water in the chamber, because air can oscillate in pressure, in step with the flexible membrane. The air power can be converted by use of a turbine.

3.2.3 Theory for Wave Energy Conversion

Wave energy impinging on a device, can be reflected, absorbed (or captured) and transmitted. To maximise wave energy capturing, a wave energy converter should be designed to minimise the other two losses. This process, the primary conversion, converts wave energy for instance into:

- mechanical energy
- air compression (second conversion by means of an air turbine)
- potential energy of water (second conversion by means of a hydraulic turbine)

Subsequently, the captured wave energy has to be converted into electricity. Both phases of the conversion operate with a certain efficiency, the first one is called the 'capture efficiency' or 'primary efficiency' and the second the 'generation efficiency' or 'secondary efficiency'. Sometimes both are estimated at a quite low value of 50%. When for instance the average wave energy is 50 kW/m, then 12 kW/m could be converted into useful electricity.

The primary conversion of many devices can be represented by a floating body modelled as a simple spring-and-damper system. The capture efficiency is a good measure of the performance and thus of the possibility of a device. The theory is shown in **Appendix B** and some conclusions are given below. This general theory is important to understand the behaviour of devices and to comprehend other theories based on it.

A highly efficient device is one of which the amplitude of waves downstream, produced by the forced oscillation of the body in the absence of the incident waves (radiation waves), is as small as possible compared to the amplitude of the waves produced upstream. It can be concluded that for a symmetrical two-dimensional body, with the same amplitude downstream and upstream, the maximum captured wave power is half the mean wave power, $P_{\text{cap,max}} = 1/2 \cdot P_w$.

For an asymmetrical oscillating body, the efficiency can be improved when it generates little wave motion downstream compared to upstream and a maximum efficiency $E_{\text{max}} = 100\%$ is obtained at a particular frequency. This maximum efficiency is reached when the energy extraction rate equals the rate of radiation damping and the floating body is kept in resonance. Also for devices oscillating in more than one direction, the maximum efficiency of 100% can be reached.

When oscillating bodies are tested in three-dimensional conditions, capture efficiencies higher than 100% can be obtained. This is caused by the wave focusing, that results from the interaction between the incident waves and the radiation waves at or near the condition of resonance. The capture efficiency is called the capture width, defined as the width of a two-dimensional wave crest having the same mean power as the power that is captured by the device: $w_{\text{cap}} = P_{\text{cap}} / P_w$. In literature, often the non-dimensionalised capture width is given, which is the capture width divided by the width of the device ($W_{\text{cap}} = w_{\text{cap}} / \text{width}$). See also Section 3.3.2, where this phenomenon is called point absorbing.

3.3 Classification of Wave Energy Converters

Many ways exist of describing and classifying energy converters. Often, they are described in terms of their location (Section 3.3.1), theoretical considerations and general arrangement (Section 3.3.2), or energy use (Section 3.3.3). McCormick made a division into nine basic types in his book 'Ocean Wave Energy Conversion' of 1981 as described in Section 3.3.4 [McCormick;1981].

3.3.1 Location

A wave energy converter may be placed in the ocean in various possible situations and locations. It may be located on the shore or on the sea bed in relatively shallow water. Such a converter on the sea bed may be completely submerged, surface-piercing or placed on an offshore platform. An advantage of these systems is that operation and maintenance are relatively easy. Drawbacks are that the

available wave power may be smaller than offshore, and the civil engineering work is difficult on wave-exposed shore.

It is also possible that a converter is floating or submerged in the sea offshore. Operation and maintenance are more difficult, but construction (in a shipyard) may be relatively easy. Submerged WECs are even less accessible for maintenance, but they are less exposed to corrosion and to extreme wave forces. [Elliot;1981] [Carmichael et al.;1992]

3.3.2 Point absorbers, Attenuators and Terminators

Wave energy converters have also been classified (mainly by theoretical hydrodynamicists) according to their size and orientation. Devices which are very small compared to a typical wavelength, have been termed point absorbers. Since the power rating of a point absorber is typically a few hundred kilowatts, a large power plant would consist of many of such units, which are dispersed in a very long and relatively narrow array along the coast.

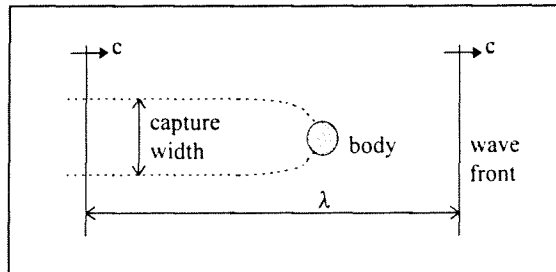


Figure 3.3 Capture width of a point absorber

Point absorbers can gather energy to itself from a width of the wave crests called the capture width. The maximum capture width occurs at resonance operation and is equal to:

$$\frac{\lambda}{2\pi} \quad \text{when the radiated wave field is axi-symmetric, as in the case with a heaving body}$$

$$\frac{\lambda}{\pi} \quad \text{when the radiated wave field is non-symmetric with respect to the incident wave crests, as in the case with a rolling or swaying body or a oscillating body in more than one direction simultaneously (see also Section 3.3.4 about heaving and pitching bodies)}$$

The derivation of the capture width is given in **Appendix B**.

The counterpart of point absorbers are elongated structures of a length which is comparable to or larger than one wavelength. A wide structure which is aligned perpendicular to the incident wave direction is defined as a terminator. It is not surprising that these types of devices are more fully understood than others at this stage of the development of wave energy conversion devices, since early experimental work has been done in narrow wave tanks and theoretical calculations have mostly been two-dimensional. In both cases, devices of infinite width are being simulated.

If converters are aligned parallel to the wave propagation, they are termed attenuators. The term came from the belief that energy could be progressively extracted along the length of the device, but later studies have shown that for optimal operation the rear element of such a device would have to extract as much energy as the front one. Theory indicates that the maximum capture efficiency of a terminator is somewhat less than that of an attenuator. [Count;1982] [Carmichael et al.;1992] [Evans;1982]

The different types of converters are shown schematically in Figure 3.4.

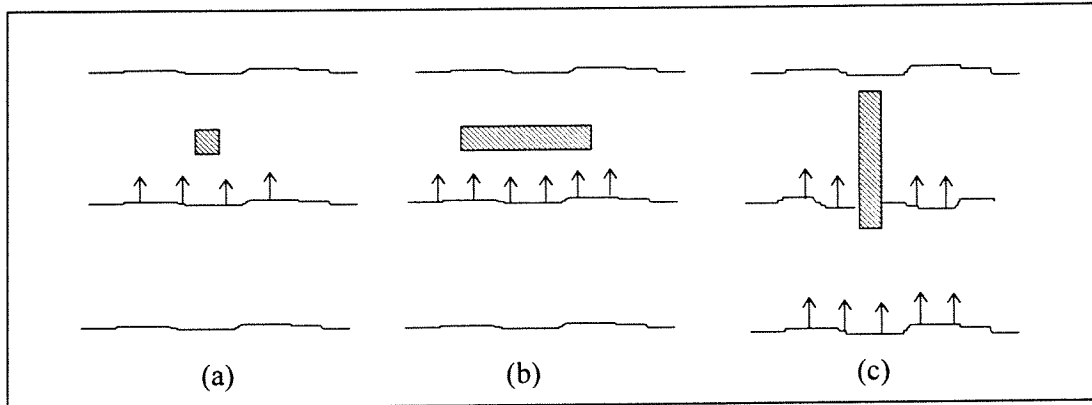


Figure 3.4 Top view of (a) point absorber; (b) terminator; (c) attenuator

3.3.3 Types of converted Energy or Energy Use

Types of converted energy

Various methods of wave energy conversion exist and there are different forms of the use of the converted energy. The primary conversion of wave energy into some other kind of energy may be of different types. In oscillating water column (OWC) devices, the energy is pneumatic. In other systems waves fill an elevated basin, which supplies potential energy to run a hydro-electric plant. Many proposed devices utilise relative motion between bodies, where hydraulic cylinders and hydraulic motors are used to transmit and convert energy.

Considering how wave energy manifests itself, the devices can be divided according to the method which they use to capture the wave energy. Wave energy can be obtained from:

1. Variations in surface profile (slope, height) of travelling deep water.

This category includes many proposals for floats, converting the energy of the motions between the float and the connected seabed, shore or a larger float. Other proposals utilise the relative motion of a column of water or the flow of air caused by the oscillating column in the structure.

2. Sub-surface pressure variations.

The fluctuation in pressure below the water surface can also be utilised in a number of ways. Oscillation of a water column inside a vertical tube could drive a turbine or the column displaces air to drive an air turbine. It is also possible to construct oscillating bodies below the water surface.

3. Sub-surface fluid particle motion.

The easiest way of using sub-surface motion of fluid particles, is to hinge a vertical flap about its lower edge and to convert the oscillating motion into energy. The low efficiencies inherent to this concept can be overcome by using asymmetric concepts with peak capture efficiencies close to 100% (at resonance frequency) for two-dimensional conditions or a peak capture width of λ/π for three dimensional conditions.

4. Uni-directional motion of fluid particles in a breaking wave (naturally or artificially induced).

For getting an uni-directional motion of the fluid, sloping ramps and converging channels are used. The motion of the fluid can be converted directly into electricity by a turbine or can be stored in the form of potential energy.

Types of energy use

Converted wave energy may be used for various purposes. It may be used in addition to electricity production for delivery to a grid or for local use, for desalination of sea water, for water pumping, for heating or cooling or for the propulsion of vessels.

3.3.4 The Nine Basic Types

It is also possible to distinguish nine basic types of converters, on which most conversion techniques are based [McCormick;1981]. The first five types have been suggested and patented in one form or another since the turn of the twentieth century. The last four are more advanced techniques, that have been proposed over the past few decades. The primary conversion of heaving and pitching devices can be represented by a floating body modelled as a simple spring-and-damper system. This is shown in **Appendix B** 'Theory of Oscillating Bodies', also some conclusions are given. The theory and the calculation of the capture efficiency of the other devices is given in **Appendix C** 'Theory of Several Converters'. This capture efficiency is important, because when it is too low, the device will not have much chance to become economically attractive.

1. Heaving and Pitching Bodies

Heaving and pitching bodies are the most common wave energy conversion devices. Three directions of motion of a floating (two-dimensional) body exist: (1) horizontal displacement, called sway or sometimes surge, (2) vertical displacement, called heave and (3) angular displacement, called roll or pitch. Several variations of devices are sketched in Figure 3.5. Although, these bodies are efficient when in resonance with a monochromatic wave, they are less efficient in off-design waves and in random seas. The ease of mooring (usually a single-point mooring) and the simplistic design make these bodies attractive from a cost point of view.

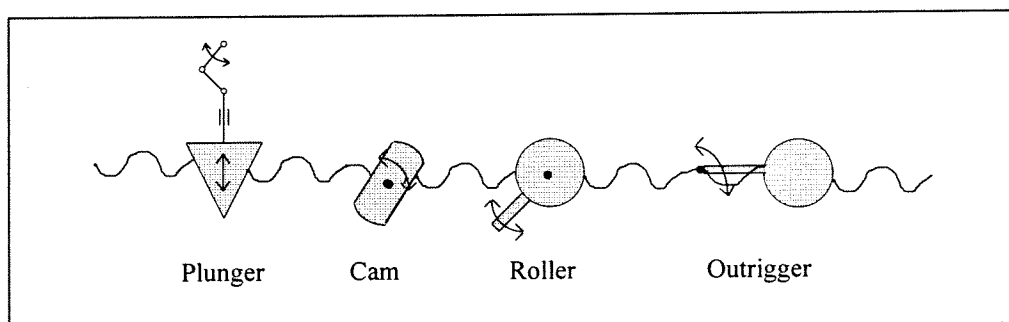


Figure 3.5 Several heaving and / or pitching schemes

2. Oscillating Water Column (OWC) Devices or Cavity Resonators

The concept is that an entrained water column will be excited into motion by wave action and will therefore act as a massive piston, pumping large volumes of air. The varying pressure can be used to drive a turbine. Masuda, a Japanese inventor, developed in the 1960-s wave-powered navigation buoys, which are used world-wide [Carmichael et al.;1992]. A well known turbine is the 'Wells self-rectifying turbine'. This one has the quality that its rotor is driven in the same direction whether air is forced through it from one side or the other.

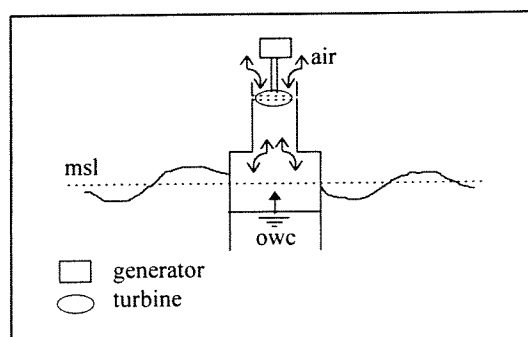


Figure 3.6 Oscillating water column device

Several different designs of devices, based on the oscillating water column concept, are possible. Efficiency reaches 50% for symmetric devices, up to 100% (at resonance) for devices with a reflecting vertical wall behind the air chamber.

3. Pressure Devices

The pressure beneath a wave is constantly varying because of the change in water level (affecting the hydrostatic pressure) and the motion of the water particles (affecting the dynamic pressure). Systems can consist of a flexible membrane responding to pressure changes caused by the passage of a wave

or of a moving piston. The wave power conversion is calculated at about 5% and because of the massive constructions involved in these systems the pressure devices are cost-ineffective.

Floating pressure device, like the Lancaster Flexible Bag seemed to have some promise. It worked like an attenuator, had however a modest efficiency and high structural costs, so in course of time it became unattractive [French et al.;1995].

4. Surging-Wave Energy Converters

On a very gradual beach, a shallow water swell will act as a surge over a moderate distance before plunging on the beach. There have been a number of suggested methods for capturing the energy of a wave just as it enters the surf zone. The wave power conversion for a idealised device is less than 8%. Consequently, the surging device operating in or near the surf zone is rather inefficient. In view of the high capital costs of such a device it is not a cost-effective system.

5. Particle Motion Converters

To convert the energy of the moving particles, the device should have motions that are approximately equal to those of the particles. A very popular idea is the water wheel, with an optimum design when the axis of rotation is just above the crest of the wave, see **Appendix C**. In this case, wave power is only converted when a crest passes or over one-half of the wave period. It can be assumed that this device is not cost-effective because of its low efficiency.

Another popular device is the bottom-mounted compliant flap sketched in Figure 3.7. It has a maximum theoretical capture efficiency of 50% at resonance, when the piston is optimally tuned. The flap in shallow water is more feasible since the horizontal motions of the water particles do not vary significantly from the free surface to the sea bed, see **Appendix A**. Furthermore the capital costs will be lower than in deep water. Unfortunately, the total wave energy is less than in deep water.

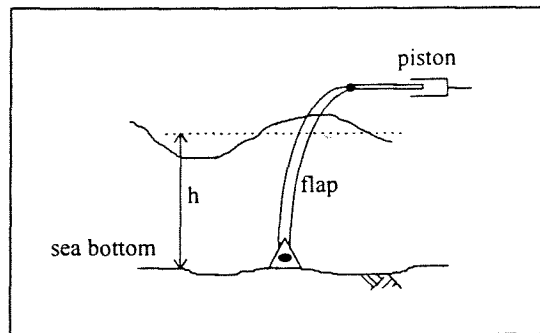


Figure 3.7 Compliant flap converter

6. Salter's Duck

The 'Salter's Duck' was the earliest of the high efficiency devices. It has a maximum theoretical capture efficiency of 90% and an experimental efficiency of 80% [Evans;1985]. The duck is an asymmetrically shaped device, that oscillates about a spine connecting many ducks. The ducks bob up and down at different moments as the waves hit them. The variation in timing helps to even out the strain on the spine. More recently, interest has centred on the case of a single duck, which acts more like a point absorber. A nodding duck converts both the kinetic and potential energies of the wave into rotational mechanical energy. The rotational motion is then converted into electrical energy by a hydraulic-electric subsystem.

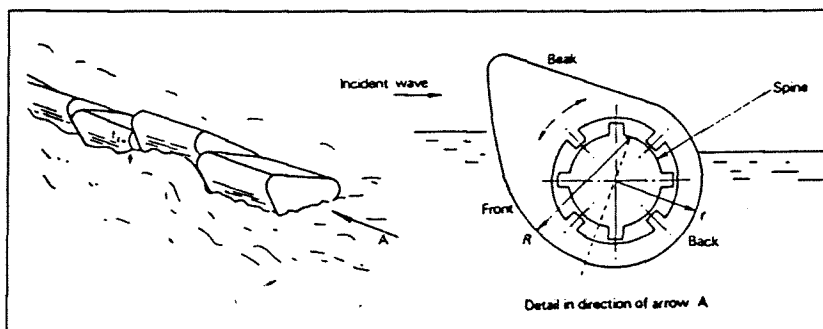


Figure 3.8 Salter's Duck - original concept

7. Cockerell's Rafts

The principle of this device is using wave contouring rafts. These rafts are hinged together and an energy conversion subsystem (usually hydraulic) is located at each hinge. This energy conversion depends on the relative angular motions of raft pairs. Within a short period of time after his original idea, Cockerell redesigned his contouring rafts to include varying raft lengths. The three-raft system appears to be the most cost effective. However, there are two major problems. The physical size is excessive and the mooring is difficult.

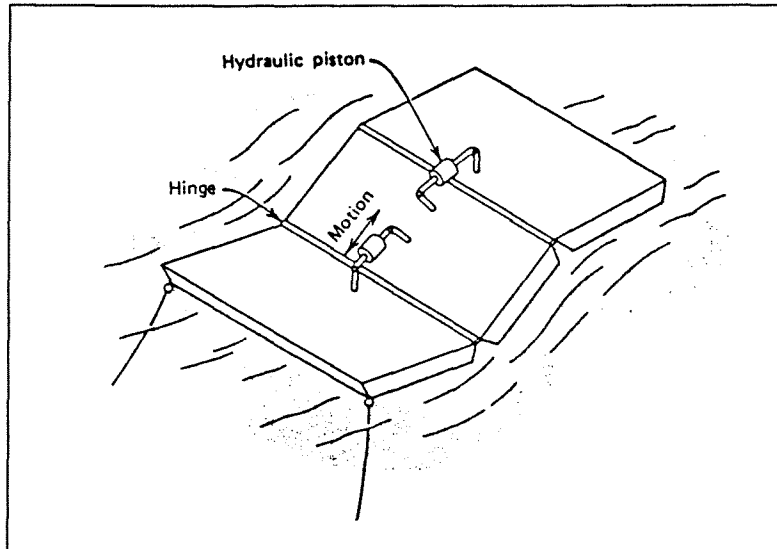


Figure 3.9 Wave contouring raft system

8. Russell's Rectifier

The Russell's or H.R.S. Rectifier has been initiated at the Hydraulics Research Station by R.C.H. Russell in 1975. It is a large rectangular hollow caisson with a series of narrow inlet and outlet compartments. The front faces of the inlet compartments are fitted with non-return flap valves, allowing water entry under the pressure of wave crests, whilst the outlet compartments have flap valves which open to allow discharge into a wave trough. Water flows from the higher level of the inlet compartment through a Kaplan low head turbine into the outflow compartments.

The condition for maximum capture efficiency of operation exists when the length (perpendicular to the wave crests) of the structure approximates to one fifth of the wave length. This maximum efficiency reaches about 20 %, as shown in **Appendix C**. The units would be operated in a water depth of about 15 m and would be faced with a ramp from the sea bed to a level 5 m up the front face, to prevent the intrusion of sediment.

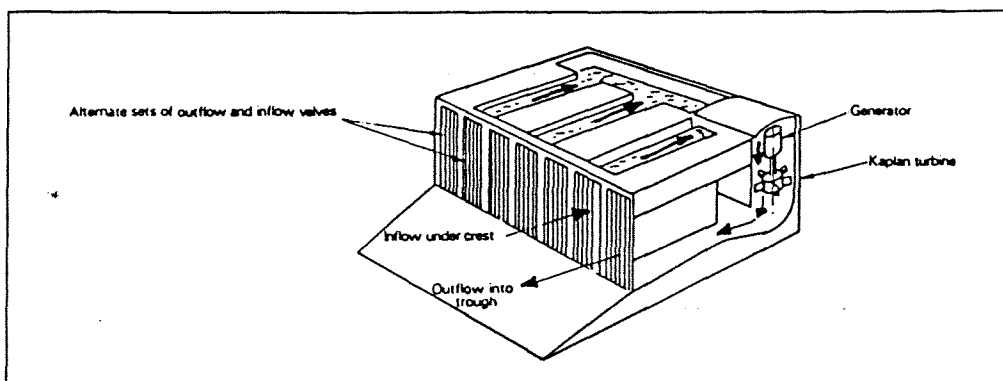


Figure 3.10 Russell's Rectifier

9. Wave Focusing Techniques

With the realisation that it is impractical to have large sections of coastal waters occupied by wave energy converters, engineers began to seek methods of focusing wave power on conversion devices occupying relatively small regions. Their efforts have resulted in three promising techniques: (1) point absorbing, mentioned in Section 3.3.2, (2) 'island' focusing, caused by refraction over the slopes of an artificial 'atoll' and (3) 'lens' focusing due to refraction over a lens-shaped submerged platform. See for the last two techniques the next figure.

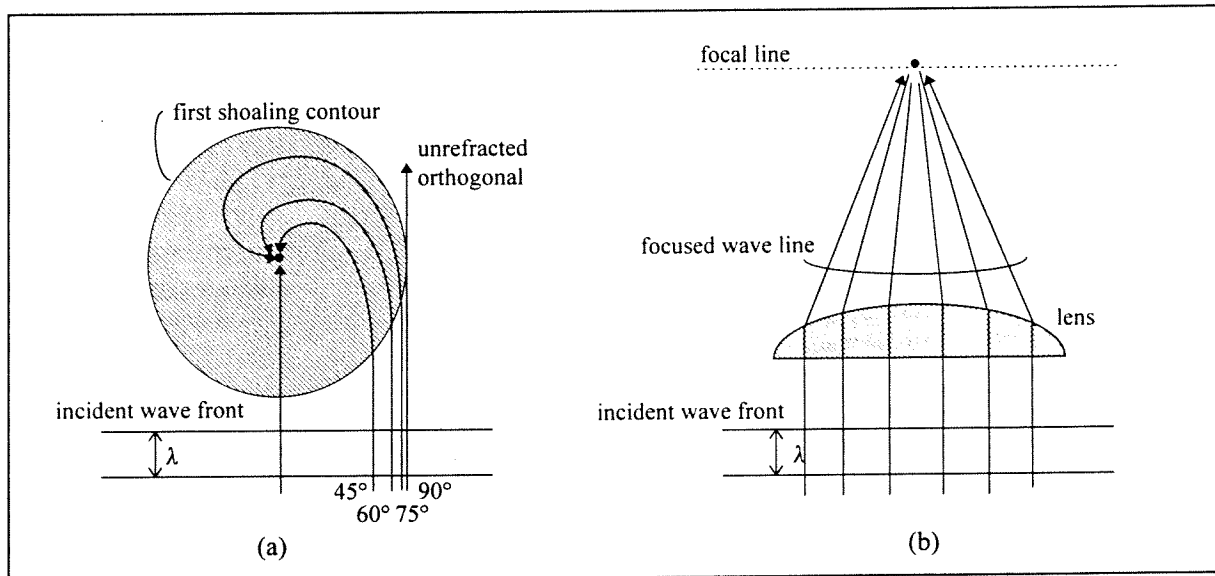


Figure 3.11 Wave focusing techniques: (a) island focusing; (b) lens focusing

3.4 Research Activity around the World

Quite some countries are involved in wave energy conversion development. There is and has been significant research in the United Kingdom, Norway and Japan. In fact Japan is arguably the most active country in wave energy at the present time. The activities of some of these countries are described below. The used literature is given in the last section.

Japan

The wave climate around Japan is considerably different from that of the North Atlantic. As well as being rather seasonal the annual average wave power in the sea of Japan and in the Pacific is generally of the order of 10 kW/m. The maximum electricity demand occurs in summer due to the air conditioning load. [Duckers;1991]

Probably, the most famous energy device in the world is the 'Kamei'. This floating vessel has a length of 80 m and a number of oscillating water columns are installed. Research was started in 1976 and continued until 1981. [Funakoshi et al.;1993] [Simeons;1980]

Some shore mounted devices, based on the principle of an oscillating water column have been constructed (Sanze) and some others were constructed in front of a breakwater (Neya port, Niigata). [Duckers;1989]

Recently an OWC type wave power extracting caisson breakwater has been developed. The caisson incorporates a hollow box air chamber of which the front wall has some gaps to allow entry of water, see Figure 3.12. By absorbing wave energy and thus

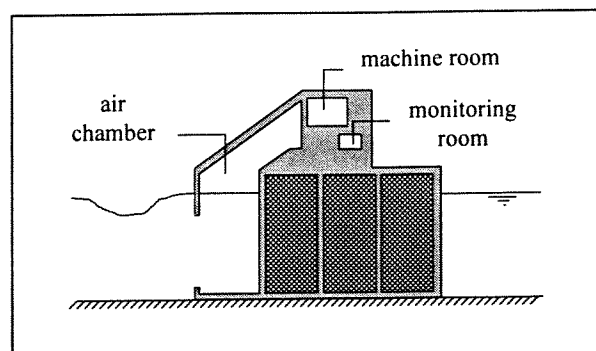


Figure 3.12 Shape of the caisson breakwater

producing electricity, the caisson has low reflection characteristics. Field trials started in 1989 in Sakata Port. [Funakoshi et al.;1993] [Nakada et al.;1992] [Takahashi et al.;1992]

Some other techniques are also used. The 'Pendulor' is a pendulum gate which swings backwards and forwards in the front of a chamber. The back of the chamber is a fixed wall, located at a quarter wavelength (of the corresponding mean wave period) behind the axis of the pendulum pivot. A 5 kW system has been in operation in the bay of Uchiura near to Muroran [Watabe et al.;1986].

A somewhat similar device called 'Flap', differs from the 'Pendulor' in that the hinge axis is submerged at the bottom of the flap.

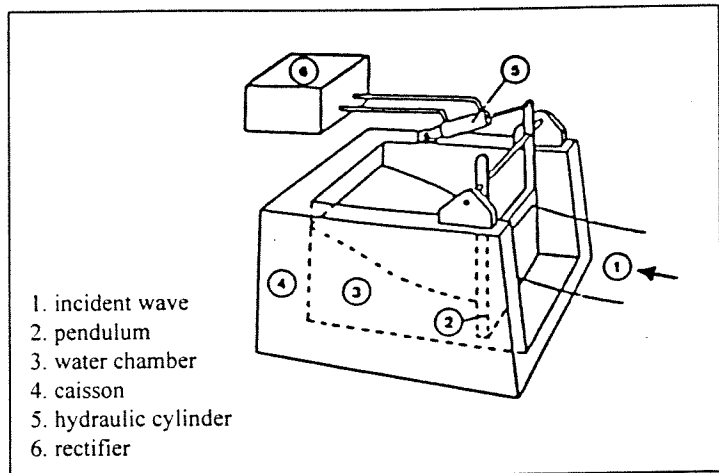


Figure 3.13 Pendulor

[Duckers; 1989, 1991] [Funakoshi et al.; 1993] [Hagerman; 1992]

Experiments are going on with wave pumping systems. These systems pump sea water into an upper reservoir as a storage of potential energy [Funakoshi et al.; 1993].

China

The density of wave power on the coastline is small and the mean density is only 3 kW/m. The wave energy along the coasts of islands is larger than along the coast of the mainland. Since 1980, more than ten institutions have begun to study electricity generation by wave energy. The work concentrates on navigation buoys and developing wave energy on the islands .

India

The average wave power density along the Indian coast is only 5 to 10 kW/m. A sea trial of a 150 kW multiresonant OWC device (see also Norway), placed into a breakwater, has been started at the Trivandrum coast. Probably, the costs are shared between the breakwater and the energy conversion system. This device is expected to deliver an average of 75 kW from April to November and 25 kW from December to March. However, many more harbours are planned on the Indian coastline and the potential application of wave energy breakwaters will therefore be considerable. [Duckers;1991] [Neelamani et al.;1995]

United Kingdom

From 1975, quite some research has been done in the United Kingdom. The first two designed devices were the 'Salter's Duck' and 'Cockerell's Raft', followed by the 'Russell's Rectifier' and the NEL Oscillating Water Column Wave Energy Converter (NEL stands for National Engineering Laboratory) [Grove-Palmer;1982]. This last device consists of a partially submerged hollow structure, which is open to the sea below the water line as shown in Figure 3.15. Later the 'Lancaster Flexible Bag' that works as a attenuator and the 'Bristol Cylinder' were suggested. This last device is a submerged circular cylinder which rotates around its longitudinal axis.

At the moment, attention is paid to the circular CLAM wave energy converter, a floating device consisting of interconnected air cells with rectangular flexible membranes [Lockett;1991] and to the sea bed mounted NEL Breakwater OWC [Hunter;1991] [Moody et al.1982].

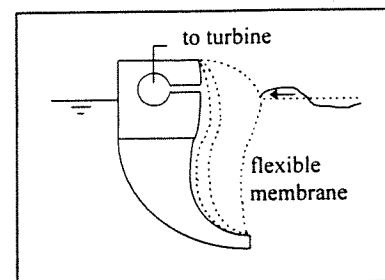


Figure 3.14 CLAM device

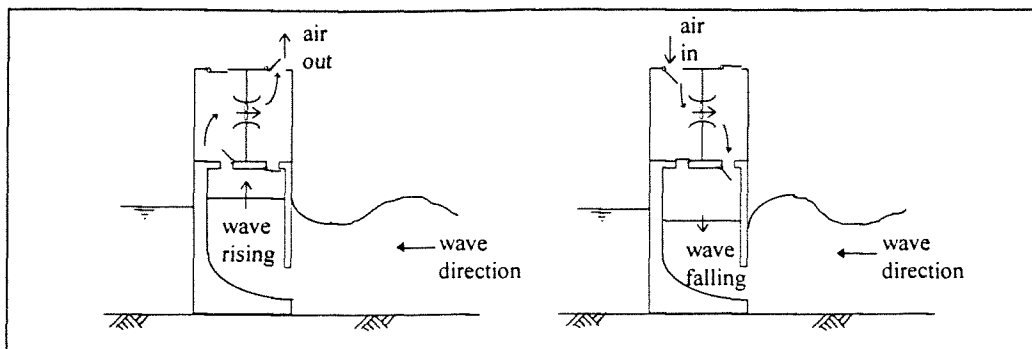


Figure 3.15 The initially principle of the NEL Breakwater: Uni-directional air flow drives a turbine

Ireland

The West coast of Ireland is particularly suitable for the development of both shore mounted and offshore wave energy converters. Research in Ireland has concentrated on OWCs and self rectifying air turbines as alternatives to the Wells turbine. The Queens University of Belfast has supervised the construction of the shore mounted OWC device of the Isle of Islay. The power generation of this system with an installed capacity of 75 kW has been started in 1991. [Carmichael et al.;1992] [Curran et al.;1995]

United States

The U.S. developments of wave energy have mainly been funded from private sources, with some funding of the government. The Sea Energy Corporation configured the Articulated-Raft, which is similar to the British Cockerell's raft [Burdette et al.;1986] Also experimental and theoretical studies of rigid flap devices have been done. The Q Corporation developed the Tandem Flap device. The experiments have demonstrated good performance in regular waves [Scher;1985]. The 'island' focusing method has been used for the Dam-Atol device [McCormick;1981].

Denmark

There has been a research effort in Denmark based upon a tethered buoy system. The large floating buoy responds to wave activity by pulling a piston in a sea bed unit. This piston pumps water through a submerged turbine. An array of these buoys could be deployed and arranged to have an integrated and hence smoothed, output. [Hagerman;1992]

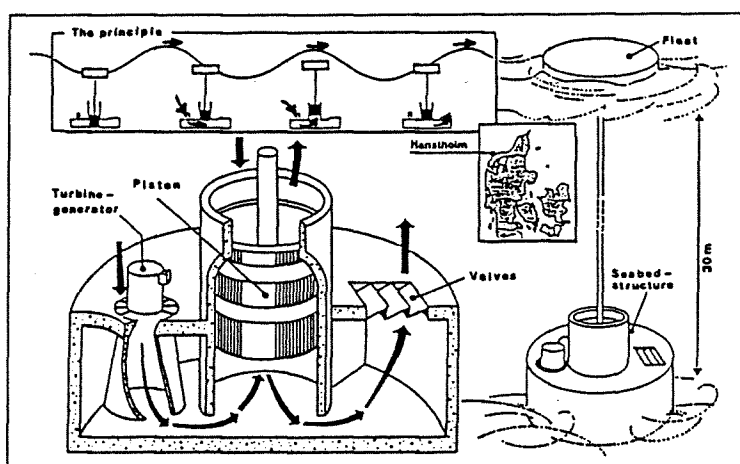


Figure 3.16 Danish heaving buoy system

Norway

In Norway two types of devices have been developed. The 'TAPCHAN', a tapered channel device at the coast has operated since 1986. As the waves run up the narrowing and rising channel they increase in height but reduce in width and spill into a lagoon a few metres above the sea level. Energy is extracted by a low head Kaplan water turbine. [Hagerman;1992] [Mehlum;1985]

An other device is the 'Multi Resonant Oscillating Water Column' (MOWC) using a 'resonant harbour' in front of the air chamber. This device, has a better efficiency than devices with a single resonance frequency. A field experiment started in 1985 at the coast of Bergen, with a 500 kW device installed in a steep cliff, but it was destroyed in January 1989. [Ambli et al.;1982] [Hagerman; 1992]

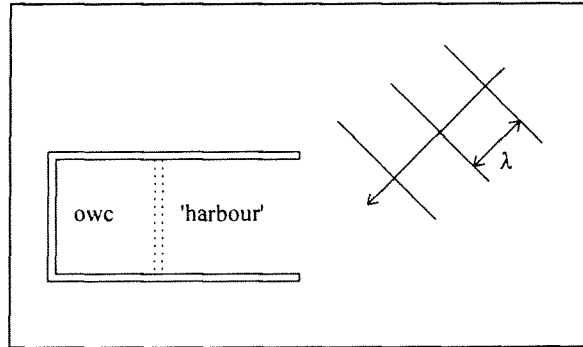


Figure 3.17 Topview of the 'harbour' type OWC

Sweden

In Sweden the 'Götaverken's Hose Pump' was investigated. This is a similar concept to the Danish buoys, but using reinforced rubber hose as the tether and pumping mechanism. [Berggren;1992] The research appears to have ceased due to lack of funding.

The Netherlands

Until the nineties, little research in wave energy conversion has been carried out in the Netherlands. This because of the unfavourable wave conditions for energy conversion at the coast of the North Sea. In 1993 a new principle was patented: 'The Archimedes Wave Swing'. Two or more vessels are placed under the sea level upside down and the air compartments are connected by a tube. The amount of air in the vessel is influenced by the water pressure at the water surface in the vessel. The air in the several vessels forms a constant pressure system. The water level in the vessel will rise if the water pressure will become higher than the air pressure. Since the water pressure is affected by the variation of the waves, it will change as a function of these waves.

As the amount of air in the vessel is varying, the buoyancy will vary. If the vessels are balanced to neutral buoyancy at mean sea level, a vessel will want to float if the underwater pressure decreases and it wants to sink if the underwater pressure increases. These motions are shown in Figure 3.18. The vertical oscillation of the vessels is converted into a rotating movement and from that into electrical energy. [Jongeneel;1996] [Hekking;1996] [Vriesema;1995]

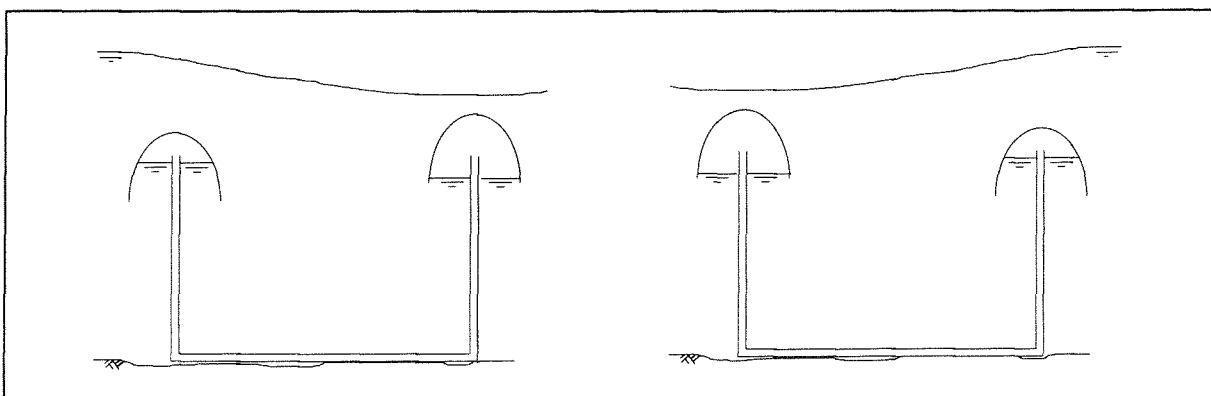


Figure 3.18 Principle of a two module Archimedes Wave Swing

The waves which are used are swell waves, which are generated by the wind far away from the system. These waves have a relatively large wavelength (some hundred metres) and are much more commonly present than wind waves. The estimated electricity costs range from 0.09 to 0.15 Hfl/kWh. Portugal seems to be good location for installing these devices, because of good wave conditions and a retail price of electricity, generated by renewable sources of Hfl 0.13 per kWh. When the costs will be about Hfl 0.10 per kWh, then the Archimedes Wave Swing will be cost-effective.

Portugal

A 300 kW OWC is planned for the island of Pico, part of the Azores in the North Atlantic. This will be located at the sea bottom, close to the rocky shoreline. A Wells air turbine will be incorporated into the column. Future developments might include air chamber flow latching and variable pitch turbine blades in order to improve overall performance. [Carmichael;1992] Recently, there have been contacts with the Netherlands about the possibilities of the 'Archimedes Wave Swing' at the coast of Portugal.

South Africa

The South African coast enjoys wind systems in two directions. The east coast has a rather constant wave power of about 10 kW/m near the shore. The west coast shows a seasonal variation and values are considerably higher than that of the east coast. The research concentrates on a device which works like a piston that compresses air into a chamber, from which it is expanded through a turbine. [Simeons;1980]

3.5 Evaluation of Wave Energy Converters

After describing many types of devices and the research activity around the world, the advantages and disadvantages of wave energy converters can become clear. A device must be constructive feasible and durable. Besides, a wave energy converter must be economically attractive, thus the investment costs must be low and the conversion efficiency has to be high.

The main problem with energy converters is that a device has to resist the most severe storm during its life time and that the energy conversion takes place during average wave conditions. Consequently, structural considerations and subjects which influence the performance of energy conversion are important for the evaluation. [Leishman et al.;1976] Also maintenance criteria can be used. [Taylor;1981,1982]

3.5.1 Evaluation Criteria

The devices can be evaluated on the following criteria:

Results of research and experiments

An important consideration is whether somewhere in the world a device has been designed and a scaled model or prototype has been tested. Reliable results can be used to select a converter or to improve it. Specific results of a particular device can also be used for the following criteria.

Capture efficiency

Wave energy impinging on a converter can be reflected, absorbed (captured) and transmitted. The capture efficiency and subsequent phases of the conversion should be as high as possible. From the theory of wave energy conversion and from experiments, the capture efficiency of many converters is known and can be used as a first criteria to determine whether a device is suitable or not.

Number of intermediate stages between wave energy and electrical output

It may be that a large number of intermediate stages of energy is required, to match the random nature of the waves to a smooth electrical output. However, a large number of stages implies higher losses and a larger number of components, which all can give rise to failure and require maintenance. Consequently, the number of intermediate stages of energy must be small.

Sensitivity of electrical output to wave height

The wave energy is proportional to the square of the wave height. The influence of the wave height on the captured energy has to be checked.

Sensitivity of electrical output to wave length

Most energy converters have a maximum efficiency for a particular wave length (resonance frequency). Because real waves have a spectrum of wave lengths, it is important that the converter has a broad bandwidth of the efficiency curve, so that also waves with an other length can be converted with a reasonable efficiency. Multi resonant devices, like the 'harbour' type OWC devices of Norway have been developed. The best converter should be tuneable to every wave length, however, so far this has been impossible.

Difficulty of achieving tidal compensation

A floating converter without a connection to the seabed and converters which make use of sub-surface pressure variations, will have hardy problems with the tidal variation. The largest difficulty is expected with shore and sea bed based structures, which are surface piercing and make use of the variations in surface profile.

Possibility of wave energy conversion of waves from more than one direction simultaneously

Waves may be arriving from more than one direction. Converters, that are axi-symmetric about the vertical axis, can extract energy from whatever direction waves are coming. Terminator type converters operate mainly by normally incident waves. Energy of waves in the sector 90° either side of this direction can still be converted, but with decreasing efficiency as the angle approaches 90° .

Possibility of realigning the structure to suit principal wave direction

The principal wave direction can change over the year. Floating structures can, if necessary, be rotated, though this gives difficulties with the moorings. Fixed structures cannot be rotated, but maybe an other adjustment is possible. Close to the shore, most waves are normally incident to the shore, because of refraction by the bottom contours.

Construction complexity

The complexity of construction of a device has to be low. This means that the construction of several components of the device and their assembly must be low. The development of special tools has to be avoided, because of the accompanying high costs. The employment of existing construction facilities and expertise has to be preferred.

When a converter will be constructed in-situ, also the location is of influence on the construction complexity. In severe wave conditions and hardly accessible locations, it is difficult to construct a converter.

Difficulty of transportation of the structure or of building material

When converters are not constructed in-situ, but for instance in a shipyard, the construction has to be transported. In most cases this transport is possible, however some floating structures will have better towing characteristics than others.

When systems are constructed in-situ, the towing characteristics of the structure are not of influence, but the transport of building-materials between the supply site and the construction site .

Complexity of maintenance and repair

The level of maintenance and repair depends on the type of device and the quality of the used components. The quality of the components is related to the investment costs and to the loading by severe waves. When maintenance and repair are needed, it is important whether the converter is easily accessible.

The maintenance and repair of offshore floating structures is more difficult than of shore or sea bed based systems. Submerged converters are even less accessible for maintenance and repair, but they are less exposed to corrosion and extreme wave forces. In general, it has to be possible to replace major components or to repair them at the operating site.

Likelihood of damage to the system in severe sea conditions (with or without electricity generation)

Submerged types of energy converters are protected from severe sea conditions. Floating converters can have problems with the moorings, surface piercing structures based on the sea bed or shore must be able to endure storm conditions. The energy conversion of the device during storm conditions may be suited to the circumstances or stopped for a period.

Linkage complexity

The mechanical links in a converter are in general the weakest parts of the device. The number of mechanical links within the converter and the complexity of these links should be minimised.

Degree of stress concentration in principal components

Concentrations of stress should be avoided wherever possible.

Extent of exposure of components to sea water

The structure, in particular moving parts, must be prevented from or not vulnerable to corrosion by sea water and fouling by marine flora and fauna.

Extent of hazard presented to navigation, fishing, environment, etc.

The consequences of an energy converter for several topics must be determined.

Likelihood of adverse criticism on credibility and aesthetic considerations

Even if a scheme is technically and economically feasible it may still appear ridiculous in both the public and professional eye, so the design and the operation of a wave energy converter must have as much credibility as possible. Aesthetic and credibility criteria are very closely connected being expressed in the adage 'if it looks right it is right'. For instance, a converter with many external moving parts may be considered as unsightly.

3.5.2 Results of the Evaluation

From the classification of converters into point absorbers, terminators and attenuators (Section 3.3.2), it becomes clear that the point absorber has a fundamental advantage in economy, because it can capture energy of incident waves over a longer distance than its own width. To compete with a point absorber, any terminator needs some substantial compensating advantage. [French et al.;1995]

Apart from wave-powered navigation buoys and the Japanese vessel 'Kamei', most of the constructed prototypes so far have been placed at or near the shore. Consequently, the working of sea bed based devices is much better investigated and tested. An advantage with such systems is that operation and maintenance are relatively easy. But, drawbacks are lower wave power than offshore and the difficult civil engineering work on a wave-exposed shore. Moreover, all types of floating devices in the ocean present problems with moorings and energy transmission to the mainland.

The commercial export of offshore systems is expected to lag behind that of land- and- caisson based systems. Significant improvement in cost and performance will not occur until a floating device is successfully operated at full scale for a period of years. Commercial sales will not occur without a demonstration and without sales, the developers will not have the financial sources or operating experience, necessary to make significant improvements.[Hagerman;1992]

Many workable types of converters have been suggested, but the economics of most are unfavourable, mainly because the construction is large compared to the converted energy quantity. Practical problems of many devices are the moving parts for conversion of the wave energy into mechanical energy. These parts are sensitive to damage in severe sea conditions.

In Table 3.1, the different types of devices are given with some information and the main considerations on which the prospects are based.

Table 3.1 Several devices and their prospects

Type of device	Practical considerations	Interested countries	Devices	Theoretical efficiency	Prospect
Heaving, pitching body	- sensitive to particular wave lengths - sensitive to damage	several countries	- in general floating devices	++	low
OWC	- no moving parts, except the air turbine - good performance - well investigated - high credibility - combination with a breakwater possible	Japan	- breakwater mounted experiments (Sakata et al.) - shore mounted (Sanze)	+++ +++	good moderate
		Norway	- Multi-resonant KVaerner device (Bergen)	++++	good
		UK	- NEL Breakwater - shore mounted (Isle of Islay)	+++ +++	good
		India	- Breakwaters (Trivandrum)	+++	good
Pressure device	- in general using a flexible membrane and air turbine - when below water level, not attacked by severe waves	- UK	- bottom mounted - Lancaster Flexible Bag - CLAM device	- ++ ++	low abandoned investigating, probably good
		NL	- Archimedes Wave Swing	+++	investigating, probably good
Surging wave device		-	- see Figure C.1	--	none
Particle motion converter	- rather sensitive to damage (moving parts) - simple design - combination of Pendolor with a breakwater possible	Japan	- Pendolor (prototype tested)	++	moderate
		US	- Tandem Flap	++	low
Salter's Duck	- sensitive to damage, - complex hydraulic system	UK	- original concept - Solo Duck	++ +++	abandoned investigating
Russell's Rectifier	- large structure - combination with a breakwater possible	UK		-	abandoned
Raft	- sensitive to damage - large structure	UK	- Cockerell's Raft	++	abandoned?
		US	- Articulated-Raft	++	abandoned?
Point Absorbing	- small structures - not sensitive to wave direction	Norway	- Multi-resonant Kvaerner device (shore mounted)	++++	moderate
		UK	- new NEL Breakwater	++++	good
		Denmark	- Heaving Buoy	++++	investigating
		Sweden	- Hose pump	++++	investigating
'island focusing'	- large structures	USA	- Dam-Atoll	+	abandoned?
'lens focusing'	- large structures	Japan	- investigating	?	low
Tapchan	- using large area - using potential energy - not possible with a large tidal variation	Norway	- 350 kW plant Toftestallen - designs for Indonesia and Tasmania	++	good

Most attention (Japan, United Kingdom, India and Norway) at the present is paid to the oscillating water column devices. This fact shows the confidence, investors have in this type of converter. It has no moving parts and a good performance, namely a high capture efficiency with a reasonable broad bandwidth for different wave lengths.

It can be concluded that, when a wave energy converter is only used to produce electricity it has to be a point absorber. Several heaving buoy systems and the circular CLAM are still investigated for this purpose. These devices will be installed offshore, in areas with large wave power.

The other useful device is the shore based TAPCHAN, which is easy to construct and can survive severe storms (prototype in Toftestallen, Norway). [Hagerman;1992]

When a converter can be combined with other benefits, a terminator has the best prospects. [French et al.;1995] Converters which are still in research and have been tested are the Japanese wave energy extracting breakwaters operated by OWCs, the 'Pendulor' device and the NEL Breakwater.

3.6 Wave Energy Conversion in Combination with a Breakwater

As mentioned, because of the high initial capital costs of wave energy converters it is attractive to combine the energy conversion with other benefits. Since ordinary caissons reflect most wave energy, there is the possibility of a distinct low-energy 'shadow' developing behind them. Caissons are ideal candidates for combining wave energy conversion with breakwater protection at coastal harbours. Even in remote coastal areas, an occasional wave energy breakwater might be acceptable for creating a harbour of refuge for small craft in the event of sudden storms, medical emergencies or engine problems. An other purpose can be sheltered water for sea farming.

The costs and performance projections of wave energy converting breakwaters are very site-specific. The costs are influenced by the need for sea bed foundation levelling, by the availability of suitable rock for a rubble mound on which the caissons would rest, as well as by the local availability of aggregate material when cast-in-situ concrete construction is used. The sheltering effect of coastal features, such as headlands and peninsulas and the effects of wave refraction and shoaling are large near the shore. Consequently, the part of deep water wave power which can be converted by the breakwater is highly dependent on the exact coastal location of it.

In the past, some energy breakwaters have been suggested and are still investigated. The design of the NEL OWC Breakwater started in 1976 in the United Kingdom. In Japan in 1989, a test breakwater was constructed in Sakata Port, also based on the principle of oscillating water and an other breakwater of 1.5 MW, based on the 'Pendulor' has been designed (these devices are briefly described in Section 3.4). By functioning both as a breakwater and energy converter, the Japanese believe that the system is cost effective. These systems will be further developed, when the results of the prototype at Sakata Port are firmly established. The Japanese caisson-based systems are expected to enter the market within some years. However, the method of exploiting the converted electricity has to be studied. [Funakoshi et al.1993] [Hagerman;1992]

Under this scenario, wave power conversion development in industrial countries will be largely limited to caisson-based systems, deployed as breakwaters at locations where their environmental impact is consistent with the existing level of onshore harbour development. These breakwaters would be designed primarily for harbour protection. Simultaneously, they are functioning as pilot plants for various offshore wave energy systems, for the purpose of long-term endurance testing. Therefore, energy converting breakwaters are an important stepping stone in the commercialisation of wave power conversion [Hagerman;1992]. In many places throughout the world, where much smaller quantities of wave power are required than in the industrial countries, like small islands in the southern pacific, these energy converting breakwaters could be usefully employed.

3.7 Conclusions

With the help of the 'linear wave theory' the energy of waves can be calculated. This energy consists of potential and kinetic energy. The transfer of it from point to point in the direction of the wave is called 'wave power'. For a quite some places around the world this wave power is estimated. In the North Atlantic 50 kW per metre is typical, whereas around Japan 10 kW per metre is more usual.

The wave energy can be captured by a floating or fixed structure. Any technique that can effectively create waves can also be used to convert wave energy. It can be concluded that energy can be produced by an oscillating body or may be generated by an oscillating water column (OWC) which drives air through a turbine.

Wave energy converters (WECs) can be described in terms of their location, theoretical considerations and general arrangement or energy use. It is also possible to distinguish basically nine types of converters. Four of them are more advanced techniques, the other types have been suggested in one form or another.

More than ten countries are involved in wave energy development. In fact Japan is at present, arguably the most active country in wave energy research. In the United Kingdom a considerable number of converters have been designed and tested (mostly scaled models). Also the Scandinavian countries have developed some devices. The prototypes so far tested have been placed mostly at or near the shore. The most important progress has been made in the oscillating water column devices and the TAPCHAN.

When wave energy converters are classified according to their size and orientation, three types exist. Devices which are very small compared to a typical wavelength, have been termed point absorbers. A wide structure which is aligned perpendicular to the incident wave direction is defined as a terminator. If converters are aligned parallel to the wave propagation, they are termed attenuators. These types of converters are shown schematically in Figure 3.4.

A point absorber has a fundamental advantage in economy, because it can capture more energy than that of the incident waves with a width equal to its own width. To compete with a point absorber, any terminator needs some substantial compensating advantage. Consequently, when a wave energy converter is only used to produce electricity it has to be a point absorber. Several heaving buoy systems and the circular CLAM are still investigated for this purpose. The other useful device is the shore based TAPCHAN, which is easy to construct and can survive severe storms (prototype in Toftestallen, Norway).

Because of the high initial capital costs of wave energy converters, it is attractive to combine the energy extracting with other benefits. When a converter can be combined with other benefits a terminator has the best prospects. Converters which are still in research and have been tested are the Japanese wave energy extracting breakwaters operated by OWCs, the 'Pendolor' and the NEL breakwater.

Caissons are ideal candidates for combining wave energy conversion with breakwater protection at coastal harbours. An other purpose can be sheltered water for sea farming. Several energy converting breakwaters have been suggested (NEL Breakwater) and are still investigated (breakwaters in India and Japan). By functioning both as a breakwater and an energy converter, the system can be cost effective.

Wave power development in the foreseeable future, in industrial countries, will be largely limited to caisson-based systems deployed as breakwaters. These breakwaters would be designed primarily for harbour protection. Simultaneously, they will be functioning as pilot plants for various offshore wave energy systems. In many places throughout the world, where the electricity demand is much lower than in the industrial countries, these wave power converting breakwaters could be usefully employed.

It is for these reasons that in the continuation of this study, the possibilities and the design of a sea bed based (not floating) wave power converting breakwater will be investigated.

3.8 References and Literature

References

- Ambli, N.; Bønke, K.(1982); Malmo, O.; *The Kværner multiresonant OWC*; Proceedings of The 2nd International Symposium on Wave Energy Utilization, The Norwegian Institute of Technology, Trondheim, Norway
- Atlas of the Oceans* (1983); The Times Atlas, Couper A.D. Times Books Limited, London
- Berggren, L.(1992); *Energy take-out from a wave energy device, A theoretical study of the hydrodynamics of a two-body problem consisting of a buoy and a submerged plate*; Department of Hydraulics, Chalmers University of Technology, Göteborg, Sweden
- Brin, A.(1979); *Energy and the Oceans*; Deputy for Industrial Matters, Mission Interministrelle de la Mer
- Burdette, E.L., Gordon, C.K.(1986); *Available Ocean Wave Power and Prediction of Power extracted by a Wave Contouring Raft Conversion System*; Proceedings of ASME, Offshore Mechanics Arctic Engineering Symposium, Tokyo
- Carmichael, A.D., Falnes, J.(1992); *State of the Art in Wave Power Recovery*; Ocean Energy Recovery, The state of the Art; Scripps Institution of Oceanography, University of California at San Diego; Offshore Technology Research Center, Texas A&M University, USA
- Count, B.M.(1979); *Wave power - A problem searching for a solution*; Power from Sea Waves, Conference on Power from Sea Waves, University of Edinburgh, England
- Count, B.M.(1982); *On the hydrodynamic characteristics of wave energy absorption*; Proceedings of The 2nd International Symposium on Wave Energy Utilization, The Norwegian Institute of Technology, Trondheim, Norway
- Curran, R., Raghunathan, R.S., Stewart, T.P., Whittaker, T.J.T.(1995); *Matching a Wells Turbine to the Islay Oscillating Water Column Wave Power Converter*; Proc. of the 14th Int. Conf. On Offshore Mechanics and Arctic Engineering, Copenhagen, Denmark, Vol. I-A, pp. 147-154
- Duckers, L.J.(1989); *Wave Energy Devices*; The Solar Energy Society Conference Proceedings, England
- Duckers, L.(1991); *Wave energy research and development around the world*; Wave Energy, IMechE, Institution of Mechanical Engineers, Seminar, England
- Elliot, G., Roxburgh, G.(1981); *Wave energy studies at the UK National Engineering Laboratory*; Second Int. Symposium on Wave and Tidal Energy, BHRA, Cambridge, England
- Evans, D.V.(1982); *A comparison of the relative hydrodynamic efficiencies of the attenuator and terminator wave energy devices*; Proceedings of The 2nd International Symposium on Wave Energy Utilization, The Norwegian Institute of Technology, Trondheim, Norway
- Evans, D.V.(1985); *The Hydrodynamic Efficiency of Wave-Energy Devices*; Hydrodynamics of Ocean Wave-Energy Utilization, Symposium Lisbon, Portugal
- French, M., Bracewell, R.(1995); *The Systematic Design of Economic Wave Energy Converters*; The Fifth International Offshore and Polar Engineering Conference, The Hague, June 1995
- Funakoshi, H., Ohno, M., Takahashi, S., Oikawa, K.(1993); *Present Situation of Wave Energy Conversion Systems*; Civil Engineering in Japan, Vol.32, pp. 108-134
- Grove-Palmer, C.(1982); *Wave energy in the United Kingdom- A review of the programme June 1975-March 1982*; Proceedings of The 2nd International Symposium on Wave Energy Utilization, The Norwegian Institute of Technology, Trondheim, Norway

-
- Hagerman, G.(1992); *Economics of Wave Power*; Ocean Energy Recovery, The state of the Art; Scripps Institution of Oceanography, University of California at San Diego; Offshore Technology Research Center, Texas A&M University, USA
- Hekking, H.D. (13-1-1996); *Archimedes Waterschommel haalt stroom uit de golven (Dutch)*; Nieuwe Noord-Hollandse Courant, the Netherlands
- Hunter, R.(1991); *Future possibilities for the NEL Oscillating Water Column wave energy converter*; Wave Energy, IMechE, Institution of Mechanical Engineers, Seminar, England
- Jongeneel, C. (17-1-1996); *Waterschommel haalt energie uit deining (in Dutch)*; *Waterschommel is een vliegwiél van 1000 ton (in Dutch)*; Technisch Weekblad, The Netherlands
- Leishman, J.M., Scobie G.(1976); *The Development of Wave Power, a Techno-Economic Study*; Department of Industry, NEL, Scotland
- Lockett, F.P.(1991); *The CLAM wave energy converter*; Wave Energy, IMechE, Institution of Mechanical Engineers, Seminar, England
- McCormick, M.E.(1981); *Ocean Wave Energy Conversion*; U.S. Naval Academy, Annapolis, Maryland, Willey-Interscience Publication, USA
- Mehlum, E.(1985); *Tapchan*; Hydrodynamics of Ocean Wave-Energy Utilization, Iutam Symposium Lisbon, Portugal
- Moody, G.W., Elliot, G.(1982); *The development of the NEL Breakwater wave energy converter*; Proceedings of The 2nd International Symposium on Wave Energy Utilization, The Norwegian Institute of Technology, Trondheim, Norway
- Nakada, H., Suzuki, M., Takahashi, S., Shikamori, M.(1992); *Development test of wave power extracting caisson breakwater*; Civil Engineering in Japan, Vol.31, pp.146-164
- Neelamani, S. Thiruvankatasamy, K.(1995); *Wave Forces on an Array of Oscillating Water Column Type Free Standing Wave Energy Caissons*; Proceedings of the Fifth International Offshore and Polar Engineering Conference, The Hague, The Netherlands
- Scher, R.M.(1985); *Progress on Flap-type Wave Absorbing Devices*; Hydrodynamics of Ocean Wave-Energy Utilization, Iutam Symposium Lisbon, Portugal
- Simeons, C.(1980); *Hydro Power, The Use of Water as an Alternative Source of Energy*; Pergamon Press
- Takahashi, S., Nakada, H., Ohneda, H., Shikamori, M.(1992); *Wave Power Conversion by a Prototype Wave Power Extracting Caisson in Sakata Port*; Chapter 262, International Congress of Coastal Engineering
- Taylor, R.J.(1981); *Wave energy: the influence of maintenance/repair requirements Wave and Tidal Energy*; Second International Symposium on Wave and Tidal Energy, BHRA, Cambridge, England
- Taylor, R.J.(1982); *The availability, reliability and maintenance aspects of wave energy*; Proceedings of The 2nd International Symposium on Wave Energy Utilization, The Norwegian Institute of Technology, Trondheim, Norway
- Vriesema, B.(1995); *The Archimedes Wave Swing, A New Way of Utilising Wave Energy*; Netherlands Energy Research Foundation ECN, the Netherlands
- Watabe, T.; Kondo, H. Yano, K.(1986); *Studies on a pendulum-type wave energy converter*; Water for Energy, 3rd Internatinal Symposium on Wave, Tidal, OTEC, and Small Scale Hydro Energy, BHRA, Brighton, England

Literature

Wave and Tidal Energy; International Symposium on Wave and Tidal Energy, BHRA, University of Kent, Canterbury, England (1978)

Wave and Tidal Energy; Second International Symposium on Wave and Tidal Energy, BHRA, Cambridge, England(1981)

Water for Energy; 3rd International Symposium on Wave, Tidal, OTEC, and Small Scale Hydro Energy, BHRA, Brighton, England (1986)

Power from Sea Waves, Conference on Power from Sea Waves, University of Edinburgh, Academic Press, England (1979)

Ross, D.(1979); *Energy from the Waves*; Pergamon Press, England

Shaw, R(1982); *Wave Energy, a design challenge*; University of Liverpool, England

Wave Energy Utilization, Proceedings; Proceedings of The 2nd International Symposium on Wave Energy Utilization, The Norwegian Institute of Technology, Trondheim, Norway (June 1982)

Hydrodynamics of Ocean Wave-Energy Utilization; Symposium on Hydrodynamics of Ocean Wave Energy Utilization, Iutam, Lisbon, Portugal (1985)

Utilization of Ocean Waves, Wave to Energy Conversion; Proceedings of the International Symposium, ASCE Speciality Conference, Scripps Institution of Oceanography, USA(1986)

Wave Energy, IMechE, Institution of Mechanical Engineers, Seminar, England (1991)

4 Wave Energy Devices for Combination with a Breakwater

4.1 Introduction

For floating breakwaters, in fact all devices which convert wave energy can be used. They do not only reflect the waves but also convert wave energy. Therefore, they are considered to have a better capability as a breakwater than ordinary floating breakwaters, as well as a higher stability. [Funakoshi et al.;1993]

In this study, only the combination of a seabed based breakwater with wave energy conversion devices will be investigated.

Some types of energy converters are more suitable than others for combination with a breakwater, because of their shape and form. For this combination, three types of energy converting systems seem to be suitable. These are (1) the potential energy converting devices, (2) the flap type devices and (3) the oscillating water column devices. These types of converters can be caisson-like constructions and thus ideal candidates for combination of a breakwater with wave energy conversion. Devices which extract potential energy exist in several concepts, they are described in Section 4.2. One of the first designed converters is the Russell's Rectifier, but this one has been decided in an early stage to have no possible future because of high capital costs.

The flap type devices are a bit pushed into the background, some devices are being investigated but only one scheme, the 'Pendulor', has been tested in Japan. This last one is proposed by Watabe and Kondo for application in a breakwater. Several flap type devices are described in Section 4.3.

As known, the oscillating water column devices are an important and well investigated group of converters. Several designs of these devices are proposed. A breakwater with oscillating water column devices has been proposed by the Japanese and British inventors. Some different types of OWCs exist, like a multi resonant design with extended side-walls or a phase controlled device. Information about the oscillating water column devices is given in Section 4.4.

For selecting a type of device for the combination with a breakwater, it is necessary to investigate and to compare the possible converters. Extensive study of the literature has been carried out for this purpose, described in the Sections 4.2, 4.3 and 4.4. The accompanying theory is described in several appendixes. In Section 4.5, some conclusions are drawn about the feasibility of the different types of converters for combination with a breakwater. The references are given in Section 4.6.

4.2 Potential Energy Converting Devices

4.2.1 Russell's Rectifier

General Information

The Russell's Rectifier is already briefly described in Section 3.3 and the theory is explained in **Appendix C**. The large rectangular hollow caisson exists of narrow inlet and outlet compartments of 10 m width, to keep reflections low. The front faces of the inlet compartments are fitted with non-return flap valves, allowing water entry under the pressure of wave crests, whilst the outlet compartments have flap valves which open to allow discharge into a wave trough. These valves have to be small compared to the orbit length of the wave (0.5 m), because they have to respond quickly to small pressure differences. Water flows from the higher level in the inlet compartment through a Kaplan low head turbine to the outlet compartment. See Figure 4.1, for the illustration of the operation.

[Cranfield;1979] [McCormick;1981] [Shaw;1982] [Simeons;1980]

The units would be operated in around 15 m of water. A proposal of a design consists of caissons with a height of 20 m, a length of 30 m and a width of 50 to 100 m. [Cranfield;1979] Because of this size and hence its high costs per unit output of electricity, the device is fallen from favour.

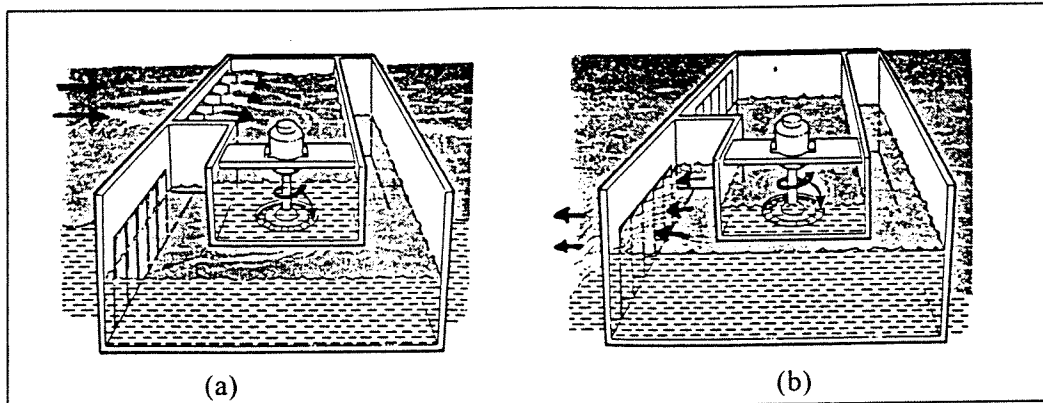


Figure 4.1 Operation of the Russell's Rectifier; (a) inflow, (b) outflow

Theory

In **Appendix C**, the theory developed by McCormick is shown. Experience of the Hydraulics Research Station showed that the condition for maximum efficiency of operation exists when the length (front-to-back dimension) of the inflow basin approximates to one fifth of the wave length, however the device is not highly frequency dependent. The theory of McCormick shows a maximum capture efficiency of about 20 %, though his assumption of resonance in the inlet basin seems to be debatable. Other authors indicate an efficiency of the same magnitude.

Conclusions

The proposed units would be operated in around 15 m of water. This depth is quite normal for breakwater circumstances. For breakwater design, the required length (parallel to normally incident waves) of the caisson for stability, depends on the wave conditions. The required length for energy conversion of 1/5 of the wave length, is in the same order of that of other types of devices like the OWC.

The rectifier must have a certain weight to withstand severe wave conditions. In the existing literature, the designs of the Rectifier do not have a large weight because the largest part of the structure is filled by water. Consequently, not only the dimensions of the Russell's Rectifier are large but it needs also more weight.

The combination of a quite low capture efficiency, large dimensions and the required extra weight causes that this device is decided to be not very suitable for combination with an energy converting breakwater. However, when the Russell's Rectifier would be used as a breakwater, the design has to be a compromise between capture efficiency and structural efficiency (length, width, height and weight).

4.2.2 Converging Channel

General Information

In the converging channel device, waves are led through convergence banks for overflow into an upper reservoir. A low head hydraulic turbine is used for the secondary conversion. The concept of the device is shown in Figure 4.2. In the converging channel, the height of the waves increases, the waves overflow a sill and the water is stored in the reservoir. The principle is the same as that of the in Norway designed shore based TAPCHAN, however the devices will be considerable smaller.

Theory and Experiments

In order to obtain an optimum configuration some experiments were conducted in Japan [Suzuki et al.; 1981]. Some parameters have been varied, namely the angle of convergence (θ), the water bed gradient (i) and the ratio of the width of the channel at the entrance to that at the inner end (b/B). The outline of the concept with the parameters is shown in Figure 4.2.

The angle of convergence was varied from 15° - 30° , the water bed gradient from $1/5$, $1/3$, $1/1$ and the ratio b/B from $1/10$ - $1/5$. It turned out that the highest capture efficiency is obtained for a model with an angle of convergence of 30° , a water bed gradient of $1/3$ and the width ratio of $1/10$. However, the highest efficiency reached, was only about 20%.

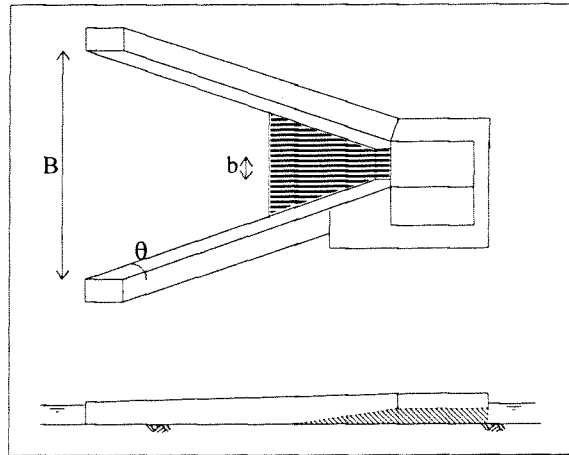


Figure 4.2 Concept of the converging channel

Conclusions

The devices will have large dimensions and a low capture efficiency. Moreover, the variation in water level (tidal variation) and waves is difficult to solve in the design. Consequently, these kind of devices are decided to be not suitable for combination with a breakwater.

4.2.3 Other Concepts

General Information

To make use of the potential energy of the waves also other concepts can be designed. Caisson-like components with a ramp can bring the water on level in a storage reservoir. Subsequently, the water can be let out through a hydraulic turbine. The components could be placed in a closed row to form a breakwater. In this case long convergence banks can be avoided. It must be investigated whether the water must flow out on the lee side with the still water level or on the wave site during the troughs of the waves (as in the case of the Russell's Rectifier).

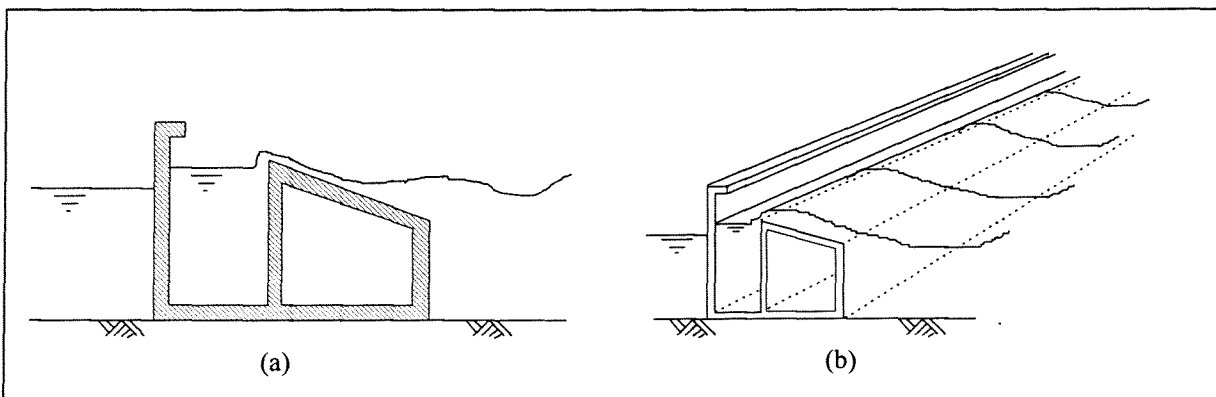


Figure 4.3 Concept of a potential energy extracting breakwater; (a) cross section; (b) 3-D view

Conclusions

The difficulty with systems using a ramp with a certain slope to bring water on level, is the variation in water level (tidal influences) and in wave height (because of the wave spectrum and seasonal variation). A movable ramp will be complex to construct and very expensive. From the other experiments can be expected that efficiencies of potential energy converting devices will be low.

When this last concept would be used for a breakwater, several design parameters have to be investigated. Some of these are the angle and length of the slope, the height to overflow, the size of the basin and the system of outflow.

4.3 Flap Type Devices

4.3.1 Introduction to Flap Type Devices

The flap type devices, in comparison to many others, are too simple to be eye-catching. In essence, the devices consist of a thin, vertical plate, usually (but not necessarily) at the free surface. The plate is arranged to respond in sway or roll, pivoted about an axis. The axis may be above or below the surface, as desired. The simplicity of these devices suggests certain economies in fabrication and also valuable simplifications in analysis. Nonetheless there are certain disadvantages as well.

Most importantly, from the outset, the performance of the flap type devices was expressed by the '2-D Efficiency', which is the ratio of captured to incident wave power in a two-dimensional situation. This ratio, for a symmetric device oscillating in a single degree of freedom, was very early shown to have a maximum value of 50%, at optimal tuning and damping (see also **Appendix B**). By contrast, devices that are asymmetric, or that oscillate in two or more degrees of freedom, were shown to be capable to capture all of the incident wave power, at least within the context of the linear wave theory. Thus, inevitably, the single-flap device was widely judged as 'inferior' by a factor two [Sher;1985]

In some countries the flap type devices have been investigated and tested. In the United Kingdom a wave power machine with free floating vertical plates was designed. In the United States research has been done to the Tandem Flap Device and in Japan the 'Pendolor' has been developed. By studying these converters the operation and possibilities of the flap type devices will become clear.

In the existing configuration, the wave power machine with free floating plates is not suitable for a breakwater. However, these devices are described below to investigate the operation principles and to get a better understanding of flap type devices. Also the Tandem Flap Device requires some adaptations when it will be used in combination with a breakwater.

4.3.2 Power Machine with Free Floating Vertical Plates

The Two plate machine

The 'Two plate machine' consists of two large vertical plates (the plates have a ballast at the underside), floating with most of their depth below the water line. The plates are oriented more or less parallel to the wave crests. They are maintained in position by moorings with sufficient play for them to move to and from with the waves. Between the two plates a number of double acting pumps is connected. The machine is shown in Figure 4.4a. [Farley et al.;1978]

The horizontal component of the wave motion causes the plates to move towards and away from each other, operating the pumps. A difficulty in this system is that perfect tuning of the device to the incoming waves is provided by a free floating unloaded plate (plate 1). The water on the right side of plate 1, provides just the right amount of resistance to capture all the incoming power without reflection. As soon as the plate is loaded by a pump, reflections are inevitable.

Consequently, as shown in **Appendix D**, with this arrangement at most an efficiency of 50% can be reached. The reflections can be avoided by a asymmetric 3-plate system or 'Triplate machine', designed to remove the water resistance on the right side of the first plate.

The Triplate machine

The 'Triplate machine' looks like the Two plate machine, but consists of three large vertical plates. The machine is shown in Figure 4.4b. [Farley et al.;1978]

Plate 2 and 3 are connected by jointed tie rods at a distance of half a wave length. Because the wave forces on the two plates cancel, such an arrangement does not move to and from horizontally. Consequently, their separation is fixed, but they are free to move vertically. No waves are transmitted beyond plate 3, thus plate 2 acts as a fixed reflector. A standing wave is set up in front of plate 2. A node for the vertical motion and an anti-node for the horizontal motion exist at a quarter wave length in front of plate 2, see also **Appendix A**. Plate 1, which is placed at this point, can move very freely in the horizontal direction. The damping presented by plate 1 to the incoming waves is very small. By adding pumps between plate 1 and 2, the optimum damping can be selected tuned to the incoming waves.

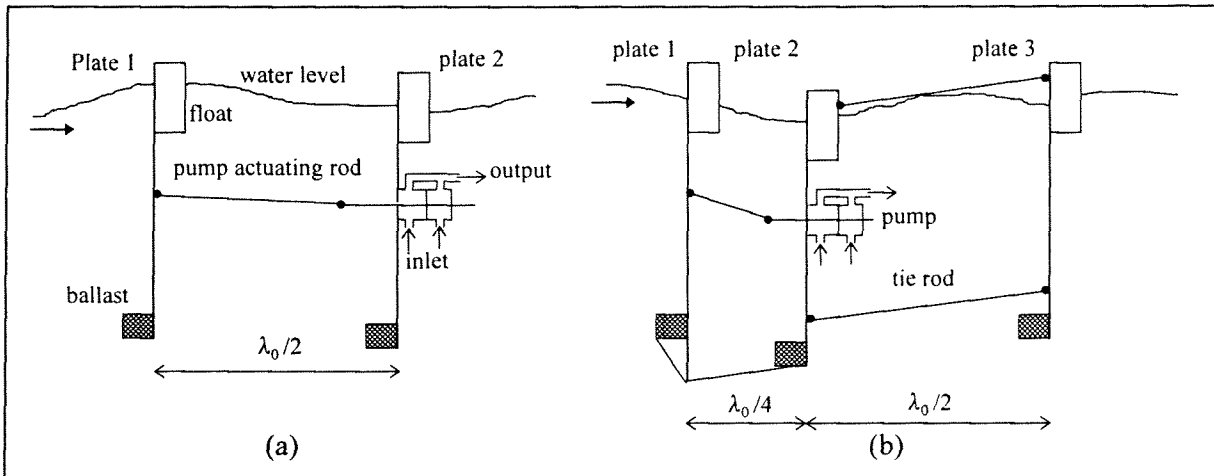


Figure 4.4 (a) Two plate machine. The plates move horizontally in anti-phase operating the pump; (b) Triplate machine. Plate 2 and 3 remain almost stationary, while plate 1 operates the pump

Theory and Experiments

A mathematical analysis is described in **Appendix D** for as well the Two plate as the Triplate machine. [Parks;1979] The plates are considered mass-less, infinite in depth and they can sway to and from following the exponential profile of the waves. The pump is replaced by an optimum linear loading (force proportional to the velocity).

The theory shows a maximum capture efficiency of 50% for the Two plate machine. For the Triplate machine a maximum efficiency of 100% at the design wavelength can be reached. The machine gives a reasonable broad response covering a factor two in wave length. This theoretical efficiency is reduced by a factor of about 0.86 because of the limited depth of the plates and a factor 0.64 due to non-ideally loading of the pumps. Adding hydraulic and friction losses one can expect an overall power conversion efficiency of the Triplate machine of about 50%. Measured efficiencies of model tests agree well with the theory.

It has been suggested to use instead of three plates an asymmetrical Two plate device, having one light and one heavy plate. The heavy plate can be realised by trapping a length of water between it and a third plate, with the surface wave suppressed however.

Conclusions

The Triplate (and the Two plate machine, in the case of an infinite length of the trapped water of plate 2), operates in fact like a device with a vertical wave absorbing plate and a fixed vertical reflector. Agreements exist with the Pendulum, described in Section 4.3.4. Both systems consist of a moving flap, located at a distance of a quarter of the wave length from a vertical reflector, however the way of motion is different (horizontal displacement for these devices and roll about an axis for the Pendulum). The maximum efficiency of 100% can be reached theoretically for the design wave length, but in practise this value is lower because of the non optimal loading of the power take-off.

Investigations in the machines with free floating plates started around the year 1978. It has been shown that the Triplate machine has the highest overall efficiency of about 50%. However, in later years nothing has been published about progress of the research. The inventors of the machine proposed in 1981 a new concept of a buckling resonant raft [BHRA;1981].

Likely, they have stopped the research because of problems with a full scale model. It is a floating system, consequently it must have moorings and flexible cables. The plates must be strong enough to survive in severe wave conditions and to transmit the wave forces to the pumps, for this requirement thin plates and flexible joints are needed. It can be concluded that the machine has some difficult parts to construct and vulnerable linkages. Particularly the upper part of the machine is exposed to severe storms.

4.3.3 Tandem Flap Wave Power Device

General Information

The Tandem Flap Device has two flaps which are hinged at the bottom edge and allowed to move in the direction of the wave propagation. The motions of the flaps are restrained by linear springs and hydraulic dampers. Experiments were performed with the supporting structure rigidly fixed in normally incident wave conditions. [Carmichael et al.;1992] Maximum 2-D efficiencies of 100% were confirmed. Also a 3-D numerical method has been derived and comparison with experiments showed good correspondence [Sher;1985].

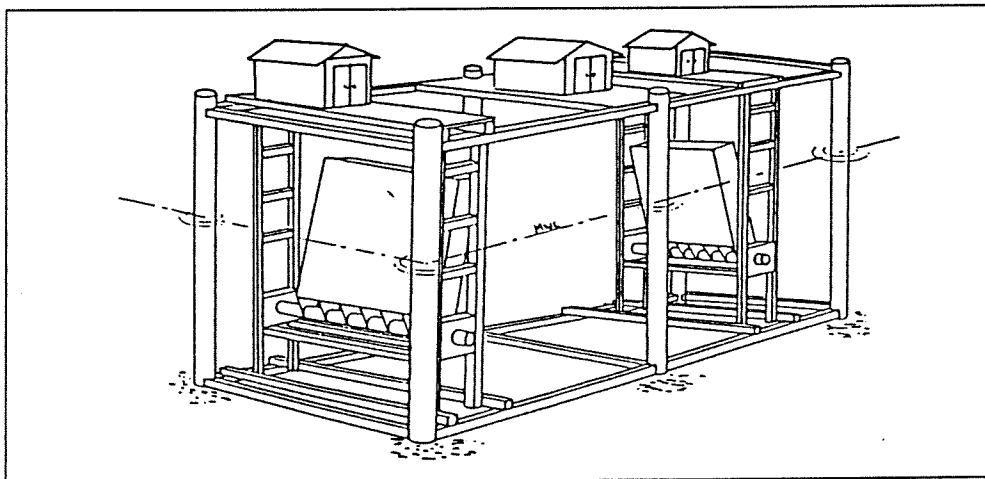


Figure 4.5 The Tandem Flap Device

Theory and Experiments

Several broad conclusions could be drawn after the experiments in a tank at the University of Michigan [Sher;1985]. The tests were carried out with a pure sway arrangement and with a rolling device, pivoted about an axis near the bottom of the flap. This last arrangement offers several advantages in terms of design, construction and operation. These include the avoidance of alignment problems, reduction in structural forces and moments and the ability to operate the flap at large angles of inclination, away from the free surface, thus shedding some exiting force. However, it has some mechanical parts under the water level, which hamper the maintenance of the device.

To the extent that flap width remains small with respect to wave length, the maximum capture width, obtainable at any frequency has been shown to be primarily a function of the wave length and not of the width of the device. A flap type device operating in relative long wave lengths, is in effect a 'point absorber'. The maximum theoretical capture width is π/λ . This point absorber limit is reached, for practical purposes, at a wave length of about three times the flap width. At shorter wave lengths, the flap-type device gradually becomes a terminator. [Sher;1985]

The flap motion amplitude varies approximately inversely with the flap width. Therefore the selection of an appropriate flap width cannot be made independent of the motion limits, imposed by power take-off machinery and the incident wave amplitude. [Sher;1985]

The flap draft has also no effect on maximum power capturing. However, the corresponding motion amplitude at maximum power conversion varies approximately with the inverse square of the flap draft. For this reason, flap draft, even more strongly than flap width, is the primary design variable for tuning the size of the device to the maximum stroke of the power take-off machinery. In addition, for the bottom pivoted flap the draft is also the primary design variable for tuning the device to a given wave frequency. [Sher;1985]

In 3-D, with a finite width of a twin-flap device, it is obvious that not all the radiation waves can be completely cancelled at any frequency, although radiation can be reduced. The effect of the twin-flap device is to recapture part of the energy that would otherwise be lost as a radiation waves. However, the condition for optimal tuning and damping of the twin-flap in 3-D is not as easily solved as in 2-D. The results of numerical runs have shown that a twin-flap device in 3-D can absorb twice the power of a single-flap device of equivalent width. Further study is required to investigate whether a twin-flap device is economically superior to a single-flap of equivalent flap width. [Sher;1985]

Conclusions

The flap devices have been investigated as well by theoretical as by model tests. The device with a rolling flap, pivoted about an axis near the bottom turned out to be the best configuration. The influence of several design parameters is described. When the device is operated in two-dimensionality (in practice, when devices are placed side by side in a breakwater) good efficiency is possible. When the device acts as a point absorber (in practise, when devices are placed at intervals in a breakwater) the maximum theoretical capture width π/λ is reached when the wave length is about three times the flap width.

The drawbacks of the Tandem Flap Device are the moving parts and thus the high chance on damage and costly maintenance. When the tandem flap is operating at non resonance frequencies, not all wave power will be captured and thus, behind the device there will exist waves. This is not permitted in the case of a breakwater.

For constructing a breakwater with these Tandem Flap Devices, the design has to be adapted. A possibility is to make a reflecting back wall, behind the second flap. When this wall is placed at a quarter wave length behind the flap, it will oscillate very good (like the 'Pendulor' device). In that case the wave power is decreased in two phases and the back wall will not receive severe wave attack. The breakwater can be formed by structures consisting of a frame with two flaps and a back wall, fixed to the sea bottom. The advantage of such a system is that no large expensive caissons and foundation material have to be used. For such a breakwater more study is required.

4.3.4 The Pendulor

General Information

The Pendulor has been developed in Japan and is mentioned already in Section 3.4. Its configuration is shown in Figure 3.13 and its principle in Figure 4.6. The system consists of a caisson or the like, which has an open chamber facing the sea. When the incident waves come into the chamber, they become standing waves by reflection from a back wall, located at a quarter of the wave length. The energy of the waves is fully changed into the reciprocating motion of the water at the nodal point of the standing waves.

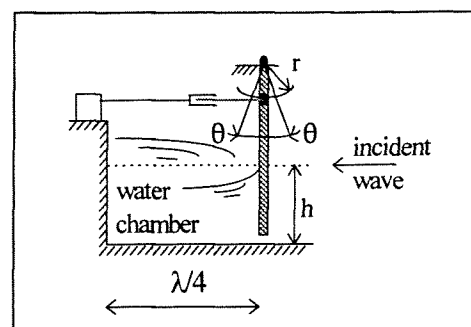


Figure 4.6 Pendulor (schematically)

The pendulor - a kind of pendulum with a flat surface - is driven by the oscillation of the standing waves, being hung down in the water. The pendulor drives a generator through a simple hydraulic transmission [Watabe et al.;1986] [Hagerman;1992].

Theory

A theory to calculate the efficiency has been derived by Asano. The load F_c , which acts on a hydraulic cylinder, is proportional to the angular velocity θ' of the pendulor and the cylinder has elastic deform x_c in proportion to the load F_c . The wave condition is sinusoidal regular. [Watabe et al.;1986] The theory and results are described in **Appendix E**.

Experiments

The efficiency of the pendulor has been checked in a model test. It was proved that the maximum efficiency η is about 80% of the incident waves, when the load coefficient of the pendulor equals the damping coefficient due to radiation waves. The test was carried out using a two dimensional model driven by a sinusoidal regular wave.[Watabe et al.;1986]

A 5 kW prototype (hydraulic motor rating) has been investigated at a coastal site, Muroran Port, during a period of almost 20 months. The water depth ranged from 2.5 m at low tide to 4 m at high tide. Two capture chambers have been built into the caisson, but only one has been fitted with a Pendulor. The maximum ratio of power conversion was above 50%. During severe sea conditions the output was 18 ~ 35 kW, while the mean incoming wave power was estimated at 55 kW. [Watabe et al.;1986] The pendulor system was sufficiently durable at this condition. However, during a next severe storm the pendulor was deformed and after that the flap had been lost. The shock absorbers for the end-stops, which prevent over-stroking of the cylinder had to be redesigned. A new Pendulor was installed in 1985 and has survived several severe storms since then, without damage [Hagerman;1992].

Conclusions

The system has a simple principle, is sea bed based, well investigated by models and prototypes and the efficiency in real sea conditions can be 50%. As the first pendulor was broken by a storm, the design has to be made very carefully. Also some other engineering problems must be solved before the commercial use of this system. The mechanical parts are out of the water, but the system has the flap as a moving part, which always is a drawback compared to systems without moving parts.

The pendulor can be set in coastal defensive structures, like breakwaters, dikes and revetments. Watabe and Kondo (1989) have developed a conceptual design for a 1.5 MW breakwater at Muroran Port. The breakwater consists of caissons with three Pendulors of a width of 5.3 m. Each pendulor drives two cylinders. The total height, length and width of the caisson are 10 m, 13 m and 25 m respectively [Hagerman;1992]. The caisson is shown in Figure 4.7.

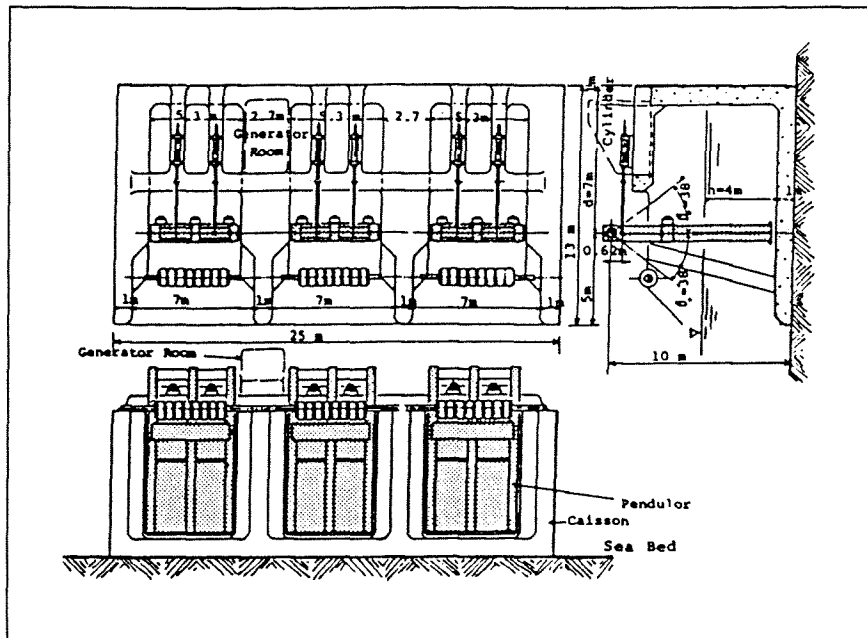


Figure 4.7 Caisson based Pendulor design; a component with three Pendulors

4.4 Oscillating Water Column Devices

4.4.1 Introduction to Oscillating Water Column Devices

In an oscillating water column device both the kinetic and the potential energy of waves is converted into piston like motions of a water column inside a structure. The air, trapped in the chamber above the water surface, is vented to the atmosphere through a turbine-generator which converts the cyclically reversing air flow into rotary motion and then into electrical output. In this section the development and theory of the oscillating water column will be explained. Because the breakwater in this study are sea bed based, only the results of investigation of non-floating OWC devices are given.

Single Acting

In the course of years, several concepts of devices have been designed. Single and double-acting systems exist.

A single-acting OWC device converts energy only from the fall or the rise of the water column. The Takenaka Corporation in Japan developed such a device [Hagerman;1992]. It consists of relatively narrow caissons which act as capture chambers. Output of air from several caissons is manifolded into a high-pressure air tank, which drives a conventional impulse turbine. Air is drawn into the caissons through check valves as the water column falls. When the water column rises, the air is directed to the outlet through a different set of check valves, see Figure 4.8.

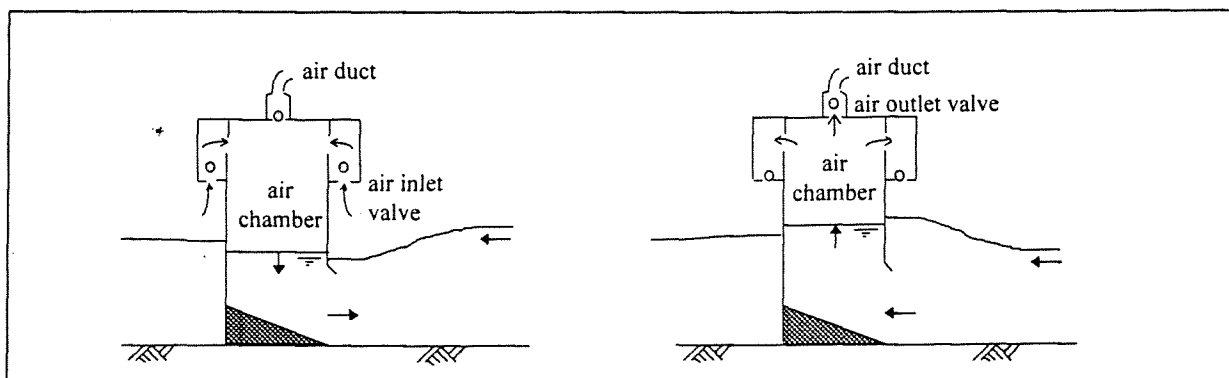


Figure 4.8 Takenaka Corporation's single-acting OWC concept

Double Acting

Most other OWC devices are double acting. In that case, as well with the rise as with the fall of the column, energy is absorbed by an air turbine. By the use of valves, it is possible to convert the bi-directional flow into an uni-directional pulse, which can be utilised by a conventional turbine, this is shown in Figure 3.15 for the NEL breakwater. When a self-rectifying turbine is used, like the Wells turbine, bi-directional flow can drive the turbine. These kind of turbines are self rectifying, since they are symmetric. The Wells turbine combines high efficiency with simplicity as there is no requirement for control valves and ducting to rectify the airflow.

Manifolding

Most designs of OWC devices deploy one turbine on each water column. There are distinct advantages in terms of reduced capital costs of electro-mechanical equipment if the air flow from a number of columns could be fed into a common duct and hence to a single large turbine. This is known as manifolding. The disadvantages are possible cost penalty due to the requirement of additional space, but primarily a reduction in the efficiency due to the loss of control of the individual column behaviour and sub-optimal damping. Tests and sea trials showed for terminator type devices, incorporating a manifolded system, a considerably drop in performance [Count;1982].

Load Control

From the theory of the spring-and-damper system it is known that maximum power extraction occurs when the damping due to energy extraction equals the radiation damping ($D_e = D_L$) and when the device is kept in resonance ($S=\omega^2M$). The equalisation of the two damping constants depend on the optimisation of the air chamber and the turbine load. The aim of load control is to adjust the turbine generator to match the performance of the air chamber and in this way maximising the electric output of the generator.

Multi Resonant

For the demand of keeping the device in resonance, it is impractical to have the column continually tuneable to the resonance frequency (by changing the column inertia or stiffness), so giving the device more than one resonance frequency is a good solution.

Part of the design process involves ensuring that the natural frequency of the column corresponds to the wave frequency at which most wave energy is delivered to the specific target site. The device's natural frequency and its ability to convert energy efficiently from a wide frequency range, are determined by and are very sensitive to the choice of the device dimensions. For instance, reducing the column length (front-to-back dimension), can increase the natural frequency and reduce the device's bandwidth of the efficiency curve. Several methods have been developed to make the column multi resonant. In Norway the Kværner prototype device, a 'harbour' type OWC device with projecting side walls, is designed and built. A proposal for a device with two columns of varying length within one structure has been made by the University of Belfast [Whittacker;1985].

As mentioned (Section 3.3.2), wave energy converters working at resonance will capture energy from a crest width larger than the width of the device, the so called capture width. Consequently, waves can be focused by making the column multi resonant.

Phase Control

The best method to increase the efficiency of a converter is to make it operating at resonance in any sea conditions, however, this seems to be impossible. The relative phase difference between the oscillation of the water column and the incident waves has also an important influence on the efficiency. By controlling this phase difference it is possible to improve the efficiency at non-resonant conditions.

The aim of phase control is trying to bring a non-resonant device into phase with the incident wave force by controlling the energy conversion mechanism. This means that the peaks in column velocity and excitation coincide. [Hoskin et al.;1985,1986] [Hotta et al.;1985][Hunter;1991]

Phase control can take place by regulating the air flow between the column and the turbine by a valve. If uncontrolled, the water column is excited into oscillation by the incident wave force and acts like a piston, driving air through the open valve and through the turbine. The valve can be controlled to modify the pressure in the air chamber, in order to improve the average energy conversion.

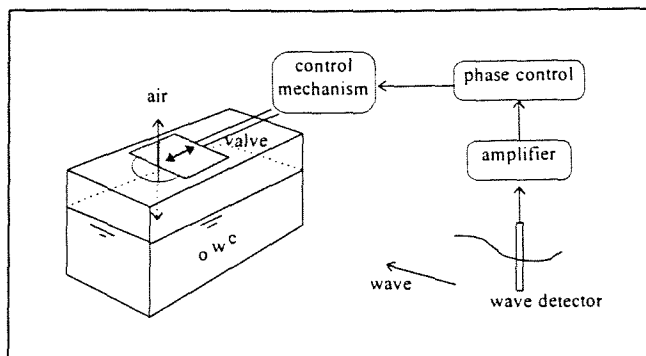


Figure 4.9 Phase control by a valve

When the valve is closed and power-generation is halted, the motion of the column persists, since the air in the chamber does not provide an infinite restoring force. When the natural frequency is higher than the incident wave frequency, the valve remains closed so that the pressure restrains the column motion, effectively lowering the natural frequency, in this way phase control slows the device. But for a much larger ratio, additional high frequency harmonics may be introduced by the control.

When the natural frequency is lower than the incident wave frequency, the valve closes before maximum displacement is reached and opens again when the column is moving down, the air spring stiffens the system and raises the natural frequency ($\omega_0 = \sqrt{S/m}$), the optimal control acts to speed up the system.

For an oscillating water column with a natural frequency of 2.12 rad/s and the incident wave frequency of 1.0 rad/s, a typical periodic uncontrolled and controlled response is given in the Figures 4.10(a) and 4.10(b). The response of a column to irregular waves with a mean frequency of 1.34 rad/s is shown in figure 4.11. [Hoskin;1986]

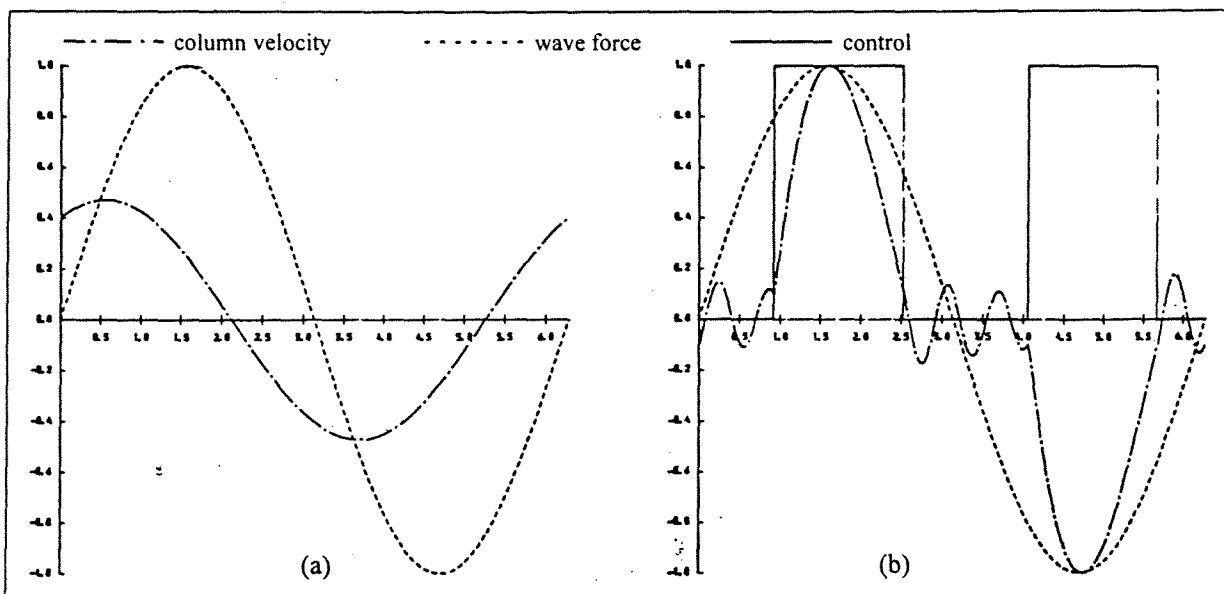


Figure 4.10 (a) Uncontrolled OWC; (b) Controlled OWC in regular waves

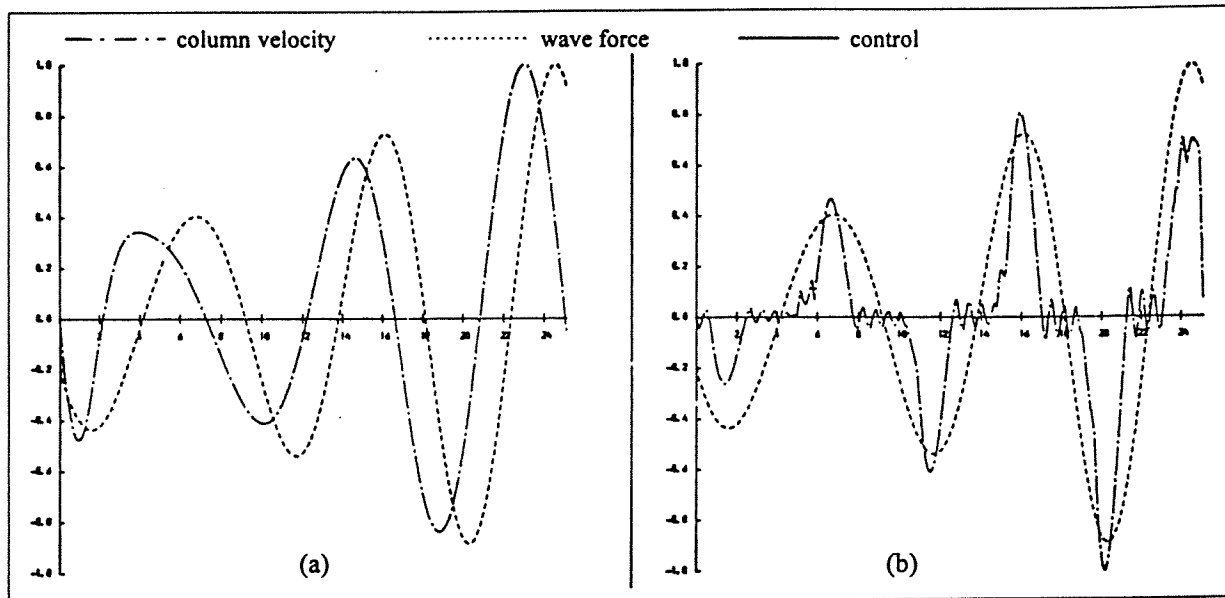


Figure 4.11 (a) Uncontrolled OWC; (b) Controlled OWC in irregular waves

Changes in the airflow due to the phase control causes some losses on the air turbine, but significant increases in efficiency of energy conversion can be achieved by optimal phase control. Implementation of such a mechanism requires forward prediction of the wave exciting force, however, further investigation of filtering techniques to provide this information is necessary.

A practical phase control device has been proposed by Sarmiento et al. [Sarmiento et al.;1990]. They describe a modified version of the well known Wells turbine. It is self-rectifying and has a mechanism that controls the rotor-blade setting angle, while the turbine is in motion, as in Kaplan water turbines. In this way, the air-flow through the turbine can be controlled independently from the air pressure difference and can take the instantaneous value defined by the optimum control strategy. However, at the moment no good control strategies exist to predict the incoming waves.

Theory

The earliest theory of the behaviour of an oscillating water column device, is modelling the column as a simple spring-and-damper system of a rigid body. This is described in **Appendix B** as the theory suitable for many types of devices. In the case of an oscillating water column, this usually involves replacing the free surface of the column by a thin weightless piston and it requires the determination of the added mass and the damping of the piston. However, these added mass and damping are hard to determine.

After this first theory, Evans has developed a new hydrodynamic method for the oscillating water columns systems, described in **Appendix F**. The potential flow theory is used and it is supposed that the pressure in the air chamber is proportional to the vertical velocity of the water column. This method correctly allows for the applied surface pressure and the consequent spatial variation of the internal free surface. The results, which are based on the classical linear wave theory, show the close analogies which exist with the theory of oscillating bodies.

The main conclusion of comparing these two theories is that power capturing can be calculated by both theories with the same equations, however the parameters have different meanings [Evans;1985].

4.4.2 Japanese Wave Power Converting Caisson

General Information

Since the perforated wall caissons had been invented, they were increasingly used as seawalls and breakwaters. This is because wall perforated caissons have low wave reflection and overtopping characteristics and they are highly stable due to their wave absorbing capability. The Japanese Ministry of Transport has been developing a wave power converting caisson breakwater, which can absorb the energy and can convert it into useful electricity.

The breakwater consists of caissons on a rubble mound foundation. The caisson has an air chamber, which is attached to the ordinary caisson. The waves enter into the air chamber from the opening under the immersed front wall and cause the vertical oscillation of the water surface in this chamber. Then, the air flow activates the turbine and generates the electricity.

Theory

The theory used for the breakwater design has been named as the thermodynamics and wave kinematics method [Nakada et al.;1993] [Ojima et al.;1984] [Takahashi;1988]. It comprises two thermodynamics equations in the air chamber and one wave kinematics equation at the air chamber opening under the front wall. The equations have to be solved numerically. The theory includes air compressibility. An illustration of the theory is shown in Figure 4.12.

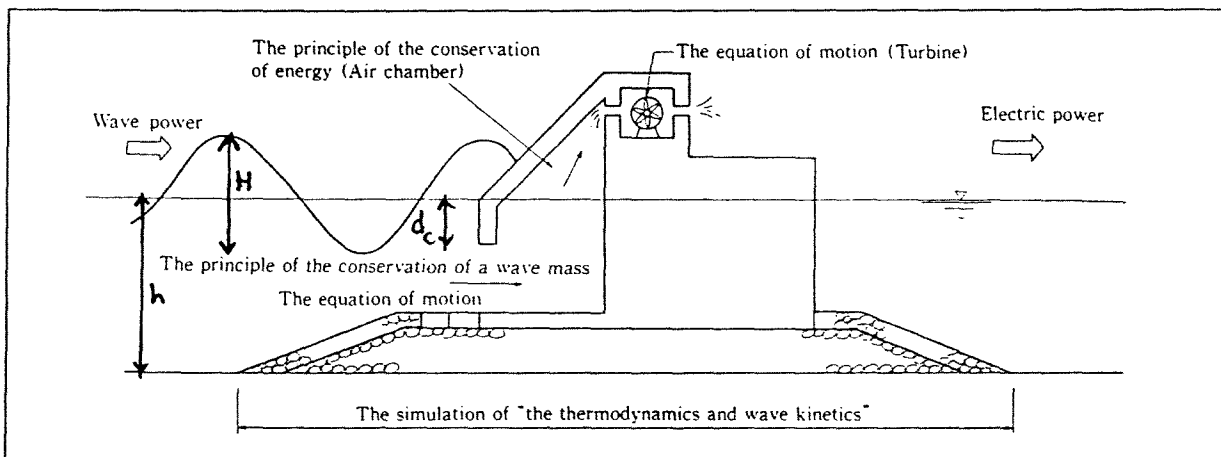


Figure 4.12 Wave energy and the thermodynamics and wave kinematics method

The theory has been verified by experiments with models. [Ojima et al.;1984] The maximum capture efficiency (wave power to air power) is reached at an chamber length of 11-15% of the wave length.

The effect of the immersion depth of the front wall d_c , shown in Figure 4.13, can be explained as follows. When the depth is zero ($d_c/h = 0$), the efficiency is rather low with a value less than 50%. As it is immersed deeper, the efficiency is increased up to a certain value. The maximum efficiency is obtained at the condition that the immersion depth is half to one times the wave height ($d_c/H = 0.5 \sim 1.0$). Beyond that level the efficiency turns to decrease because of narrowing

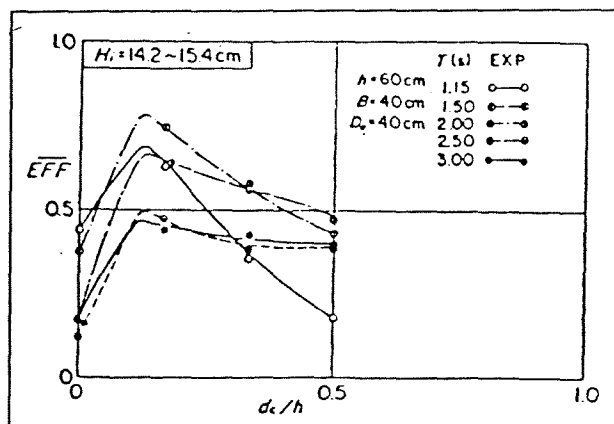


Figure 4.13 Capture efficiency versus immersion depth

the entrance of the chamber. The low efficiency at the condition $d_c/h = 0$ is caused by the fact that the air pressure in the chamber is released to the atmospheric value at the time of the wave troughs.

Experiments

A pilot plant breakwater was constructed in the summer of 1989 at Sakata Port. The depth of the water at the construction site is 18 m. The system was designed to operate using waves of a height of 1 to 5 m. The wave with $H_{1/3} = 2.2$ m and $T_{1/3} = 7$ s was selected as a main wave to discuss the conversion efficiencies. However, the design wave for stability of the caisson is $H_{1/3} = 10.2$ m and $T_{1/3} = 14.5$ s. The caisson has a width of 20 m and has a height of 12.5 m above low water level. The air chamber has a length of 7 m and the total horizontal area is 115 m^2 (not including the thickness of the walls). The sloped front face increases the stability under wave conditions. [Funakoshi et al.;1992] [Nakada et al.;1992] [Takahashi;1988]

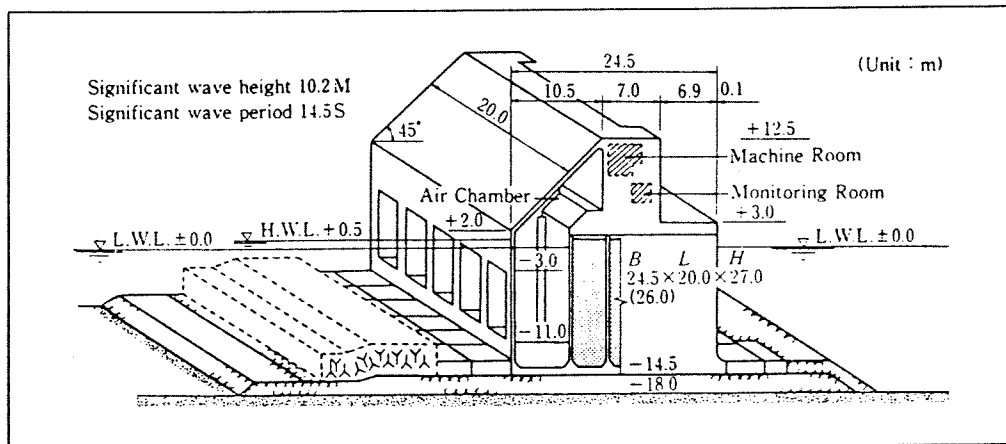


Figure 4.14 Shape of the caisson breakwater at Sakata Port

Two Wells turbines of 1.337 m in diameter are employed and sandwich the generator to make a tandem type arrangement, cancelling the forces that work in the axial direction of the turbines. The generator is a 200 V synchronous generator with a rated output of 60 kW and a maximum revolution of 3000 rpm.

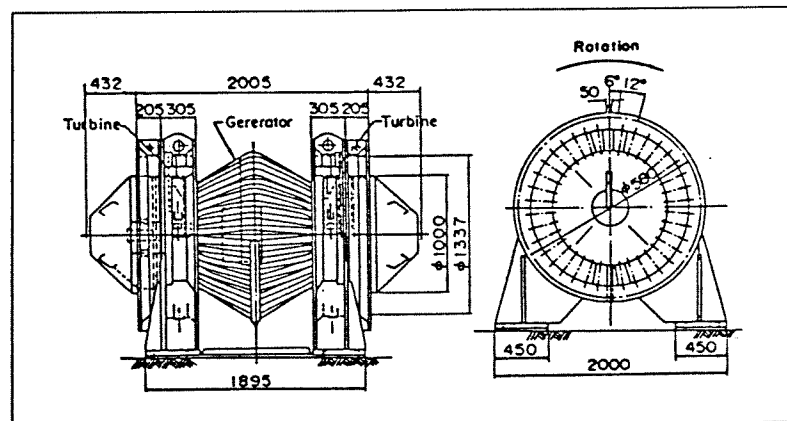


Figure 4.15 Turbine and generator (unit: mm)

The experiment shows the following conversion efficiencies. The efficiency from wave power to air power (capture efficiency) is between 0.4 and 0.8, the efficiency from air power to turbine power (turbine efficiency) is between 0.2 and 0.5 and the efficiency from turbine power to electric power (generator efficiency) is about 0.5. The total efficiency which is given by the product of last-mentioned efficiencies varies between 0.1 and 0.3. However, it should be noted that the diameter of the turbines is set to be much smaller than that of the optimum turbine, predicted by the amount of air power from the air chamber. Two dummy nozzles are installed to release the extra air power, which corresponds to almost half of the total air power. Consequently, for a full-size system with a larger turbine generator, the actual total efficiency should be divided by the air power utilisation rate.

Conclusions

From the theory it is concluded that the power conversion is affected by many parameters, so optimisation in every parameter is difficult. For simplicity the immersion depth of the front wall can be set at $d_c = H_{\text{operating}}$ (wave height under operation condition) or $0.25 H_D$ (H_D = wave height of design storm). The height of the air chamber (the internal freeboard) can be set at $D_0 = 0.5 H_D$. The height of the crest of the breakwater is determined by the demand of overtopping and transmission. These values can roughly be recognised in the design of the Sakata Port Breakwater.

The prototype at Sakata Port has shown that wave energy conversion by a full-size system is possible. The field experiment was conducted very successfully, although several severe storms attacked the caisson. The experimental values of the conversion from wave to air power were even higher than the predicted values by the theory. This is because only one wave power converting caisson was installed between reflective caissons. In that case reflected waves from neighbouring caissons can increase the incident wave power into the caisson with wave power conversion. In this way, also within a breakwater the phenomenon of point absorbing occurs.

4.4.3 Kværner Harbour Type OWC

General Information

From the very beginning, there was in Norway the idea of having an absorber continually tuneable to resonance. However, several problems appeared and as consequently that method has been abandoned. To solve the problem of a narrow bandwidth of the efficiency of small wave energy converters, the so-called 'harbour' in front of the device has been introduced, see Section 3.4. It is a passive way of broadening the bandwidth of the efficiency without mechanical components and without a wave prediction method as needed for phase control. The 'harbour' is formed by a pair of walls, protruding from the opening of the oscillating water column, thereby partly enclosing a rectangular basin.

The simplest analogy is that in this basin the phenomenon of harbour resonance occurs, with large amplification of the waves inside the 'harbour'. It is possible to select dimensions such, that this device has two resonance frequencies, one for the column and one for the 'harbour' [Ambli et al.;1982].

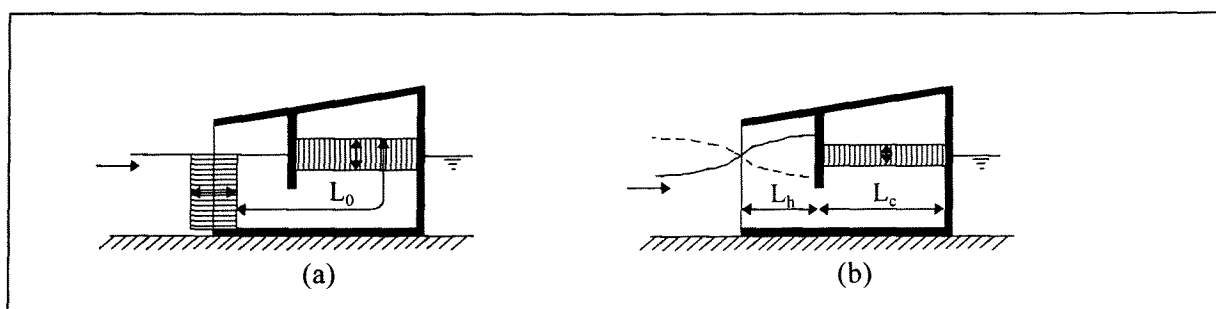


Figure 4.16 Resonance oscillations in the Kværner 'harbour' type OWC device: (a) normal OWC resonance; (b) quarter wave length resonance introduced by the 'harbour'

Wave energy converters working at resonance frequency will focus the wave energy, consequently this 'harbour' type device acts as a point absorber. The combination of these two properties (double resonance and point absorbing) results in an OWC device, that yields more kilowatt hours per ton material used to build it, than other OWC concepts.

Theory and Experiments

Originally, the idea was to place the 'harbour' type OWC device in the open sea, anchored or resting on the sea bottom. However, civil work in an offshore environment was too expensive. The site finally chosen for a prototype of 500 kW is Toftestallen west of Bergen, an almost vertical wall of

rock on a peninsula. [Malmo et al;1985] This change in location has influenced the derivation of the theory. The first developed theory is for single devices in open sea, later the theory was extended for devices placed in a reflecting wall.

The theory of 'harbour' type OWC devices is explained in **Appendix G**. An approximate theory based on the results of springer-damper system by Malmo and Reitan and another approximate method of Evans are given. These two theories agree well. It is shown that the addition of side walls to an OWC can improve the performance markedly. The peak performance is increased and shifted to the lower frequencies (longer wave lengths with more energy). When the 'harbour' length equals the chamber (i.e. the column) length then the performance is close to the upper limit of complete impedance matching over a broad bandwidth.

4.4.4 NEL Breakwater

General Information

The National Engineering Laboratory of the United Kingdom started in 1976 with the study of an OWC station. This resulted in three designs, namely the 1980, 1981 and finally the 1982 NEL Breakwater. This last one is situated at South Uist, in a water depth of 21 m, consisting of modules of several columns. The columns have a length and width of 15 m, a vertical opening dimension of 9 m and a nose immersion of 6 m. An internal freeboard of 5.5 m is provided for the air volume. Above each column is located the generator room containing a conventional axial bulb turbine, rectifying and isolating valves and some other equipment [Hunter;1991].

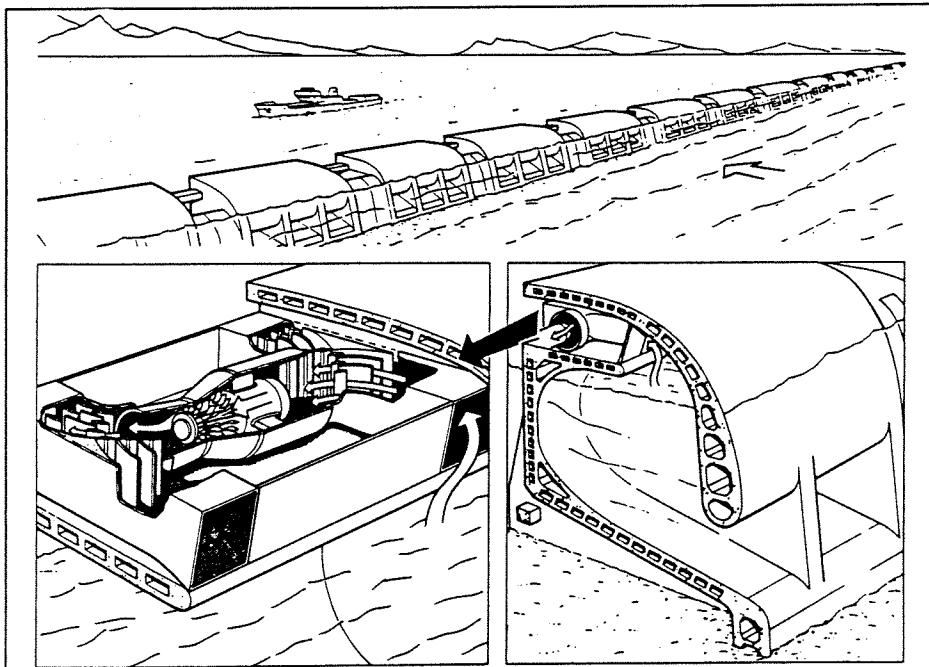


Figure 4.16 Design of the 1982 NEL OWC Breakwater

Later on, renewed attention was given to the NEL Breakwater for further improvements. The first change is a self-rectifying turbine like a Wells turbine. A method to improve the efficiency, is to build protruding 'harbour' walls like the Norwegian device. Tuning the device to the energy available in the target location, a 'harbour' length of between 20 and 25 m would seem to be about maximum (see also Figure 4.18).

A better design, with a more suitable combination of dimensions has been made. The column length is reduced to 10 m and the 'harbour' has a length of 17 m (see also Figure 4.19 and 4.20). The design gives a good broad bandwidth of the efficiency. It is believed that the optimum design would consist

of a long reflecting breakwater, along which, at carefully chosen intervals, 'harbour' type OWC devices would be placed [Hunter;1991]. However, a full-size construction still has not been made.

Theory and experiments

Theory for 'harbour' type OWC devices placed in a reflecting wall (in practise a breakwater) has been developed by the Norwegians Malmo and Reitan and the Englishmen McIver and Evans. These methods are mainly numerical and the results show the influences of several design parameters. It is shown that the 'harbour' type OWC in a reflecting wall has a good broad performance and capture width. The NEL Breakwater has been designed by the three-dimensional theory of Evans [Count et al;1984] which is applicable to a single column placed in open sea. The influence of 'harbour' length, damping level of the turbine and phase control has been considered.

The influence of adding the 'harbour' is clearly illustrated in Figure 4.18. The dotted line corresponds to the two-dimensional breakwater design of 1982 without a 'harbour', whilst the upper solid line indicates the maximum attainable efficiency according to the point absorber theory. Increasing the 'harbour' length increases the maximum capture width ratio and tunes the device to longer wave lengths.

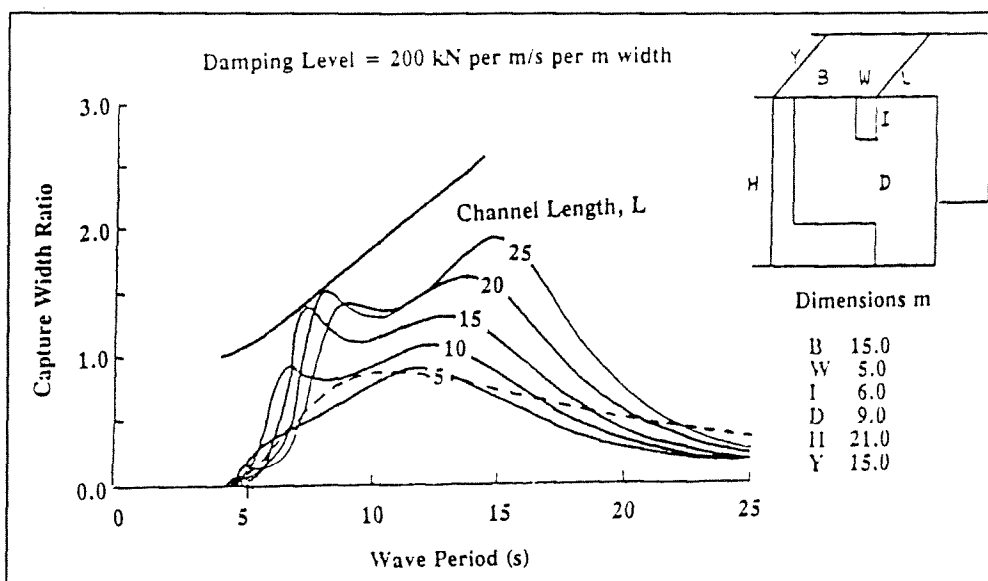


Figure 4.18 Capture width versus wave period for various harbour lengths

The influence of the damping level of the turbine is shown in Figure 4.19. Low damping gives rise to peaky resonance and high efficiencies at 7 and 12 seconds, whereas higher damping gives a flatter response and hence improved performance at mid range periods around 10 seconds. Also the magnification factor (the ratio of the chamber amplitude to the incident wave amplitude) is a consideration involved in the design. Low damping gives rise to unacceptable column amplitudes, see Figure 4.20. Usually, a value of two for the magnification factor is chosen as maximum desirable.

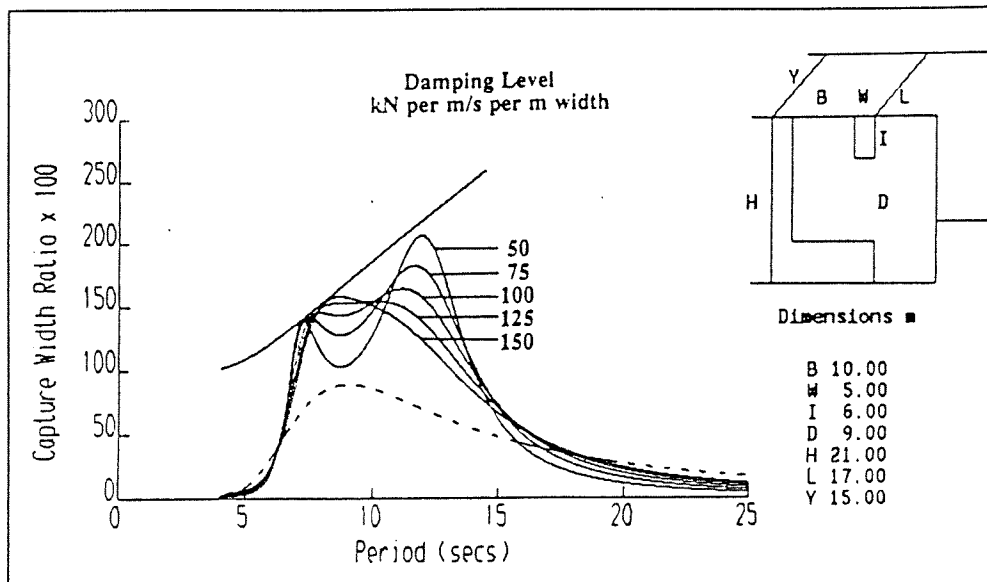


Figure 4.19 Capture width ratio versus wave period for various damping levels

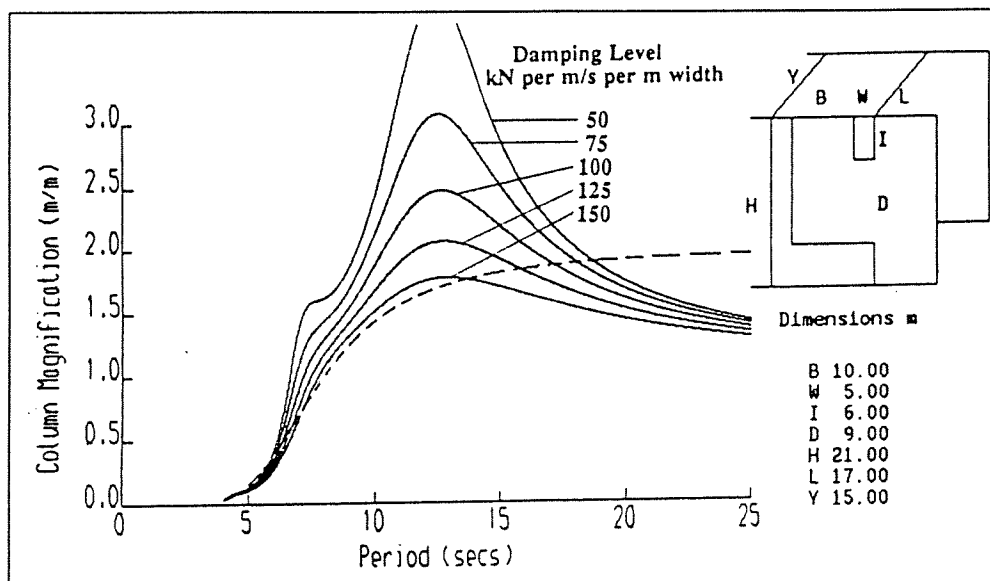


Figure 4.20 Column magnification factor versus wave period for various damping levels

Conclusions

The most recent NEL Breakwater design shows that also the British inventors believe that the best prospects are using the 'harbour' type OWC in their breakwater. Considerable theoretical research has been done verified by experimental model tests. The technique of phase control is not already available. The results showed in the Figures 4.18, 4.19 and 4.20 of varying several design parameters are clear illustrations of the behaviour of the 'harbour' type OWC in a breakwater. The spacing between the two devices is set as a first assumption at slightly more than half the wave length (75 m).

4.4.5 The Q.U.B. Multi-Resonant Converter

General information

The Queen's University of Belfast, Northern Ireland, has designed, as part of the UK wave energy program, a 2-GW OWC power plant. [Whittacker;1985] The first design was an array of bottom standing axi-symmetric structures, with six-columns and an outer diameter of 22 m at the waterline, as shown in Figure 4.21. Excitation in the landward facing columns was primarily due to the wave diffraction around the structure. The devices had to be spaced at least 2.5 diameters apart to enable this diffraction.

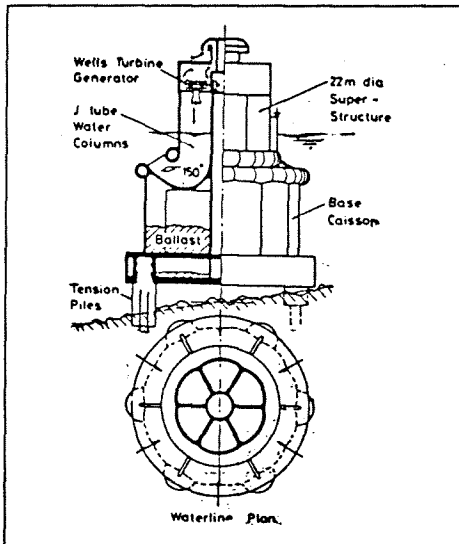


Figure 4.21 Six-column axi-symmetric device

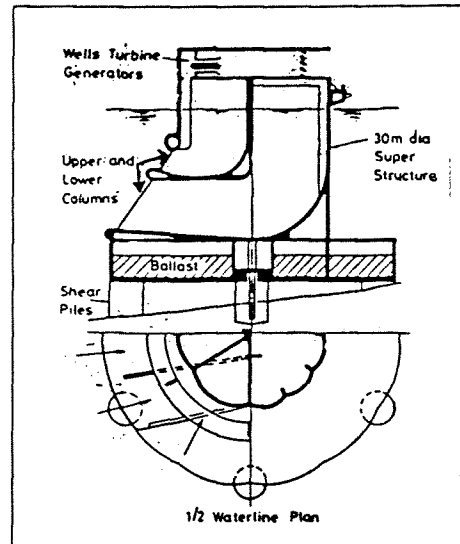


Figure 4.22 Two frequency device

The second design which included the multi-resonant concept was developed from the six-column axi-symmetric device. As known, an OWC is a tuned system with a resonant frequency determined by the mass and stiffness of the oscillating water column. The frequency bandwidth of this design is widened by incorporating columns of varying dimensions within the one structure. Figure 4.22 shows the two frequency device with two sets of columns. The original three seaward facing columns, in Figure 4.22 at the left side, are virtually unchanged, while the remaining three columns are combined into one column beneath the top columns.

Theory and Experiments

Experiments showed that no interaction occurs between adjacent columns and only at some frequencies there is some interaction between the bottom column and top columns. At these frequencies, the combined performance of the two columns can be up to 20% less than predicted by the superposition. One model has been tested and it is considered that the degree of interaction is primarily a function of the shape, relative position and orientation of the entrances and the hydrodynamic characteristics of the water columns.

The large bottom column has a natural period of 11 s compared to the 6.5 s period of the top columns. The total device performance is roughly the summation of the two performances of the columns. The capture width ratio of the different columns and of the total device is given in Figure 4.23, taking into account the interaction losses.

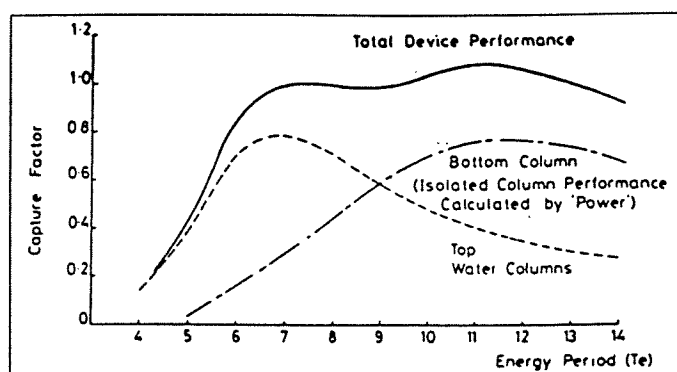


Figure 4.23 Capture width ratio of the two frequency device

Conclusions

The frequency bandwidth can be broadened by introducing two column lengths within one device. However, the structure becomes more complicated and every column needs a turbine. In this way the device will become more expensive also. The device is not fully investigated and no prototype at large scale has been tested.

When the concept of two different column is used in a breakwater design, one top and one bottom column are needed with consequently two turbines. Another possibility is using columns of different dimensions alternately in a breakwater, each tuned to a specific wave length. The application of this last suggestion depends on the wave spectrum of the location of the breakwater and in what way the electricity is required (high during short periods, or less during longer periods). An optimisation has to be made for the column dimensions (all devices the same dimension or devices with different optimal dimensions) and the spacing between them.

4.5 Selection of the Device for Combination with a Breakwater

By comparing the three types of converters, namely potential energy converting, flap type and OWC type devices, it becomes clear that the first mentioned are not very suitable for combination with a breakwater. The main problems are a low capture efficiency, the variations in sea water level and the required large structures.

The flap type devices can have different configurations. It can be concluded that a flap hanging before a reflecting back wall has the best prospect for combination with a breakwater. It is believed that the flap must not have very large dimensions. Consequently, flap type devices can be used for breakwaters in less heavy attacked locations, i.e. in shallow water with no large wave power values.

Pendulors, can be installed in a caisson, side by side or at intervals. When placed at intervals, the point absorbing capability is used. An other configuration, without caisson, is a structure consisting of a frame with a reflecting back wall and one or two flaps, as shown in Figure 4.24 (the structure with two flaps). This device has not been investigated, may be for breakwater construction these structures will be economically superior to caisson like structures. If necessary, the back wall can be perforated to avoid too large wave forces on it, however in that case the reflection will be lower (less motion of the flap) and the wave transmission higher (in general not wanted in a port).

However, the drawbacks of the flap type devices are the moving parts, therefore in the design, special attention has to be paid to the strength of these parts and the linkages.

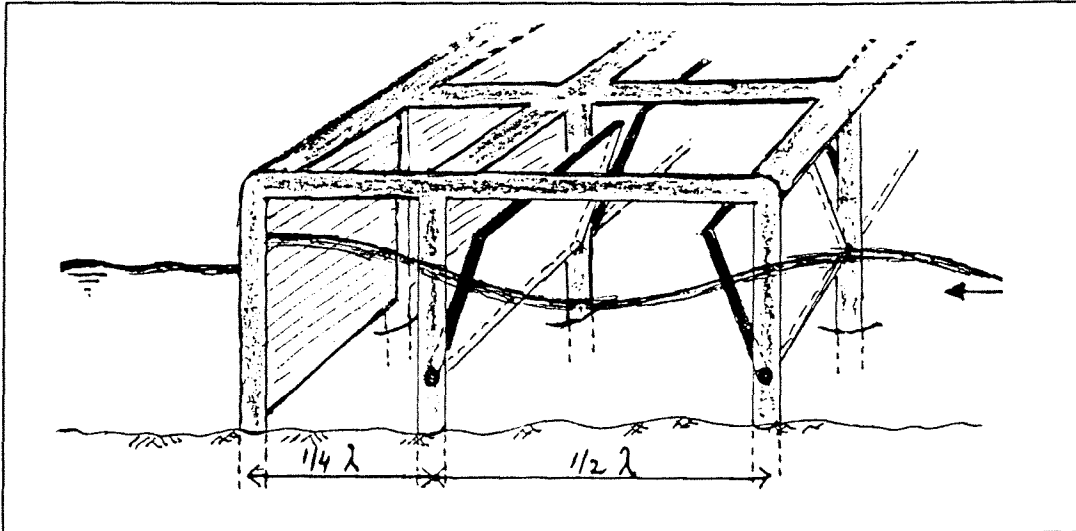


Figure 4.24 Structure consisting of a frame with a reflecting back wall and two flaps

Several OWC type devices exist. The Japanese breakwater at Sakata Port is functioning well, both as a breakwater and an energy converter. Multi resonant devices are preferred for the broad bandwidth of the capture efficiency and the large capture width. The 'harbour' type device is the best investigated multi resonant OWC device at present. These devices can be installed at intervals in a breakwater. In that case, the total number of devices in a breakwater can be less and the performance of a device in a row is better than of a single placed device. The British inventors believe that this type of converting breakwater will have the best prospects.

Summarising, the results of the comparison of the devices are given in Table 4.1.

Table 4.1 Several devices and their prospects for combination with a breakwater

Type of device	Device	Considerations	Prospects for combination with a breakwater
Potential energy converting	Russell's Rectifier	- low efficiency - large structure	- no
	Converging channel	- low efficiency - large structure - problems with sea water level variations	- no
	Other concepts	- low efficiency - large structure - problems with sea water level variations	- no
Flap type	Free floating plates	- abandoned?	- no
	Tandem Flap Device	- good performance - well investigated - sensitive to damage	- has to be investigated
	Pendulor	- good performance - well investigated - full scale tests - sensitive to damage	- possible for locations with no large wave power - placed side by side or at intervals
OWC	Sakata Breakwater	- good performance - well investigated - full scale tests - not sensitive to damage (no moving parts)	- good
	Kvaerner device	- multi resonant	- good, devices placed at intervals as in the improved NEL design
	NEL Breakwater 1982	- in fact the same as the Sakata Breakwater	- less good, than the improved design
	improved NEL Breakwater (with 'harbour' type devices)	- multi resonant devices - believed to be economically superior to the design of 1982	- good
	Q.U.B. Two frequency device	- two resonance frequencies - each column a turbine	- has to be investigated

It can be concluded that the OWC type devices are the best for combination with a breakwater. In this study the combination of 'harbour' type OWC devices, installed at intervals in a breakwater will be investigated.

4.6 Conclusions

In this chapter, three types of energy converters which seemed to be suitable for combination with a breakwater have been investigated. These are (1) the potential energy converting devices, (2) the flap type devices and (3) the oscillating water column devices.

The drawbacks of the potential energy converting devices are in general (1) the low capture efficiency, (2) when using a ramp with a certain slope, the problem of variation in water level and in wave height and (3) the required large structures.

Three flap type devices have been investigated, the wave power machine with free floating vertical plates, the Tandem Flap Device and the 'Pendolor'. In the existing configuration, only the last device is suitable for a breakwater. However, these devices have been described to investigate the operation principles and to get a better understanding of flap type devices.

The flap type devices show that a good capture efficiency is possible with two flaps hanging behind each other or with a flap in front of a reflecting wall like the 'Pendolor'. This last one has been tested in Japan. It showed a good performance in real sea conditions (50%), however during a severe storm the pendolor was broken. The Pendolor is already proposed for application in a breakwater, but the design of the Pendolor must be improved.

An interesting consideration is to make use of the point absorbing capability of a device. In **Appendix B**, it is shown that the maximum capture width of devices that operate in sway motion is λ/π , which is twice the maximum capture width of devices that operate in the heaving mode. The caissons which are proposed by Watabe and Kondo have flaps over the total width of the caisson (three flaps per caisson). By using the capture width of each flap, the total number of Pendolors to install in a breakwater is considerably less.

The oscillating water column devices are an important group of converters. Several designs are shown, like the Japanese wave energy converting caisson and two multi resonant devices ('harbour' type device and the Q.U.B. Two frequency device). The OWCs have in general a high capture efficiency in comparison to other types of devices. When multi resonant, they have also a good broad bandwidth of the efficiency. A design with a 'harbour' in front of the column is at the present the most promising OWC device, because of its good performance and point absorbing capabilities. Phase control is a promising application for the future, however at this moment no good method exists for real sea conditions.

The experiments and theoretical models with a 'harbour' type OWC device, indicate that adding a 'harbour' will give the same effect for any other wave energy device that operates well in the two dimensional case [Count et al.;1984]. Up to now, no other devices than the oscillating water column devices have been designed with a 'harbour'. This last fact illustrates that all attention is paid to the OWC devices because of their credibility (no moving parts, well experimented) and good performance.

It can be concluded that the OWC type devices are the best for combination with a breakwater. In this study the combination of 'harbour' type OWC devices, installed at appropriate intervals in a breakwater will be investigated. In the next chapter, the principle of wave energy conversion and several design parameters of this device will be investigated.

4.7 References

- Ambli, N.; Bønke, K.(1982); Malmo, O.; *The Kværner multiresonant OWC*; Proceedings of The 2nd International Symposium on Wave Energy Utilization, The Norwegian Institute of Technology, Trondheim, Norway
- BHRA(1981);; Second International Symposium on Wave and Tidal Energy, BHRA, Cambridge, England
- Carmichael, A.D., Falnes, J.(1992); *State of the Art in Wave Power Recovery*; Ocean Energy Recovery, The state of the Art; Scripps Institution of Oceanography, University of California at San Diego; Offshore Technology Research Center, Texas A&M University, USA
- Count, B.M.(1982); *On the hydrodynamic characteristics of wave energy absorption*; Proceedings of The 2nd International Symposium on Wave Energy Utilization, The Norwegian Institute of Technology, Trondheim, Norway (June 1982)
- Count, B.M.; Evans, D.V.(1984); *The influence of projecting sidewalls on the hydrodynamic performance of wave-energy devices*; Journal of Fluid Mechanics, Vol. 145, pp. 361-376
- Cranfield, J.(1979); *Interest in wave power growing*; Ocean Industry, February, pp. 67-76
- Evans, D.V.(1985); *The Hydrodynamic Efficiency of Wave-Energy Devices*; Hydrodynamics of Ocean Wave-Energy Utilization, Iutam Symposium Lisbon, Portugal
- Funakoshi, H., Ohno, M., Takahashi, S., Oikawa, K.(1993); *Present Situation of Wave Energy Conversion Systems*; Civil Engineering in Japan, Vol.32, pp. 108-134
- Hagerman, G.(1992); *Economics of Wave Power*; Ocean Energy Recovery, The state of the Art; Scripps Institution of Oceanography, University of California at San Diego; Offshore Technology Research Center, Texas A&M University, USA
- Hoskin, R.E.; Count, B.M. Nichols, N.K., Nicol D.A.(1985); *Phase control of the Oscillating Water Column*; Hydrodynamics of Ocean Wave-Energy Utilization, Iutam Symposium Lisbon, Portugal
- Hoskin, R.E, Nichols, N.K.(1986); *Optimal strategies for phase control of energy devices*; Utilization of Ocean Waves, Wave to Energy Conversion, Proceedings of the International Symposium, ASCE Speciality Conference, Scripps Institution of Oceanography, USA
- Hotta, H. Miyazaki T., Washio Y.(1985); *Increase in Absorbed Wave energy by the phase Control for Air flow on OWC Wave Power Device*; Hydrodynamics of Ocean Wave-Energy Utilization, Iutam Symposium Lisbon, Portugal
- Hunter, R.(1991); *Future possibilities for the NEL Oscillating Water Column wave energy converter*; Wave Energy, IMechE, Institution of Mechanical Engineers, Seminar, England
- Malmo, O. Reitan, A.(1985); *Development of the Kvaerner Multiresonant OWC*; Hydrodynamics of Ocean Wave-Energy Utilization, Iutam Symposium Lisbon, Portugal
- McCormick, M.E.(1981); *Ocean Wave Energy Conversion*; U.S. Naval Academy, Annapolis, Maryland, Willey-Interscience Publication, USA
- Nakada, H., Suzuki, M., Takahashi, S., Shikamori, M.(1992); *Development test of wave power extracting caisson breakwater*; Civil Engineering in Japan, Vol.31, pp.146-164
- Ojima, R., Suzumura, S. Goda, Y.(1984); *Theory and experiments on extractable wave power by an oscillating water-column type breakwater caisson*; Coastal Engineering in Japan, Vol.27, pp. 315-326
- Parks, P.C. (1979); *Wedges, plates and waves - Some simple mathematical models of wave power machines*; Conference on Power from Sea Waves, University of Edinburgh, England

Sarmento, A.J.N.A.; Gato, L.M.C; Falcão, A.F. de O.(1990); *Turbine-controlled wave energy absorption by oscillating water column devices*; Vol. 17, No. 5, pp. 481-497

Shaw, R. (1982); *Wave Energy, a design challenge*; University of Liverpool, England

Scher, R.M.(1985); *Progress on Flap-type Wave Absorbing Devices*; Hydrodynamics of Ocean Wave-Energy Utilization, Iutam Symposium Lisbon, Portugal

Simeons, C. (1980); *Hydro Power, The Use of Water as an Alternative Source of Energy*; Pergamon Press

Suzuki, H.; Yamamoto, M.; Miyazaki, H.; Shioiri, M.; Ogawa, K.(1981); *Comparison of wave power electricity generation systems by model experiments*; Second International Symposium on Wave and Tidal Energy, BHRA, Cambridge, England

Takahashi, S.(1988); *Hydrodynamic Characteristics of Wave-Power-extracting Caisson Breakwater*; Int. Conf. on Coastal Engineering, pp. 2489-2503

Watabe, T.; Kondo, H. Yano, K.(1986); *Studies on a pendulum-type wave energy converter*; Water for Energy, 3rd International Symposium on Wave, Tidal, OTEC, and Small Scale Hydro Energy, BHRA, Brighton, England

Whittacker, T.J.T., Leitch, J.G., Long, A.E., Murray, M.A.(1985); *The Q.U.B. Axisymmetric and Multi-Resonant Wave Energy Converters*; Journal of Energy Resources Technology, Vol.107, pp. 74-80

5 Design of the 'Harbour' Type OWC in a Breakwater

5.1 Introduction

The influence of the shape and form on the performance of an OWC has been investigated by several researchers. A review is given in Section 5.2. The optimal shape for application in the breakwater will be selected. The harbour type OWC is the best one, the immersed front wall has to guide the flow into the device smoothly.

When harbour type oscillating water columns will be used in a wave power converting breakwater, the optimal design (i.e. when the performance of these devices is the best), has to be known. Furthermore, the appropriate spacing between these devices is an interesting parameter.

The theory of 'harbour' type devices is briefly discussed in Section 5.3. In Section 5.4, several theories of 'harbour' type devices are compared to each other. The results of this investigation are given in the same section. All theories which have been investigated are developed for a rectangular chamber, without streamlining. With the results of this section, it has to be possible to determine for a certain location the dimensions of devices as well as the spacing between them.

In Section 5.5, it is mentioned that caisson breakwaters are usually designed by the theory of Goda. In this study that theory will be used. In Section 5.6 the conclusions are drawn and in Section 5.7 the references are given.

5.2 Shape of the Oscillating Water Column Device

5.2.1 Reflecting Back Wall

In the development of the OWC devices, it was already discovered at an early stage that an asymmetric design with a reflecting back wall had a good performance. This improvement of the efficiency (higher value and broader bandwidth) is very clearly illustrated in Figure 5.1 [Elliot et al.;1981]. The NEL Breakwater is based upon the shape with the best performance.

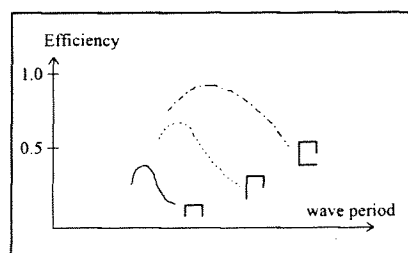


Figure 5.1 Efficiency and column shape

5.2.2 Rectangular or Circular Chamber Area

Two chamber geometries have been compared by McCormick, using model tests in a wave tank [McCormick et al.;1986]. The water surface area of the chambers are equal, one being square and one being circular. The entrance width b of the chambers has been varied. The highest efficiency values for both devices, correspond to the smallest entrances, while the lowest peak values correspond to the widest entrances. Although the efficiency has highest value for the smallest entrance width, the total captured energy increases as the entrance width increases. The efficiency values of the square chamber for each entrance width are higher than those of the circular one. It is concluded that the circular device produces more radiation waves. The conclusion of the experiment was that a rectangular device with an entrance width of the total length ($b = B$) is the best for converting wave power to air power.

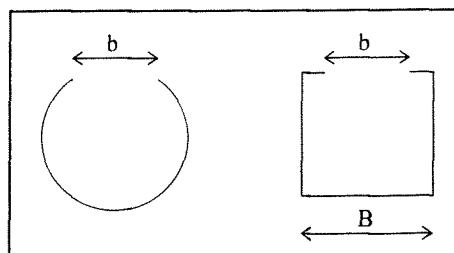


Figure 5.2 Circular and rectangular chamber

5.2.3 Optimal Shape of a Rectangular OWC Device

A number of OWC shapes (two-dimensional, maximum efficiency 100%) were tested by Rao and Koola, using a computer program [Rao et al., 1986]. The efficiency of a device with optimal load control (frequency dependent loading, phase control, see Appendix B: $\Lambda = \bar{Z}$), can be calculated by solving the diffraction problem. The program solves the diffraction problem by calculating the incident and scattered velocity potentials at various points along the free surface. Four parameters were investigated: (1) the depth of immersion of the bottom plate, (2) the front barrier thickness, (3) effect of the shape of entry and (4) effect of streamlining the device.

Bottom depth

From investigation of the depth of the bottom plate of a rectangular OWC two conclusions are drawn. Higher efficiencies are obtained when the depth is larger, while the bandwidth of the efficiency curve increases with increase of the depth. This can be seen in Figure 5.3.

Front barrier thickness

To study the effect of different front barrier thicknesses, the relative performance of a rectangular OWC ($D/L_D=1$) is shown in Figure 5.4. Three different thicknesses are shown, namely 1, 2 and 3 (ascending progression). It can be seen that thinner front barriers give higher efficiency.

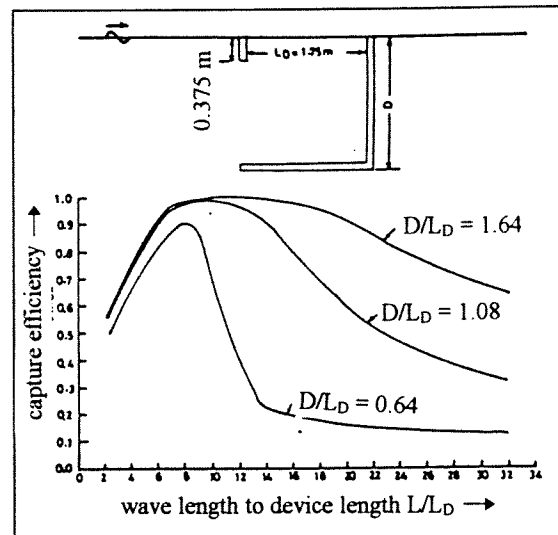


Figure 5.3 Variation of efficiency with depth of immersion

Shape of entry and streamlining

To investigate the influence of the shape of the entrance, devices with a convex and a concave entry below the mean water level have been tested. A comparison has been made between the rectangular type and the streamlined device. The efficiency curves are shown in Figure 5.5. The device equipped with a convex entry, has a high efficiency at a relatively low L/L_D value ($L/L_D = 3$), but the bandwidth is rather small. The device with the concave entry shows a double peaked nature, with a broader bandwidth centred around the second peak. The rectangular OWC shows a peak efficiency at around $L/L_D = 6.5$. The efficiency of the streamlined OWC is the highest and also the bandwidth is very broad.

From the experiments can be concluded that the streamlined OWC device has the best performance. This design has a relatively thick front barrier, that contradicts the results of studying the influence of this thickness. This shows that it is not the thickness that matters but it is the amount of obstruction to the flow that decreases the efficiency. The streamlined front barrier guides the flow into the device smoothly.

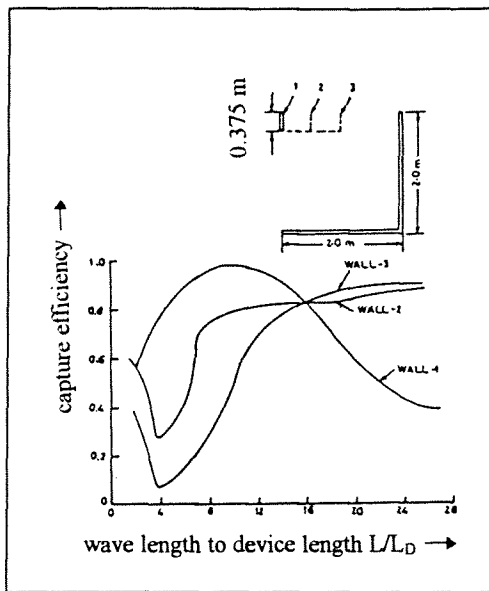


Figure 5.4 Variation of efficiency with front barrier thickness

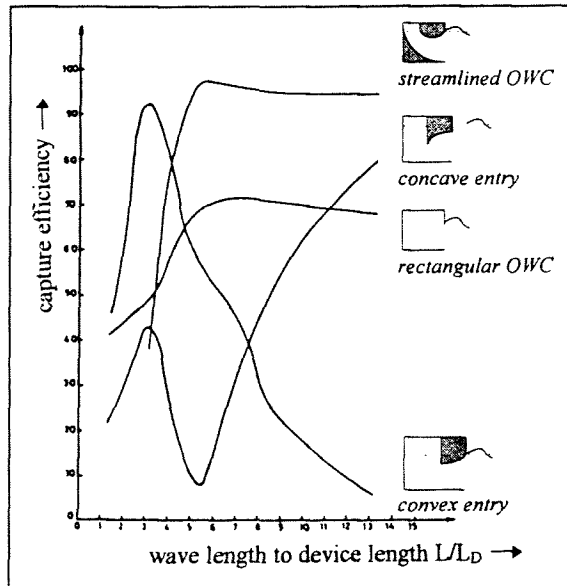


Figure 5.5 Variation of efficiency for different 2-D OWC shapes

5.2.4 Comparison with the 'Harbour' Type OWC

Indian investors who were involved with the research of the best shape of the OWC device made a comparison with the 'harbour' type OWC [Koola et al.;1994]. They report that the best performance of the 'harbour' type OWC occurs when the 'harbour' length equals the chamber length.

The comparison of the rectangular, streamlined and the 'harbour' type device is shown in Figure 5.6. The 'harbour' type device has a chamber length equal to the 'harbour' length.

The peak efficiencies arise at a value of $L_0/L_D = 6.6, 5$ and 11 . This means that the rectangular and streamlined devices have a chamber length L_D of respectively 0.15 and 0.20 times the wave length (assumed that peak efficiency is caused by chamber resonance).

From other literature it is believed that the resonance of the 'harbour' type device is caused by device resonance and not by the chamber resonance, 'harbour' resonance does not appear in the figure. In that case the 'harbour' type device has a total length of 0.18 times the wave length (device length is two times the chamber length).

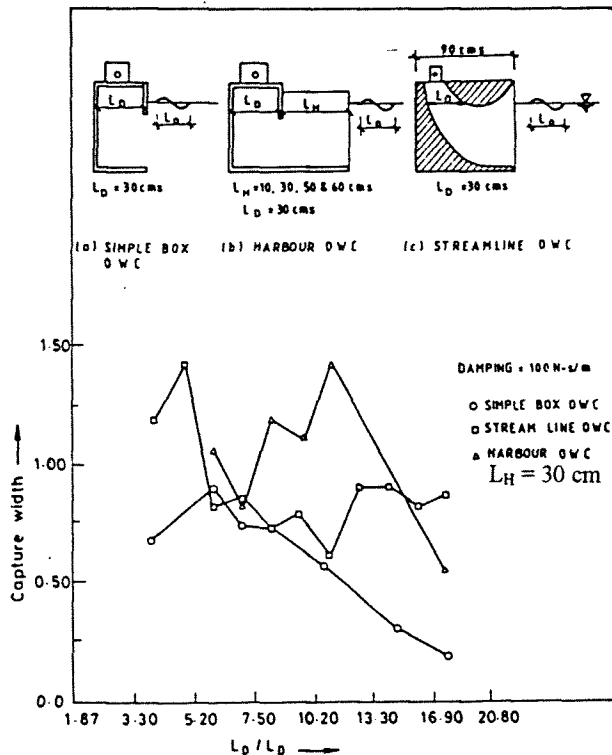


Figure 5.6 Variation of capture width for three different OWC devices

Koola et al. concluded, that for a given wave length the 'harbour' device has the smallest chamber dimensions. Moreover, the total length of this device is of the same order of that of the simple OWC ($0.18 \cdot L_0 \approx 0.2 \cdot L_0$).

The results are in agreement with observations of Count and Evans, see **Appendix G**. They also conclude that a 'harbour' type device with a chamber length equal to the 'harbour' length, has the best performance. The values of device resonance are the same, namely 0.18 times the wave length.

5.2.5 Shape of the 'Harbour'

Gallachóir et al. considered an oscillating water column with a tapered 'harbour' [Gallachóir et al.;1995] It is mentioned that Whittaker and Stewart (1993) have demonstrated experimentally in wave tank as a first result, that a tapered 'harbour' device has a better performance than a device with a rectangular 'harbour'.

A comparison has been made between a device with a rectangular 'harbour' and a tapered 'harbour', see Figure 5.7. However, the results of Gallachóir et al. do not show a significantly better performance of the tapered 'harbour' device. Based on this fact, the rectangular 'harbour' type device is believed to be a good design.

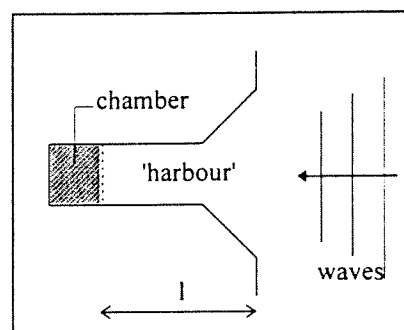


Figure 5.7 Geometry of the tapered 'harbour' OWC device

5.2.6 Pilot Plant Design for Ennore

A prototype wave power converter was proposed for the port at Ennore, India, by Haskoning in association with NEL [Haskoning;1989]. This prototype is based on the NEL 'harbour' type device and incorporated into a rubble mound breakwater. The design is shown in Figure 5.8. In this figure can be seen that some rounding of the entrance is suggested. The width of the chamber and 'harbour' is 8 m.

In the report, the optimal design of the device has been investigated by the NEL specialists. They show that the damping level of the turbine, the incident wave height and the tidal range influence the immersion depth of front wall.

It is mentioned that the height of the entrance of the chamber (4.5 m), effects the performance of the device: if it is too large the bandwidth of the efficiency curve is impaired and if it is too small excessive turbulent losses occur at the immersed front wall as water flows in and out of the chamber.

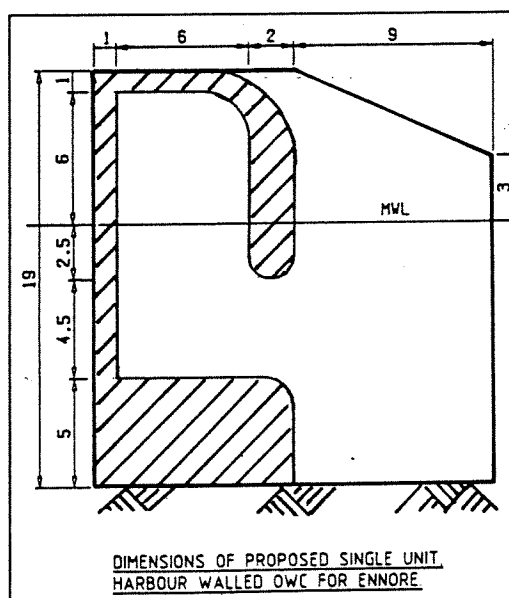


Figure 5.8 Design of the prototype 'harbour' OWC device for Ennore (dimensions in m)

The prototype device for Ennore, is designed by the specialists of NEL. Two 'harbour' type devices are proposed to be incorporated into a rubble mound breakwater. It is mentioned that a device in a reflecting wall has a higher efficiency (up to 40%), than a device in open sea or a non-reflecting wall [Haskoning;1989]. Because of this reason, reflecting vertical sidewalls of 20 m are added at each side of the device, see Figure 5.10.

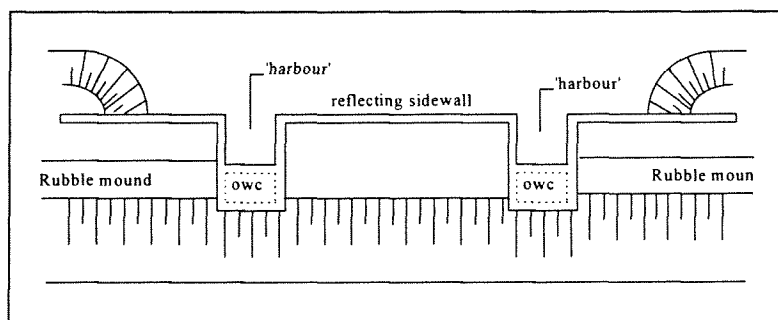


Figure 5.10 Layout of the prototype device for Ennore (schematically)

5.2.7 Conclusions about the Shape of 'Harbour' Type OWC Device

From the experimentally and theoretically obtained performances of the different devices, some general conclusions can be drawn. It was already concluded in the last section of Chapter 4, that the 'harbour' type is decided to be the best applicable device. From the results of Section 5.2, it follows for the design of the harbour type OWC that:

1. The chamber has to be rectangular in plan (Section 5.2.2)
2. The bottom plate has to be as deep as possible, this means that the opening in the front wall must reach to the bottom (Section 5.2.3), however in the report of Haskoning it is mentioned that the height of the entrance must not be too large (Section 5.2.6).

In this study the height of the entrance will be chosen, depending on the water depth at a certain selected location. Further investigation is needed for a theoretical determination of the optimum height of this entrance.

3. The flow into the chamber must be smoothly (low scattering), this fact influences the design of the front barrier (as less as possible obstruction) (Section 5.2.3)
4. The design with the streamlined chamber has in the experiments the best performance (Figure 5.5), in practice, with real dimensions, it is believed that a smooth design of the front barrier is sufficient (Section 5.2.6)

Other design parameters and factors which are of influence on the performance of the device, will be investigated in the next sections.

5.3 Theory of the 'Harbour' Type Device in a Reflecting Wall

5.3.1 Development of the Theory

Malmo and Reitan have studied the performance of a 'harbour' type OWC in a reflecting wall. Firstly they considered a single device symmetrically placed in a channel or equivalently an infinite row of identical and equidistant devices. The waves approaching the device are normally incident [Malmo, Reitan;1985].

The next investigation was a single device placed in an infinitely wide wall and an infinite sea with waves of different angles of incidence [Malmo, Reitan;1986]

Finally, the intermediate case of a finite row of devices in an infinitely reflecting wall and an infinite sea is discussed [Malmo, Reitan;1986]. This case has also been investigated by McIver and Evans [McIver, Evans;1988].

The theory of Malmo and Reitan is based on the oscillating surface-pressure distribution (Appendix H: Part I, II, III). The theory of McIver and Evans (Appendix H: Part IV) and the NEL Breakwater is based on the oscillating body theory.

A review of these articles and the references are given in **Appendix H**. The results, which are based on numerical methods, are important illustrations of the influences of several design parameters.

5.3.2 Vertical Caisson Breakwater instead of a Rubble Mound Breakwater

In part I of Appendix H, the influence of the reflecting sidewalls is investigated. It follows that a device in a reflecting wall has a better performance than a device in open sea or in an absorbing beach (Figure H.2, H.3, H.4). The bandwidth of the efficiency is broader and peak values are higher.

The absorbing beach can be compared to a rubble mound breakwater. In the report of the prototype device for Ennore it is mentioned that the efficiency of a device in a reflecting wall is increased by 40%. It is for this reason, that a wave power converting breakwater constructed by means of caissons has a better performance than a rubble mound breakwater, in which 'harbour' type devices are placed.

5.4 Design Parameters of the 'Harbour' Type Device

5.4.1 Method of Determining the Design Parameters

When an optimum design of a wave power converting breakwater has to be made, for a certain location with a certain wave spectrum, a full numerical approach is the best method. However, the development of a numerical method is time-consuming.

In this study devices for a wave power converting breakwater will be designed, using mainly:

- Appendix H
- design of the NEL Breakwater of South Uist (see Section 4.4.4)
- prototype device of Ennore (see Section 5.2.6)
- Japanese breakwater of Sakata (see Section 4.4.2)

The NEL breakwater for South Uist, has to operate in a water depth of 21 m and for wave periods of about 7 to 20 s. The corresponding wave lengths can be calculated by the linear wave theory using the dispersion relation.

The prototype device for Ennore consists of two devices with reflecting side walls, incorporated in a rubble mound breakwater. The peak periods at which wave energy is highest, lie in the range 8.5 to 9s. Good performance is required in the range of 7 to 11 s. The wave height in operating conditions varies between 0.5 and 1.7 m.

The breakwater at Sakata port is located in 18 m deep water and is designed to operate for waves of 1-5 m. The standard wave for conversion is selected at $H_{1/3} = 2.2$ m and $T_{1/3} = 7$ s. The design wave height for stability is $H_{1/3} = 10.2$ m and $T_{1/3} = 14.5$ s [Takahashi et al.;1992].

Other considerations are structural design and construction requirements. In general, caissons are made of concrete. A concrete caisson is usually divided into a number of inner cells. The size of these cells is limited to 5 m or less. In these ordinary caissons, the use of pre-tensioned concrete is not advantageous. For caissons with special shapes, for instance wave power converting caissons, pre-tensioned concrete can be used [Goda;1992]. Long spans of concrete parts have to be pre-tensioned and must be avoided.

The results of the different theories will be compared as much as possible in the next sections. To compare the results of the different theories, the design parameters have in general been made dimensionless. The purpose is to illustrate clearly the influence of varying the design parameters and to obtain reliable values to design a wave power converting breakwater.

5.4.2 Dimensionless Presentation of Various Design Parameters

The length of the chamber and 'harbour' are important design parameters. In this study the next symbols are used:

- the 'harbour' length, l (in the figures of NEL $l = L$)
- the chamber length, a (in the figures of NEL $a = B$)
- the width of the 'harbour' and the chamber, b (in the figures of NEL $b = Y$).

Device resonance

As known, two resonance frequencies exist for a 'harbour' type device. The first peak, at low frequency (and thus long wave length) can be seen as the quarter-wave resonance of the total device. The resonance of the device can be expressed in the dimensionless factor $(a+l)/\lambda$, which is the total device length divided by the wave length. In the theory of Malmo and Reitan (Appendix H), this resonance frequency occurs at the first peak of the ratio ξ_0 .

'Harbour' resonance

The second peak, at high frequency (and thus short wave length) can be seen as the quarter-wave resonance of the 'harbour'. The resonance of the device can be expressed in the dimensionless factor l/λ , which is the 'harbour' length divided by the wave length. In the theory of Malmo and Reitan (Appendix H), this resonance frequency occurs at the first peak of the ratio π_1 .

Ratio 'harbour' length to device length

A long 'harbour' length compared to the chamber length has advantages. The capture width becomes larger and the peak is shifted to the range of longer wave lengths (Figure H.10; H.20). However, the peak of capture width becomes narrower. An other advantage follows from Figure H.13, the larger the ratio $l/(a+l)$ is, the smaller the turbine can be.

'Harbour' length as a multiple of the chamber length

In most literature, the length of the 'harbour' is expressed as a multiple of the chamber length. The width of the 'harbour' and chamber is also expressed as a multiple of the chamber length.

The dimensions of the NEL Breakwater of Figure 4.18, 4.19 and 4.20 can be expressed in this way, when the 'harbour' length ($l = 5, 10, \dots$ m) is divided by the chamber length ($a = 15$ m). The device has a total length of the chamber, 'harbour' and the thickness of the front wall.

The design of Figure 4.18 has a 'chamber' with a square plane $a = b$. The ultimate design of the NEL Breakwater (Figure 4.19, 4.20) has a 'harbour' length of $l = 17$ m and a chamber length of $a = 10$ m, thus $l/a = 1.7$. The chamber has a width $b = 15$ m, thus $b = 1.5 \cdot a$.

Blocked part of the water depth

The immersed front barrier has a certain depth below the water level. The symbols used are different:

- d (Malmo and Reitan; Fig. 7a, b, c)
- d_c (Japanese breakwater; Fig. 4.12)
- I (NEL; Fig. 4.18, 4.19, 4.20)

The entrance of the chamber is blocked by the immersed part of this front wall and, in the case of the NEL design, by the thickness of the bottom plate. To compare the various results, the part of the water depth which is blocked has been made dimensionless.

In all experiments and designs, the water depth is less than half the wave length, which is the depth influenced by waves. The blocked part of the water depth is made dimensionless by dividing it by the total water depth, this factor is called the blocked part of the water d/h . Because the wave influence decreases with the water depth, different weights should be given to the different depths at which the entrance is blocked.

The blocked part of the devices of Malmo and Reitan is only influenced by the depth of immersion of the front barrier. The entrance of the chamber of the NEL device is blocked by the depth of

immersion of the front wall and by the thickness of the bottom plate. The blocked part by the bottom plate, is given a weight half that of the blocked part by the front wall. This gives for the NEL design a value of $d/h = (6+0.5 \cdot 6)/21 = 0.43$.

5.4.3 Length of the Chamber and 'Harbour'

A good selection of the 'harbour' and chamber length strongly depends on the local wave length spectrum, this can be clearly seen in the Figures 4.18, H.5, H.10, H.13, H.19 and H.20.

From Appendix H, Part I, Figure H.2, H.3 and H.5, the resonance frequencies for devices with various 'harbour' lengths can be derived. In the Figures H.7a, b and c, the influence of the immersion depth is shown.

In Appendix H, Part II, the resonance frequencies for devices with various 'harbour' lengths are shown in Figure H.9 and H.10. In Figure H.12 the influence of varying the length of the chamber is shown, the width of the device is constant ($b = 0.5$ m). Consequently, this figure shows also the influence of the ratio chamber width to chamber length, b/a . The resonance frequencies of a single device given in Figure H.15 and H.16 (Part III) have roughly the same values as in Part II.

In Part IV, results are shown for a device with a width $2a$. The resonance frequencies for an optimal damped device are shown in Figure H.20. The resonance frequencies of a real and constant damped device are shown in the other figures. The frequencies at which resonance of an optimal damped and real constant damped device occurs, are roughly the same.

Influence of the 'harbour' length on device resonance

- (1) Part I; Fig. H.7a,b,c; $d/h = 0$;
 $a = b$
- (2) Part I; Fig. H.7a,b,c; $d/h = 0.3$;
 $a = b$
- (3) Part I; Fig. H.7a,b,c; $d/h = 0.5$;
 $a = b$
- (4) Part I; Fig. H.7a,b,c; $d/h = 0.7$;
 $a = b$
- (5) Part I; Fig. H.5; $d/h = 0$;
 $a = b$
- (6) Part II; Fig. H.10; $d/h = 0$;
 $a = b$
- (7) NEL; Fig. 4.18; $d/h = 0.43$;
 $a = b$
- (8) Part IV; Fig. H.20; $d/h = 0$;
 $2a = b$

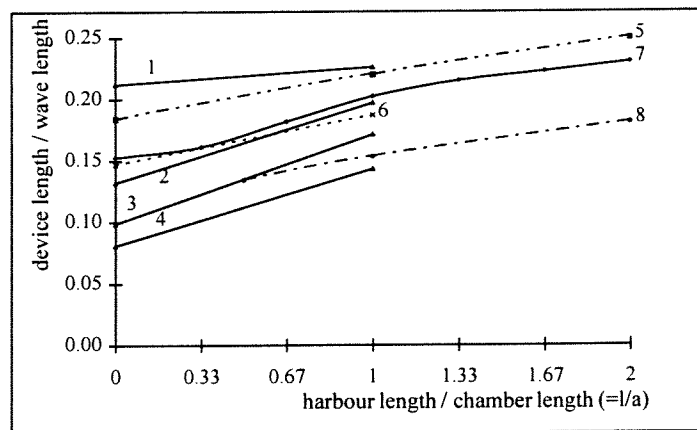


Figure 5.11 Resonance of the device, versus 'harbour' length / chamber length, obtained from various results

An effort has been made to clarify the differences between the various results. The values of (1) and (5) are rather high. This can partly be caused by the fact that $d/h = 0$ (see the influence of immersion depth, Figure 5.18) and partly by the influence of the differences in test conditions. The values of 'harbour' resonance (see the next figure) of the same results (1) and (5), are also higher than those of the others results. The differences between line (1) and (5) can be induced by differences in the width of the device (Fig. H.5: $b = 0.5$ m; Fig. H.7a, b: two-dimensional).

Line (2), (3) and (4) show the influence of an increasing blocked part of the water depth. The results of Part II are shown as line (6). When values of the same theory with $d/h = 0.43$ would exist, the line would probably be close to the results of NEL (line (7); $d/h = 0.43$).

The results of McIver and Evans are shown as line (8). The values are lower than those of line (7), the effect of $d/h = 0$ raises the line, but the effect of a chamber width of $b = 2a$, lowers the line (see the influence of the chamber width, Figure 5.16).

Influence of the 'harbour' length on 'harbour' resonance

- (1) Part IV; Fig. H.20; $d/h = 0;$
 $2a = b$
- (2) Part I; Fig. H.5; $d/h = 0;$
 $a = b$
- (3) NEL; Fig. 4.18; $d/h = 0.43;$
 $a = b$
- (4) NEL; Fig. 4.19; $d/h = 0.43$
 $1.5a = b$
- (5) Part II; Fig. H.9, 10; $d/h = 0;$
 $a = b$

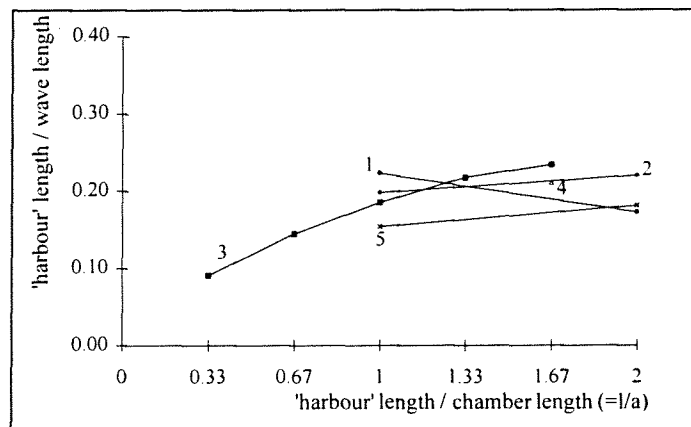


Figure 5.12 Resonance of the 'harbour' versus harbour length / chamber length, obtained from various results

The values of 'harbour' resonance of the various results are quite different. The behaviour of line (1) differs from the others. Although the values of line (1) descend for longer 'harbour' lengths, the resonance frequencies occur at longer wave lengths (see Figure 5.13).

The influence of d/h is not strong (see Figure 5.19) and the influence of the large chamber width $b = 2a$ is not significant (see Figure 5.18). Line (2) has higher values than line (5), this is because line (2) is based on the results of a device in a channel (Part I) and line (5) on the results of a device in open sea (Part II).

The differences between the lines can be caused by some differences between the experiments or designs. For instance, the damping level is not the same (see for the influence of the damping on the resonance frequencies Figure 4.19).

Influence of the 'harbour' length on wave length resonance

Making the 'harbour' length longer, shifts the resonance frequencies of device and 'harbour' to the longer wave lengths. To show this fact, Figure 5.13 is given. It is clear that at longer 'harbour' lengths resonance occurs at longer wave lengths.

- (1) NEL device resonance Fig. 5.11 line (7)
- (2) device resonance Fig. 5.11 line (8)
- (3) NEL 'harbour' resonance Fig. 5.12 line (3)
- (4) 'harbour' resonance Fig. 5.12 line (1)

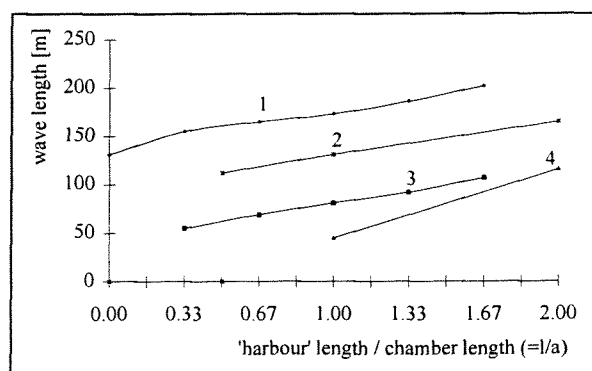


Figure 5.13 Resonance wave length of the device and the 'harbour' of the NEL Breakwater versus l/a

Conclusion

Figure 5.11 and 5.12 show the influence of the 'harbour' and chamber length for the device resonance and the 'harbour' resonance. However, the results of the several theories are not completely the same,

this partly because of variation in parameters (e.g. width of the device) and because of variation in the theories themselves. To select the length of the harbour and chamber of a device at a certain location, universal design rules are desirable.

The NEL design is made for a real situation, namely South Uist. In this design the front wall is immersed below the water level and the entrance opening to the chamber is limited. The device has a constant damping level (selected at two times the optimum damping level at resonance frequency), what means that a real turbine can be used that is frequency independent. It is for these reasons that the NEL design is assumed to be representative for other practical designs.

The values for device resonance in this study, are determined in the following manner:

- The NEL Breakwater result with $a = b$ and $d/h = 0.43$ (line (7); Fig. 5.11), is assumed to be representative for other practical designs.
- Also the results for a device in an infinite sea of Malmo and Reitan with $a = b$ will be used. The device with an immersion depth of the front barrier $h = 0$, is shown as line (6) in Figure 5.11. However, the values of this line would be lower when the value of d/h is not zero. A change from $d/h = 0$ to $d/h = 0.43$, has been made in the same way as the change of line (1) to line (3) in Figure 5.11. The points are fitted by lines, which go asymptotically to a value of 0.25, since resonance values are assumed to be roughly quarter-wave resonances.

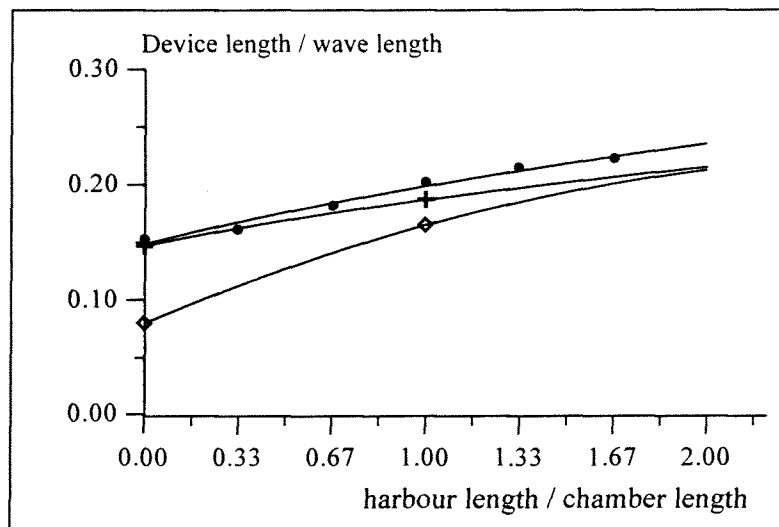


Figure 5.14 Device resonance versus l/a

- + Fig. H.9, H.10, infinite sea: $d/h = 0$, $a = b$
- Fig. 4.18, NEL: $d/h = 0.43$, $a = b$
- ◊ estimation, infinite sea: $d/h = 0.43$, $a = b$

The estimated line with $d/h = 0.43$ differs from the line based on the NEL design. However at values of l/a higher than about 1.5 the results are close together.

As mentioned, the NEL design is assumed to be representative for other practical designs. In this study, the line derived from the NEL designs will be used. For the design of a device with a square chamber ($a = b$) at a certain location, the optimal length of the device can be selected from Figure 5.14.

The 'harbour' resonance can be determined in a similar way as the device resonance. The results of the NEL Breakwater (Fig. 5.12; line (3)) and the device in an infinite sea of Malmo and Reitan (Fig. 5.12; line (5)) are used. The influence of d/h on the 'harbour' resonance is assumed to be neglectable (see Fig. 5.19). The results are fitted by lines, which go asymptotically to a value of 0.25, since resonance values are assumed to be roughly quarter-wave resonances.

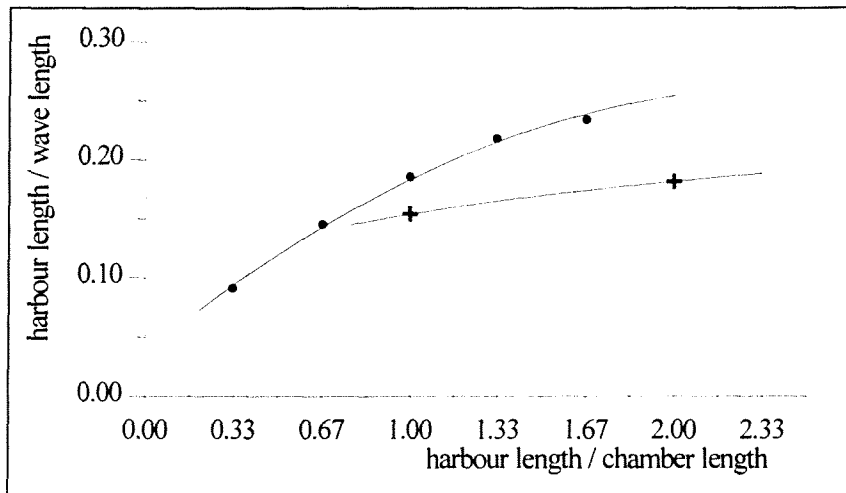


Figure 5.15 Device resonance versus l/a

- + Fig. H.9, H.10, infinite sea: $d/h = 0$ $a = b$
- Fig. 4.18, NEL: $d/h = 0.43$ $a = b$

The two lines do not agree very well. Because the design of the NEL device is assumed to be representative for other practical designs, this line will be used. For the design of a device with a square chamber ($a = b$) at a certain location, the optimal length of the 'harbour' can be selected from Figure 5.15.

5.4.4 Width of the Chamber and 'Harbour'

As mentioned, the width of the chamber and 'harbour', b , can be expressed as a multiple of the chamber length, a . In most cases of Part I to III the chamber has a square plane $a = b$, in Part IV the width is two times the chamber length: $b = 2a$.

The design of the NEL Breakwater shows two different widths of the device, $a = b = 15$ m (Figure 4.18) and $b = 1.5 \cdot a = 15$ m (Figure 4.19, 4.20). Figure H.10 (Part II) shows the resonance frequency of a device with and without a 'harbour' for different widths. Figure H.20 (Part IV) shows the results of a device with a width $2a$.

The influence of the width of the device on the resonance frequency of the device and the 'harbour' is shown in the next two figures. It must be noted that, differences in other parameters between the various theories exist, like different values of d/h and l/a .

Influence of device width on device resonance

- (1) Part II; Fig. H.10; $l/a = 1$; $d/h = 0$
- (2) NEL; Fig. 4.18, 20; $l/a = 1.7$; $d/h = 0.43$
- (3) Part II; Fig. H.10; $l/a = 0$; $d/h = 0$
- (4) Part IV; Fig. H.20; $l/a = 2$; $d/h = 0$
- (5) Part IV; Fig. H.20; $l/a = 1$; $d/h = 0$
- (6) Part IV; Fig. H.20; $l/a = 0.5$; $d/h = 0$

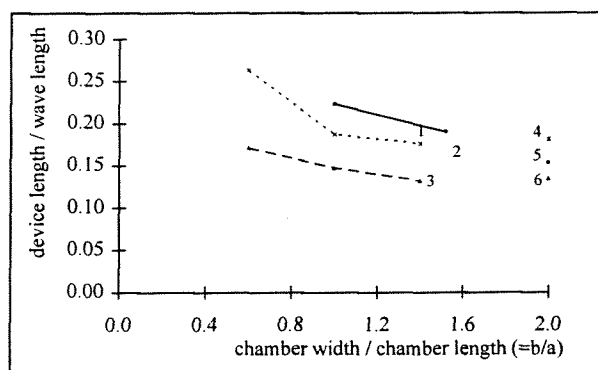


Figure 5.16 Resonance of the device versus b/a

The general trend of all results is the same, however some differences exist. Line (1) has higher values than (3) because of the 'harbour'. The results of NEL are derived from two designs (Fig 4.17 and 4.18) with $l/a = 1.7$, $d/h = 0.43$. Compared to the other lines, the value $l/a = 1.7$ increases the results, but $d/h = 0.43$ lowers them. It is assumed that, when the NEL Breakwater would have a value $l/a = 1$ (see Figure 5.11) and the device of line (1) a value of $d/h = 0.43$ (see Figure 5.18), these two lines will agree better. The points (4), (5) and (6) are roughly in line with the other results. Point (5) can be seen as the last value of line (1).

The resonance in the design of the Japanese breakwaters, which have no 'harbour' occurs at a chamber length of 0.13 times the wave length [Ojima et al.;1984] [Takahashi;1988]. The devices in these breakwaters are placed beside one another and consequently act like a terminator. In that case, the factor b/a is very high. For high values of b/a the value of device length / wave length of 0.13 is in agreement with Figure 5.16.

Influence of device width on 'harbour' resonance

- (1)NEL; Fig. 4.18, 20; $l/a = 1.7$; $d/h = 0.43$
- (2)Part II; Fig. H.9; $l/a = 2$; $d/h = 0$
- (3)Part II; Fig. H.10; $l/a = 1$; $d/h = 0$
- (4)Part IV; Fig. H.20; $l/a = 1$; $d/h = 0$
- (5)Part IV; Fig. H.20; $l/a = 2$; $d/h = 0$

The results of McIver and Evans point (4) and (5) are not in agreement with the other results. It can be expected that point (5) would have a higher value than that of (4). This remarkable fact was already discussed for line (1) of Figure 5.12.

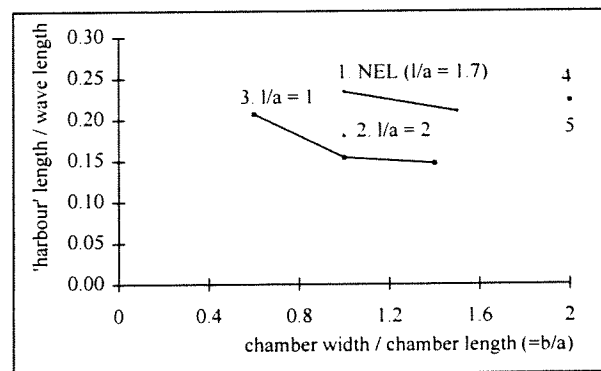


Figure 5.17 Resonance of the 'harbour' versus b/a

However, the influence of the width of the device on the 'harbour' resonance is not clearly shown in this figure. The Figures H.6 and H.10 of Appendix H, show that the longer the width of the device, the more the device will act like a two-dimensional device with a 2-D efficiency of 1 or capture width of 1.

Conclusion

It can be seen in the Figures 5.16 and 5.17 that, the lower the value b/a , the shorter the resonance wave length become, in particular when b/a is lower than 1. In the range of $b/a = 1-2$, the influence of the width is less important. Consequently, the width will be selected between 1-2 times the chamber length.

When the width is changed from $b = a$ to $b = 1.5 a$, the device length / wave length value is decreased by a factor 0.88 and the 'harbour' length / wave length value is decreased by a factor 0.9.

The width of the device is also influenced by the structural considerations of concrete.

5.4.5 Immersion Depth of the Front Barrier

The influence of immersion depth is shown in Figure H.7a, b, and c. The deeper the immersion, the narrower the peak performance of the device and the more the device resonance is shifted to the longer wave lengths. This influence is shown in the next two figures.

The resonance values of the NEL Breakwater are also shown. The device width of the NEL design is the same as in Figure H.7a, b and c, namely $a = b$. The value of the blocked part is assumed to be 0.43, which seems to be reasonable.

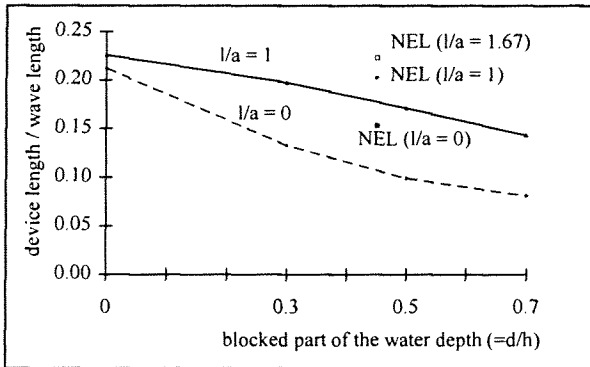


Figure 5.18 Influence of the blocked part of the water depth on device resonance

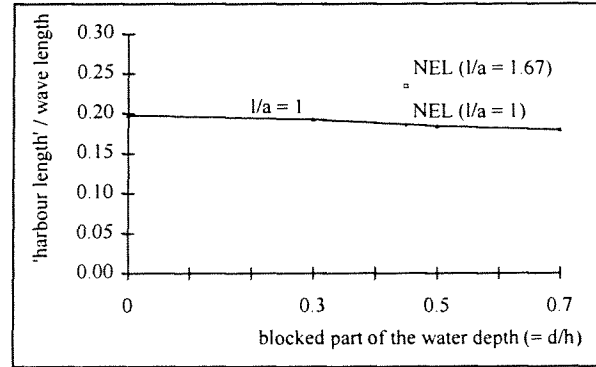


Figure 5.19 Influence of the blocked part of the water depth on 'harbour' resonance

The immersion depth of the front barrier, depends on the wave height at operating conditions. During operation the barrier must remain submerged. In most calculations of Appendix H this depth is zero. In practice, when the depth is zero, the efficiency will be rather low. When it is immersed deeper, the efficiency is increased up to a certain value. The Japanese inventors mention that maximum efficiency is obtained when the immersion depth equals $0.5 \sim 1.0$ · wave height, see Fig. 4.13. Beyond that level the efficiency turns to decrease, because of narrowing the entrance of the chamber.

For determination of the immersion depth the next information is given:

Immersion depth in Japanese literature:

theory: - $0.5 \sim 1.0$ · wave height of operation, for best performance [Ojima et al.;1984]
 - $0.25 \cdot H_{\max}$ (= maximum wave height in storm conditions), for not receiving severe impact air pressure [Takahashi;1988]

design Sakata: - immersion depth 3 m below LWL (3.5 m below HWL)
 - water depth of 18 m
 - bottom plate 3.5 m
 - rubble mound foundation 5.5 m
 - entrance opening 9 m
 - entrance opening / water depth = $9/18 = 0.5$
 - wave heights in operating conditions 1-5 m
 - wave heights in storm conditions 10.2 m
 - maximum wave heights in storm conditions $H_{\max} = 15.3$ m
 - immersion depth = $3.25/15.3 = 0.21 \cdot H_{\max}$

[Nakada et al.;1992]

Immersion depth in NEL designs:

theory: - the wave height in the chamber has to be less than two times the incoming wave height (column magnification less than 2), this can be arranged by a good selection of the damping
 - consequently, an immersion depth of about the wave height in operating condition is needed

design South Uist: - immersion depth 6 m below MWL
 - water depth 21 m
 - bottom plate 6 m
 - entrance opening 9 m
 - entrance opening / water depth = $9/21 = 0.43$
 - wave heights in operation conditions are assumed at 1- 5 m, thus an immersion depth of about $1.0 H_{\text{operating}}$

- assumed $H_{\max} = 0.8 \cdot \text{water depth} = 17 \text{ m}$, thus an immersion depth of $0.35 \cdot H_{\max}$ [Hunter; 1991]

- design Ennore:
- immersion depth 2.5 m below MWL
 - water depth 12 m
 - bottom plate 5 m
 - entrance opening 4.5 m
 - entrance opening / water depth = $4.5/12 = 0.38$
 - wave height in operating condition 0.5-2.5 m, thus an immersion depth of about $1.0 H_{\text{operating}}$
 - assumed $H_{\max} = 0.8 \cdot \text{water depth} = 9.6 \text{ m}$, thus an immersion depth of $0.26 \cdot H_{\max}$ [Haskoning; 1989]

Conclusion

The recommendation of an immersion depth of $0.25 \cdot H_{\max}$ by the Japanese theory is also valid for the NEL designs. The design of South Uist has a higher value what is probably caused by the high tidal variation at this location.

The Japanese devices have an immersion depth of $0.5 \sim 1.0 \cdot \text{wave height}$ in operating conditions. The NEL design have an immersion depth of about $1.0 H_{\text{operating}}$. This difference is caused by the fact that the Japanese devices have no 'harbour'. The NEL designs with a 'harbour' have (theoretically) standing waves in the 'harbour' and in the total device, in that case the wave height is two times the height of incoming waves and the immersion depth has to be $1.0 \cdot H_{\text{operating}}$. The wave height in the chamber is less than two times the incoming wave height, what is arranged by a good selection of the damping level.

It follows that the two methods ($0.25 \cdot H_{\max}$ and $1.0 \cdot H_{\text{operating}}$) do not differ very much. By using both methods, the immersion depth of a 'harbour' type device at a certain location can be determined. The height of the entrance opening to the chamber is in all design about 0.4-0.5 times the water depth.

5.4.6 Height of the chamber

The major design requirement of the chamber height (internal freeboard) is the avoidance of water ingress into the turbine. Consequently, the height of the chamber depends on the wave amplitude magnification in the chamber and thus of the damping (Figure 4.18). The chamber height is also dependent on the total height of the breakwater (which depends on overtopping and stability demands).

Chamber height in Japanese literature:

- theory: - internal freeboard $0.5 \cdot H_{\max}$ [Takahashi; 1988] [Ojima et al.; 1984]
 design Sakata: - the internal freeboard is about 10 m (the crest height is 12.5 m above LWL)
 - $H_{\max} = 15.3 \text{ m}$
 - see also Section 5.4.7 about crest height

Chamber height in NEL designs:

- theory: - magnification factor normally not more than 2 [Hunter; 1991], consequently a minimum chamber height of the wave height in operating condition
- design South Uist: - 5.5 m internal freeboard
 - damping level with a chamber wave magnification of less than 2 (about twice the damping level which will maximise the efficiency at the column's resonance frequency) [Hunter; 1991]
- design Ennore: - 6 m internal freeboard, damping level with a wave magnification of less than 2 [Haskoning; 1989]

Conclusion

The recommendation of an internal freeboard equal to the wave height in operating conditions (NEL) is not sufficient to prevent water intrusion during rough sea conditions. In the Ennore design a considerable higher value is used. The recommendation of the Japanese theory of an internal freeboard of $0.5 \cdot H_{\max}$ in design conditions (high water level, rough sea) is better to protect the turbine. Consequently, this value will be used in the design of a device at a certain location.

5.4.7 Crest Height of the breakwater

The crest height of the breakwater is dependent on overtopping demands and its stability. The overtopping demands depend on the function of the breakwater. Due to overtopping of the breakwater, waves are transmitted to the area behind the breakwater. When a breakwater has to protect a port, the overtopping demands are determined by the economical loss when the port activities are annoyed and the costs of constructing a higher breakwater.

Sometimes no overtopping is permitted to provide under all conditions a calm harbour for ships, in other cases overtopping is allowed only in severe wave conditions. The part of transmitted waves can be expressed as the transmission coefficient, i.e. the ratio between the transmitted wave height behind the breakwater to the incoming wave height.

In Japan the caisson breakwaters have a relatively low crest height. The recommendation for ordinary breakwaters is a crest height of $0.6 \cdot H_{1/3}$ above high water level in design condition (storm), see Figure 5.20. For the design storm condition, this elevation is certainly insufficient to prevent wave agitation by overtopping waves. In Japan the design waves are accompanied by strong gale and storm winds. In these conditions, safe mooring of large vessels in parts of the harbour cannot be guaranteed, even if wave overtopping should be reduced to minimum. The storm waves within the return period of one year or less, are much lower than the design wave. Therefore, the crest elevation is thought to be sufficient for maintaining a harbour basin calm at the ordinary stormy conditions. [Goda;1992].

Sloping front wall caissons, like the Sakata Breakwater, need a crest height of wall $1.0 \cdot H_{1/3}$ above high water level in design condition (storm), see Figure 5.20. At this crest height, wave transmission is reduced to a level as low as that by an ordinary caisson breakwater with a height $0.6 \cdot H_{1/3}$. When the sloped front wall caisson converts wave power, the wave transmission is probably lower [Takahashi;1988].

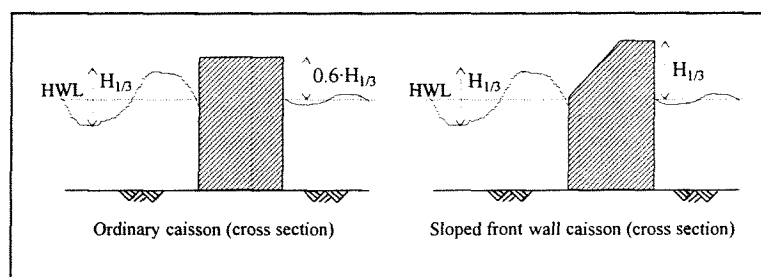


Figure 5.20 Crest height of an ordinary and a sloped front wall caisson in Japan

The breakwater at Sakata has a crest height of 12 m above HWL. The design storm wave height $H_{1/3} = 10.2$ m. This means a crest height of $1.18 \cdot H_{1/3}$.

In Europe crest heights of vertical breakwaters are in general higher than in Japan [Oumeraci;1994(a)]. According to the PIANC recommendations, 1976, the crest height should be $1.3 - 1.5 H_u$. About the influence of the geometry of the caisson nothing is mentioned. H_u is the design wave height related to the limit state of use, which is $H_z 1/10$. $H_z 1/10$ is the average weight of the highest one tenth of all wave heights H_z [Oumeraci;1994(b)].

For determination of the crest height of rubble mound breakwaters, other recommendations are used, which are not discussed in this study.

Conclusion

The height of the crest of a breakwater depends on several subjects like caisson geometry, stability and overtopping demands. In Europe in general higher crests are used than in Japan. However, no good design method is given. In this study the Japanese recommendations will be used.

5.4.8 Turbine characteristic and damping level

In Appendix F is concluded a good air turbine will be linear, which means that the pressure drop across the turbine is linear to the flow through it. No phase control method is already available, what means that a real turbine characteristic will be used. The damping will have a fixed value (frequency independent, standard turbine without variable settings). This value must be chosen in a proper way.

Information for determination of a fixed damping level:

- damping equal to twice the optimum damping (twice the damping level which maximises the efficiency at the resonance frequency) [Hunter;1991]
- damping such that column magnification is not to large (less than two) [Hunter;1991]
- damping in relation with the available wave power, when lower damping is used, a larger part of the capacity can be considered as firm power [Dawson;1979] [Haskoning;1989]
- lower damping means smaller turbine and consequently, lower costs [Dawson;1979]
- lower damping requires lower transmission capacity and consequently, lower costs [Dawson;1979]

5.4.9 Spacing between the devices in the breakwater

The distance between the OWC's is an important parameter in the design of a wave power converting breakwater. This distance has been investigated in **Appendix H**, in particular in Part III and IV. Placing more devices in a reflecting wall at a well selected distance from each other, can increase the captured power considerably. Even when the waves are not normally incident, the captured power can be increased. The spacing depends on the number of devices and the wave spectrum.

McIver and Evans say that this spacing can be chosen without reference to the characteristic of the device [McIver, Evans;1988]. However, Malmo and Reitan show that for instance the length of the 'harbour' affects the value of spacing slightly, see Figure H.19. This figure shows that the spacing for a system of two devices must be $0.6 - 0.7 \lambda$, dependent on the 'harbour' length.

The selection of the appropriate spacing depends strongly on the number of devices. The spacing must be chosen not too close to the maximum power amplification, because it decreases very fast at the right side of this maximum, in particular for systems comprising a lot of devices (Figure H.18). In practice the spacing must be chosen dependent on the local wave spectrum with the power amplification value higher than $I_p = 1$. This means a value of about $0.6 - 0.8$ times the wave length.

In the NEL design, discussed in Chapter 4, the appropriate spacing in a system of two devices is slightly more than half the wavelength, for which the system is tuned [Hunter;1991]. Also in the design for Ennore a spacing in the order of half the wave length is proposed [Haskoning;1989].

The influence of the angle of incidence on the appropriate spacing has not been investigated in the used literature [Malmo,Reitan;1986,b] [McIver,Evans;1988]. When waves are obliquely incident, further investigation for the appropriate spacing is required.

Conclusion

The optimum spacing depends on the number of devices and the wave length of the incident waves. The angle of incidence influences the value of the amplification factor. In this study the optimum spacing for normally incident waves is used.

5.4.10 Reflection of the breakwater

The waves reflected by the breakwater can be harmful to anchoring and navigation of ships in the offshore area of this breakwater. The reflected part of the waves can be expressed by the reflection coefficient of the breakwater, i.e. the ratio between the reflected wave to the incoming wave height.

This reflection is influenced by the degree of dissipation of the wave energy. When a very low part of the waves is allowed to reflect, then the breakwater must be able to dissipate (i.e. capture and convert) the wave energy in any sea state. Consequently, wave power converting breakwaters have less reflection than other caisson breakwaters [Takahashi;1988].

Conclusion

A Japanese wave power converting breakwater, like that at Sakata, will likely have a lower reflection coefficient than a breakwater, along which at intervals 'harbour' type OWC devices are placed, like the proposed NEL Breakwaters. Although, no information is given in literature about the reflection of this last type of breakwater, a rough estimation can be made by calculating the wave power conversion.

5.5 Theory for Caisson Breakwaters

To calculate the stability of caissons attacked by waves, some methods exist. In Italy a method based on the pressure distribution of Sainflou is used. In Japan, for years design manuals for waves and breakwaters have been published. In the 1980 edition of technical standards, the Goda formulas to calculate the design wave forces on the upright section of breakwaters were adopted as a standard method in the design of composite breakwaters [Goda;1992]

Many breakwaters in Japan have been constructed, using the Goda formulas for the design. Also new type breakwaters, like the breakwater at Sakata can be designed with this method.

Conclusion

In this study, the Goda method for the design of a caisson breakwater will be used.

5.6 Conclusions

The optimal shape of the 'harbour' type device has been determined. The plan of the chamber and 'harbour' have to be rectangular. The Indian researchers concluded that the deeper the bottom plate is, the better the performance of the device. However, the NEL specialists mention that a too large entrance of the chamber impairs the bandwidth of the efficiency curve. In this study the height of the entrance will be chosen, depending on the water depth at the location. Further investigation (numerical methods or experimental models) is needed for a theoretical determination of the optimal height of this entrance.

The front barrier has to be rounded, so that the movement of water flow into the chamber is smooth. The depth of the front barrier depends on the wave height at operating conditions. Two values for determination of the immersion depth can be used, namely a depth of 0.5~1.0·wave height in operation conditions and a depth of $0.25 \cdot H_{max}$ (= maximum wave height in storm conditions). The values of these two methods do not differ very much in general. By using both methods, the immersion depth of a 'harbour' type device at a certain location can be determined. The height of the entrance opening to the chamber is in all design about 0.4-0.5 times the water depth.

A device in a reflecting wall has a better performance than a device in open sea or in an absorbing beach (Appendix H, Part I). The bandwidth of the efficiency is broader and peak values are higher. It is for this reason, that a wave power converting breakwater constructed by means of caissons has a better performance than a rubble mound breakwater, in which 'harbour' type devices are placed.

When an optimal design of a wave power converting breakwater has to be made, for a certain location with a certain wave spectrum, a full numerical approach is the best method. However, the development of a numerical method is time-consuming. In this study a breakwater will be designed by using the results of several designs and theories.

To design a device, the 'harbour' and chamber length and the corresponding resonance frequencies of the device and the 'harbour', can be selected from two figures (Figure 5.14 and 5.15). These figures are believed to be representative for practical design with a device width equal to the chamber length.

The longer the width of the device, the more the device will act like a two-dimensional device with a capture width equal to the device width. It can be seen in the Figures 5.16 and 5.17 that, the lower the value b/a , the shorter the resonance wave length become, in particular when b/a is lower than 1. In the range of $b/a = 1-2$, the influence of the width is less important. Consequently, the width will be selected between 1-2 times the chamber length.

The major design requirement of the chamber height (internal freeboard) is the avoidance of water ingress into the turbine. Consequently, the height of the chamber depends on the wave amplitude in the chamber and thus of the damping. Two methods for determination exist, namely an internal freeboard of $0.5 \cdot H_{\max}$ or $1.0 \cdot H_{\text{operating}}$, when the magnification factor is less than two.

In Japan the caisson breakwaters have a relatively low crest height. The recommendation for ordinary breakwaters is a crest height of $0.6 \cdot H_{1/3}$ above high water level in design condition (storm). Sloped front wall caissons, like the Sakata Breakwater, need a crest height of wall $1.0 \cdot H_{1/3}$. According to the PIANC recommendations, 1976, the crest height should be $1.3-1.5 H_u$ (H_u is the design wave height related to the limit state of use, which is $H_{z 1/10}$).

The turbine will be linear and without phase control. The damping will have a fixed value, what means a standard turbine without variable settings. This value must be chosen in a proper way.

Placing more devices in a reflecting wall at a well selected distance from each other, can increase the captured power considerably. The selection of the appropriate spacing depends on the number of devices. In practise the spacing must be chosen dependent on the local wave spectrum with the power amplification I_p higher than 1. This means that the spacing has a value of about $0.6 - 0.8$ wave length.

The wave reflection is influenced by the degree of dissipation of the wave power. A Japanese wave power converting breakwater, like that at Sakata, will likely have a lower reflection coefficient than a breakwater, along which at intervals 'harbour' type OWC devices are placed, like the proposed NEL Breakwaters. Although, no information is given in literature about the reflection of this last type of breakwater, a rough estimation can be made by calculating the wave power conversion.

To calculate the stability of caissons attacked by waves, some methods exist. In Japan, in 1980 the Goda formulas were adopted as a standard method to calculate the design wave forces on the upright section of breakwaters. Since then, many breakwaters have been constructed, using these formulas. In this study, also the Goda method to calculate the stability of the breakwater, will be used.

5.7 References

Dawson, J.K.(1979); *Wave Energy*, Energy Paper Number 42; Department of Energy, Harwell, England

Elliot, G., Roxburgh, G.(1981); *Wave energy studies at the UK National Engineering Laboratory*; Second Int. Symposium on Wave and Tidal Energy, BHRA, Cambridge, England

Gallachóir, B.P.O., Sarmiento, A.J.N.A., Thomas, G.P.(1995); *The Hydrodynamic of a Wave-Power Device in a Tapered Harbour*; Proc. of the Int. Offshore and Polar Engineering Conference, The Hague, The Netherlands

Goda, Y.(1992); *The Design of Upright Breakwaters*; Proc. of the Short Course on Design and Reliability of Coastal Structures, attached to the 23rd Int. Conf. on Coastal Engineering, pp. 547-568

Haskoning, Tebodin, Rites (1989); *Paradip - Ennore Coal Transport Feasibility Study, Final Report*; Haskoning, The Netherlands

Hunter, R.(1991); *Future possibilities for the NEL Oscillating Water Column wave energy converter*; Seminar on Wave Energy, Imeche, England

Koola, P.M., Ravidran, M., Aswathanarayana, P.A.(1994); *Studies on the Relative Performance of Three Oscillating Water Column Wave Energy Devices*; Journal of Energy Resources Technology, Vol. 116, pp. 287-289

McCormick, M.E., Altera, A.G.(1986); *A comparative study of two capture chamber geometries*; Proc. of the Int. Symposium on Utilization of Ocean Waves, Wave to Energy Conversion, ASCE, Scripps Institution of Oceanography, USA

Nakada, H., Suzuki, M., Takahashi, S., Shikamori, M.(1992); *Development test of wave power extracting caisson breakwater*; Civil Engineering in Japan, Vol.31, pp.146-164

Ojima, R., Suzumura, S. Goda, Y.(1984); *Theory and experiments on extractable wave power by an oscillating water-column type breakwater caisson*; Coastal Engineering in Japan, Vol.27, pp. 315-326

Oumeraci, H.(1994(a)); *Japanese Experience on Composite Breakwaters*, Discussion; Proc. of the Int. Workshop on Wave Barriers in Deepwaters, Yokosuka, Japan

Oumeraci, H.(1994(b)); *Review and analysis of vertical breakwater failures - lessons learned*; Coastal Engineering, 22, pp. 3-29

Rao, C.L., Koola, P.M.(1986); *Analytical studies on optimal shape of a two-dimensional water column*; Water for Energy, Third Int. Symposium on Wave, Tidal, OTEC and Small Scale Hydro Energy, BHRA, Brighton, England

Takahashi, S.(1988); *Hydrodynamic Characteristics of Wave-Power-extracting Caisson Breakwater*; Int. Conf. on Coastal Engineering, pp. 2489-2503

Takahashi, S., Nakada, H., Ohneda, H., Shikamori, M.(1992); *Wave Power conversion by a prototype Wave Power Extracting Caisson in Sakata Port*; Int. Conf. on Coastal Engineering, pp. 3440-3453

Whittaker, T.J.T., Leitch, J.G., Long, A.E., Murray, M.A.(1985); *The Q.U.B. Axisymmetric and Multi-Resonant Wave Energy Convertors*; Journal of Energy Resources Technology, Vol.107, pp. 74-80

6 Location of the Breakwater and Design Conditions

6.1 Introduction

In this chapter a location for a wave power converting breakwater is selected and described. In the following section various suitable sites are selected. The Port of Bilbao, Spain, is preferred as the location for the design conditions of the wave power converting breakwater. A description of the location is given in Section 6.2.3.

The water level and wave climate are discussed in Section 6.3. The water level is influenced by the tide and by the wind set-up. The wave climate is described by the wave height, period, direction and steepness. The wave steepness is an important parameter to show the correlation between wave height and period. With this correlation the wave power, corresponding to a particular wave length can be estimated.

In Section 6.4, the design conditions are described. Two design conditions exist, namely the ultimate limit state, U.L.S and the serviceability limit state, S.L.S. The first state is important for the stability and strength of the breakwater. The second condition is formed by the frequently occurring water levels and wave climate, which are important for functioning of the breakwater for harbour protection as well as for wave energy conversion.

Finally, some conclusions are drawn in Section 6.5 and the references are given in Section 6.6.

6.2 Selection of the Location

6.2.1 Selection Criteria

To select the location for the wave power converting breakwater, the availability of wave data is important, the wave climate has to be attractive for wave power conversion and it is preferred that a breakwater is desired. The choice for a caisson breakwater (Section 5.3.2), implies that the water must be relatively deep, otherwise a rubble mound breakwater would probably be more economically attractive. The following criteria are used in this study:

Quantity of wave power

From general figures of wave height, wave length and wave power the places in the world where substantial wave power is available, are known, see Figure 3.1.

Availability of wave data

In this study no wave measurement program is possible, consequently the wave data have to be available. Not only averaged values of wave height and length have to be known, but also the distribution over the year and the direction of the waves.

Suitability of the wave power for conversion by the breakwater

To convert the wave power, it has to be fairly homogeneously divided over the year. When for instance most of the wave power exists during the monsoon, the suitability for conversion is lower than when wave power exists during the whole year. Another factor is the difference in water level. A small tidal range is preferred.

Desirability of a breakwater

When a breakwater is needed, construction costs can be shared. At present, the experience with full-scale wave power converting breakwaters is still modest. Consequently, a breakwater only for wave power conversion has less good prospects, see also Section 3.6.

Availability of topographical data

Also other information about the location has to be known, like water level (tide), bottom depth, soil quality, etc.

Water depth

The breakwater must be located in a water depth, which is deep enough to make a caisson breakwater more economically attractive than a rubble mound breakwater.

6.2.2 Possible Locations

India is interested in wave power conversion. Based on the 'harbour' type OWC device (MOWC principle), a 150 kW capacity wave power converting caisson, has been constructed at the South West Coast near Trivandrum, during 1990. Other proposed designs consists of 'harbour' type OWC devices placed into a rubble mound breakwater at Ennore [Haskoning;1989] and Thangassery, near Quillon town [Neelamani et al.;1995]. These designs would be test facilities, because of the non-maximal utilisation of wave power by a rubble mound breakwater [Haskoning;1989]. However, the annual average wave power along the Indian coast of 5 to 10 kW/m is relatively low compared to other countries.

Some countries in East Asia are constructing harbours and artificial islands. For these locations breakwaters are needed. In Korea, near the city of Pusan, an artificial island with a breakwater of 4.3 km is proposed. This caisson type breakwater is located at a water depth of about 25m [Lee et al.;1994]. Japan and Taiwan have many caisson breakwaters [Kuo;1994]. The available wave power is considerable in Japan, Korea and Taiwan.

South Africa and South America have considerable wave power. South Africa is involved in the development of wave power conversion.

In Europe, England and the Scandinavian countries are interested in wave power converting. Spain and Portugal are exposed to rather high wave power. In Spain more than 20 ports have vertical breakwaters [Ligteringen;1994]. It can be concluded, that there are possibilities for a caisson breakwater combined with 'harbour' type OWC devices.

New breakwaters are necessary in the Port of Bilbao, a harbour at the Spanish Cantabric Coast, within the Bay of Biscay, see Figure 6.1, 6.2 and 6.3.

These breakwaters are part of an ambitious extension project, called 'Abra Exterior'.

- The proposed breakwaters will be rubble mound and are located at a depth of 20 to 25 m.
- The wave climate has been analysed. As well as wave height, length and direction have been determined.
- A glance at Figure 3.1, shows a considerable amount of wave power [Iribarren et al.; 1992] [Sierra et al.;1994].

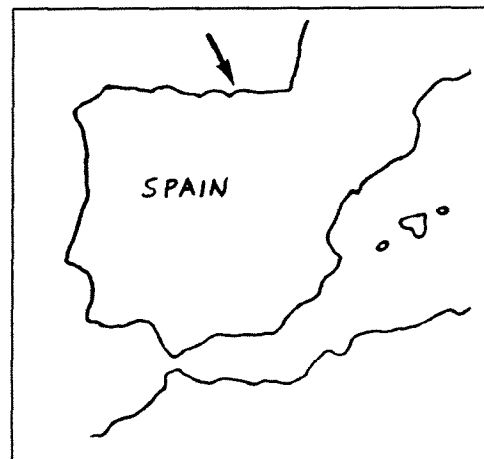


Figure 6.2 Location of Bilbao

Because of these reasons this location is selected for the design of the caisson type breakwater, combined with the 'harbour' type OWC devices.

6.2.3 Description of the Location

The Port of Bilbao is the largest harbour in Spain in terms of volume of traffic. It also holds a relevant position in the international context. In 1971, the works for the construction of the Punta Lucero Breakwater started. For this one, water depths of 32 m were achieved.

In 1976 the breakwater was damaged by an exceptional storm. For this reason the construction of the Punta Galea Breakwater, which would have closed the outer estuary, was permanently stopped. The Punta Lucero Breakwater was repaired between 1980 and 1985.

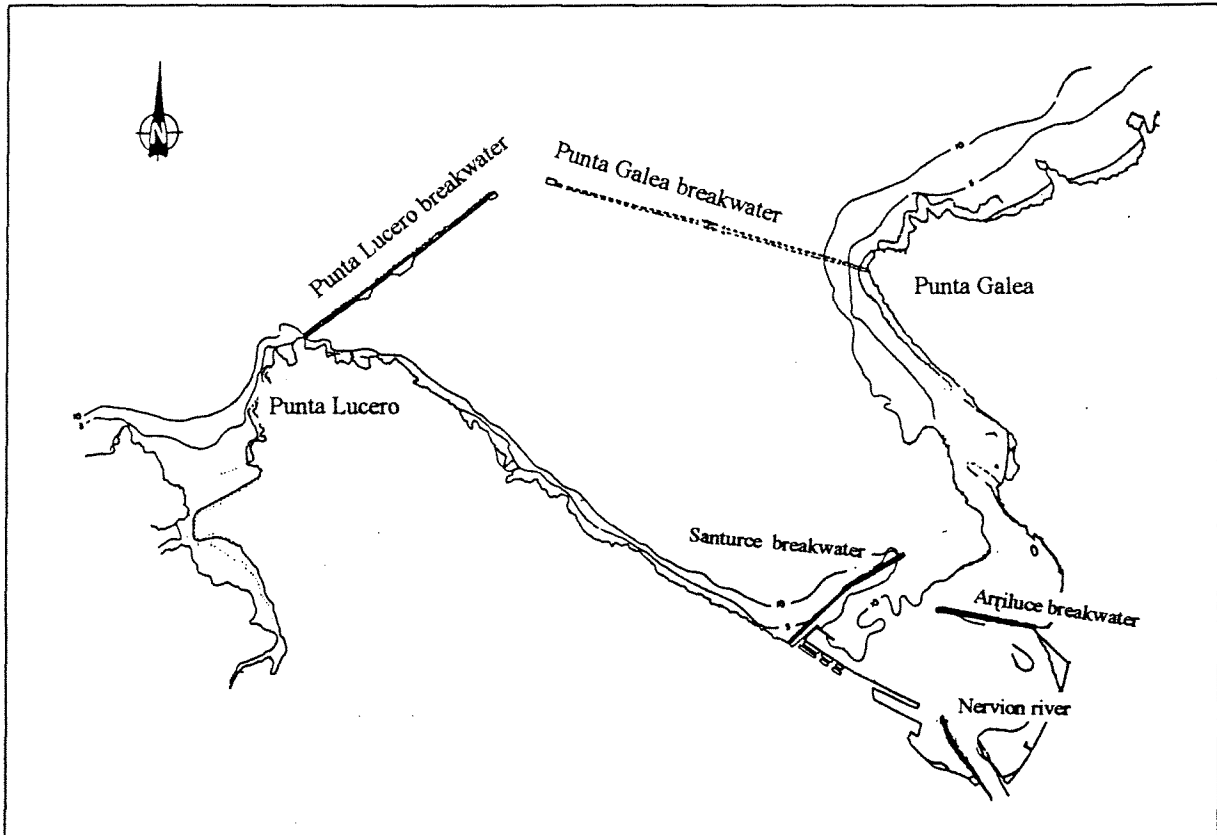


Figure 6.2 Layout of Bilbao Harbour

In 1989, a new extension project was initiated, to expand the surface of the harbour. After various technical and economic studies, it was proposed to construct new breakwaters with a total length of 3150 m. This project provides the harbour 8 km of dockline and 350 ha of new land surface. The construction with a total duration of 62 months is scheduled to start in 1997.

The new breakwaters are proposed to be rubble mound. They will be constructed by concrete blocks of 100 tons weight (the outer armour layer), which have to be able to withstand waves of a height of 11 m. A structure will be placed on top of the breakwater to avoid overtopping [Sierra et al.;1994]. A more detailed description of the design conditions is given in 'Experimental studies for the Port of Bilbao extension' and will be given in Section 6.4.1 [Iribarren et al.;1992].

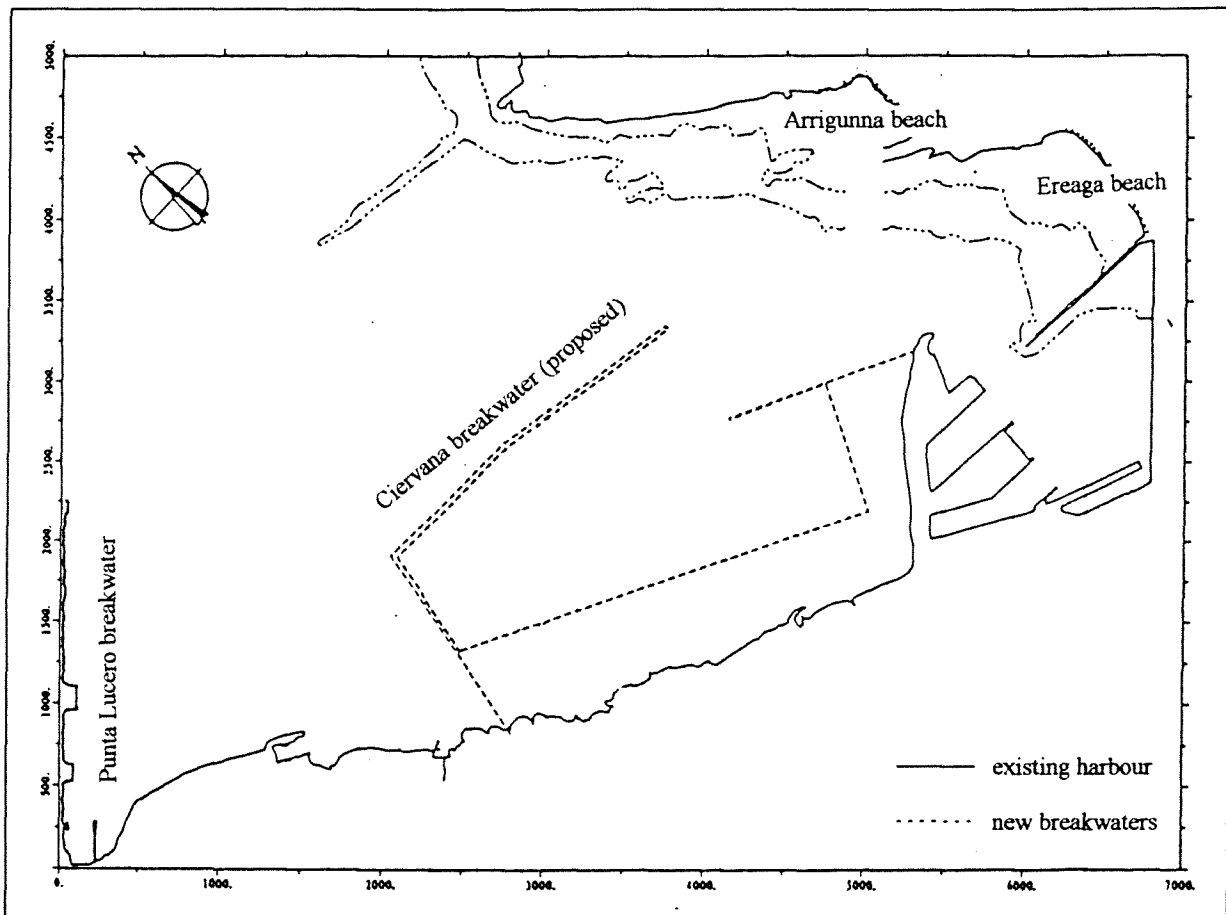


Figure 6.3 Layout of new breakwater and the extension project

6.3 Water Level and Wave Climate

6.3.1 Water Level

Tidal levels

The water level is an important parameter to design the breakwater. As well for the stability and strength calculations of the breakwater, as for the design of the wave energy converter the water level has to be known. The tidal levels of the port of Bilbao are given by the 'Admiralty Tide Tables' [Admiralty Tide Tables; 1981]. The levels are referred to Chart Datum.

C.D. = Chart Datum

The same as the zero of the tidal predictions in all cases. By international agreement, Chart Datum is defined as a level so low that the tide will not be frequently below it.

M.H.W.S. = Mean High Water Springs = 4.0 m

M.L.W.S. = Mean Low Water Springs = 0.5 m

The height of mean high / low water springs is the average, throughout a year of two successive high / low waters during periods of 24 hours when the range of the tide is greatest.

M.H.W.N. = Mean High Water Neaps = 3.1 m

M.L.W.N. = Mean Low Water Neaps = 1.4 m

The height of mean high / low water neaps is the average, throughout a year of two successive high / low waters during periods of 24 hours when the range of the tide is least.

M.T.L. = Mean Tide Level = 2.25 m

The mean of the heights of M.H.W.S., M.L.W.S., M.H.W.N. and M.L.W.N.

The values of the water levels are valid for average meteorological conditions, consequently higher and lower levels than those given can occur. These variations in tidal heights are mainly caused by strong or prolonged winds and by unusually high or low barometric pressure. Tidal predictions are computed for average barometric pressure. A low barometer will tend to raise the water level and a high barometer will tend to depress it. The water level only responds to the average change in pressure over a considerable area, the change in water level seldom exceeds 0.3 m. The effect of wind depends largely on the bathymetry of the area. In general, the effect of wind straight blowing onshore is to set up the water, while winds blowing off the land will have the reverse effect. The result of both influences is that during extreme springs, the range of the tide will be increased by an amount which varies from 20 - 30 % [Admiralty Tide Tables; 1981].

Wind set up

The influence of the wind on the water level at Bilbao is roughly investigated. When the wind blows, shear stresses occur at the surface of the sea. For this event, an equilibrium of forces can be derived [Thijsse;1951].

When the shear stress at the bottom is neglected ($F_1 = F_2$) follows:

$$i = c \cdot \frac{U^2}{gh} \quad (6.1)$$

with	c_1	= friction coefficient	[-]
	ρ_1	= density of air	[kg/m ³]
	ρ_w	= density of water	[kg/m ³]
	h	= water depth	[m]
	g	= gravitational acceleration	[m/s ²]
		= 9.81 m/s ²	
	i	= slope of water surface	[-]
	c	= coefficient	[-]
		= 3.5-4.0·10 ⁶	[-]
	U	= wind velocity	[m/s]

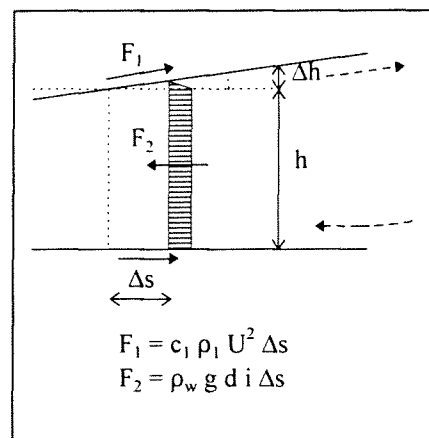


Figure 6.4 Water level set up

The waves reaching the Spanish North Coast are generated in the North Atlantic by the action of extratropical storm. The polar mass oscillations through the year define the path of the storms through the Bay of Biscay. Under such conditions, the winds come from West to North with the dominant gradient North West and NNW. The wind speed can be as much as 40 m/s [Valdecantos, Carnero; 1994]

The Cantabrian Sea becomes deep at very short distance from the coast, see for instance 'The Times Atlas of the World' [The Times Atlas of the World;1992]. At about 25 km from the harbour of Bilbao, the sea has a depth over 200 m and at less than 40 km over 2000 m. The depth of the sea along the French coast is less than 200 m over a distance of about 120 km from the shore. The length over which the wind blows (fetch) depends on the direction and the magnitude of the wind field. When the winds come from the North along the French coast, this length is about 325 km at a water depth of less than 200 m. When the winds come from the North West the fetch is the magnitude of the wind field. The length is estimated at about 850 km, based on a figure of wind field in 'Coastal Actions' [Taboada;1991]. With these values estimations of the set up of the water level can be made.

Wind from North:

U = 40 m/s	U = 40 m/s
Fetch = 325 km	Fetch = 25 km, 15 km, 150 km
h = 200 m	h = 100 m, 1100 m, 2000 m
$\Delta h \approx 1.05$ m	$\Delta h \approx 0.25$ m

Wind from North West:

U = 40 m/s	U = 40 m/s
Fetch = 850 km	Fetch = 33 km, 25 km, 800 km
h = 3000 m	h = 100 m, 1100 m, 3000 m
$\Delta h \approx 0.2$ m	$\Delta h \approx 0.4$ m

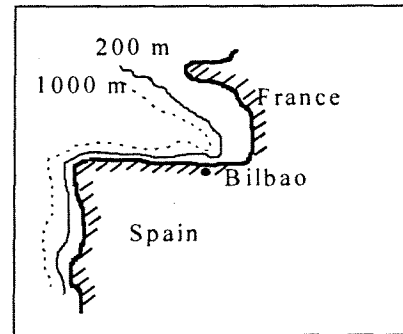


Figure 6.5 Water depth of the Cantabrian Sea

It can be concluded that the maximum set up is caused by wind coming from the North, with a maximum increase of water level of about 1 m. In 'Hydro Port '94 Volume II', the maximum tidal range is mentioned as 4.6 m [Sierra et al.;1994]. This value agrees with the range of tide given by the 'Tide Tables' increased by 30 % ($4.0 - 0.5 = 3.5$ m; $3.5 * 130\% = 4.6$ m) or increased by a value of about 1 m ($3.5 + 1.0 = 4.5$ m).

Seasonal changes in water level

The seasonal changes in mean tide level of Bilbao are given by the 'Tide Tables':

Table 6.1 Seasonal changes in mean tide level [m]

Jan. 1	Feb. 1	Mar. 1	Apr. 1	May 1	June 1	July 1	Aug. 1	Sep. 1	Oct. 1	Nov. 1	Dec. 1
0.0	- 0.1	- 0.1	- 0.1	0.0	0.0	0.0	0.0	0.0	+ 0.1	+ 0.1	0.0

It can be concluded that the seasonal changes have no high values and consequently they will be ignored.

Conclusions

In further calculations a maximum spring tide level of 5.0 m above Chart Datum will be assumed. This value seems to be good, because the maximum water level for the breakwater at Punta Lucero is mentioned as + 5.2 m C.D. [Valdecantos et al.;1994]. The minimum water level is assumed to be Chart Datum.

The design water levels for the breakwater functioning as a wave power converter, are different from the levels for stability and strength of the breakwater. The design water levels for wave power converting influence the immersion depth of the front wall.

The design water levels for strength and stability are those, which in combination with severe waves cause the most serious loading.

6.3.2 Wave Climate

Introduction

The wave climate has to be known to design the wave power converter and to calculate the stability and strength of the breakwater. The wave climate can be described by wave length (or period), height and direction.

The wave climate is measured by a waverider buoy located in open water, in front of the Punta Lucero Breakwater. In 'Hydro Port '94, Volume II', the sea state curves of H_s (significant wave height) and T_z (mean wave period) and the (smoothed) energy-density of an average year are given [Sierra et al.;1994]. The first of October was taken as the origin of this year. The sea-state curves are shown in the following figures.

Wave Height

The significant wave height varies between 0.5 and 5.5 m. For wave power conversion the probability of occurrence, which is the distribution over the year, is important. For stability and strength of the breakwater an extreme wave height has to be considered.

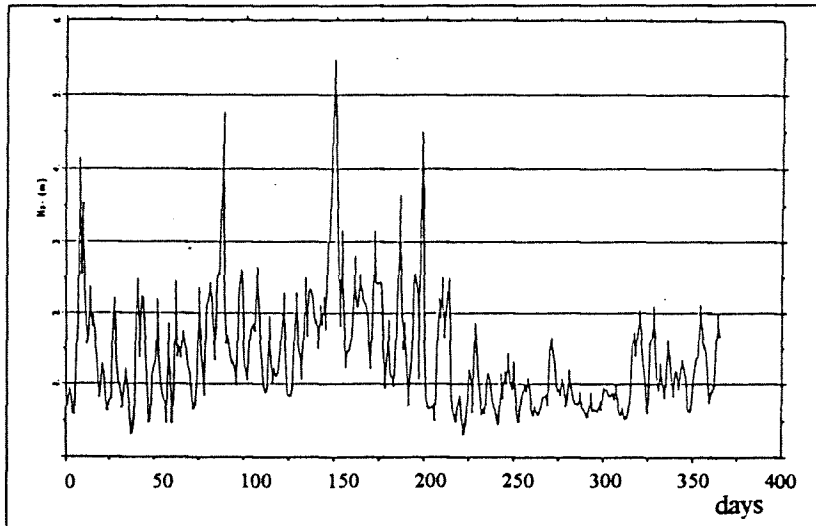


Figure 6.6 Sea-state curve of the wave height H_s

Wave Period

The mean wave period varies between 3 and 13 s. This distribution of the wave period, in relation with the wave height distribution is important for wave power conversion. For the stability and strength of the breakwater, extreme wave conditions are important. These conditions consist of a combination of wave height and period.

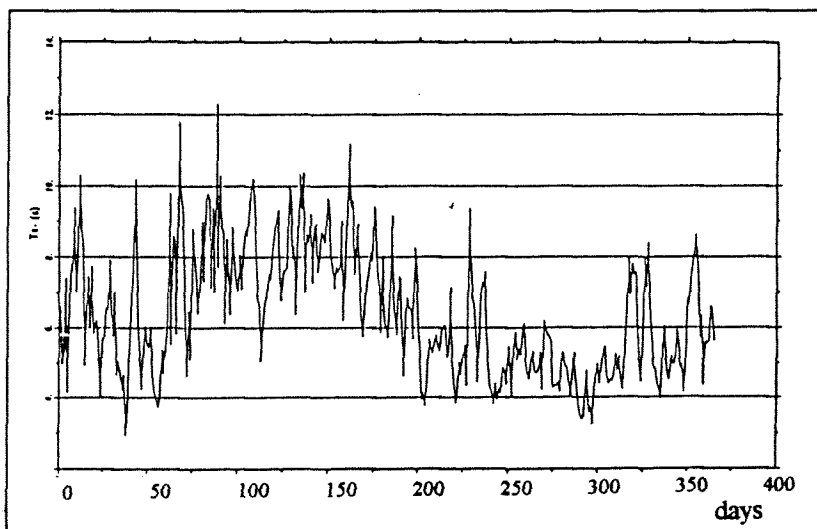


Figure 6.7 Sea-state curve of the wave period T_z

Energy Density

The averaged sea-state curve of energy density was obtained with the criteria of maintaining the same area under the curve. The energy density is in fact the variance density of the wave amplitude, with the unit m^2/Hz or m^2/s [Battjes;1992]. This density can also be roughly considered as the wave power. It can be concluded that in general the mean wave power in the first 200 days is about 25 kW/m (peak values of 300 kW/m are possible) and in the remaining part of the year about 7.5 kW/m.

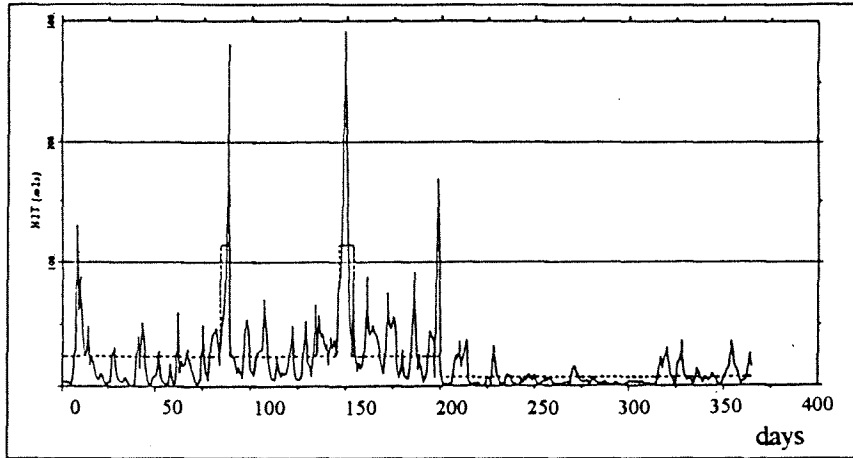


Figure 6.8 Averaged sea-state curve of the energy density

Wave Direction

The wave direction has also been determined by the buoy. Figures are shown in 'Coastal Actions' [Taboada; 1991]. Sierra et al. give a table of the average annual frequency for each direction, see Table 6.2 [Sierra et al.;1994]. It can be seen that the prevailing wave direction, comes from the fourth quadrant (W to N).

(Sierra et al. mention for NW 29.7% instead of 24.7%. It seems that an error has been made, because the total frequency is 105%.)

Table 6.2 Frequency of wave direction

Direction	Frequency (%)
W	13.9
WNW	18.2
NW	24.7
NNW	22.8
N	12.1
NNE	4.7
NE	3.6

Wave steepness

The correlation between the wave height and period can be expressed in the wave steepness. The expression of wave steepness is [Vrijling;1995]:

$$s_p = \frac{H_s}{L_p} \quad (6.1)$$

with s_p = wave steepness [-]
 L_p = length of wave with peak wave period [m]

$$= \frac{gT_p}{2\pi} \quad (6.2)$$

g = gravitational acceleration [m/s^2]
 T_p = peak wave period [s]

Equation (6.1) can be rewritten as:

$$H_s = C \cdot T_p^2 \quad (6.3)$$

$$\text{with } C = (s_p \cdot g) / (2\pi) \quad (6.4)$$

To obtain the peak period from the mean wave period the relation between them has to be known. The wave climate at Bilbao can be represented by a Jonswap spectrum [Iribarren et al.; 1992] [Clemente;1990]. The relation between T_p and T_z for this spectrum is given by the following ratio [Vrijling;1995]:

$$T_p / T_z \approx 1.2 \quad (6.5)$$

The significant wave height and mean wave period are given in curves, shown in Figure 6.6 and 6.7, data was not available in this study. Consequently, data had to be extracted from these curves. In this way the values of s_p are determined, shown in the Figure 6.9.

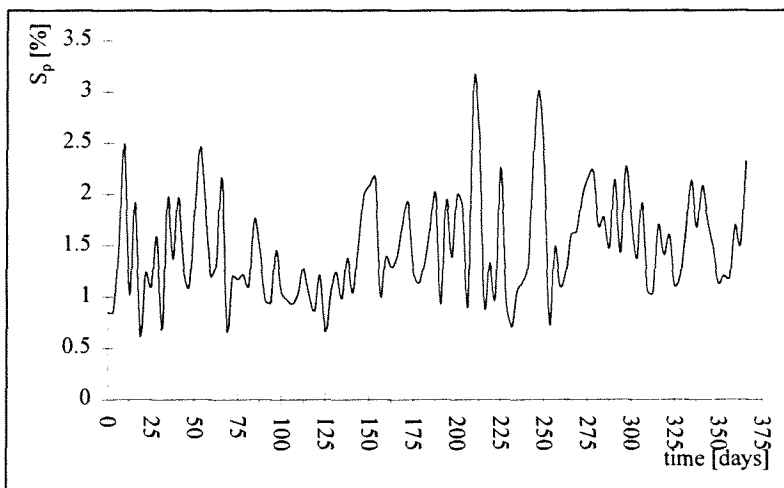


Figure 6.9 Sea-state curve of the wave steepness

When the wave power converter has to be designed, the values of wave power has to be known. This value depends on as well the wave height as the wave length. This is shown in equation (3.5) and **Appendix A**. The wave power is related to the second power of the wave height and to $n \cdot c$ (which is the product of the factor for the depth of water and the wave celerity).

The probability of occurrence of the wave height can also be derived from Figure 6.6. To calculate the wave power and its probability, a corresponding wave period has to be known. To find this corresponding wave period, the following method has been used.

The year is divided into two parts. One part consists of the first 175 days of the year, from October till almost the end of March, or the winter. The other part is formed by the remaining days, the summer. In winter the steepness can be set at 1.3%, in summer at 1.6%. This is shown in the Figure 6.10.

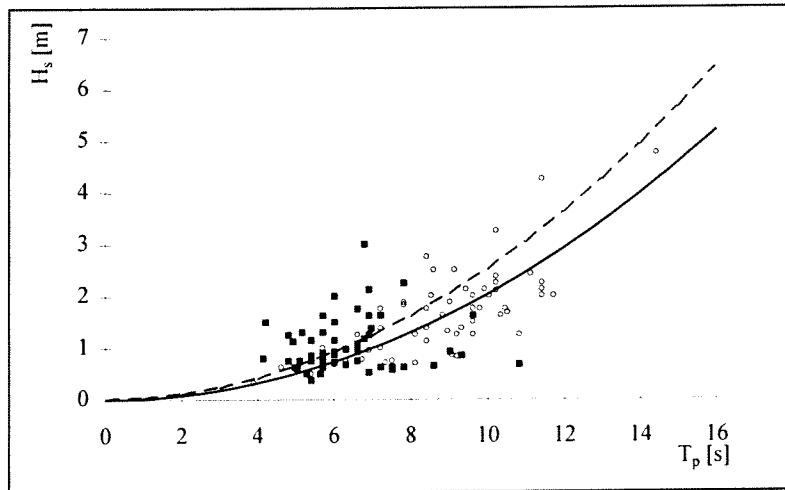


Figure 6.10 H_s versus T_p and the wave steepness
 summer values: ■ ---- 1.6%
 winter values: ○ — 1.3%

When this method is used, there may be no correlation between H_s and s_p [Vrijling;1995]. This is checked by showing s_p versus H_s , for as well the winter as the summer. The following figure shows, that no clear correlation exists between H_s and s_p .

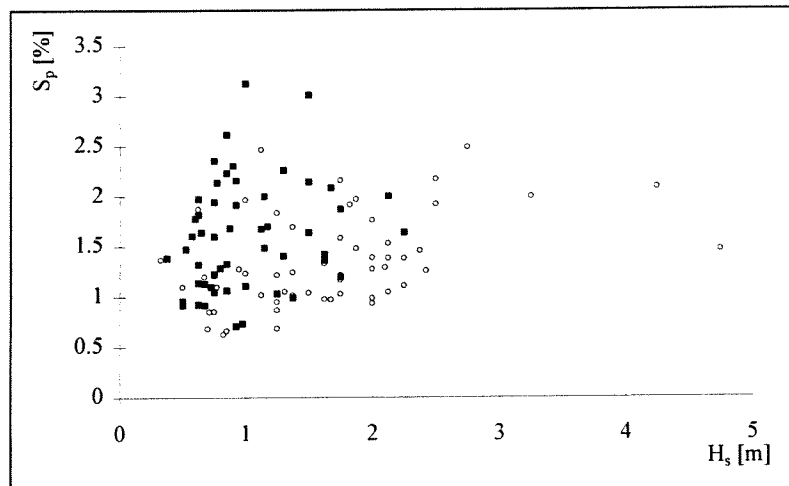


Figure 6.11 s_p versus H_s summer values: ■
 winter values: ○

The relation between peak wave period and significant wave height is also used by Iribarren [Iribarren et al.;1992]. He used the expression of the British Standard Code of Practice for Maritime Structures:

$$T_p = (4.2 - 6.0) \cdot H_s^{1/2} \quad (6.6)$$

This means a steepness of 1.8 - 3.7%. However, from Figure 6.9 appears that these values are rather high. Some wave conditions used in tests, are mentioned by Iribarren and Sierra [Iribarren et al.;1992] [Sierra et al.;1994]:

The tests conditions given by the table show a wave steepness varying mostly between 1.3 and 2.6 %.

Table 6.3 Wave conditions used in tests

Iribarren et al.				Sierra et al.			
wave direction	H_s [m]	T_p [s]	s_p [%]	wave direction	H_s [m]	T_p [s]	s_p [%]
N-33-W	4.75	14.7	1.4	N-45-W	4.0	14.0	1.3
	7.50	19.0	1.3		2.0	7.0	2.6
N-18-W	7.50	14.5	2.3	N-35-W	2.0	7.0	2.6
	5.50	19.0	1.0				
N-7-W	3.00	12.0	1.3	N	3.5	9.0	2.8
	4.75	14.5	1.4				
N-43-E	3.00	9.0	2.4				
	3.00	12.0	1.3				

To show the reliability of the selected steepnesses of 1.3 and 1.6%, the wave period is calculated by using the wave height from Figure 6.6. Also the wave height is calculated by using the peak wave period T_p , obtained from Figure 6.7 (after multiplying by the factor 1.2).

The wave power has been calculated too. For calculation the mean period is used. Three methods are used. The exact wave power is calculated by H_s and T_p both given in Figure 6.6 and 6.7. The other two methods have derived respectively the wave height or the period from these figures, the wave period and height is estimated by the steepness relation. The results are shown in the following three figures.

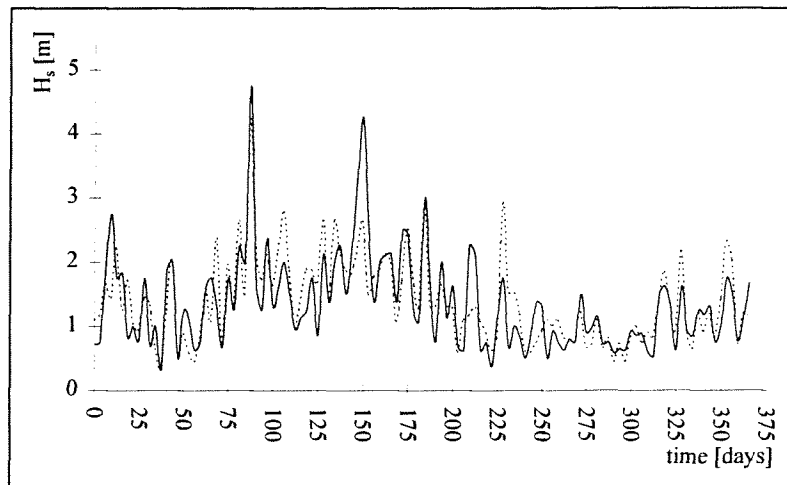


Figure 6.12 — H_s from Figure 6.6
 H_s estimated by T_p (from Figure 6.7)

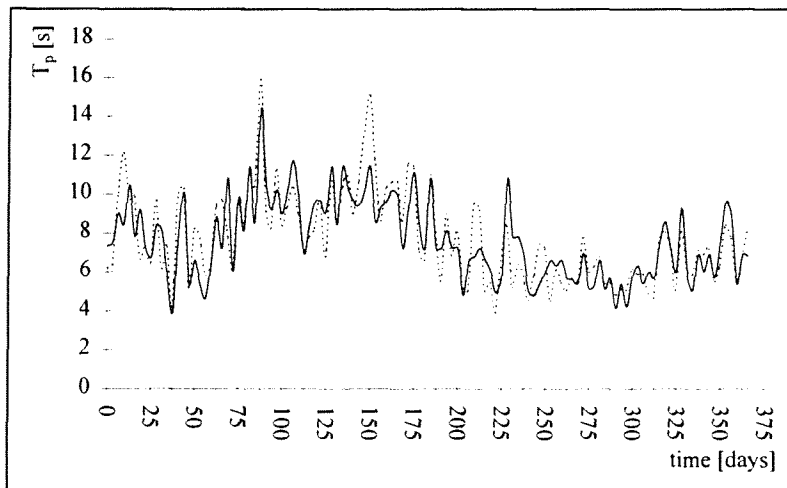


Figure 6.13 ——— T_p from Figure 6.7
 T_p estimated by H_s (from Figure 6.6)

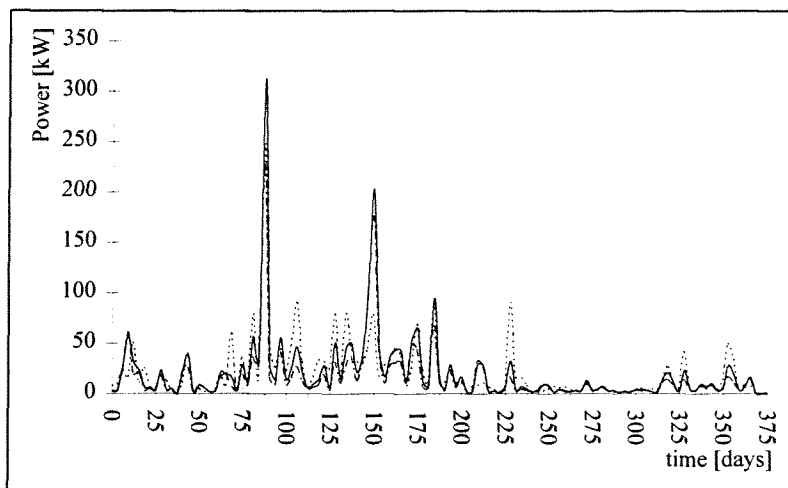


Figure 6.14 ——— Actual power calculated by H_s and T_z from Figure 6.6 and 6.7
 - - - - - Power calculated by H_s from Figure 6.6 and T_z estimated by H_s
 Power calculated by T_z from Figure 6.7 and H_s estimated by T_p

The estimation of T_p calculated by the values of H_s from Figure 6.6 is better than the estimation of H_s calculated by T_p from Figure 6.7. This is because of the relation $H_s = C \cdot T_p^2$. A deviation in the steepness coefficient C between the fixed value ($s = 1.3$ or 1.6%) and the real value, causes a more significant error in the value of H_s , than in the value of T_p .

In general the peak values of wave height and length have the largest errors, likely this is because at these peak values, the fixed steepness value differs from the real value.

The wave power calculated by a given H_s from Figure 6.6 and T_p estimated, does better agree with the actual wave power, than calculated by a given T_z and estimated H_s . This is because the error in the estimation of H_s is more serious than the error in the estimation of the wave period. Moreover, the calculation of the wave power is more strongly effected by an error in the wave height than by an error in the peak period ($\text{Power} \sim H_s^2$).

In general, the following trend can be seen. The power calculated by given H_s and estimated T_z (- - - - -), has too low values at the peak values of wave power. The power calculated by given T_z and estimated H_s (.....), has too high values at the peak values of wave power.

6.4 Design conditions

Two design conditions exist, namely the ultimate limit state, U.L.S. and the serviceability limit state, S.L.S. The first state is important for the stability and strength of the breakwater. The second condition is formed by the frequently occurring water levels and wave climate, which are important for functioning of the breakwater for (1) sheltering the harbour from waves and (2) converting the incoming wave power into electricity.

6.4.1 U.L.S. Ultimate Limit State

Water level

In the ultimate limit state, the extreme conditions occur. During these periods the breakwater must be able to withstand the most unfavourable combination of water level and wave attack. In this state, the breakwater has not to function as a wave power converter. The extreme water levels are given in Section 6.3.1. The lowest water level is set at Chart Datum and the highest at + 5.0 m C.D.

Extreme wave height at the proposed rubble mound breakwater

In 'Experimental Studies for the Port of Bilbao Extension' the extreme wave height distribution has been selected [Iribarren et al.;1992]. A Weibull distribution function with shape parameter $c = 2.0$ turned out as the best fit. The predictions are shown in the following figure, for the Bilbao Buoy, which is the buoy in front of the Punta Lucero Breakwater, see Figure 6.16. This buoy is located at - 32 m C.D., which means in a mean water depth of about 34 m.

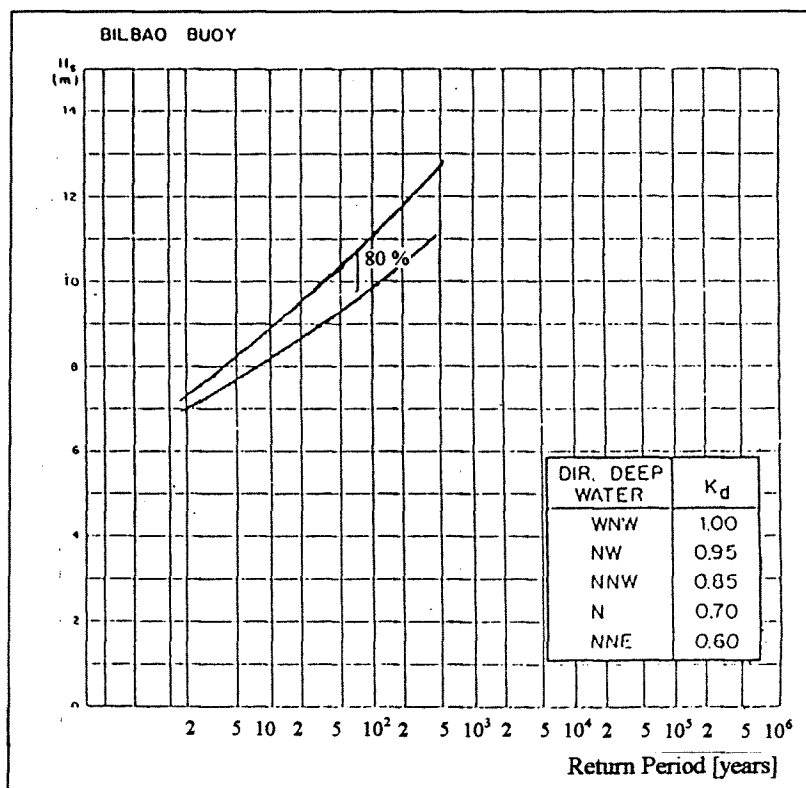


Figure 6.15 Extreme wave height distribution

The extreme wave height at the new breakwater depends on the wave directions which can effect it and the propagation of the waves. To determine this extreme wave height, the extreme wave height of the Bilbao Buoy is multiplied by a direction factor K_d and a propagation factor K_a .

The direction which produces the maximum wave height has a K_d value of 1. For the other directions it was supposed that the extreme wave height is reduced by the factor. The K_d values are shown in Figure 6.15.

The propagation of waves is influenced by refraction, shoaling, diffraction and reflection. Because these phenomena can differ along the new breakwater, it has been divided in representative segments. Each of these segments is characterised by an average propagation factor K_a , which takes into account all the phenomena mentioned.

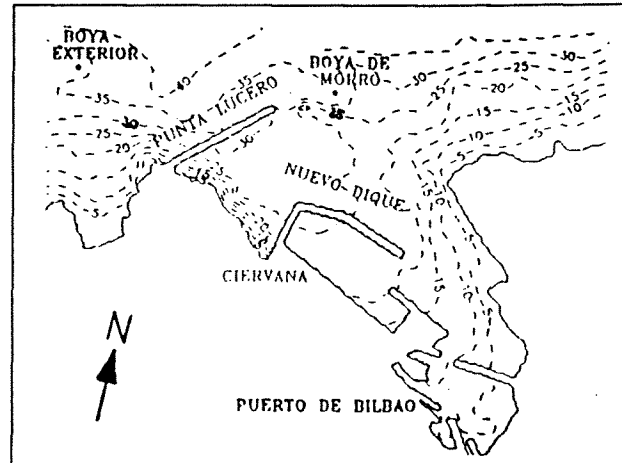


Figure 6.16 General layout of the Port of Bilbao and bottom depth [m below C.D.]

In this way the wave heights at each of the segments are calculated, using the equation shown in Figure 6.17. This figure also includes the different final design wave heights and the associated wave directions.

In the equation the significant wave height with a return period of 200 years is used, see Figure 6.15.

The design wave height given in 'Hydro Port '94' is 11 m [Sierra et al.;1994].

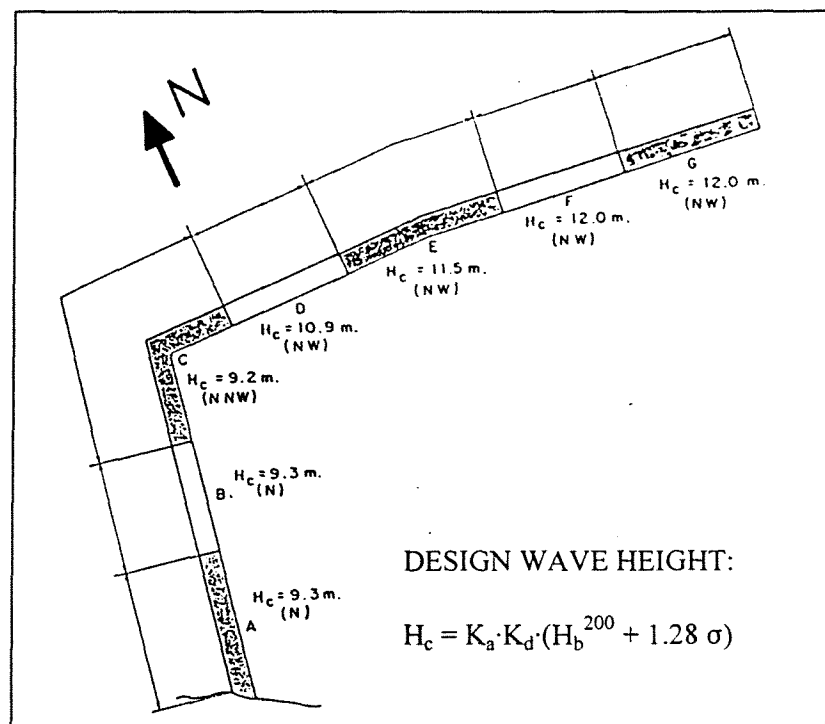


Figure 6.17 Final design wave heights and associated directions of the rubble mound breakwater of the Port of Bilbao

Structural lifetime and accepted failure probability

The extreme design wave height for the rubble mound breakwater has a return period of 200 years. Its lifetime and failure probability are not given. The relation between these three design parameters is shown in the following expression [Burcharth;1992].

$$p = 1 - \left(1 - \frac{1}{R}\right)^T \quad (6.7)$$

with p = failure probability, probability that the R-year return period event will be exceeded during its lifetime
 R = return period of an event
 T = lifetime of the structure

The relation between this failure probability p , the return period of an event and the structure lifetime is illustrated in Figure 6.18.

The accepted failure probability of a rubble mound breakwater differs from the accepted failure probability of a caisson breakwater. This is caused by the consideration that a rubble mound breakwater will not be completely destroyed and can be repaired, but a caisson breakwater is completely destroyed at once.

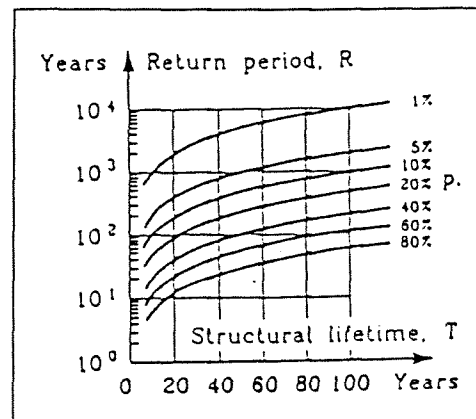


Figure 6.18 Probability p in relation with return period and lifetime

For determination of lifetime and failure probability of structures, some tables are given by Lamberti [Lamberti;1992].

Table 6.4 Minimum structural lifetimes for works or structures of definitive character

Type of work	Required security level		
	1	2	3
	Structural lifetime [year]		
General use infrastructure	25	50	100
Specific industrial infrastructure	15	25	50

Legend:
General use infrastructure: general character works, not associated with the use of an industrial installation or of a deposit
Specific industrial infrastructure: works in the service of a particular installation or associated with the use of transitory natural deposits of resources (e.g. industry service port, loading platform of a mineral deposit, petroleum extraction platform, etc.)

Level 1: Works and installations of local auxiliary interest. Small risk of loss of human life or environmental damage in case of failure. (Defence and coastal regeneration works, works in minor ports and marinas, local outfalls, pavements, commercial installations, buildings, etc.).
Level 2: Works and installations of general interest. Moderate risk of loss of human life or environmental damage in case of failure. (Works in large ports, outfalls of large cities, etc.).
Level 3: Works and installations for protection against inundations or of international interest. Elevated risk of loss of human life or environmental damage in case of failure. (Defence of urban or industrial centers, etc.).

Table 6.5 Maximal accepted failure probability during the lifetime

Damage initiation		
Economic repercussion	Possibility of human loss	
	reduced	expected
Low	0.50	0.30
Average	0.30	0.20
High	0.25	0.15
Total destruction		
Economic repercussion	Possibility of human loss	
	reduced	expected
Low	0.20	0.15
Average	0.15	0.10
High	0.10	0.05
<p>The damage initiation or total destruction maximum accepted failure probability shall be adopted according to the deformation characteristics and ease of repair of the structure.</p> <p>For brittle works, without possibility of repair, the total destruction probability shall be adopted.</p> <p>For flexible, semi-rigid or generally reparable works the damage initiation probability shall be adopted (damage initiation refers to a damage level present according to the structural type). In these type of works, the total destruction risk shall also be analysed (presenting to the structural type the damage level to be considered as total destruction)</p>		
<p>Legend:</p> <p>Possibility of human loss:</p> <ul style="list-style-type: none"> - reduced: when human loss is not expected in case of failure or damage - expected: when human loss is foreseeable in case of failure or damage <p>Economic repercussion:</p> <ul style="list-style-type: none"> - low: $r \leq 5$ - average: $5 < r \leq 20$ - high: $20 < r$ <p style="text-align: center;">with $r = \frac{\text{total costs of direct or indirect losses if work is disabled}}{\text{investment for the work}}$</p>		

The lifetime of the structure can be determined by Table 6.4. Bilbao Harbour is an industry service port and of international interest [Iribarren;1992: 'leading port in Spain', Oil Terminal at Punta Lucero, 'relevant position in the international context']. Consequently, a structural lifetime of 50 years is selected.

A caisson breakwater is completely destroyed when failure occurs, no repair is possible (brittle structure). The possibility of human loss is reduced and the economic repercussion is assumed to be high. For these reasons the accepted failure probability is 0.10.

Altering the breakwater from rubble mound to a caisson type means, that an other extreme design wave height has to be used. Instead of the significant wave height with a return period of 200 year, an extreme significant wave height with a return period of 500 year is needed.

Extreme wave height at the wave power converting breakwater

The extreme significant wave height with a return period of 500 year at the location of the buoy is 11.8 m, see Figure 6.15. The caisson breakwater will be designed by the method of Goda, see Appendix I.

In this method, instead of the significant wave height, the highest wave in the design condition is used, $H_{\max} = H_{1/250}$. The relation with the significant wave height, $H_s = H_{1/3}$ outside the surf zone (before breaking) is given by Goda [Goda;1992]:

$$H_{\max} = H_{1/250} = 1.8 H_s$$

Within the surf zone, this relation is not valid. The maximum wave height is determined by the largest wave height of random breaking waves at a distance of $5 \cdot H_s$ seaward of the breakwater. For more information about the calculation of the maximum wave height H_{\max} , see **Appendix I**.

In Figure 6.17, the final design significant wave height with a return period of 200 year is given for each segment of the breakwater. At the buoy the significant wave height, H_s^{200} is 11 m. With this information, the wave propagation factor K_a is calculated, assumed that $\sigma = 0$. Subsequently, the significant wave height H_s^{500} and the maximum wave height H_{\max}^{500} are estimated ($H_{\max}^{500} = 1.8 \cdot H_s^{500}$). During the highest water level (+5.0 m C.D.), the water depth is maximum, h_{\max} . The breaker index is $H_{\max}^{500} / h_{\max}$.

Table 6.6 Estimation of K_a , the maximum wave height H_s^{500} , H_{\max}^{500} and the breaker index

location	H_s^{200} [m]	K_d	K_a	H_s^{500} [m]	H_{\max}^{500} [m]	h_{\max} [m]	$H_{\max}^{500} / h_{\max}$
Bilbao Buoy	11.0	-	-	11.8	21.2	37	0.57
segment A	9.3	0.70	1.21	10.0	18.0	27	0.67
segment B	9.3	0.70	1.21	10.0	18.0	30	0.60
segment C	9.2	0.85	0.98	9.8	17.6	31	0.57
segment D	10.9	0.95	1.04	11.7	21.1	31	0.68
segment E	11.5	0.95	1.10	12.3	22.1	30	0.74
segment F	12.0	0.95	1.15	12.9	23.2	28	0.83
segment G	12.0	0.95	1.15	12.9	23.2	26	0.89

In literature different values of the breaker index are given as a limit for breaking. For a horizontal bottom, the solitary wave theory gives a value of 0.78 [LeMehaute;1976].

In the theory of Miche the limit is given by $H_{\max} = 0.14 \cdot L \cdot \tanh(2\pi h/L)$, with L the wave length. This gives in deep water $H_{\max} = 0.14 \cdot L$ and in shallow water $H_{\max} = 0.88 \cdot h$ [Miche;1951].

A frequently used limit for irregular waves is 0.5.

Goda uses empirically derived formulas for the determination of H_{\max} [Goda;1992]. Because, the method of Goda for the stability calculation will be used, also his formulas of wave breaking will be applied. In his formulas the deep water wave height is used. However, the given extreme significant wave height distribution of Figure 6.15, is valid for the location of the buoy at an averaged water depth of 34 m. Consequently, the deep water wave height has to be derived from the H_s^{500} , which is 11.8 m. It is assumed that waves reaching the buoy are not refracted. The method is shown schematically in the Figure 6.19.

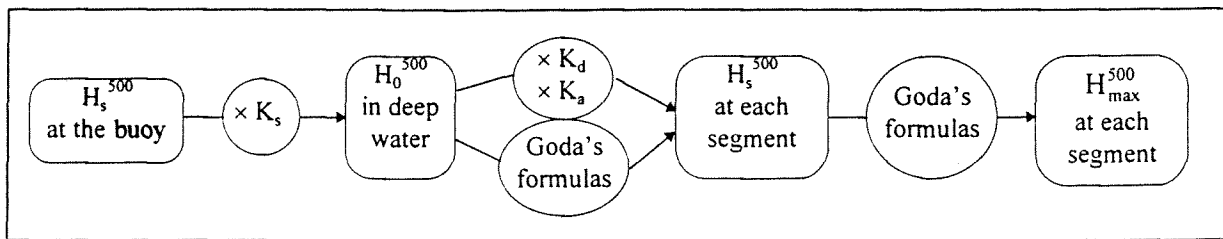
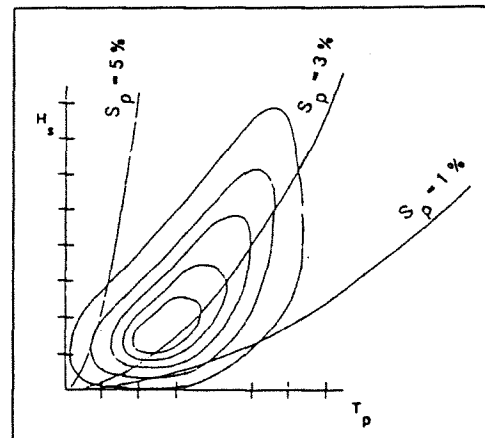


Figure 6.19 Method of determining the maximum wave height H_{\max}^{500} at each segment of the breakwater

- The shoaling factor K_s is given by the linear wave theory, **Appendix A**.

- The calculations are executed for different wave steepnesses. It is believed, that very high waves will not have a low steepness, also very high wave steepness is not expected, because these waves will be broken before reaching the breakwater. This is illustrated by Figure 6.20, which shows the general relation between wave height and period.

The four highest measured waves in Figure 6.6 (day 8, 88, 149, 198) are 4.2, 4.8, 5.5 and 4.5 m. The corresponding steepness is respectively 3.0, 2.0, 3.75, 4.2 %.



For these reasons the used range of wave steepness is 2.0 to 4.0 %.

Figure 6.20 General relation between significant wave height and peak period

The calculations are shown in **Appendix J**. The resulting design waves for each segment are given in the following table. The wave height varies with the wave steepness.

Table 6.7 Calculation of the maximum wave height H_s^{500} and H_{\max}^{500} by the breaking formulas of Goda

location	H_s^{500} [m] (with breaking)	H_{\max}^{500} [m] (without breaking)	$H_{\max}^{500} / h_{\max}$	H_{\max}^{500} [m] (with breaking)	$H_{\max}^{500} / h_{\max}$
segment A	10.0	18.0	0.67	18.0	0.67
segment B	10.0	18.0	0.60	18.0	0.60
segment C	9.8	17.6	0.57	17.6	0.57
segment D	11.4-11.7	21.1	0.68	20.5-21.1	0.66-0.68
segment E	11.4-11.9	22.1	0.74	20.5-21.0	0.66-0.70
segment F	11.4-11.9	23.2	0.83	19.6-20.1	0.70-0.72
segment G	11.4-11.9	23.2	0.89	18.3-18.8	0.70-0.72

The caisson breakwater will be designed for these wave heights and lengths, which form the most unfavourable combination for stability and strength.

6.4.2 S.L.S. Serviceability Limit State

Water level

The water level is important for as well functioning as a breakwater as functioning as a wave power converter. The water level influences the wave overtopping. Due to overtopping of the breakwater, waves are transmitted into the harbour. Sometimes no overtopping is permitted to always provide a calm harbour for ships, in other cases overtopping is allowed only in severe wave conditions. The overtopping depends also upon the geometry of the breakwater and the wave condition.

It is mentioned that no overtopping will be permitted for the proposed rubble mound breakwater of the Bilbao harbour. Consequently, a superstructure would be placed on the top [Sierra et al.;1994]. Overtopping of a vertical wall breakwater of caissons is a subject which is not fully understood at the present. Depending on which design philosophy is used, the crown height is selected as a determinative wave height multiplied by a factor.

In the following chapter the crest height of the breakwater will be determined.

The wave height and water level influence the depth of immersion of the front wall and the height of the chamber in combination with the damping level of the turbine. Wave power conversion has to be possible during as well low water as high water. The mean low water at spring tide (M.L.W.S.) is + 0.5 m C.D., given in Section 6.3.1. When the system is able to convert wave power during this period, it will be also possible to convert the power during periods with higher water levels (however, the performance will be changed, caused by the change in immersion depth of the front wall, see Section 5.3.2.3).

Wave conditions

The frequently occurring wave conditions are also important for functioning as well as a breakwater as functioning as a wave power converter. The design of the converter is particularly sensitive to the wave length. The wave height influences the depth of the front wall and the overtopping of the breakwater. The direction of the waves is important for the efficiency of wave power conversion.

Figure 6.6 shows the significant wave heights of a standard year. From this figure it is concluded that the system will be designed such, that operation is possible for waves with a height of 1 to 4 m.

As mentioned, the wave length is also important, because the performance of the device depends on the resonance of the 'harbour' and the resonance of the total device. The determination of the chamber and 'harbour' length strongly depends on the probability distribution of the wave length and the corresponding probability distribution of wave power. From the Figures 6.6 and 6.7 several figures are derived.

The main purpose of these figures is to get an good understanding of the relation between the wave height, period and wave power and their probability of occurrence.

Wave height

In the Figures 6.21 - 6.23, the probability of the wave height is shown in winter, summer and in a year. The probabilities are obtained from Figure 6.6.

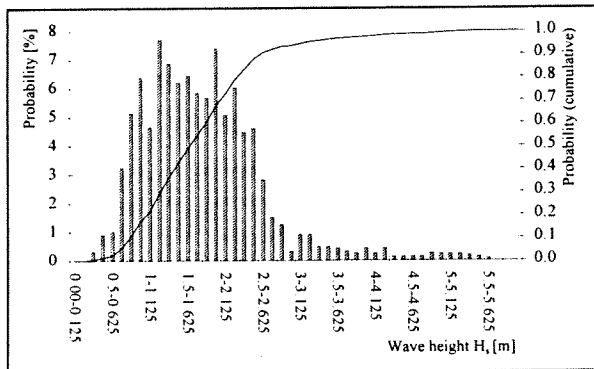


Figure 6.21 Probability of the significant wave height in winter (day 0-175)

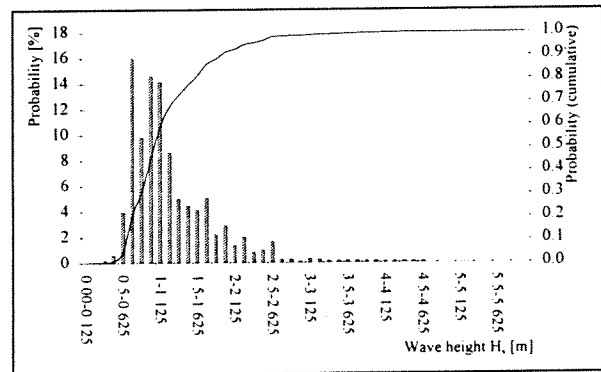


Figure 6.22 Probability of the significant wave height in summer (day 175-365)

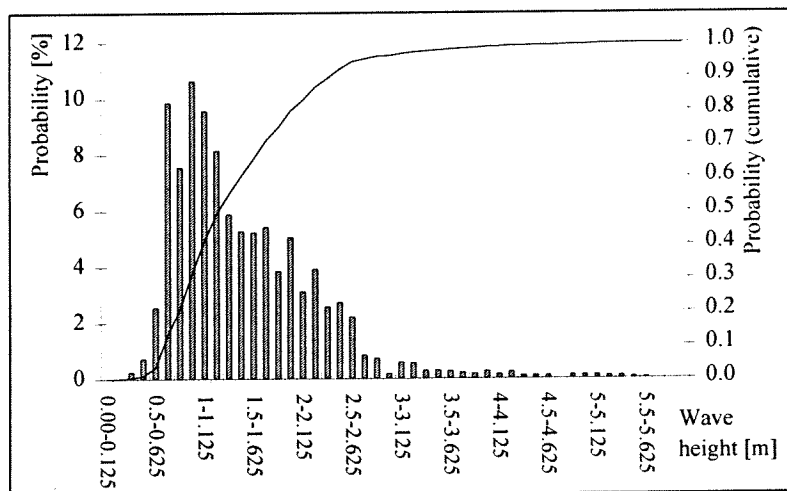


Figure 6.23 Probability of the significant wave height in a year (day 0-365)

Wave period

In the Figures 6.24-6.26, the probability of the wave length is shown in winter, summer and in a year. The probabilities are obtained from Figure 6.7.

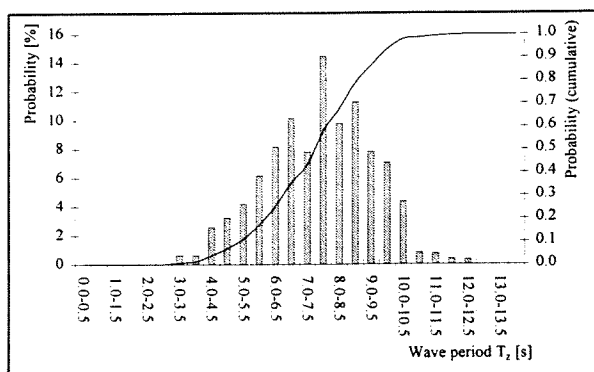


Figure 6.24 Probability of the wave period in winter (day 0-175)

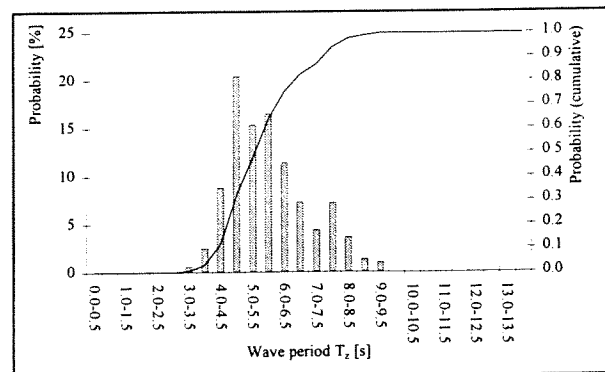


Figure 6.25 Probability of the wave period in summer (day 175-365)

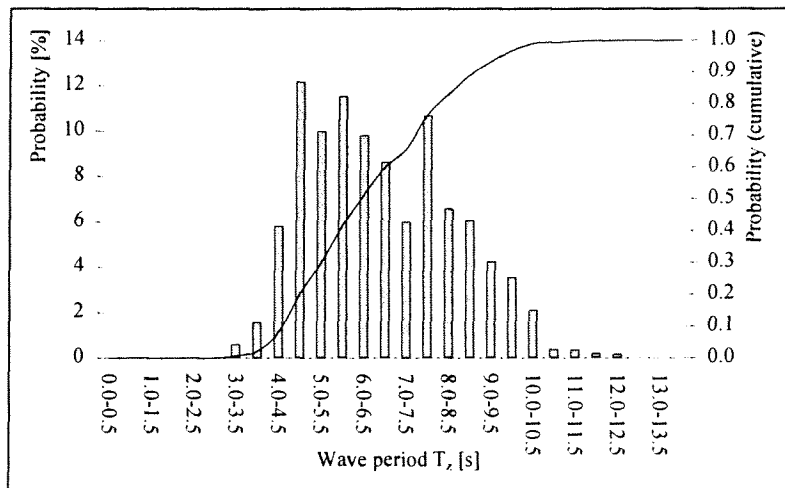


Figure 6.26 Probability of the wave period in a year (day 0-365)

Wave power

Generally, the longer the wave length, the higher the wave height and the higher the wave power. The relation between wave period and wave power is shown in Figure 6.27. In the figure also the probability of the wave period in a year is shown.

Figure 6.27 shows the wave power calculated by the given wave period and the estimated wave height. It can be concluded that wave power values higher than about 100 kW do not occur frequently, because the wave period is not frequently longer than about 10 s. The wave power corresponding to the wave periods is calculated by a steepness of 1.3%.

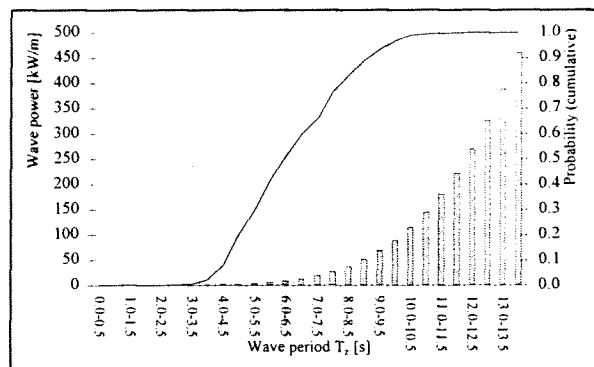
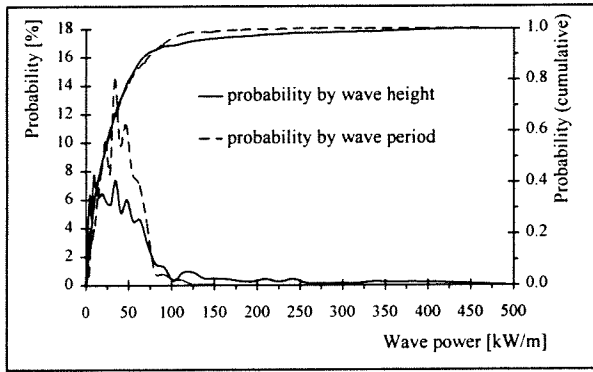


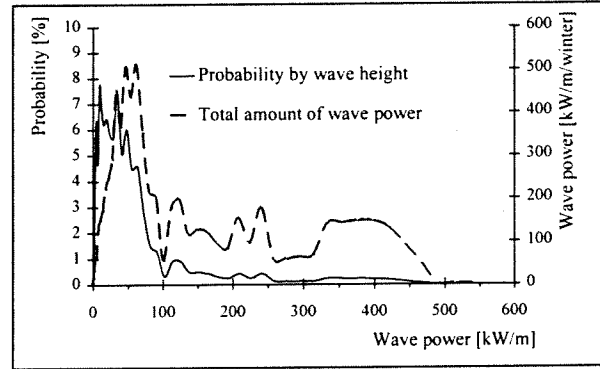
Figure 6.27 Probability of wave period (cumulative) and wave power versus period

As mentioned (Section 6.3.2), the wave power can be calculated by the given H_s and estimated T_z or by given T_z and estimated H_s . In the first case, the probability of the calculated wave power is based on the probability of the significant wave height, in the second case on the probability of T_z .

The wave power and its probability is shown for the winter and the summer in the following figures for both methods. Also the total amount of wave power is shown for winter and summer. The total amount of wave power is the product of wave power, its probability and the number of days in winter (175) or summer (190).

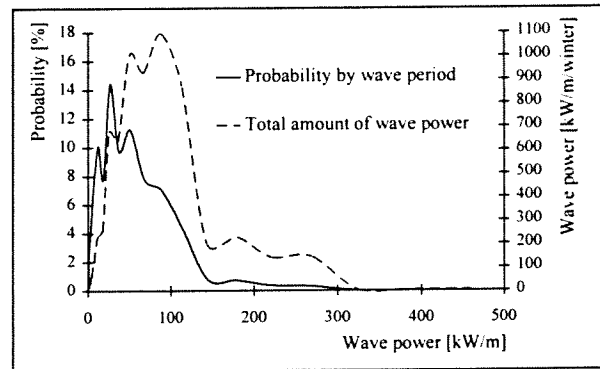


(a)

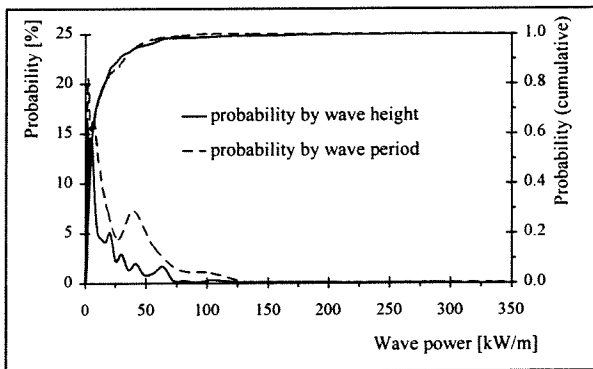


(b)

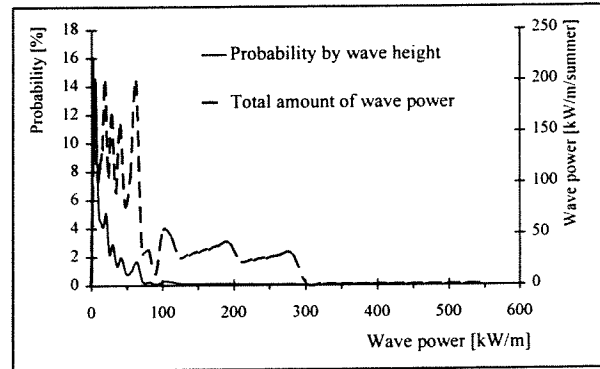
Figure 6.28 (a) Probability of wave power in winter, (day 0-175)
 (b) Probability and total amount of wave power in winter, calculated by probability of wave height
 (c) Probability and total amount of wave power in winter, calculated by probability of wave period



(c)

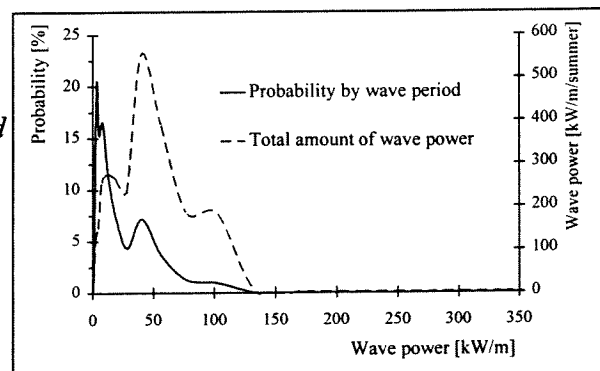


(a)



(b)

Figure 6.29 (a) Probability of wave power in summer, (day 175-365)
 (b) Probability and total amount of wave power in summer, calculated by probability of wave height
 (c) Probability and total amount of wave power in summer, calculated by probability of wave period



(c)

To show the shift of the total amount of wave power to the longer periods more clearly, the following figures are shown. Both methods are illustrated again, for winter, summer and a year.

Winter

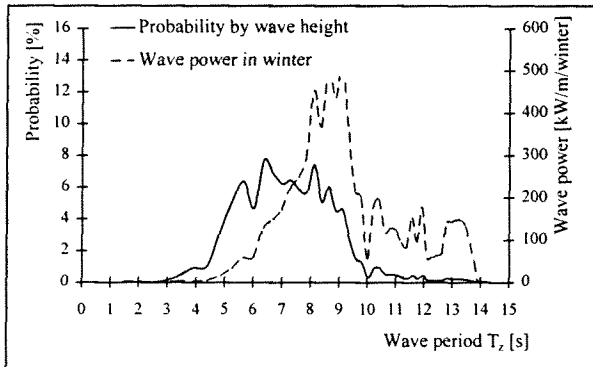


Figure 6.30 Probability of wave period (calculated by the probability of wave height) and wave power in winter

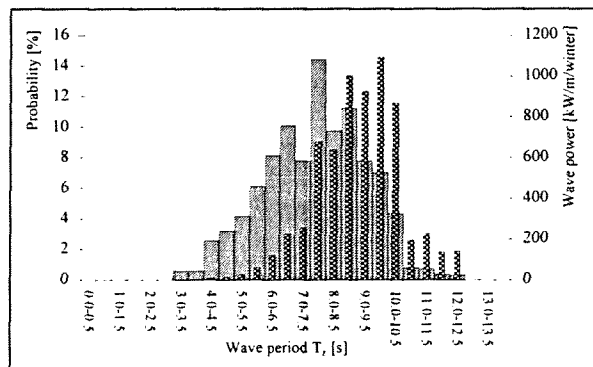


Figure 6.31 Probability of wave period (plain) and wave power in winter (pattern)

The shift to the longer periods is roughly the same for both figures, however the calculated total amount of wave power for $T_z = 8 - 10$ s in Figure 6.30 is lower than in Figure 6.31. This is mainly caused by the underestimated probability of these periods.

The figures show that in the range of wave period of 6.5 - 12 s, the total amount of wave power is considerable. However, the probability of wave periods larger than about 10 s is low.

Summer

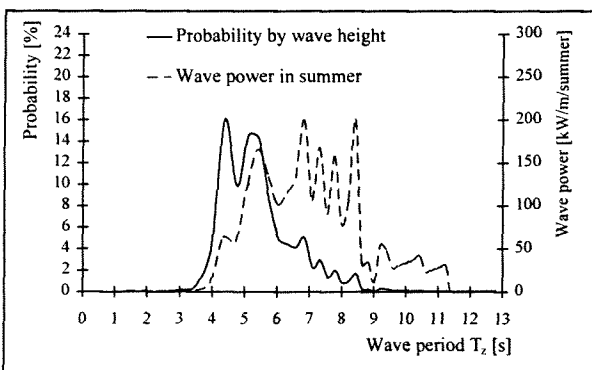


Figure 6.32 Probability of wave period, calculated by the probability of wave height and wave power in summer

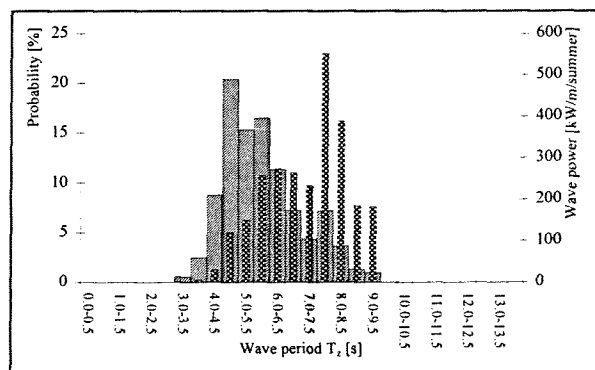


Figure 6.33 Probability of wave period (plain) and wave power in summer (pattern)

The shift to the longer periods is roughly the same for both figures, the calculated wave power for $T_z = 7.5 - 8.5$ s is larger in Figure 6.33, because these wave periods occur relatively frequently.

The figures show that in the range of wave period of 4.5 - 9.5 s, the total amount of wave power is considerable. However, the probability of wave periods larger than about 8 s is low.

Year

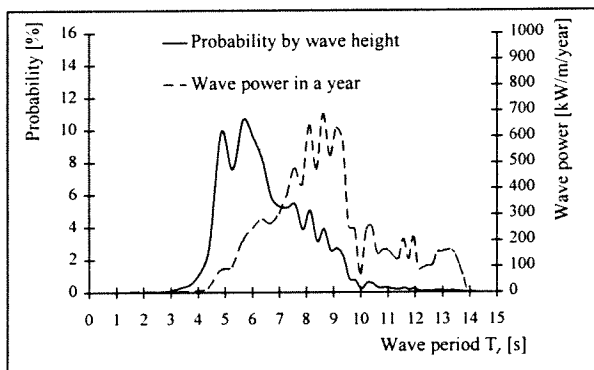


Figure 6.34 Probability of wave period, calculated by the probability of wave height and wave power in a year

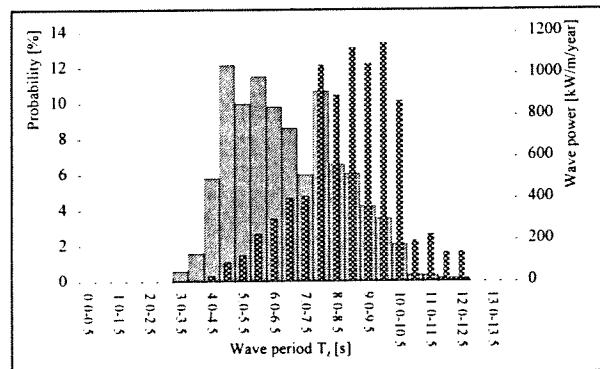


Figure 6.35 Probability of wave period (plain) and wave power in a year (pattern)

The Figures 6.34 and 6.35 are in fact a combination of respectively Figure 6.30; 6.32 and Figure 6.31; 6.33. These two figures show that in the range of wave period of 4.5 - 10.5 s, the total amount of wave power is considerable. However, the probability of wave periods larger than about 10 s is low.

Results of the investigation of the wave climate

From the figures of this section can be concluded, that the higher the wave power, the lower the probability is. However, at low probability still a considerable total amount of wave power is available.

The estimated wave power values can be compared to the values of wave power of Figure 6.8. This is shown in Table 6.8

Table 6.8 Comparison of the estimated wave power to the wave power of Figure 6.8

	Figure 6.8	Figure 6.28b, 6.29b	Figure 6.28c, 6.29c	Factor of overestimation
Winter (day 0-175)	5545 kW/m (162 days: 25 kW/m, 13 days: 115 kW/m)	6855 kW/m	6595 kW/m	1.2
Summer (day 176-365)	1863 kW/m (25 days: 25 kW/m, 165 days: 7.5 kW/m)	2494 kW/m	2637 kW/m	1.4

It can be concluded that the estimation of the total amount of wave power in winter or summer is higher than in practice. Consequently, when the total amount of wave power is estimated, the values have to be divided by the factors of overestimation.

For the design of the device a selection has to be made for which value of wave power the system has to be tuned. This tuning of the device depends mainly on the wave length. A choice has to be made between a system that can convert frequently occurring values of wave power well and a (more expensive) system that can convert a higher total amount of wave power, occurring less frequently, during relatively short periods. In the first design a higher part of the converted power, can be considered as firm power.

6.5 Conclusions

The Port of Bilbao, a harbour at the Spanish Cantabric Coast, is the proposed location for the design of a wave power converting breakwater, constructed by caissons. In this harbour new breakwaters are needed. For the proposed rubble mound breakwaters, the wave climate has been analysed.

The water level is influenced by a tidal range and wind set up. The low water level is Chart Datum and the high water level +5.0 m C.D.

The significant wave height in the year varies between 0.5 and 5.5 m. The mean wave period varied between 3 and 13 s. The prevailing wave direction is from North to West. By investigating the relation between wave height and period, the wave steepness has been derived. In summer the standard steepness is estimated at 1.6% and in winter 1.3%. With the use of these steepness values, the wave power corresponding to a certain wave length can be calculated quite well.

Two design conditions exist, namely the ultimate limit state, U.L.S. and the serviceability limit state, S.L.S. The first state is important for the stability and strength of the breakwater. The second condition is important for functioning of the breakwater for (1) sheltering the harbour from waves and (2) converting the incoming wave power into electricity.

For the proposed rubble mound breakwater, a design wave height with a return period of 200 years is used. In the case of a caisson breakwater, a return period of 500 years is needed.

The caissons will be designed by the method of Goda. In this method the maximum wave height, H_{\max} is used. These wave heights can break, during travelling into less deep water. The maximum wave heights for the caisson breakwater for each segment have been calculated (Table 6.6). Some wave heights are limited by the water depth. This limit is calculated by the formulas of Goda for breaking waves.

For the S.L.S., the distribution of the wave height, period and power over a year has been investigated. The figures of the wave power show, that the higher the power, the lower the probability is. In the Figures 6.31-6.36, the shift of the total amount of wave power to the longer periods with lower probabilities, is shown. However, the estimated values of the total amount of wave power in winter or summer are too high.

A design has to be made, that can convert the available power well. For this design, a choice has to be made between the high power during short periods, or less power during longer periods and thus more firm power.

A design will be made in the following chapter. The ultimate design has to be an optimisation influenced by as well stability and strength as functioning criteria.

6.6 References

- Admiralty Tide Tables, Volume I, 1982* (1981); European Waters, The Hydrographer of the Navy
- Battjes, J.A.(1992); *Wind Waves*; Technical University of Delft, The Netherlands, (in Dutch *Windgolven*, B78)
- Battjes, J.A.(1993); *Short Waves*; Technical University of Delft, The Netherlands, (in Dutch *Korte Golven*, B76)
- Burcharth, H.F.(1992); *Reliability Evaluation of a Structure at Sea*; Proc. of the Short Course on Design and Reliability of Coastal Structures, attached to the 23rd Int. Conf. on Coastal Engineering, pp. 511-546

-
- Clemente, M.M., Lopez, J.C.S., Perez, L.S.(1990); *Spanish network for wave measurement, R.E.M.R.O.*; The 27th Int. Navigation Congress, Osaka, pp. 69-78
- Goda, Y.(1992); *The Design of Upright Breakwaters*; Proc. of the Short Course on Design and Reliability of Coastal Structures, attached to the 23rd Int. Conf. on Coastal Engineering, pp. 547-568
- Haskoning, Tebodin, Rites (1989); *Paradip - Ennore Coal Transport Feasibility Study, Final Report*; Haskoning, The Netherlands
- Iribarren, J.R., Martin, M.J.(1992); *Experimental studies for the port of Bilbao extension*; Proceedings of the Int. Conf. of Coastal Engineering in the Oceans, pp. 149-157
- Kuo, C.T.(1994); *Recent Researches and Experiences on Composite Breakwaters in Taiwan*; Proc. of the Int. Workshop on Wave Barriers in Deepwaters, Yokosuka, Japan, pp. 217-238
- Lamberti, A.(1992); *Example Application of Reliability assesment of Coastal Structures*; Proc. of the Short Course on Design and Reliability of Coastal Structures, attached to the 23rd Int. Conf. on Coastal Engineering, pp. 669-698
- Lee, D.S., Park, W.S., Suh, K.D., Oh, Y.M.(1994); *Hydraulic Experiments for Basic Design of Offshore Breakwater fro Protecting Artificial Island*; Hydro-Port '94; Prcoceedings of the Int. Conf. On Hydro-Technical Engineering for Port and Harbor Construction, pp. 563-580
- Lee, D.S., Hong, G.P.(1994); *Korean Experiences on Composite Breakwaters*; Proc. of the Int. Workshop on Wave Barriers in Deepwaters, Yokosuka, Japan, pp. 172-183
- LeMéhauté (1976); *Hydrodynamics and waterwaves*; Springer
- Ligteringen, H.(1994); *Other European Experience on Deep Water Breakwaters*; Proc. of the Int. Workshop on Wave Barriers in Deepwaters, Yokosuka, Japan, pp. 199-216
- Miche, R.(1951); *Le pouvoir réfléchissant des ouvrages maritimes exposés a l'action de la houle*; Ann. des Ponts et Chaussées, 121 Année, pp.285-319
- Sierra, J.P., Jiménez, Sánchez-Arcilla, A., Picó, J.M., Viñuales, A., Villanueva, E.J.(1994); *Physical Impact of Bilbao 'harbour' New Breakwater on Adjacent Beaches*; Hydro-Port '94; Prcoceedings of the Int. Conf. On Hydro-Technical Engineering for Port and Harbor Construction, pp. 1041-1058
- Taboada, L.F.P.(1991); *Coastal Actions 1988-90*; MOPU Direccion general de puertos y costas
- The Times Atlas of the World* (1992), 9th Comprehensive Edition
- Thijsse, J.,Th.(1951); *Technische Vraagbaak*; deel W, pp.283, Kluwer, Deventer, the Netherlands
- Valdecantos V.N., Carnero, O.V.(1994); *H₀ Parameter for Preliminary Design of Conventional Breakwater Structural Head. Data Analysis of Spanish North Coast Harbours*; Int. Conf. on Coastal Engineering 1994, pp. 1657-..
- Vrijling, J.K.(1995); *Probabilistic Design in Hydraulic Engineering*; Technical University of Delft, The Netherlands, (in Dutch *Probabilistisch ontwerpen in de waterbouwkunde*, F30)

7 Design of the Wave Power Converting Breakwater

7.1 Introduction

In this chapter the wave power converting breakwater of the Port of Bilbao will be designed. Firstly, it has to be discussed in which part of the new breakwater the devices will be installed.

Figure 6.17, shows that the segments A, B and a part of C will only be attacked by waves coming from the North to NNWest direction. These segments are sheltered from waves coming from the West to North West by the Punta Lucero Breakwater. The waves from North and NNW have an angle of incidence of about $0 - 30^\circ$ at this part of the breakwater. At these angles of incidence, the performance of wave power converting devices is not good.

It is for this reason that the devices will be installed only in that part of the breakwater with the East West direction (part of segment C, segment D, E, F, and G).

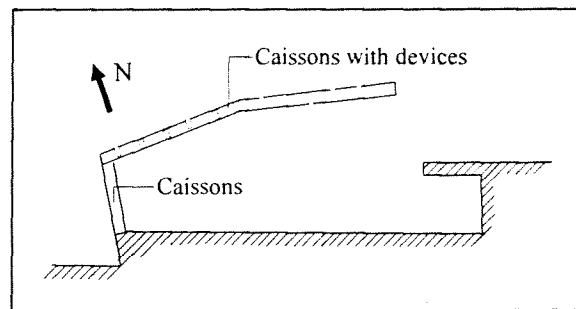


Figure 7.1 Breakwater of Bilbao

The main part of this chapter will be formed by the design of the caissons with devices. The caissons without devices for the segments A, B and part of C will not be designed.

In Section 7.2, the design method of the caissons with the devices will be explained. A figure illustrates the relation between the design of the device for wave power conversion and the design of the caisson for stability. In the following sections, several design parameters are determined and the global design is shown. In Section 7.4, some general information about wave power conversion is discussed and the dimensions of the devices are determined. In Section 7.5, the theory for calculating the stability of the caissons is given. The Goda theory is modified for a sloping top caisson and for the wave power converting device. The final design of the caissons with and without wave power converting devices is given in Section 7.6. At the end of the chapter sections with conclusions (7.7) and references (7.8) are presented.

7.2 Design Method

For the design of the wave power converting breakwater, two subjects have to be considered. The design of the devices to operate well and the design of the caissons for stability and strength. The two designs must be made in relation with each other.

The stability of the caissons will be calculated by the method of Goda, see **Appendix I**. The caissons must be stable against sliding and overturning. In most cases, the danger of sliding is more severe than that of overturning [Tanimoto et al.;1994]. However, at increasing water depth (with higher waves and as a result a larger required weight of the caisson) the force at the bottom plate (the slab reverse force) becomes also very important. This bottom slab reverse force is influenced by the area of the bottom slab and by the bearing capacity of the rubble mound foundation [Hou et al;1994].

The relation between the two designs and several design parameters which are of influence are shown in the next figure.

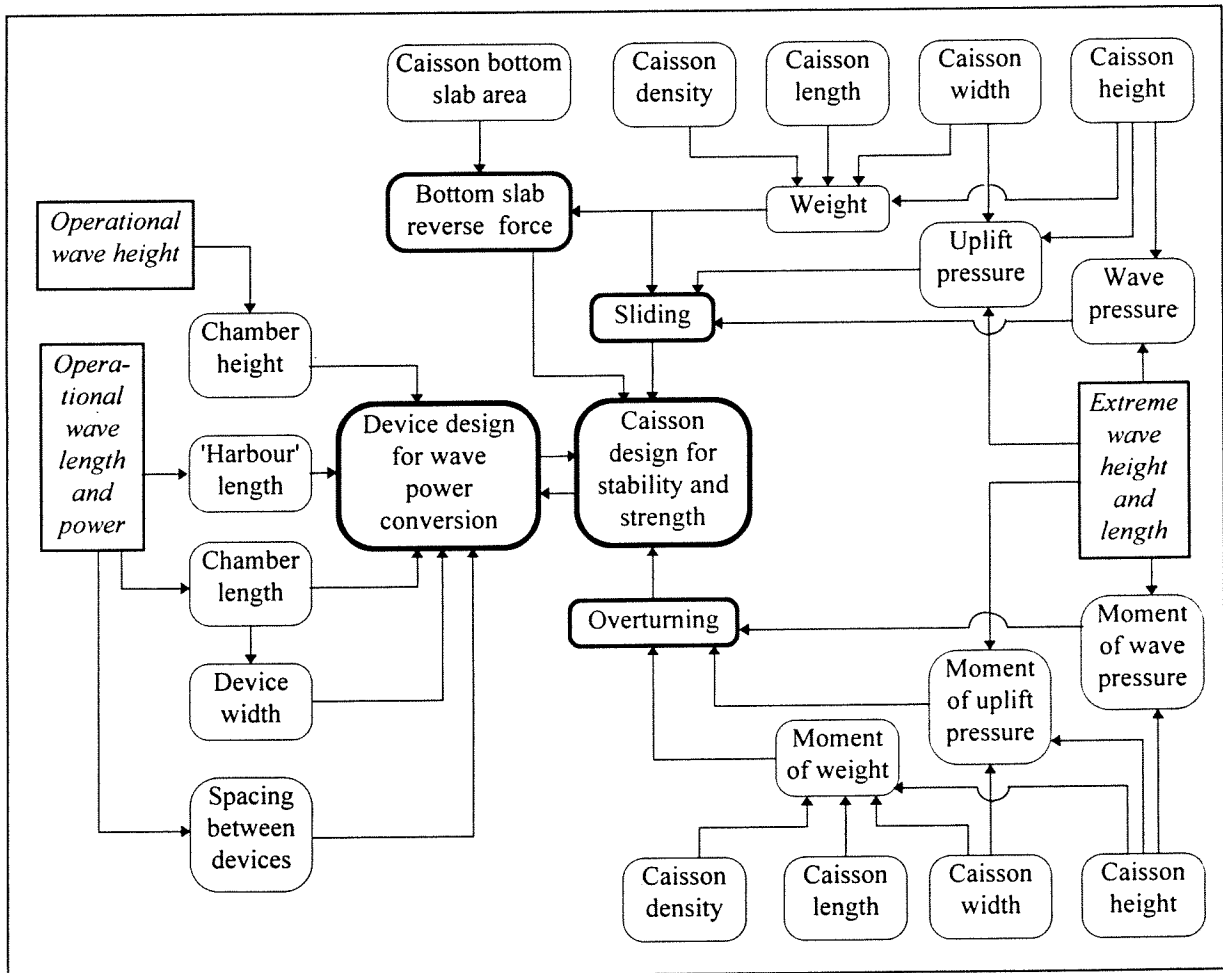


Figure 7.2 Relation between the design parameters

The following design method will be used to arrive at a final design:

1. A rough global design, which shows the shape of the caisson and the combination of the device and the caisson.
2. Determination of some design parameters.
3. First approximation of the dimensions of the caisson, required for stability.
4. Determination of the dimensions of the device.
5. Checking of the stability of the caisson with a device.
6. Final design.

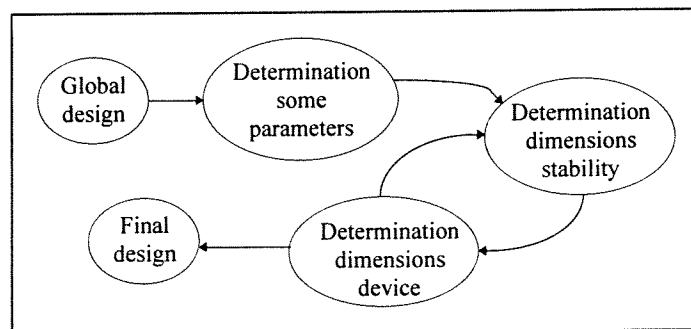


Figure 7.3 Design method, schematically

7.3 Global Design of the Caissons with a Device

Before determining the dimensions of the devices and the caissons, the shape and an estimation of the dimensions of a global design have to be known.

Sloping top caisson

The caisson will have a sloping top, like the Sakata Breakwater (Figure 4.13). The advantage of a sloping top caisson is a reduced horizontal wave force in rough seas and thus a better stability. Also the impact pressure can be much reduced by the slope [Takashi et al.;1994 b].

As mentioned in Section 5.3.2, devices in a reflecting wall have a better performance than in a non-reflecting wall. However, the lower the starting point of the slope the better the stability of the caisson.

Waves in front of the caisson are reflected and thus the wave height in front is twice the incoming wave height. Consequently, the sloping top has to start above the water level increased by the wave height. The mean water level is + 2.25 m C.D. (Section 6.3.1) and the devices have to operate at wave heights of 1 - 4 m (Section 6.4.2). The wave power converting breakwater of Bilbao will have a sloping top, starting at + 6.5 m C.D. with an angle of the slope of 45°. At higher water level, for instance M.H.W.S., + 4.0 m C.D., waves with a height up to 1.25 m are completely reflected, however higher waves will have some run up on the slope.

Crest height of the caisson

Following the Japanese design philosophy, the crest height of the caissons has to be $1.0 \cdot H_{1/3}$ above high water level in design condition. The high water level is + 5 m C.D. (Section 6.3.1) and the significant wave height with a return period of 500 years is about 12 m for most seriously attacked segments of the breakwater (Table 6.6). In this study the crest height will be + 17 m C.D., but further investigations on overtopping of the breakwater is required.

Rubble mound foundation

Generally, caissons have a rubble mound foundation. The determination of the height of the caisson and the height of the rubble mound foundation, is part of an optimisation of the price of the complete breakwater. The foundation level of the breakwater varies between -21 and -26 m C.D. (see Figure 6.16).

When breaking waves can act on a breakwater, a low rubble mound foundation is strongly recommended. The water depth d , above the rubble mound berm has to be at least more than $0.6 \cdot$ the water depth h ($d/h > 0.6$) [Takahashi et al.;1994 a]. The berm in front of the breakwater will have a thickness of 1.5 m above the rubble mound foundation and a length of about 15 m.

In this study the foundation can have a height of 1.5 - 10 m, which means a layer of rubble mound from the sub-soil up to a level of -17.5 m C.D. The recommendation $d/h > 0.6$ is satisfied, during as well low water as high water, for all segments of the breakwater, see table 7.1.

Table 7.1 Water depth above rubble mound

bottom depth	- 21 m C.D.	- 26 m C.D.
low water: C.D.	$16/21 = 0.76$	$16/26 = 0.62$
high water: +5 m C.D.	$21/26 = 0.81$	$21/31 = 0.68$

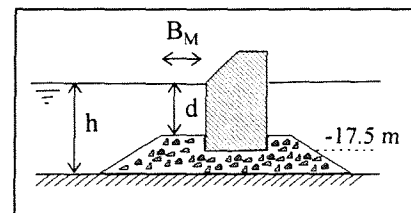


Figure 7.4 Depth of the rubble mound berm

No information about the bottom material at the location of the new breakwater is available in this study. However, a figure of the cross section of the Punta Lucero Breakwater shows that the rubble mound is put down immediately on the sub-soil. Consequently, it is believed that the sub-soil has a sufficient bearing capacity.

Device completely or partly placed in the caisson

Two possibilities exist to place the devices in the caissons. When the device is placed completely in the caisson, the total device length (chamber and 'harbour' length) has to be smaller than the length of the caisson, see Figure 7.5 a. The other possibility is to have the 'harbour' or part of the 'harbour' in front of the caisson, in that case protruding side walls are needed, see Figure 7.5 b.

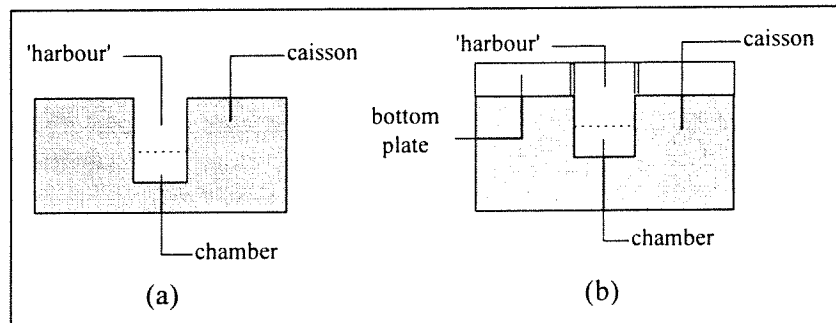


Figure 7.5 (a) Top view of device completely in the caisson
(b) Top view of device partly in the caisson

The influence of this change in configuration on the performance of the devices is not known. Probably, the performance will be less good. An disadvantage of the design 7.5 b is that protruding walls are sensitive to damage by the waves. These walls need a foundation plate, which results in a larger bottom plate of the caisson. In the design in this study the devices will be placed completely in the caisson.

Toe at each side of the caisson

The caissons will have on both sides a toe. The minimum length of these toe will be 1 m. The addition of toes is a measure to get a better stability, to decrease the rubble mound stress and to reduce the danger of scour. In front of the toe, in general two or three foot protection blocks are placed. The rest of the rubble mound foundation has to be protected by armour units [Tanimoto et al.;1994].

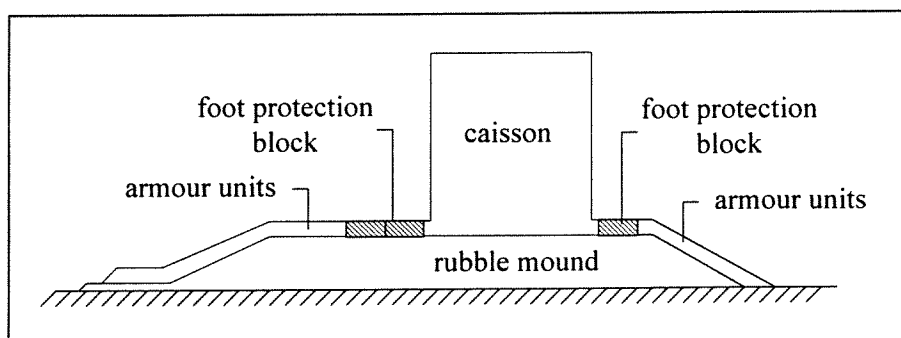


Figure 7.6 Toes of the caisson and rubble mound protection

Global design

First approximations of the stability of the caisson show a required length of the caisson of 25 - 30 m. With the information of this section, a rough design of the caisson with a device can be made, shown in the next figure.

The length (perpendicular on the direction of the breakwater) and the width (in the direction of the breakwater) of the caisson are shown in this figure.

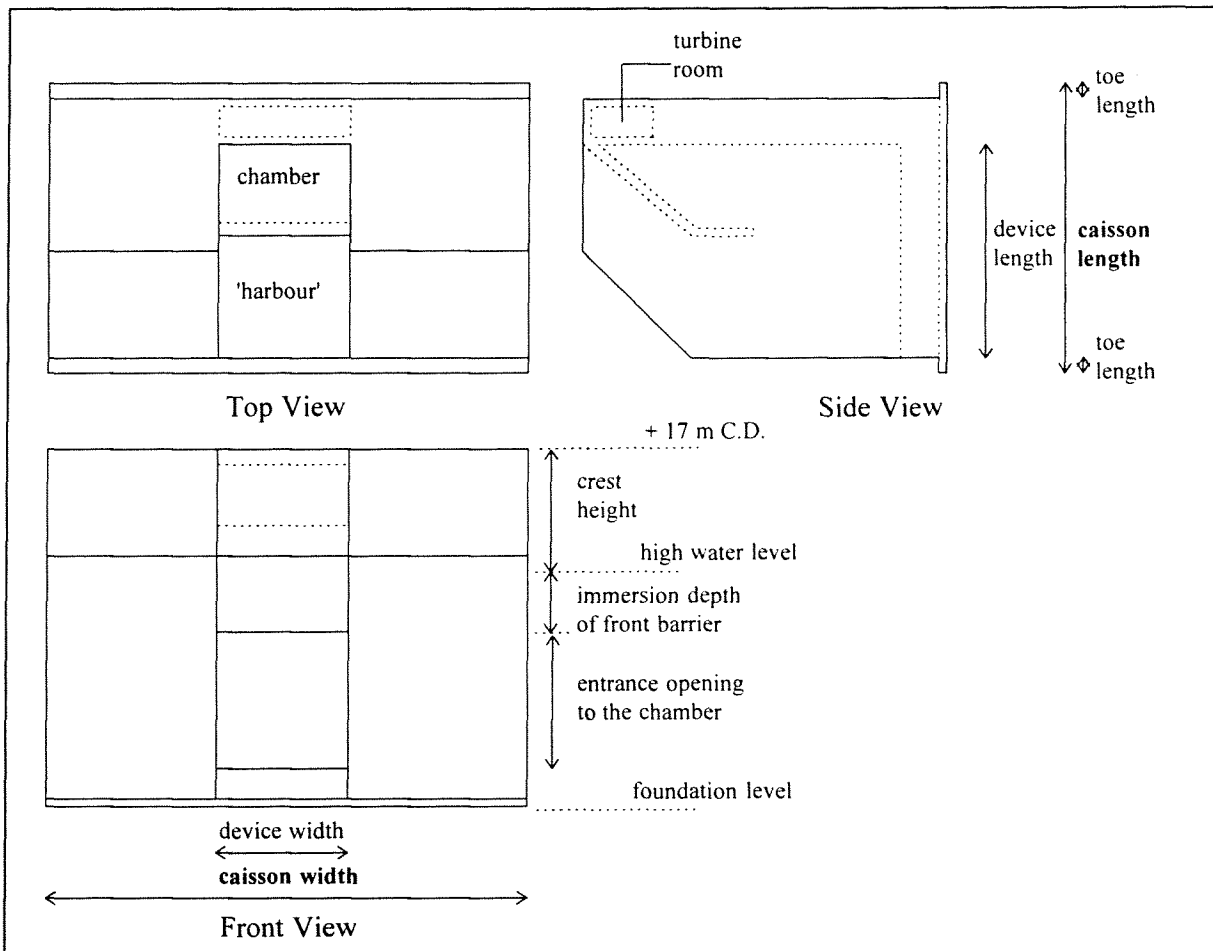


Figure 7.7 Global design with some important dimensions

7.4 Dimensions of the Device

General information about wave power conversion

Before determining the dimensions of the device, firstly some basic information about wave power conversion will be discussed. The available wave power does not only have short-term fluctuations (depending on the wave spectrum), but also longer term fluctuations caused by the day-to-day variations of the sea state and the seasonal variations of weather pattern. In winter and part of spring (day 0-200), the mean wave power is in general 25 kW/m, but in summer even less than 10 kW/m (see Figure 6.8).

Thus, there are a significant number of occurrences where the power is much greater than the mean wave power. The device will have fixed dimensions and consequently the performance will be best at the resonance wave lengths (and corresponding wave power values). A selection has to be made which values of power will be converted at high efficiency and which are less significant for conversion [Dawson 1979]. This is illustrated in Figure 7.8.

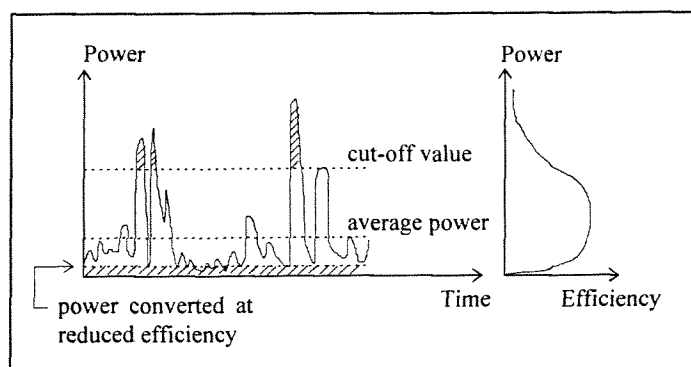


Figure 7.8 Wave power conversion and efficiency

Three considerations exist for selecting the cut-off level:

1. Will the device be tuned to the average winter power level, the average summer level or the average year level.

It is assumed, that it is more desirable to have devices that operate well in winter with a large total amount of converted wave power, than devices that operate during the whole year, resulting in a smaller total amount of power. This means that, even in winter, the converted wave power can fall to negligibly low values from time to time. In summer, the periods with considerable values of converted wave power only occur for short periods and very low or zero values can last for a week or more (see, for instance Figure 6.8).

2. In which way is the electricity desired, high electricity peak demand during short periods or more firm electricity during longer periods.

This consideration is in fact the same as the last one, however for the day-to-day fluctuations. When a device is tuned to a lower power level, a larger part of the capacity of the device can be considered as firm power, resulting in a more smoothly electricity output. Standard rules are not available for solving this issue.

In 'Wave Energy' it is mentioned that probably an annual load factor of about 45%, would be optimum i.e. in a year the proportion mean converted power to installed turbine generator capacity is 45% [Dawson; 1979]. An illustration is given for the determination of this value, see Figure 7.9.

However, this estimation is valid for devices which are constructed only for wave power conversion, in this study the caissons will be used also as a breakwater.

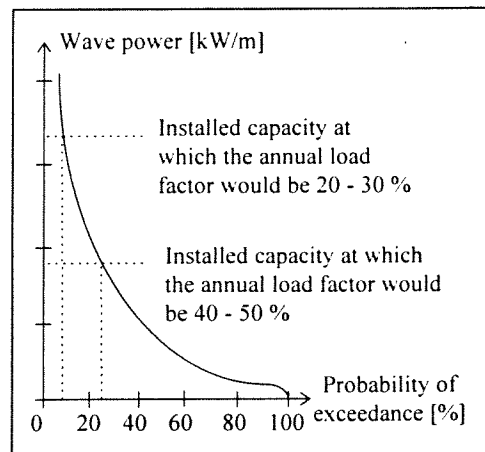


Figure 7.9 Effect of installed capacity on the load factor

3. Will the costs be higher, when higher power levels are converted.

The costs can be divided into capital costs and operating costs. The capital costs of the caissons are increased, when larger caissons are needed, for devices which operate at a high wave power level than for devices which convert lower levels. In general, the higher the converted wave power, the larger the turbines and the higher the costs of turbines and generators. Lower values of wave power conversion require lower transmission capacity, thus lower transmission costs [Dawson; 1979].

Figure 6.8 shows that the wave power will not be frequently larger than 100 kW/m. When the wave steepness is 1.3% (the average value in winter), the corresponding wave period will not be higher than about 10 s. This is illustrated by Figure 7.10.

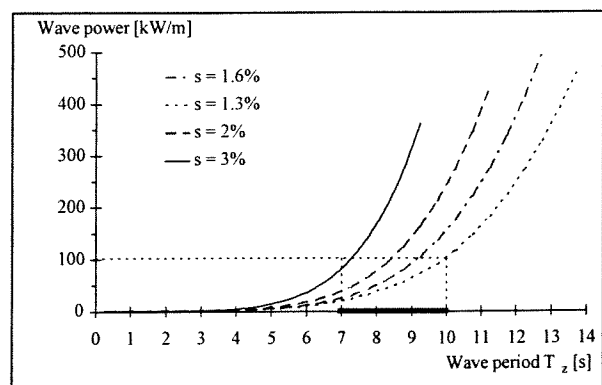


Figure 7.10 Relation between wave power and period for different wave steepness

Determination of the 'harbour' and chamber length

From Figure 5.14 and 5.15, the values of device resonance and 'harbour' resonance can be obtained for a device with a device width equal to the chamber length ($a=b$), for different values of l/a ('harbour' length/ chamber length).

In the design of the devices of Bilbao a device width of 1.5 times the chamber length will be used ($b = 1.5 \cdot a$). In that case the the device length / wave length value is decreased by a factor 0.88 and the 'harbour' length / wave length value is decreased by a factor 0.9 (see Figure 5.16 and 5.17). The resonance values are given in Table 7.2.

In Section 6.4.2, the probability of wave length and the corresponding wave power is shown in several figures. It can be concluded that the device has to be tuned to the long wave periods with high wave power. In the next table the dimensions for sixteen devices are determined, the highest wave periods are respectively 8.75, 9.25, 9.75 and 10.25 s. When the thickness of the immersed front wall is assumed to be 1.5 m the chamber and 'harbour' lengths can be determined.

Table 7.2 Device and 'harbour' resonance

l/a	device length / wave length		'harbour' length / wave length	
	$b = a$	$b = 1.5 a$	$b = a$	$b = 1.5 a$
1.17	0.202	0.178	0.198	0.178
1.33	0.215	0.189	0.213	0.192
1.50	0.221	0.194	0.227	0.204
1.67	0.223	0.196	0.236	0.212

Table 7.3 Dimensions of devices tuned to a wave period of 8.75, 9.25, 9.75 and 10.25 s, for several 'harbour' to chamber lengths l/a

device resonance wave period 8.75 s (107 m)					
l/a	device length [m]	'harbour' length [m]	chamber length [m]	'harbour' resonance	
				wave length [m]	wave period [s]
1.17	19.0	9.4	8.1	53	5.9
1.33	20.2	10.6	8.1	55	6.0
1.50	20.8	11.6	7.7	55	6.0
1.67	21.0	12.2	7.3	58	6.1
device resonance wave period 9.25 s (117 m)					
l/a	device length [m]	'harbour' length [m]	chamber length [m]	'harbour' resonance	
				wave length [m]	wave period [s]
1.17	20.8	10.4	8.9	58	6.1
1.33	22.1	11.8	8.8	59	6.2
1.50	22.8	12.7	8.6	62	6.3
1.67	22.9	13.4	8.0	63	6.4
device resonance wave period 9.75 s (126 m)					
l/a	device length [m]	'harbour' length [m]	chamber length [m]	'harbour' resonance	
				wave length [m]	wave period [s]
1.17	22.4	11.3	9.6	63	6.4
1.33	23.8	12.7	9.6	66	6.5
1.50	24.4	13.7	9.2	67	6.6
1.67	24.7	14.5	8.7	68	6.6
device resonance wave period 10.25 s (135 m)					
l/a	device length [m]	'harbour' length [m]	chamber length [m]	'harbour' resonance	
				wave length [m]	wave period [s]
1.17	24.0	12.1	10.4	68	6.6
1.33	25.5	13.7	10.3	71	6.8
1.50	26.2	14.8	9.9	73	6.9
1.67	26.5	15.6	9.4	74	6.9

The range of wave period at which the device is operating well is given in the next table:

Table 7.4 Range of wave period at which a device can operate well

l/a	wave length to which the device is tuned			
	8.75 s	9.25 s	9.75 s	10.25 s
1.17	5.9 - 8.75 s	6.1 - 9.25 s	6.3 - 9.75 s	6.6 - 10.25 s
1.33	6.0 - 8.75 s	6.2 - 9.25 s	6.5 - 9.75 s	6.8 - 10.25 s
1.50	6.0 - 8.75 s	6.3 - 9.25 s	6.6 - 9.75 s	6.9 - 10.25 s
1.67	6.1 - 8.75 s	6.4 - 9.25 s	6.6 - 9.75 s	6.9 - 10.25 s

All ranges of wave period are starting at periods longer than about 6 s. This means that in summer at quite a number of days the performance of the devices will not be very good.

The largest part of the converted wave power will be situated in this range of resonance periods. However, also at lower and higher periods the wave power can be converted, but at lower efficiency. From the Figures 7.11 a and b, the total amount of wave power for each device can be derived.

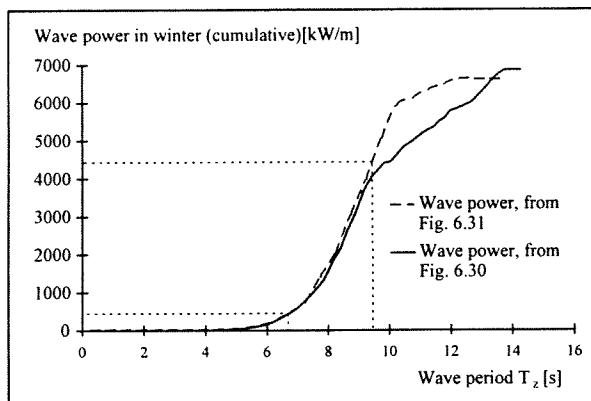


Figure 7.11 a Wave power in winter, calculated by the probability of period and wave height

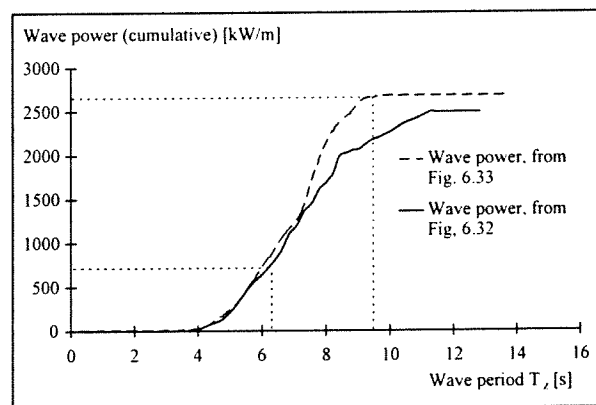


Figure 7.11 b Wave power in summer, calculated by the probability of period and wave height

The total amount of wave power, given in the next table, is estimated by these two lines, combined with the results of Table 7.4. In Section 6.4.2 it has been discussed that the estimation of the wave power values is too high, in winter the total amount of wave power is overestimated by a factor 1.2 and in summer by a factor 1.4. Consequently, in reality all values in Table 7.5 have to be divided by these factors.

Table 7.5 Wave power and probability of occurrence

device resonance period		8.75 s		9.25 s		9.75 s		10.25 s	
l/a		A	B	A	B	A	B	A	B
1.17	winter	2877	59	3756	64	4788	67	5565	67
	summer	1813	32	1886	28	1778	24	1672	21
	year	4690	45	5642	45	6566	45	7237	43
1.33	winter	2877	59	3732	61	4743	65	5520	65
	summer	1813	32	1818	26	1725	22	1619	19
	year	4690	45	5550	43	6468	43	7139	41
1.50	winter	2853	57	3698	60	4698	63	5475	63
	summer	1756	29	1778	24	1672	21	1566	18
	year	4609	42	5476	41	6370	41	7041	40
1.67	winter	2829	56	3653	58	4653	61	5377	60
	summer	1704	27	1725	22	1619	19	1470	16
	year	4533	41	5378	39	6272	39	6847	37

A = total amount of wave power in winter, summer or a year [kW/m]

B = probability of occurrence in winter, summer or a year [%]

This table shows that the higher the device resonance wave period, the higher the total amount of wave power in the range of resonance. To select the best device, some more considerations are useful.

The higher the ratio l/a, the higher the capture width at the resonance periods. This higher capture width causes that, although the total wave power in the resonance range is smaller, the total converted wave power will be higher for the devices with a higher l/a ratio.

Another consideration is the probability of exceedance of the wave period, these probabilities are given in Table 7.6. When the probability of exceedance in a year is selected at 10%, this means that about 37 days the wave period will be larger than 8.9 s. When the resonance period of the device is 9.25 s, the probability of exceedance in winter is about 14%, which means 25 days. This is an acceptable number of days, because some storm periods will occur, during which no wave power conversion is desired.

Table 7.6 Probability of exceedance of wave period

	range of interest of wave power	wave period with a probability of exceedance of:			
		5%	10%	15%	20%
winter	6.5-12.0 s	9.9 s	9.5 s	9.2	8.8
summer	4.5- 9.5 s	7.9 s	7.5 s	7.0	6.6
year	5.5-12.0 s	9.5 s	8.9 s	8.4	8.0

The following conclusions are used to select a device:

- wave power converting in winter is more important than in summer
- the selection is based on the total wave power in the range of wave periods at resonance, wave power at higher and lower periods can be converted, but at reduced efficiency
- the higher the load factor in winter, the more the firm power in this period
- the higher the ratio l/a, the higher the capture width, the higher the total converted wave power
- the probability of exceedance of the wave period must be larger than 10% in winter
- the shorter the device length, the smaller the caisson can be (although minimum dimensions for stability are required)

The device with a device resonance period of 9.25 s and a 'harbour' resonance period of 6.3 is preferred. In that case the ratio l/a has a value 1.5. The device will have a total length of 23 m. The chamber has a length of 9 m, the 'harbour' a length of 12.5 m and the thickness of the immersed front wall is 1.5 m.

Internal freeboard of the chamber

The height of the opening from the chamber to the turbine room, has to be $0.5 \cdot H_{\max}$, according to the Japanese theory. This internal freeboard is used to avoid intrusion of water into the turbine, see Section 5.4.6.

However, for the design of the breakwater in this study this value is quite high because a wave height with a return period of 500 years is used, while the common life time of a turbine is about 25 years [Whittaker;1985]. When a failure probability of 10% is accepted, a wave height with a return period of about 200 years can be used. Yet, the H_{\max} with a return period of 200 years is not much lower (about 1 m) than the wave height with a return period of 500 year. The maximum wave height is shown in Table 6.6, namely about 21 m. Consequently, the internal freeboard of the chamber has to be $0.5 \cdot 21.1 \text{ m} = 10.5 \text{ m}$ and thus the opening from the chamber to the turbine has to be higher than + 15.5 m C.D.

The minimum crest height is 17 m, in the ultimate design the crest height can be increased, when required for the openings to the turbine room and the installation of equipment.

Immersion depth of the front wall

As mentioned, the devices have to operate at wave heights of 1 - 4 m (Section 6.4.2) during common water levels. The mean low water at spring (M.L.W.S.) is + 0.5 m C.D. (Section 6.3.1). The NEL theory shows two methods of determining the immersion depth of the front barrier. The designs have an immersion depth of $0.25 - 0.35 H_{\max}$ or $1.0 \cdot H_{\text{operating, max}}$ below mean sea level.

The mean sea level is + 2.25 m C.D. (Section 6.3.1). Calculation of the immersion depth by $0.25 \cdot H_{\max}$ gives $0.25 \cdot 21 \text{ m} \approx 5 \text{ m}$, which means - 3 m C.D. Calculation by $1.0 \cdot H_{\text{operating, max}}$ gives an immersion depth of -1.75 m C.D. During the largest part of the year (and even in winter) the wave height is less than 2.5 m, see Figure 6.6. In this design the immersion depth is selected at - 2.5 m C.D., equal to $0.23 \cdot H_{\max}$. In that case, most waves can be converted even at mean low water spring. This value can be checked, by using the other dimensions of the device.

The resonance waves of the 'harbour' type devices can be seen as standing waves in the 'harbour' (wave length 60 m) and standing waves in the total device (wave length 117 m). An ideal standing wave has a wave height in front of the vertical wall of two times the incoming wave height. The 'harbour' length is 12.5 m and the device length 23 m.

Consequently, at an immersion depth of - 2.5 m C.D., even at M.L.W.S waves with a height of 4 m ($11.5/2 - 1.75$) can be converted when they resonate at the device length.

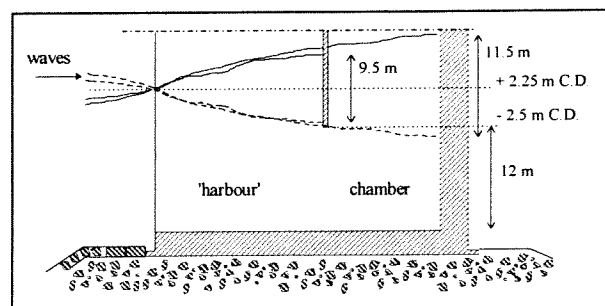


Figure 7.12 Quarter-wave resonance and the immersion depth of the front barrier

Height of the entrance opening

The influence of the height of the entrance on the performance of wave power conversion is not investigated in this study. From Section 5.4.5 it follows, that a value of 0.4 - 0.5 of the water depth is commonly accepted. In this design the averaged water depth is about 28 m. In this design, the opening is set at 12 m. ($12/28 = 0.43$, the same value as the NEL design in South Uist, section 5.4.5).

This means that the bottom plate of the device will have a thickness of 3 m, when the foundation level is - 17.5 m C.D. ($17.5 \text{ m} - 14.5 \text{ m} = 3 \text{ m}$)

Device width

In Section 5.4.4, is mentioned that the width of the device will be equal to 1-2 times the chamber length. The lines in Figure 5.14 and 5.15, on which the design in this section is based, are derived from a NEL design with a width of 1.0-chamber length. Table 7.2 shows the difference for a width of 1.0 or 1.5 the chamber length. The devices of the breakwater of Bilbao will have a width of 1.5-chamber length, which means about 13.5 m.

To avert long spans of concrete, this chamber will be divided into three chambers, as in the Sakata breakwater. The chambers will have a width of 4.25 m and the walls between are about 0.5 m thick. The total width of the device is then 13.75 m. In the upper part, the chambers are connected to each other by openings in the dividing walls.

Spacing between the devices

In Section 5.4.9 is mentioned that the optimal spacing is about $0.6-0.8 \cdot$ wave length, depending on the number of devices. The part of the breakwater in which devices will be placed has a length of more than 2 km (2280 m).

However, in this study the spacing is also dependent on the width of a caisson, which is required for stability. The smaller the width, the less the stability of the caisson, because of the loss of weight at the place of the device. The exact spacing will be determined in the section of the final design.

7.5 Dimensions of the Caisson with a Device

Stability of the caisson with device

When the dimensions of the device are known the stability of the caisson with a device can be checked, by the Goda theory, see **Appendix I**. However, the Goda theory is developed for vertical wall caissons. The breakwater in this study consists of caissons with a sloping top and a device in the middle. For these types of caissons some modifications are proposed.

Sloping top caisson

The first design method for sloping top caissons, was initially proposed by Moriha and Kunita, who modified the Goda pressure formula [Moriha et al.;1979]. Figure 7.13 shows the design wave pressure distribution in which the fundamental pressure distribution is the same as that by the Goda formula, given in **Appendix I** [Takahashi et al.;1994b].

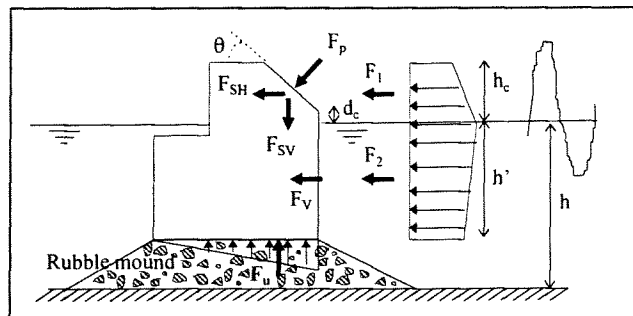


Figure 7.13 Design method of sloping top caisson

- with
- h = water depth
 - h' = height of the caisson below water level
 - h_c = crest height of the caisson
 - d_c = distance from water level to lowest point of the slope
 - F_1 = total wave force on the sloping top
 - F_2 = total wave force on the vertical wall
 - $F_V = F_2$
 - F_p = wave force normal to the sloping top
 - F_{SH} = horizontal wave force on the sloping top
 - F_{SV} = vertical wave force on the sloping top
 - F_u = uplift force

If it is assumed, that the wave force is a horizontal jet and that after collision with the slope, the fluid momentum has only a tangential component to the slope, then the total force normal to the slope F_p is $\rho \cdot Q \cdot V \cdot \sin\theta$. This is illustrated in Figure 7.14 [Takahashi et al.;1994b].

$$\text{with } F_p = F_1 \cdot \sin\theta \quad (7.1)$$

$$F_{SH} = F_1 \cdot \sin^2\theta \quad (7.2)$$

$$F_{SV} = F_1 \cdot \sin\theta \cdot \cos\theta \quad (7.3)$$

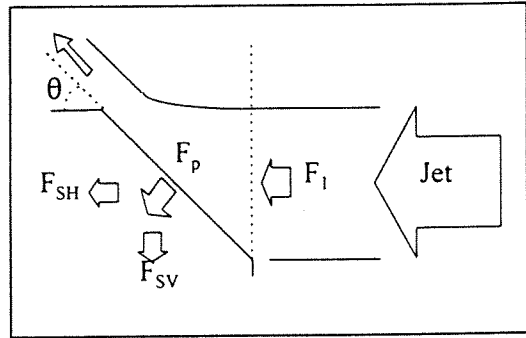


Figure 7.14 Wave force acting on the slope

Note that when $\theta = 45^\circ$, the horizontal wave force F_{SH} on the slope is one half the wave force on an equivalent vertical wall F_1 . The wave force on the vertical wall F_2 and the uplift force F_u can be directly calculated by the Goda formula.

The sliding force of the caisson F_s is increased by the vertical component of the force on the slope F_{SV} :

$$F_s = \mu (W + F_{SV} - F_u) \quad (7.4)$$

with F_s = sliding force

μ = friction coefficient between caisson and rubble mound

W = submerged weight of the caisson

F_{SV} = vertical wave force on the slope

F_u = uplift force

Takahashi et al. have improved this design method [Takahashi et al.;1994b]. Some experiments were carried out in a large wave flume. Six types of model caissons were investigated, see Figure 7.15. Type 2 is a semi-sloping top caisson, having a slope starting above the water level.

Type 2 of these caissons is comparable to the caisson in this study, for a section without device.

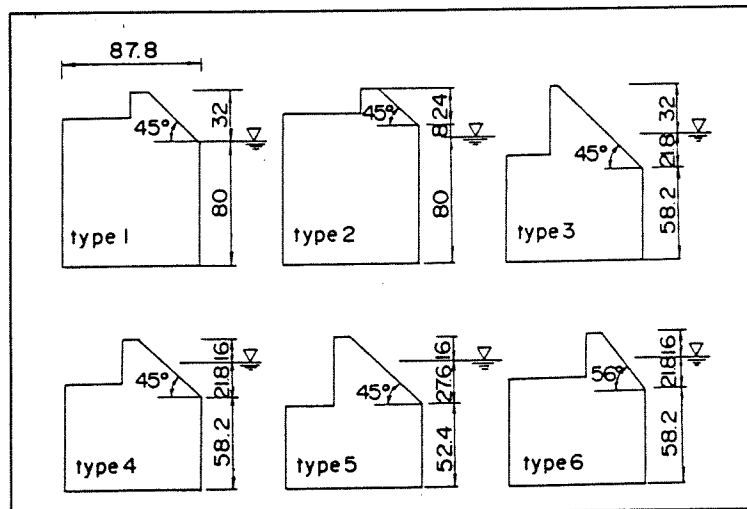


Figure 7.15 Model caisson, Type 1-6 (Unit: cm)

It turned out that the calculated horizontal wave force on the slope is underestimated, especially when the ratio H/h (wave height/water depth) is less than 0.4 and the wave period T is long. A new modification factor was introduced, namely λ_{SL} , that can express the wave force on the slope more appropriately:

$$F_{SH} = \lambda_{SL} \cdot F_1 \cdot \sin^2\theta \quad (7.5)$$

$$\text{with } \lambda_{SL} = \min \{ \max \{ 1.0, -23(H/L)\tan^{-2}\theta + 0.46\tan^{-2}\theta + \sin^{-2}\theta \}, \sin^{-2}\theta \} \quad (7.6 a)$$

$$\lambda_{SL} \cdot \sin^2\theta = \min \{ \max \{ \sin^2\theta, 23(H/L)\cos^2\theta + 0.46\cos^2\theta + 1.0 \}, 1.0 \} \quad (7.6 b)$$

A figure is given by Takahashi et al. which shows the modification factor versus the wave steepness H/L for various sloping top caissons. For the caissons with an angle of 45° of the sloping top, three regions can be defined:

- (1) When H/L is relatively small (less than 2%), $F_{SH} = F_1$
- (2) When H/L is relatively large (more than 6%), $F_{SH} = F_1 \cdot \sin^2 \theta$, as in the unmodified design method
- (3) When H/L is between (1) and (2), F_{SH} decreases as a function of H/L

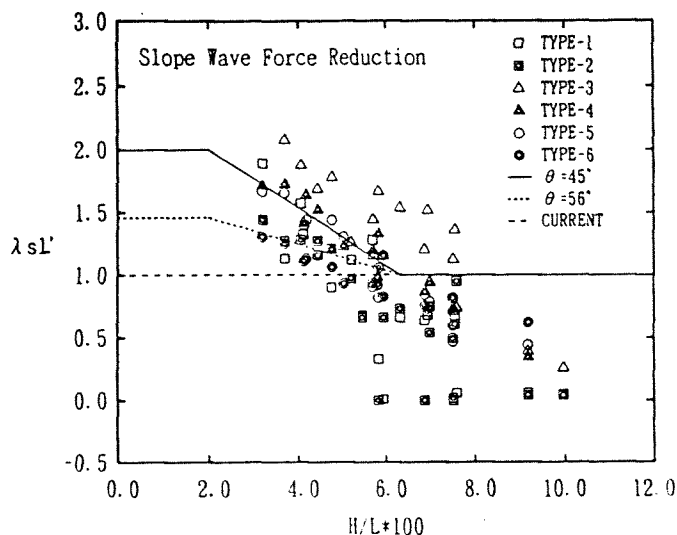


Figure 7.16 Modification factor λ_{sL}' calculated and experimental for Types 1-6

In this study all design waves have a steepness H/L larger than 6%, consequently this modification factor can be neglected in the design of the breakwater of Bilbao.

In the design method of Moriha and Kunita, the wave force on the vertical wall of the sloping top caisson is the same as estimated by the Goda formula. It was concluded on the basis of the experiments that the calculated horizontal wave force on the vertical wall is overestimated. Consequently, another modification factor was introduced, namely λ_v , to express this force:

$$F_v = \lambda_v \cdot F_2 \quad (7.7)$$

$$\text{with } \lambda_v = \min \{ 1.0, \max \{ 1.1, 1.1 + 11d_c / L \} - 5.0 H / L \} \quad (7.8)$$

Also for this factor a figure is given by Takahashi et al., which shows the modification factor versus the wave steepness H/L for various sloping top caissons. d_c is the distance from water level to lowest point of the slope, positive upward.

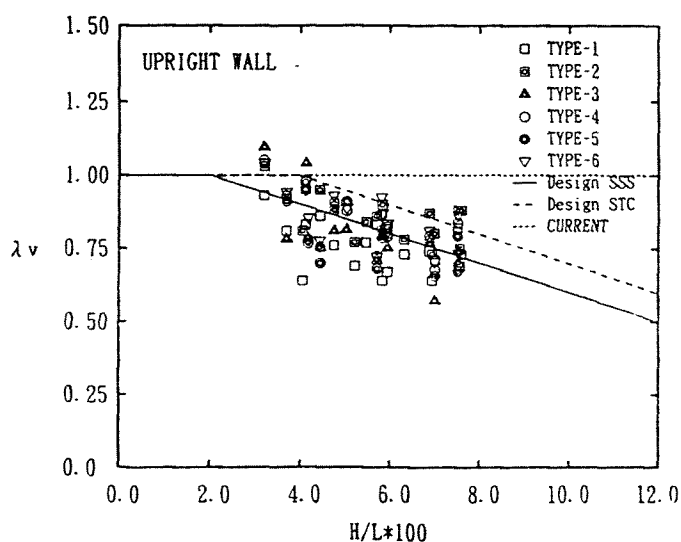


Figure 7.17 Modification factor λ_v calculated for caissons with $d_c < 0$ and Type 2 and experimental for Types 1-6

Figure 7.17 shows that experiments of waves with a steepness higher than about 8% are not executed. It is for that reason, that in the stability calculations of the caissons in this study, the value of λ_v will not be chosen lower than the value corresponding to the a steepness of 8%. In this study the minimum value of λ_v will be 0.8. Two calculations are given for example.

M.H.W.S. ($d_c = 1.5$ m, $H_{\max} = 21$ m, $L = 260$ m) $\lambda_v = 0.76$

C.D. ($d_c = 6.5$ m, $H_{\max} = 19$ m, $L = 240$ m) $\lambda_v = 1.0$

The new design method of Takahashi et al. was tested by sliding experiments. Figure 7.18 shows the results for Type 1, where W = submerged weight of the caisson. The boundary between the regions of sliding and not sliding is the minimum caisson weight against sliding. The new method gives a better estimation of the minimum weight, especially for values of H/h larger than 0.4. The minimum caisson weight is not proportional to wave height. When the wave height is large, the rate of increase in weight decreases, which means that the caisson is more resistant against severe waves than designed for.

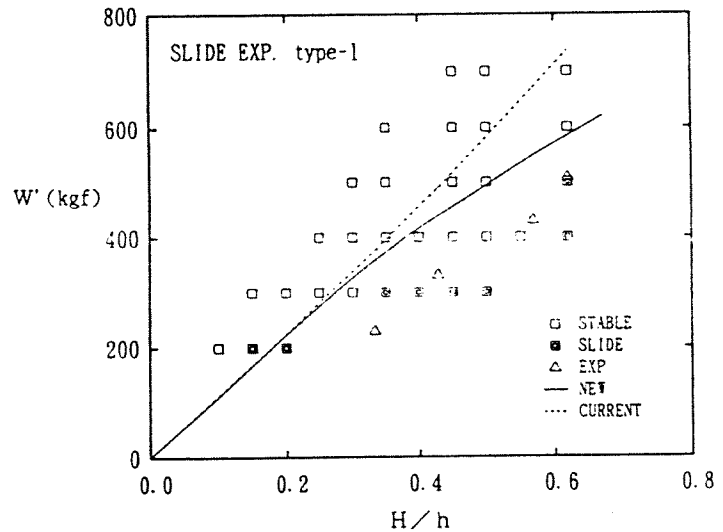


Figure 7.18 Sliding test of Type 1 and calculated minimum weight by the old and new design method -

Wave power converting device in the caisson

When a device is placed in a caisson, then the Goda formula needs some adaptations at that place. In the design of the wave power converting Japanese breakwater of Sakata, the correction factor $\lambda_1 = 1.0$ and $\lambda_2 = 0.0$. The correction factor λ_1 represents the variation in the slowly-varying wave pressure, while the factor λ_2 represents the variation of the impulsive pressure component of the wave pressure [Funakoshi et al.;1993]. For calculation of the caisson section with a device, in this study also $\lambda_1 = 1.0$ and $\lambda_2 = 0.0$ are taken.

This means that the stability of one caisson, will be calculated by the calculation of two sections, namely a section with and a section without device. The stability of the total caisson is the average calculated by the stability of these two sections, taking into account the width of each section.

The wave pressure distributions on the two sections for stability calculations are shown schematically in Figure 7.19 a and b.

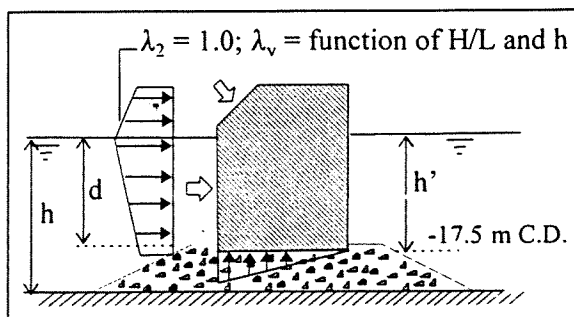


Figure 7.19a Wave pressure distribution on the section without a device

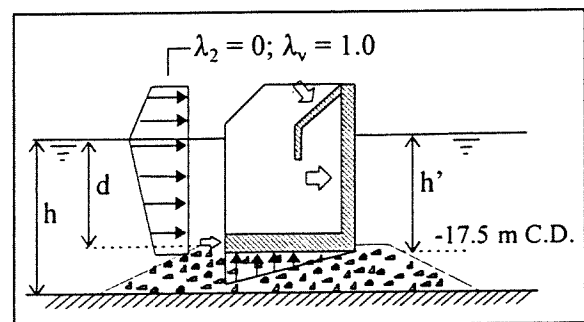


Figure 7.19b Wave pressure distribution on the section with a device

Estimations of the stability have been made for both sections. It follows that these type of caissons are possible, when the width of the caisson is large enough, to compensate for the loss of weight at the location of the device within the caisson. A minimum length of about 60 m will be required. In the next section the final design will be made, with the corresponding stability calculations.

7.6 Final Design

7.6.1 Information for Stability Calculation

For calculation of the stability of the final design, more accurate dimensions of the caisson are required.

General caisson design

Goda gives some information about general caisson designs [Goda;1992]. A caisson is divided into a number of inner cells. The size of the inner cells is limited to 5 m or less, in ordinary design. The outer wall is 40 - 50 cm thick, the partition walls are 20 - 25 cm thick and the bottom slab is 50 - 70 cm thick. Some caisson designs for specific locations in Japan, illustrate these assumptions. The accurate thicknesses have to be calculated by the stress analysis of reinforced concrete.

The calculation of these thicknesses will be given in Chapter 9.

Calculation of the weight of the caisson

- the caisson will be ballasted by sand, wet density 2000 kg/m^3
- the upper part of the caisson (part above the lowest point of the slope) will be concrete, 2400 kg/m^3
- the bottom plate of the device, thickness 3 m will be concrete, 2400 kg/m^3

Minimum dimensions of the turbine room

- the turbine to be applied will be a Wells tandem type, see Figure 4.15, as in the Sakata breakwater
- the turbine and generator will have a diameter of less than 3 m
- the distance between the turbine and the walls and roof has to be respectively 1 m and 0.5 m
- there will be two openings from the air chamber to the turbine room, having a height and width of 2.0 m
- the turbine will be installed with its centre at the same height as the centre of the openings to the turbine room, so that the air flow will drive the turbine well

Concrete dimensions

- the caisson is divided mainly into inner cells of mainly less than 5 m
- the thickness of the outer walls is assumed to be 0.5 m
- the thickness of the bottom slab is assumed to be 1.0 m
- the thickness of most inner walls is assumed to be 0.25 m
- the thickness of the dividing walls between the air chambers is assumed to be 0.5 m
- the thickness of the immersed front wall will be 1.5 m
- the thickness of the slope of and the roof of the device is assumed to be 1.0 m

Dimensions of the turbine room

- because of the required dimensions of the turbine room, the crest height of the turbine room will be + 19.5 m C.D. and consequently, the slope of the top of the device has to be 55° instead of 45° m
- the overall length (perpendicular to breakwater length) of the turbine room is 7 m, the width 14.75 m (including the two outer walls of 0.5 m) and the height 5 m (including the roof of 1.0 m)

Length of the rubble mound berm in front of the caisson

The caissons are placed on a rubble mound foundation, see Section 7.3. For the determination of the impactive pressure coefficient with the modified theory of Takahashi, see **Appendix I**, the length of the berm in front of the caisson, B_M (see Figure 7.4) is used. In the design of this study this length is assumed to be 15 m.

Caisson width and spacing

The determination of the caisson width, is influenced by as well stability requirements as by the appropriate spacing between the devices. When only one type of caissons will be constructed (no caisson without devices), then the spacing between the devices is the same as the caisson width. The ratio spacing / wave length is given in Table 7.7 for different wave lengths and a caisson width of 60-80 m

Figure H.18, Appendix H, shows the influence of the spacing on the power amplification factor. In the breakwater of Bilbao, more than 25 devices will be installed. Consequently, the power amplification will be high for values of c/λ between 0.4 - 1.0, 1.4 - 2.0,, with the highest values close to $c/\lambda = 1.0, 2.0, \dots$

When the spacing is selected at 60 m, the power amplification value has high values for wave periods up to 9.75 s. An advantage of the power amplification factor with these values is, that the relative low power values (wave periods 6.25 - 8.25 s) have the highest amplification factor. In this way, the converted power levels will be more equal for different wave lengths.

An advantage of caissons with a large width is the reduced mean wave force per unit width of the caisson for obliquely incident waves, because of the phase difference along the caisson. A width of the caisson of 60 m is possible to construct, probably steel frames and / or pre-tensioned concrete have to be used. The main purpose of this strengthening is to fulfil the required transport strength of the caisson. In Japan even a caisson with a width of 100 m has been constructed [Tanimoto et al.;1994]. In the Netherlands caissons of 68 m were used in the 'Brouwers Dam' [J.M. van Westen;1984].

Some drawings of the final design are shown in **Appendix K**.

Table 7.7 Influence of the caisson width on the spacing

T_z [s]	λ [m]	spacing / wave length = c/λ [-]				
		c = 60 m	c = 65 m	c = 70 m	c = 75 m	c = 80 m
4.25	28	2.14	2.32	2.50	2.68	2.86
4.75	35	1.71	1.86	2.00	2.14	2.29
5.25	43	1.40	1.51	1.63	1.74	1.86
5.75	51	1.18	1.27	1.37	1.47	1.57
6.25	60	1.00	1.08	1.17	1.25	1.33
6.75	70	0.86	0.93	1.00	1.07	1.14
7.25	79	0.76	0.82	0.89	0.95	0.99
7.75	88	0.68	0.74	0.80	0.85	0.91
8.25	98	0.61	0.66	0.71	0.77	0.82
8.75	107	0.56	0.61	0.65	0.70	0.75
9.25	117	0.51	0.56	0.60	0.64	0.68
9.75	126	0.48	0.52	0.56	0.60	0.63
10.25	135	0.44	0.48	0.52	0.56	0.59

7.6.2 Stability Calculation of the Caissons

Stability calculation with the modified Goda theory

The stability of the caissons is calculated by the theory of Goda, which has been modified (1) for the sections without device for the sloping top and (2) for the sections with device, for the wave power conversion.

The stability of the caissons of sections with and without device, has been checked for three water levels, namely C.D., + 2.5 m C.D. and + 5 m C.D. For each water level, five maximum design waves with a steepness of 2.0, 2.5, 3.0, 3.5 and 4.0 % have been used. This has been carried out for the segments C-G of the breakwater, see Section 7.1. The method of the stability calculation is shown in Figure 7.20.

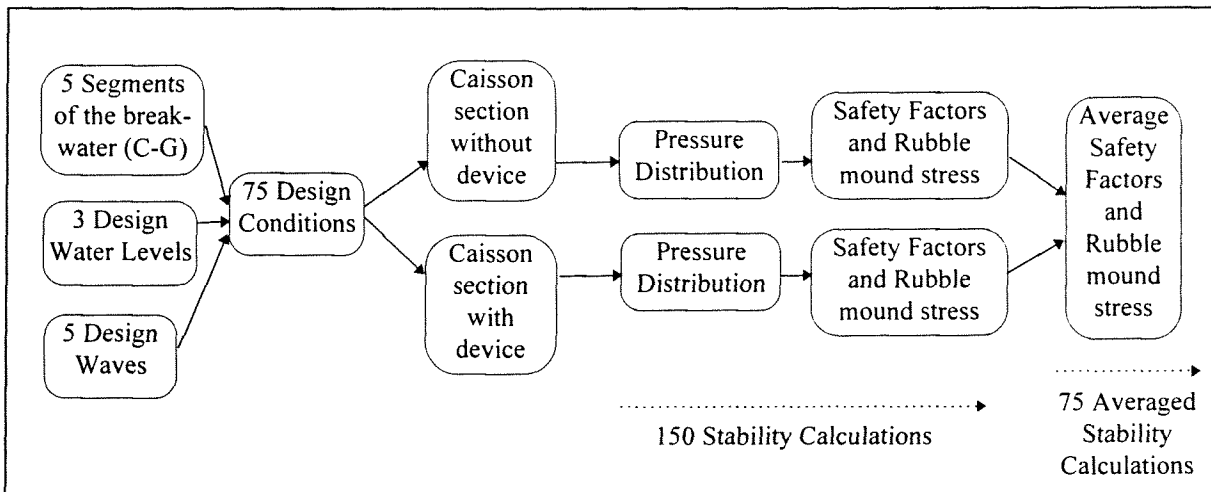


Figure 7.20 Stability calculations of the caissons

The final design is a caisson with a total length of 39 m. At the front side the caisson has a toe of 1.0 m and at the back side a toe of 4 m. The width of the caisson is 60 m. At the section without device the back side of the top structure is lowered to + 7.5 m C.D. over a length of 16 m. This has been done for two reasons, namely to shift the centre of weight to the left (which gives a opposite moment) and it is assumed that the wave transmission into the port is decreased, when waves flow over the caisson.

When the width of the caisson is 60 m, the averaged stability safety factors for overturning and sliding of the caissons with a device are higher than 1.2 (which is the minimum value of the safety factors). For the calculation of the average safety factors it is assumed that the caisson is able to distribute the wave forces of both sections (i.e. without device and with a device) over the total bottom plate. For this reason the bottom plate must have considerable rigidity.

The design method of the caissons in this way is acceptable, because in practice the wave forces may be less than in this method. This possible decrease, is caused by phase differences along the caisson (the total width of 60 m will not be attacked by a wave at one moment) and a phase difference between the wave force at the caisson sections without device and the device itself.

The stability calculations are shown in **Appendix L**.

Bearing capacity of the rubble mound foundation

The bearing capacity of the rubble mound foundation has also to be checked. It is mentioned that the maximum stress of the rubble mound, has been taken usually as 400-500 kN/m² [Tanimoto et al.;1994] This maximum stress occurs in general at the toe at the back side of the caisson. As a maximum value 600 kN/m² is used [Hou et al.;1994]. In Japan in 1989, a new calculation method for the bearing capacity of a caisson breakwater on a rubble mound foundation was included in the

Technical Standards. This calculation uses the simplified Bishop method of circular slip failure analysis [Kobayashi et al.;1987].

In this study, the rubble mound stress is less than 600 kN/m^2 and during most wave conditions the stress has been kept lower than 500 kN/m^2 .

In general, the total bottom plate area must have a positive rubble mound stress. This means that the resultant pressure force has to be situated within the middle part of the bottom plate, with a distance of $1/3$ of the bottom plate length. With this assumption the rubble mound stress can be calculated by the following equation [J.M. van Westen;1984].

$$\sigma = \frac{W}{B} \pm \frac{M}{\frac{1}{6}B^2} \quad (7.9)$$

- with σ = rubble mound stress [kN/m^2]
 W = submerged weight of the caisson [kN]
 B = length of the bottom plate [m]
 M = total moment on the caisson around the centre of the bottom plate [kNm]

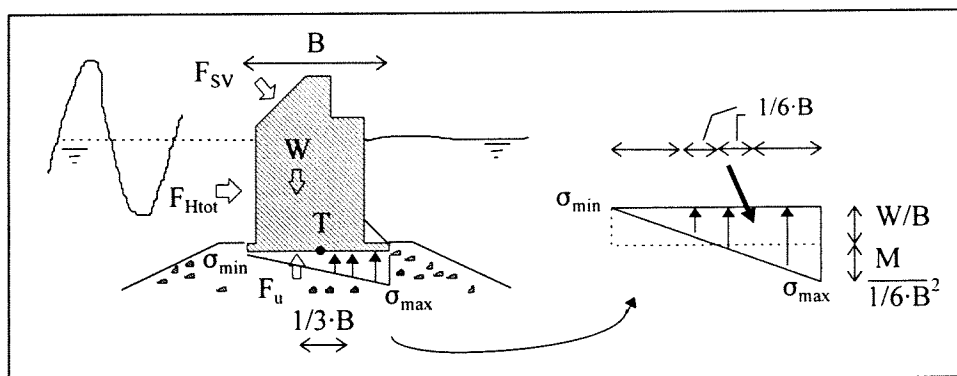


Figure 7.21 Rubble mound stress on the section without a device

For the design in this study, the rubble mound stress is the most important parameter. To fulfil the requirements of the rubble mound stress, the centre of the weight has been shifted to the left as much as possible and a toe of 4 m at the back side is needed.

For the calculation of the average safety factors it is assumed that the caisson is able to distribute the wave forces of the section without device as well as with a device over the total bottom plate. The calculations of the rubble mound stresses are shown in **Appendix L**.

Wave overtopping and the stability against sea side sliding

The method of Goda does not check the stability against sliding to the sea side. This danger exists when at the sea side a wave though occurs and, consequently, the water level behind the caisson higher is than in front of it. This danger becomes more severe when waves overtop the breakwater, causing an even higher water level at the back side.

In this study this phenomenon is investigated roughly, for a water level of + 5 m C.D. In **Appendix L**, the weight of the section with and without device is given, respectively 9006 kN/m and 19162 kN/m. The average weight per m width of the caisson is 16542 kN/m.

With a maximum significant wave height of 12 m and an ideal standing wave, the wave height in front of the breakwater is two times the incoming wave height. The water depth in front of the breakwater is 10.5 m (22.5-12 m) and behind 22.5 m (no overtopping). In this rough analysis, the water pressure is assumed to be hydrostatic (in reality the wave pressure distribution has to be used, which causes a less dangerous situation).

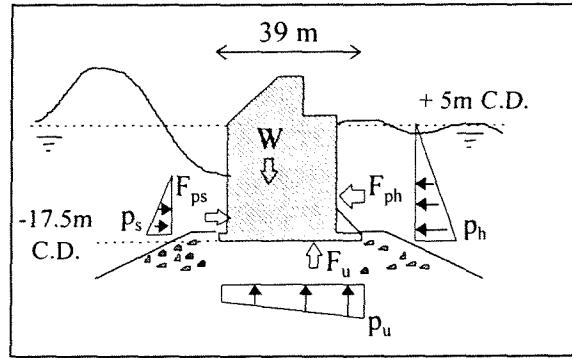


Figure 7.22 Wave overtopping of a section without device

When there is no overtopping, the resultant force F_{ph} (2558 kN) - F_{ps} (557) is 2001 kN. The resultant uplift force is 6335 kN. With a friction coefficient of 0.6, the caisson can withstand a horizontal force of 6124 kN/m ($0.6 \cdot (16542 - 6335)$). Consequently, the safety factor has a value of 3.1.

When the transmission coefficient is 0.5, behind the breakwater a wave height of 6 m exists, resulting in water level of + 8 m C.D. The resultant force F_{ph} (3285 kN) - F_{ps} (557) is 2728 kN. The resultant uplift force is 6911 kN. With a friction coefficient of 0.6, the caisson can withstand a horizontal force of 5779 kN/m ($0.6 \cdot (16542 - 6911)$). Consequently, the safety factor has a value of 2.1.

This analysis shows that the danger of sea side sliding is not large when wave overtopping is limited. However, this failure possibility has to be better investigated, because in history, most caisson breakwaters failed during heavily overtopping [Oumeraci;1994].

Dynamic response of Caisson Breakwaters

In fact, the stability calculation by the Goda theory is a static method. In that method high impact pressures can be avoided by following the design recommendations. More recently, the dynamic behaviour of caissons on a rubble mound foundation has been investigated. [Goda;1994] [Kortenhaus et al.;1994] [Oumeraci et al.;1992] [Schmidt et al.1992]

In this study, the dynamic behaviour of the wave power converting caisson has not been investigated.

7.7 Conclusions

Devices will be installed in that part of the new breakwater with the East West direction, to have a good performance of the wave power converting devices. The devices have to be designed to operate well and the caissons have to be designed for stability and strength. These two requirements are strongly related.

The caissons will have a sloping top. At the section without device, the angle of this slope is 45° and the crest height + 17 m C.D. The slope of the device is 55° and the crest height + 19.5 m C.D. The water depth in front of the breakwater above the rubble mound berm is larger than 0.6 times the water depth, to prevent high impulsive wave pressure.

The determination of the 'harbour' and chamber length of the device, is designed such that wave power conversion can take place during an acceptable number of days and the total amount of converted wave power is quite large. The device with a device resonance period of 9.25 s (wave length of 117 m) and a 'harbour' resonance period of 6.3 (wave length of 62 m) is preferred. In that case the ratio l/a has a value 1.5. The device will have a total length of 23 m. The chamber has a length of 9 m, the 'harbour' a length of 12.5 m and the thickness of the immersed front wall is 1.5 m.

The internal freeboard of the air chamber is 10.5 m, what means that the opening to the turbine room has to be higher than + 15.5 m C.D. The immersion depth of the front wall is - 2.5 m C.D. and the height of the entrance is 12 m. The device has a width of 13.75 m and the chamber is divided into three parts.

The spacing between the devices is equal to the length of the caissons, which is 60 m. With this width, the caissons are stable against sliding and overturning and the wave power conversion is high during most of the wave periods.

The stability of the caissons is calculated by the theory of Goda, which has been modified (1) for the sections without device, for the sloping top and (2) for the sections with device, for the wave power conversion. The modification for the sloping top was derived by Takahashi et al. [Takahashi et al.;1994b] and the modification for wave power conversion by Funakoshi et al. [Funakoshi et al.;1993.].

The drawings of the final design are shown in **Appendix K**.

The final design has been checked for sliding, overturning and rubble mound stress, see **Appendix L**. The caisson have a total length of 39 m and a width of 60 m. The averaged safety factors are larger than 1.2 (which is the minimum value of the safety factors recommended by the Goda theory). In general the average maximum rubble mound stress is less than about 500 kN/m^2 and in all situations much less than 600 kN/m^2 . The resultant force of the rubble mound stress is situated in the middle 1/3 part of the bottom plate. For this stability calculation, it is assumed that the bottom plate has a sufficient rigidity to distribute the wave forces over the total bottom plate area.

A rough analysis of wave overtopping and sea side sliding shows that this danger is not large when wave overtopping is limited. However, this failure possibility has to be better investigated, because in history, most caisson breakwaters failed during heavily overtopping [Oumeraci;1994].

7.8 References

- Dawson, J.K.(1979); *Wave Energy*, Energy Paper Number 42; Department of Energy, Harwell, England
- Funakoshi, H., Ohno, M., Takahashi, S., Oikawa, K.(1993); *Present Situation of Wave Energy Conversion Systems*; Civil Engineering in Japan, Vol.32, pp 108-134
- Goda, Y.(1992); *The Design of Upright Breakwaters*; Proc. of the Short Course on Design and Reliability of Coastal Structures, attached to the 23rd Int. Conf. on Coastal Engineering, pp. 547-568
- Goda, Y.(1994); *Dynamic response of upright breakwaters to impulsive breaking wave forces*; Coastal Engineering, Vol.22, pp. 135-158
- Hou, H.S., Chen, C.C., Hu, T.M., (1994); *Study of Deep Water Breakwater Design Factors*; Hydro-Port '94; Proceedings of the Int. Conf. On Hydro-Technical Engineering for Port and Harbor Construction, pp. 721-733
- Kobayashi, M., Terashi, M., Takahashi, K.(1987); *Bearing capacity of a rubble mound supporting a gravity structure*; Rept. Port and Harbour Res. Inst., Vol.26, No.5, pp. 215-252
- Kortenhaus, A, Oumeraci, H., Kohlhase, S., Klammer, P.(1994); *Wave-induced Uplift Loading of Caisson Breakwaters*; International Congress on Coastal Engineering, Chapter 94, pp.1298-1311
- Morihira, M., Kunita, O.(1979); *Model Experiments on Hydraulic Characteristics of Sloped Wall Breakwater*; Coastal Engineering in Japan, Vol.26, pp.295-288
- Nakada, H., Suzuki, M., Takahashi, S., Shikamori, M.(1992); *Development test of wave power extracting caisson breakwater*; Civil Engineering in Japan, Vol.31, pp.146-164
- Oumeraci, H., Partenscky, H.W., Kohlhase, S., Klammer, P.(1992); *Impact Loading and Dynamic Response of Caisson Breakwaters*; International Congress on Coastal Engineering, Chapter 113, pp.1475-1488
- Oumeraci, H.(1994); *Review and analysis of vertical breakwater failures - lessons learned*; Coastal Engineering, 22, pp. 3-29
- Schmidt, R., Oumeraci, H., Partenscky, H.W.(1992); *Impact Loads Induced by Plunging Breakers on Vertical Structures*; International Congress on Coastal Engineering, Chapter 118, pp.1545-1558
- Takahashi S., Tanimoto, K., Shimosako, K.(1994a); *Dynamic Response and Sliding of Breakwater Caisson Against Impulsive Breaking Wave Forces*; Proc. of the Int. Workshop on Wave Barriers in Deepwaters, Yokosuka, Japan, pp. 362-401
- Takahashi, S., Hosoyamada, T., Yamamoto, S.(1994b); *Hydraulic Characteristics of a Sloping Top Caisson - Wave forces acting on the sloping top caisson -*; Hydro-Port '94; Proceedings of the Int. Conf. On Hydro-Technical Engineering for Port and Harbor Construction, pp. 733-746
- Tanimoto, K., Takahashi S.(1994); *Japanese Experience on Composite Breakwaters*; Proc. of the Int. Workshop on Wave Barriers in Deepwaters, Yokosuka, Japan, pp. 1-24
- Westen, J.M. van(1984); *Closure of the Brouwershavensche Gat*; The Closure of Tidal Basins; Delft University Press, the Netherlands, pp. 663-727
- Whittacker, T.J.T., Leitch, J.G., Long, A.E., Murray, M.A.(1985); *The Q.U.B. Axisymmetric and Multi-Resonant Wave Energy Converters*; Journal of Energy Resources Technology, Vol.107, pp. 74-80

8 Wave Power Conversion into Electricity

8.1 Introduction

In the former chapter, the devices have been designed. This has been done in relation to stability as well as to wave power conversion. For further conversion some equipment is required, that is situated in the turbine room. The air power has to be converted into mechanical power by a turbine and the mechanical power into electricity by a generator. The required equipment will be described briefly in Section 8.2.

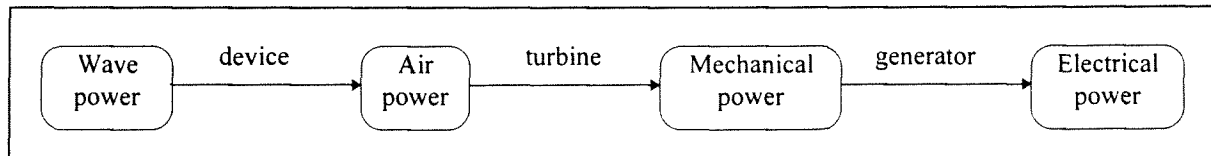


Figure 8.1 Wave power conversion

When the efficiency of all the parts of the power conversion system are known, the final electricity output can be estimated, which is given in Section 8.3. For the efficiency of the conversion from wave power into air power, called the capture width, the probability of wave length and wave direction have been taken into account. Multiplying this capture width by the power amplification factor corresponding to the spacing between the devices, gives the capture width of the devices placed next to one another in the breakwater. The efficiency of the turbine and generator are assumed to have a constant value.

By using the information of Chapter 6, about the wave length and the corresponding wave power value, the finally converted electricity is estimated.

In Section 8.4, some economic aspects of the new breakwater and the converted electricity are discussed briefly.

Finally, the conclusions of this chapter are given in Section 8.5 and the references in Section 8.6.

8.2 Turbine Room Equipment

In this section, the required equipment will be described briefly. The requirements of the turbine and generator that must be fulfilled will be discussed. The proposed layout of the turbine room is shown in Figure 8.4.

8.2.1 Turbine Generator

Principle of operation of the Turbine Generator

The turbine is assumed to have a linear turbine damping characteristic (pressure drop across the turbine linear to the volume flow through it). Several types of self rectifying turbines have been developed, like the McCormick turbine (mainly U.S.), the Wells and Reflair turbine (mainly U.K.).

The Wells turbine has become well established as the main power take-off system for oscillating water column devices. This turbine uses blades on a rotor which are symmetrical, see Figure 8.2. Air flow coming from above as well as air flow coming from below, gives a rotation in the same direction. The Wells turbine can accommodate one or two rotor planes i.e. monoplane and biplane respectively [Gato;1995]. The pressure drop across a biplane turbine is almost twice that of the monoplane due to the increase in bladed area [Curran et al.;1995].

The turbine can be directly coupled to a generator, for the turbine operates at a sufficient high rotational speed.

A tandem type arrangement, horizontally situated, is used in the Sakata Port breakwater, see Figure 4.14. This type has two turbines and only one generator. The advantage of a tandem type is that the forces in the axial direction are cancelled. This type turbine generator is expected to operate at variable rotational speed up to 1000-2000 rpm, depending on the turbine generator characteristics [Nakada et al.;1992].

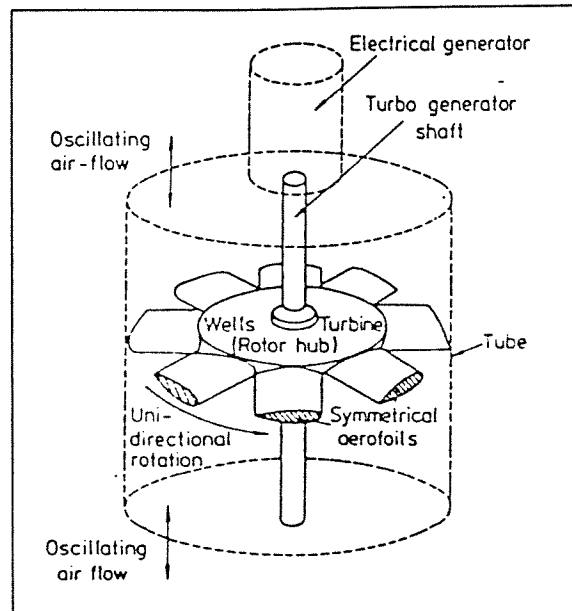


Figure 8.2 The Wells self rectifying turbine (monoplane)

Matching of the turbine generator

For the damping of the turbine generator, two principal subjects have to be considered [Curran et al.;1995].

1. The turbine generator should optimally damp the OWC.

For a good performance of the device (a good capture width), a well selected damping level is required. In this study the selection of this level is explained on basis of the oscillating body theory. In **Appendix B** and **Appendix G**, it is mentioned that for optimally wave power conversion at resonance frequency, without phase control, the damping of the turbine has to be $\Lambda = Z$ or $C_t = Z$. Consequently, the expression of the turbine constant becomes:

$$C_t = [B^2 + \omega^2 A^2]^{1/2} \quad (8.1)$$

with

$$\begin{aligned} B &= \text{radiation damping coefficient [Ns/m]} \\ A &= \text{hydrodynamic damping coefficient [kg] or [Ns}^2\text{/m]} \\ &= M + M_a - S/\omega^2 \end{aligned} \quad (8.2)$$

with

$$\begin{aligned} M &= \text{mass of the water column in the chamber [kg]} \\ M &= \text{added mass (mass of the 'harbour', frequency dependent) [kg]} \\ S &= \text{hydrostatic restoring constant [N/m]} \end{aligned}$$

Equation 8.1 shows that the optimal turbine constant has a minimum value equal to the radiation damping, but it increases for wave frequencies that are not at resonance frequency of the device. In real sea conditions, it is advantageous to apply a damping level higher than the optimal damping at resonance. The decrease in capture width at resonance wave frequencies will be outweighed by the improvement at other frequencies [Curran et al.;1995]. It is mentioned that in practice a damping close to twice the optimum damping at resonance frequency of the device is an appropriate selection [Hunter;1991] [Haskoning;1989].

In **Appendix G**, it has already been mentioned, that the value of the radiation damping coefficient B and the added mass M_a are not easy to determine. With the help of Figure G.6 of the non-dimensional radiation and added mass, a rough estimation of the optimal damping at resonance frequency of the device (wave period: 9.25 s, wave length: 117 m) can be made. The water level in this estimation is M.S.L. (+ 2.25 m C.D.).

is 15 or 50 kW/m and the capture width respectively 1.0 and 2.0, the captured wave power is respectively 206 kW and 1375 kW. Because of these differences, an appropriate turbine generator capacity has to be selected well. After discussion of the incoming wave power and the corresponding capture width in the next section, this turbine generator capacity will be selected.

Based on literature, the following assumptions can be made [Green et al.;1983] [Nakada et al.;1992] [Whittacker et al.;1985].

For the devices of the Bilbao breakwater, the tandem type Wells turbine generator will be used. The capacity will be about 1-2 MW, the exact capacity will be selected in the Section 8.3. For such a turbine an overall diameter of 2-3 m and a length of 4-5 m is assumed. The maximum number of revolutions per minute will be about 1000-1500 rpm.

8.2.2 Air Regulating Valves

When the air flow to the turbine exceeds a certain value, corresponding to an air power level higher than the capacity of the turbine, part of the air flow must be released to the open air. Regulation of this flow to the open air, will be determined by the rotational speed of the turbine generator [Takahashi et al.;1992]. Above a certain limit of rotational speed, part of the air flow will be released by air regulating valves. These valves are shown in Figure 8.4.

8.2.3 Layout of the Turbine Room

In connection with the results of the final design of Section 7.6, the layout of the turbine room including the equipment can be given. In analogy to the Sakata Port breakwater, the tandem type Wells turbine is situated horizontally behind the air chamber. The air flow from the chamber to the turbine is possible by two gaps in the back wall of the chamber. The height and width of these gaps is estimated at respectively 2.0 and 2.5 m. The proposed layout is schematically shown in Figure 8.4.

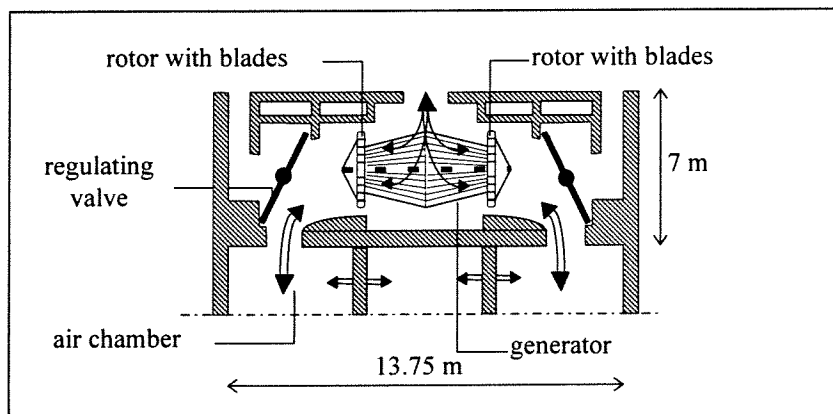


Figure 8.4 Layout of the machine room, schematically

In the theory of 'harbour' type devices, it is assumed that obliquely incident waves reach the air chamber as a normally incident wave. In that case the air pressure is roughly the same in the three parts of the air chamber.

8.3 Wave Power Conversion

8.3.1 Introduction

To estimate the converted wave power into electricity, the incident wave power has to be known and the corresponding efficiencies namely the capture width, turbine efficiency and generator efficiency. The capture width depends on the wave length and the angle of the incident waves to the breakwater.

The other two efficiencies depend mainly on the ratio of the converted power to the capacity of the turbine or generator.

8.3.2 Incoming Wave Power

The mean wave power in the first 200 days of the year is most of the time 25 kW/m and in the last 165 days 7.5 kW/m, see Figure 6.8. However, the corresponding wave length and direction have to be known, to determine the capture width. Figure 6.27 shows the relation between wave power and wave length for winter conditions (wave steepness of 1.3%).

The angle of the incident waves to the breakwater is of influence on the capture width of a device. In Section 6.3.2, Table 6.2 gives the direction of the waves. No correlation between wave length or wave power and wave direction is known. In this study no correlation is assumed.

In Figure 6.3 can be seen that waves coming from North East will not attack the new breakwater. The waves from NNEast and North are assumed to attack on respectively half and three-quarter of the length of the breakwater. This means that 91% of the incoming wave power can be converted.

The average angle of the incident waves to the devices, is calculated by its probability and direction. Only the waves that can reach the breakwater are used (91%). The calculated average angle of the incident waves is about 39°.

8.3.3 Wave Power Conversion

The devices are designed to operate at resonance wave periods of 6.3 and 9.25 s, see Section 7.4. The spacing between the devices is 60 m and the ratio spacing to wave length can be calculated. The estimated power amplification factor I_p is derived from Figure H.18. However, this figure is valid for normally incident waves. For an average angle of 39°, a reduction of 0.3 is assumed when the amplification factor has values higher than 1. This assumption is based on figures given by Thomas and Evans [Thomas et al.;1981].

The capture width of a single device is estimated based on the results of the capture width of the NEL devices, Figure 4.19. The maximum capture width is increased at 'harbour' resonance (6.3 s) with 25% and at device resonance (9.25s) with 50%, because that the devices are placed in a reflecting wall [Hunter;1991]. The values of the capture width are reduced by a factor 0.10, because of the in general obliquely incident waves of 39° instead of normally incident waves.

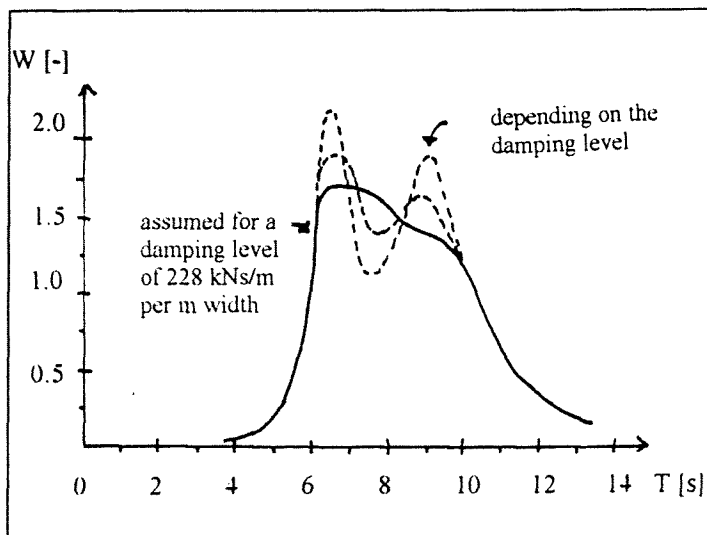


Figure 8.5 Capture width of a single device in a reflecting wall

The average turbine efficiency and generator efficiency is assumed to be 75% and 90%, respectively. These values are equal to the values proposed for the pilot plant of Ennore [Haskoning;1989].

In Table 8.1 the wave length and the corresponding wave power is given, based on the assumption of a wave steepness of 1.3 %. The the amplification factor I_p and the capture width of a single device W are also given. The generated electricity is given in kW and MWh.

Table 8.1 Wave period and the corresponding values of electricity generation in winter

T_z [s]	Probability [%]	P_w [kW/m]	c/λ [-]	I_p [-]	W [-]	$W \cdot I_p$ [-]	Air power [kW]	Electricity [kW]	Electricity [MWh]
4.25	2.6	1.2	2.14	0.6	-	-	-	-	-
4.75	3.2	2.0	1.71	1.1	0.1	0.1	-	-	-
5.25	4.2	3.4	1.40	0.9	0.3	0.3	13	-	-
5.75	6.1	5.4	1.18	0.8	0.9	0.7	53	-	-
6.25	8.1	8.4	1.00	0.3	1.7	0.5	59	-	-
6.75	10.1	12.7	0.86	1.9	1.7	3.2	564	381	161.5
7.25	7.8	18.7	0.76	1.6	1.7	2.7	699	472	154.7
7.75	14.4	26.8	0.68	1.5	1.6	2.4	884	597	361.0
8.25	9.7	37.4	0.61	1.3	1.5	2.0	1003	677	275.8
8.75	11.2	51.0	0.56	1.2	1.4	1.7	1178	795	374.1
9.25	7.8	68.1	0.51	1.1	1.4	1.5	1442	973	318.9
9.75	7.0	89.0	0.48	1.0	1.2	0.8	1469	991	291.4
10.25	4.3	114.3	0.44	0.9	1.0	0.9	1414	955	172.4
10.75	0.8	144.5	0.42	0.9	0.7	0.6	1252	845	28.4
11.25	0.7	180.1	0.39	0.9	0.5	0.5	1114	752	22.1
11.75	0.4	221.7	0.37	0.8	0.4	0.3	975	658	11.1
12.25	0.3	270.0	0.35	0.8	0.3	0.2	891	601	7.6
								average = 696 kW	$\Sigma = 2180$ MWh

In Section 6.4.2, has been concluded that the wave power in winter is overestimated by a factor 1.2. Because of the direction of the incident waves, 9% of the incoming wave power can not be converted (waves coming from North to NEast).

The total electricity supply of a device is calculated to be 2180 MWh in winter (day 0-175). This means that in reality the total supply will be about 1650 MWh (2180 MWh/1.2·0.91). Conversion takes place during 75% of the time. This means that during about 44 days no electricity will be supplied. The average generated electricity is 528 kW (696 kW/1.2·0.91) and usually the electricity is not higher than about 740 kW (975 kW/1.2·0.91). It is for these reasons that the turbine generator will have an installed capacity of 0.8 MW. The mean load factor of the generator during operating, is in that case 53% (528 kW/1000 kW).

In Table 8.2 the same information as in Table 8.1 is given, however the values are valid for the summer (day 175-365). The calculation of wave power is estimated by the assumed wave steepness of 1.6 %. The the amplification factor I_p and the capture width of a single device W are also given. The generated electricity is given in kW and MWh.

In Section 6.4.2, has been concluded that the wave power is overestimated by a factor 1.4. Because of the direction of the incident waves, 9% of the incoming wave power can not be converted.

The total electricity supply of a device is calculated to be 850 MWh in summer (day 175-365). This means that in reality the total supply will be about 550 MWh (850 MWh/1.4·0.91). Conversion takes place during 25% of the time. This means that during only about 48 days electricity will be supplied. At the other days the incoming wave power can not be converted.

Table 8.2 Wave period and the corresponding values of electricity generation in summer

T_z [s]	Probability [%]	P_w [kW/m]	c/λ [-]	I_p [-]	W [-]	$W \cdot I_p$ [-]	Air power [kW]	Electricity [kW]	Electricity [MWh]
3.75	2.5	0.9	2.73	0.9	-	-	-	-	-
4.25	8.7	1.8	2.14	0.6	-	-	-	-	-
4.75	20.4	3.1	1.71	1.1	0.1	0.1	-	-	-
5.25	15.3	5.1	1.40	0.9	0.3	0.3	19	-	-
5.75	16.5	8.2	1.18	0.8	0.9	0.7	81	-	-
6.25	11.3	12.7	1.00	0.3	1.7	0.5	89	-	-
6.75	7.2	19.2	0.86	1.9	1.7	3.2	853	576	174.1
7.25	4.3	28.3	0.76	1.6	1.7	2.7	1058	714	129.0
7.75	7.2	40.6	0.68	1.5	1.6	2.4	1340	904	273.5
8.25	3.6	56.7	0.61	1.3	1.5	2.0	1520	1026	155.2
8.75	1.3	77.3	0.56	1.2	1.4	1.7	1786	1205	65.8
9.25	0.9	103.1	0.51	1.1	1.4	1.5	2183	1474	55.7
								average = 830 kW	$\Sigma = 850$ MWh

The average generated electricity is 540 kW (830 kW/1.4·0.91) and usually the electricity is not higher than about 585 kW (900 kW/1.4·0.91). With an installed capacity of 1.0 MW, the mean load factor of the generator during operating is in summer 54% (540 kW/1000 kW).

8.3.4 Generated Electricity

With the results of winter and summer, the wave power conversion in a year is known. The total amount of electricity is in a year is 2200 MWh per device (1650 MWh in winter, 550 MWh in summer).

The total length of the breakwater is 2280 m. This breakwater will be constructed by 38 caissons of 60 m. These 38 devices, generate 83,600 MWh electricity per year and have a total installed capacity of 38 MW. The devices are operating during 179 days of the year, this is during about half of the year. The generated electricity can be compared to the average wave power in a year of Figure 6.8, giving the annual overall efficiency of the devices.

Converted wave power: $2200 / (365 \cdot 24) = 251 \text{ kW} / 13.75 \text{ m} = 18.3 \text{ kW/m}$

Incoming wave power: $(187 \cdot 25 \text{ kW/m} + 13 \cdot 115 \text{ kW/m} + 165 \cdot 7.5 \text{ kW/m}) / 365 = 20.3$

Annual overall efficiency: $20.3 / 18.3 = 90\%$

This efficiency is quite high, what is mainly caused by the point absorbing effect (i.e. a high capture width). The annual load factor of the turbine generator, see also Section 7.4, during operating is 53%. However, the annual load factor during the whole year is 26% (conversion takes place during 179 days of the year).

8.4 Economic Aspects

Two estimations of the costs of a caisson breakwater are given, namely US\$100,000 per metre length of the breakwater [Oumeraci;1994] or US\$100 per overall cubic meter caisson (in Italy) [Franco;1994]. For the breakwater in this study these two methods give roughly the same costs estimations.

As mentioned the total generated electricity is 2200 MWh per year per device.

With this information a rough estimation of the electricity costs can be made, with the following formula and assumptions [Dawson;1979][Green et al.;1983][Haskoning;1989] :

$$E.C. = \frac{(\text{cap. inv.}) \cdot (\text{fixed charge rate}) + (\text{oper. and maint. costs})}{(\text{total electricity})} \quad (8.3)$$

with E.C. = electricity costs [US\$/kWh]
 cap. inv. = capital investment
 = breakwater costs + power converting equipment costs + transmission costs
 breakw. c. = US\$ $6.0 \cdot 10^6$
 equipm. c. = US\$ $1.0 \cdot 10^6$
 transm. c. = 2% of breakwater and equipment costs
 = US\$ $0.14 \cdot 10^6$
 oper. and m.c. = operating and maintenance costs per year
 = 4% of capital investment
 = US\$ $0.29 \cdot 10^6$ /year
 fixed ch. r. = depending on interest and service life = 0.15

For the electricity costs it follows US\$ 0.62 / kWh when all costs are included. When the breakwater costs are not included, electricity costs are US\$ 0.09. It would be more reasonable to include 20% of the construction costs of the breakwater, in that case the electricity costs are US\$ 0.19/kWh.

It has been estimated that the cost of the generated electricity at Sakata Port is 20-40 yen/kWh and at other ports at the Pacific coast 15-30 yen/kWh [Nakada;1992]. Compared to these costs, the wave power converting breakwater of Bilbao can generate electricity at costs, close to the lowest estimations of the costs of a wave power converting breakwater like the Sakata breakwater (when 1US\$ \approx 120 yen).

However, in general in Europe electricity generation costs of US\$ 0.19/kWh are higher than the electricity costs of conventional power plants. The design of the breakwater in this study, shows that it is possible, even at this locations with very rough sea conditions, to design a wave power converting breakwater.

In this study the layout of the wave power converting breakwater is the same as the proposed rubble mound breakwater of Bilbao. When an other layout is used, for which a larger part of the incoming waves will be normally incident to the breakwater, the conversion efficiency will be higher and consequently the electricity costs will be lower.

In locations where the electricity costs are high, like isolated islands, these type of breakwaters become more attractive. In locations, where wave power is more equally divided over the year and the maximum design conditions for stability and strength are less severe, the electricity costs will be lower than in this study. However, probably the total generated quantity of electricity will be less.

8.5 Conclusions

To calculate the generated electricity, the efficiencies of the device and the used equipment have to be known. In the devices in this study, a tandem type Wells turbine generator will be installed. This turbine generator has to be able to damp the OWC optimally and to convert the air power efficiently.

The turbine generator will be situated in the turbine room, behind the air chamber. The air flow to the turbine is regulated by two valves, located in the openings from the air chamber to the turbine room. The regulation will be determined by the rotational speed of the turbine generator.

The incoming wave power can be estimated by the probability of the wave period and the assumed wave steepness in winter and summer. About 91% of all the waves during a year will attack the breakwater, with an average angle of incidence of 39°.

To determine the capture width of the devices placed in a row, the amplification factor and the capture width of a single device have to be known. These values have been derived from several theories. The average turbine efficiency and generator efficiency is assumed to be 75% and 90%, respectively.

In winter the average generated electricity is 528 kW during 75% of the days or 1650 MWh. In summer the average generated electricity is 540 kW during 25% of the days or 550 MWh. The installed turbine generator capacity is 1.0 MW. Consequently, the total installed capacity of the breakwater is 38 MW.

A rough estimation of the electricity costs shows that the wave power converting breakwater can generate electricity at the same or even lower costs than that of the Japanese breakwater. However, in general in Europe electricity generation costs of U\$ 0.19/kWh are higher than the electricity costs of conventional power plants. The design shows that it is possible, even at locations with very rough sea conditions to construct wave power converting breakwaters. When an other layout of the breakwater is used, which gives a better conversion efficiency, the electricity costs will be lower.

In locations where electricity costs are high, the construction of wave power converting breakwaters is more attractive. When the wave power is more equal divided over the year and the maximum design conditions for stability and strength are less severe, the electricity costs will be lower. However, probably the total generated quantity of electricity will be less.

8.6 References

- Curran, R., Raghunathan, R.S., Stewart, T.P., Whittacker, T.J.T.(1995); *Matching a Wells Turbine to the Islay Oscillating Water Column Wave Power Converter*; Proc. of the 14th Int. Conf. On Offshore Mechanics and Arctic Engineering, Copenhagen, Denmark, Vol. I-A, pp. 147-154
- Dawson, J.K.(1979); *Wave Energy*, Energy Paper Number 42; Department of Energy, Harwell, England
- Franco, L.(1994); *Vertical breakwaters: the Italian experience*; Coastal Engineering, 22, pp. 31-55
- Gato, L.M.C., Curran, R.(1995); *Performance of the Biplane Wells Turbine*; Proc. of the 14th Int. Conf. On Offshore Mechanics and Arctic Engineering, Copenhagen, Denmark, Vol. I-A, pp. 121-131
- Green, W.L., Campo, J.J., Parker, J.E., Miller, J.A., Miles, J.B. (1983); *Wave Energy Conversion with an Oscillating Water Column on a Fixed Offshore Platform*; Journal of Energy Resources Technology, Vol. 105, pp. 487-491
- Haskoning, Tebodin, Rites (1989); *Paradip - Ennore Coal Transport Feasibility Study, Final Report*; Haskoning, The Netherlands
- Hunter, R.(1991); *Future possibilities for the NEL Oscillating Water Column wave energy converter*; Seminar on Wave Energy, Imeche, England
- Nakada, H., Suzuki, M., Takahashi, S., Shikamori, M.(1992); *Development test of wave power extracting caisson breakwater*; Civil Engineering in Japan, Vol.31, pp.146-164
- Oumeraci, H.(1994); *Review and analysis of vertical breakwater failures - lessons learned*; Coastal Engineering, 22, pp. 3-29
- Takahashi, S., Nakada, H., Ohneda, H., Shikamori, M.(1992); *Wave Power conversion by a prototype Wave Power Extracting Caisson in Sakata Port*; Int. Conf. on Coastal Engineering, pp. 3440-3453
- Thomas, G.P., Evans, D.V.(1981); *Arrays of three-dimensional wave-energy absorbers*; Journal of Fluid Mechanics, Vol. 108, pp. 67-88
- Whittacker, T.J.T., Leitch, J.G., Long, A.E., Murray, M.A.(1985); *The Q.U.B. Axisymmetric and Multi-Resonant Wave Energy Converters*; Journal of Energy Resources Technology, Vol.107, pp. 74-80

9 Construction Method and Dimensions of the Caisson

9.1 Introduction

The method of construction of the wave power converting breakwater is of influence on the design of the caisson. The proposed construction method will be described briefly in Section 9.2. When the caissons will be transported, they must have a certain strength and they must be stable. The analysis for this strength and stability is given in Section 9.3. When the caissons are ballasted by water in a proper way, the caissons will be stable and no large moments will occur.

During the construction phase, the caissons must be stable against sliding and overturning. In Section 9.4, the stability of the caissons for some different wave conditions are checked. After sinking the caissons must be filled with ballast sand as soon as possible, finally the top structure can be constructed.

The dimensions of the concrete walls must be strong enough against impulsive wave pressure. The Japanese method of the pressure distribution is discussed and the thicknesses of the concrete parts are given in Section 9.5. In Section 9.6, some conclusions are drawn and in the last section the references are given.

9.2 Construction Method

The lower 24 m part of the caissons has to be constructed at first. This can be done in a dry construction dock at a certain location or in a large floating dock. It is possible to construct a part of the 24 m (bottom plate and lower part of the walls) in the dock and after that the higher part can be constructed when the caisson is placed in calm water. When the caisson is finished, it has to be transported to the location of the new breakwater. The rubble mound foundation has to be ready before sinking of the caisson. After placement of the caisson, the top structure can be made. The roof of the turbine room has to be pre-fab and can be placed finally, after the installation of the equipment in the turbine room.

The construction method can be divided into the following phases:

1. Construction of the lower 24 m part of the caisson, including the front wall, the sloping top of the device and a temporary closing of the device.
2. Construction of the rubble mound foundation.
3. Transport of the caisson.
4. Placement of the caisson and the foot protection blocks. The closing of the device can be removed.
5. Construction of the upper part of the caisson.
6. Installation of the turbine and other equipment.
7. Placement of the roof of the turbine room.

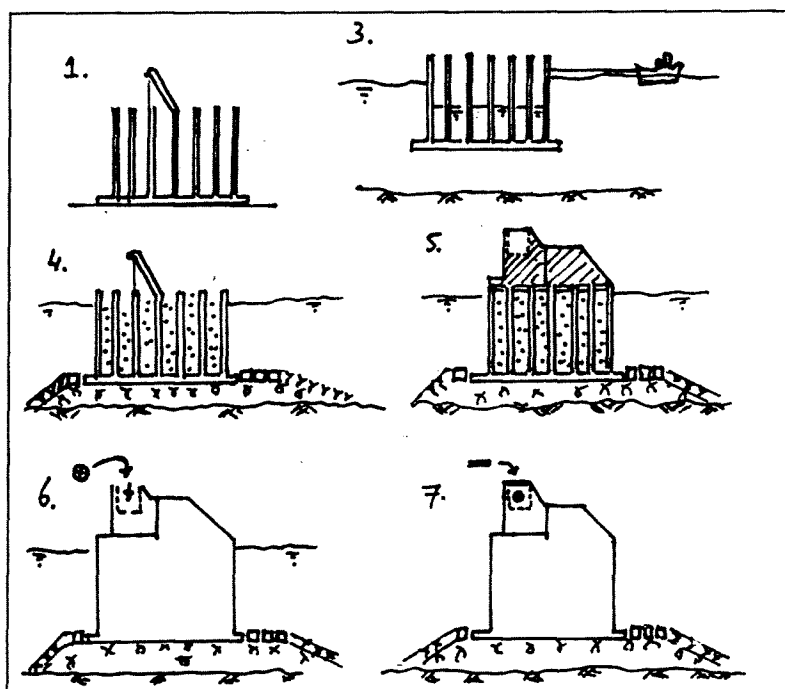


Figure 9.1 Construction method of the breakwater

For this construction method, it is required that the caissons are stable and strong enough during transport. The caissons have to be stable against sliding and overturning just after placement, when the upper part is not already constructed. This will be investigated in the next sections.

9.3 Stability and Strength during Transport

9.3.1 Stability and Wave Response of the Caisson

Stability of the caisson

During transport and sinking of the caisson it may not turn over. To check the stability, the following method is used [Mulder,1984].

The weight of the caisson is in equilibrium with the upward force according to:

$$m \cdot g = \rho \cdot g \cdot V \quad (9.1)$$

- m = mass [kg]
- g = gravitational acceleration [m/s^2]
- ρ = density of water [kg/m^3]
- V = volume of displaced water [m^3]

The weight is acting in the centre of gravity G , while the upward force acts on the pressure point B . B is situated in the centre of gravity of the displaced water. When a rotation ϕ is given to the caisson, an opposing moment is required to make the caisson stable. When B is above G the caisson is always stable.

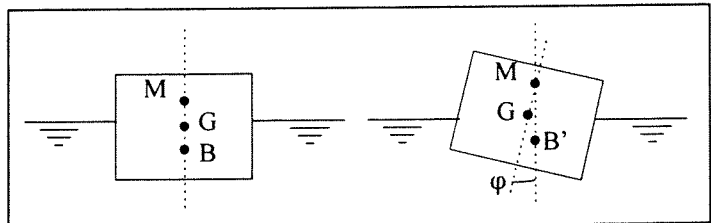


Figure 9.2 Stability of a floating caisson

M is the metacentre and the distance between G and M is called the metacentre-height. When M is above G , the caisson is stable and unstable when M is below G . The distance between B and M can be determined by:

$$BM = I/V \quad (9.2)$$

with I = moment of inertia [m^4]

When the caisson is divided into a number of inner cells and ballasted by water, the moment of inertia can be calculated by the following equation:

$$I = I_o - \sum I_i \quad (9.3)$$

with I_o = moment of inertia of the total caisson [m^4]
 I_i = moment of inertia of the inner cells [m^4]

With this theory the stability of the caissons of the breakwater can be calculated. The draught of the caisson is determined by two subjects. (1) During transport, a freeboard is required to prevent water inflow and (2) the caisson has to be placed on the rubble mound foundation of a level of - 17.5 m C.D.

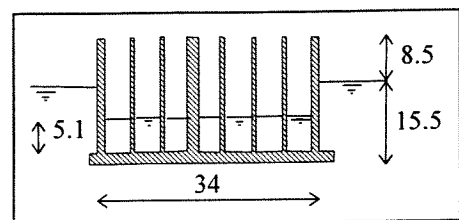


Figure 9.3 Draught and ballast water of the caisson

It is assumed that transport will take place only during periods when the significant wave height is less than 2 m, what means that the maximum wave height is about 3.6 m. A distance of about 4 m above the foundation is required for the sinking

phase. In that case the draught of the caisson is - 13.5 m C.D. The mean sea water level is 2.25 m, it is assumed that sinking of the caissons takes place during periods with a water level of + 2 m C.D. In that case, the draught is 15.5 m.

To give the caisson this draught, the caisson has to be ballasted. The ballast can consist of water or sand. The advantage of water as ballast, is that water can flow into the caisson simple and fast, what gives a fast method. An averaged layer of water in the caisson of about 4.9 m is needed for a draught of 15.5 m (weight and buoyancy in equilibrium):

$$39 \cdot 1 \cdot 2400^* + 3.25 \cdot 23 \cdot 2400^{**} + 4 \cdot (34 - 3.25) \cdot 23 \cdot 2400 / 60^{***} + (34 - 3.25) \cdot 5.1 \cdot 1030^{****} = (14.5 \cdot 34 + 1 \cdot 39) \cdot 1030^{*****}$$

- * = bottom plate
- ** = inner walls (in length direction of the caisson)
- *** = inner walls (width direction of the caisson)
- **** = ballast water
- ***** = buoyancy

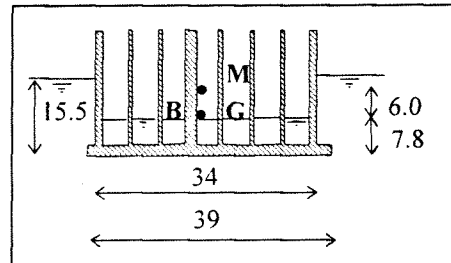


Figure 9.4 Stability of the caisson

The layer of ballast water has to be divided over the inner cells, such that the centre of gravity of the caisson is just in the middle of the length (39 m) of the caisson and that the caisson is equally loaded along the width (60 m) of the caisson by the ballast water and its own weight.

It follows that the centre of gravity G is positioned at 7.8 m and the centre of buoyancy B at 7.75 m from the bottom. B is situated at almost the same height as G and thus a righting moment is required.

The distance between B and M can be calculated by I/V .

$$I = 1/12 \cdot 1 \cdot 34^3 - 3 \cdot \{1/12 \cdot 1 \cdot 4.25^3\} - 4 \cdot \{1/12 \cdot 1 \cdot 4.625^3\} = 3223 \text{ m}^4$$

$$V = 1 \cdot 39 \cdot 1 + 1 \cdot 34 \cdot 14.5 = 532 \text{ m}^3$$

$$BM = 6.1 \text{ m}$$

It follows that M is situated about 6 m above G, what gives a sufficient righting moment.

Wave response of the caisson

Another important consideration is the caisson response to the waves during transport. A free floating caisson has, like a vessel, six modes of freedom of motion. In each of these modes, the caisson has its own natural frequency of oscillation. If excitation occurs in a particular mode, in a frequency near the caisson's natural frequency in that mode, resonance will occur.

Generally, in ship hydrodynamic theories, a so-called 'transfer function' is used to define the relationship between wave and ship motion amplitudes. The response of the caisson has to be investigated for all directions. When a natural frequency of the caisson in a certain mode causes a strong response, during a wave period which occurs very frequently during transport, the design of the caisson has to be adapted to prevent this.

9.3.2 Strength of the Caisson during Transport

As mentioned in the last section, transport will take place when the significant wave height is less than 2 m and a maximum wave height of about 3.6 m. Because of the draught of the caisson of 15.5 m, the water pressure fluctuations are very small at this depth. The bottom plate will be about 1 m thick and will be given a higher stiffness by the outer and inner walls. When the caisson is equally loaded along the width (60 m) the caisson is strong enough even in waves with a length of 60 m, which cause the most severe loading.

9.4 Stability of the Caisson during and after Sinking

When the caisson is towed to its position above the rubble mound foundation, it has to be ballasted by more water to sink. When this is done, such that the caisson is equally loaded along the width (60 m), no large moment will occur and it will sink without list.

When the height of the ballast water is the same as the sea level, the weight and buoyancy can be calculated (for a section without device):

sea level: C.D.

$$\text{weight: } 39 \cdot 1 \cdot 2400^* + 3.25 \cdot 23 \cdot 2400^{**} + 4 \cdot (34 - 3.25) \cdot 23 \cdot 2400 / 60^{***} + (34 - 3.25) \cdot 16.5 \cdot 1030^{****} = \\ 908756 \text{ kg} = 8915 \text{ kN}$$

$$\text{buoyancy: } 1 \cdot 39 \cdot 1030 + 16.5 \cdot 34 \cdot 1030 = 618000 \text{ kg} = 6063 \text{ kN}$$

sea level: + 2.5 m C.D.

$$\text{weight: } 39 \cdot 1 \cdot 2400^* + 3.25 \cdot 23 \cdot 2400^{**} + 4 \cdot (34 - 3.25) \cdot 23 \cdot 2400 / 60^{***} + (34 - 3.25) \cdot 19 \cdot 1030^{****} = \\ 987937 \text{ kg} = 9692 \text{ kN}$$

$$\text{buoyancy: } 1 \cdot 39 \cdot 1030 + 19 \cdot 34 \cdot 1030 = 705550 \text{ kg} = 6921 \text{ kN}$$

sea level: + 5 m C.D.

$$\text{weight: } 39 \cdot 1 \cdot 2400^* + 3.25 \cdot 23 \cdot 2400^{**} + 4 \cdot (34 - 3.25) \cdot 23 \cdot 2400 / 60^{***} + (34 - 3.25) \cdot 21.5 \cdot 1030^{****} = \\ 1067118 \text{ kg} = 10468 \text{ kN}$$

$$\text{buoyancy: } 1 \cdot 39 \cdot 1030 + 21.5 \cdot 34 \cdot 1030 = 793100 \text{ kg} = 7780 \text{ kN}$$

* see last section, for explanation

When the top structure is not placed, the crest height is + 6.5 m C.D. With the Goda theory, the stability can be checked for the section without device and for the section with device (which has already the sloping top structure, crest height +19.5 m C.D.). During, this phase of the construction sliding is the most dangerous phenomenon.

For wave conditions of $H_{\max} = 3.6 \text{ m}$ and $T_z = 6\text{-}12 \text{ s}$ the caisson is stable against sliding and overturning. Obviously, the rubble mound stress is in this phase not high. It is recommended to replace the water for sand as soon as possible, so that the caisson is also stable in more rough sea conditions.

Sliding to the sea side, caused by a wave though at the sea side and possibly overtopping of the caisson is a phenomenon what has to be investigated also. In fact, the period between placing the caissons and casting on site the superstructure is generally long enough to allow a relatively severe storm to occur before the superstructure is completed [Oumeraci;1994]. In this study, this sliding mode is not investigated.

9.5 Dimensions of Concrete Walls

To determine the dimensions of concrete walls the design pressure has to be known. For the design of the Sakata Port Breakwater the design pressures have been investigated [Funakoshi et al.;1993]. The following pressure distributions are used in that design, shown in Figure 9.5:

- Positive air pressure in the chamber: $1.0 \cdot \rho \cdot g \cdot H$

In practice, the measured values varied between 0.7 and $1.0 \cdot \rho \cdot g \cdot H$, in this study also a value $1.0 \cdot \rho \cdot g \cdot H$ will be used.

- Negative air pressure in the chamber: $- 0.5 \cdot \rho \cdot g \cdot H$

The measured values were slightly less. In this study also $-0.5 \cdot \rho \cdot g \cdot H$ will be used as negative air pressure.

- Wave pressure on the front wall and sloping top: $1.0 \cdot \rho \cdot g \cdot H$

The measured values showed a large variation, in the range of $0.6-1.2 \cdot \rho \cdot g \cdot H$, in particular when the wave heights were large. In this study also a value of $1.0 \cdot \rho \cdot g \cdot H$ will be used.

- Wave pressure difference on the dividing walls in the chamber: $0.25 \cdot \rho \cdot g \cdot H$

The dividing walls are subjected to pressure on both sides. For the design, the difference between these pressures is important. Depending on the incident wave direction, the pressure difference can reach $0.5 \cdot \rho \cdot g \cdot H$. For the Sakata Breakwater a value of 0.25 was sufficient. The Bilbao Breakwater has 'harbour' type devices. For these type devices it is assumed that obliquely incident waves reach the chamber as normally incident waves (Appendix G, Method of Evans). Consequently, in theory no wave pressure difference will exist between the different parts of the chamber, however in this study $0.25 \cdot \rho \cdot g \cdot H$ will be used for safety reasons.

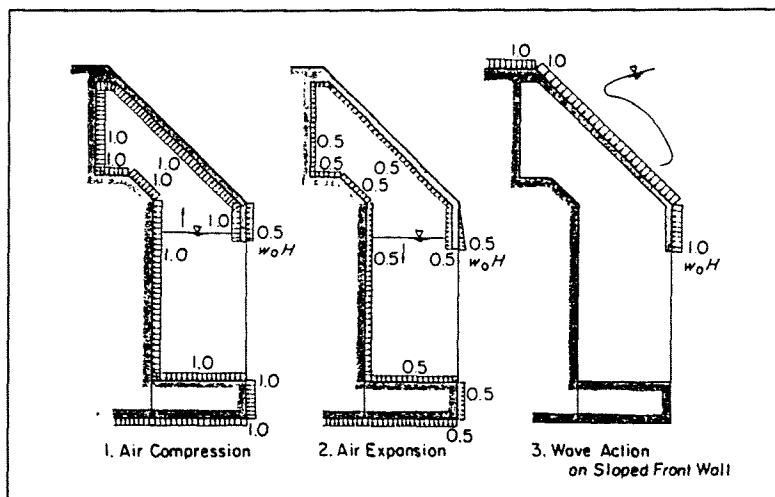


Figure 9.5 Design pressure at the Sakata Breakwater

The pressure at the bottom plate is given by the values in **Appendix L**. Several loadings exist, namely the wave uplift pressure, the rubble mound pressure and the loading of the submerged caisson weight. Values which cause a maximum loading of the bottom plate will be used to calculate the bottom plate thickness. In this study is assumed that the bottom plate has a large stiffness, so that the pressures are distributed over the total plate. This stiffness is caused by the thickness of 1.0 m and the lower parts of the walls.

In Section 7.6 the common used concrete thicknesses are given. With the pressure distribution given above and the plastic analysis with the aid of yield lines, the distribution of the forces (moments and shear forces) is known and the corresponding concrete thicknesses can be calculated.

In **Appendix M**, the calculation of the concrete thicknesses is given for the different parts of the caisson. In this study, the concrete quality B35 and reinforcement steel FeB500 are used. To get a more economically attractive caisson, the calculation has to be optimised for concrete thickness and reinforcement. When it is preferred to use less reinforcement, a higher concrete quality can be used and larger concrete dimensions.

The following dimensions are calculated:

front wall caisson:	0.5 m
front wall air chamber:	1.5 m
roof air chamber:	1.0 m
chamber dividing walls:	0.5 m
side walls 'harbour' and chamber:	0.5 m

inner cell walls:	0.25 m
inner cell (shear)walls:	0.25 m
side walls caisson:	0.5 m
back wall caisson:	0.5 m
bottom plate:	1.0 m
front toe:	1.0 m
back toe:	1.0-2.0 m
shear wall back toe:	0.5 m

At places of the highest moments and forces, the concrete thicknesses will be increased at some place, namely close to the bottom plate, see the drawings in **Appendix K**. This will be done to get also a higher stiffness of the bottom plate.

9.6 Conclusions

The construction of the caisson starts with the lower 24 m part. When this is finished, it has to be transported to the location of the new breakwater. After placement of the caisson, the top structure can be made. The roof of the turbine room has to be pre-fab and can be placed finally, after the installation of the equipment in the turbine room.

During the transport the caissons have to be stable. The draught of the caisson is determined by two subjects. (1) During transport a freeboard is required to prevent water inflow and (2) the caisson has to be placed on the rubble mound foundation of a level of - 17.5 m C.D. When the caisson is ballasted by an averaged layer of water of about 4.9 m, it has a draught of 15.5 m and it is stable.

Another important consideration is the caisson response to the waves during transport. When a natural frequency of the caisson in a certain mode causes a strong response, during a wave period which occurs very frequently during transport, the design of the caisson has to be adapted to prevent this.

When the caisson is placed on the rubble mound foundation, it is ballasted by water. In that phase, the top structure is not placed and consequently, the crest height is + 6.5 m C.D. With the Goda theory, the stability can be checked. During, this phase of the construction sliding is the most dangerous phenomenon. For wave conditions of $H_{\max} = 3.6$ m and $T_z = 6-12$ s the caisson is stable against sliding and overturning. It is recommended to replace the water for sand as soon as possible, so that the caisson is also stable in more rough sea conditions.

Sliding to the sea side, caused by a wave though at the sea side and possibly overtopping of the caisson is not investigated in this study. In fact, the period between placing the caissons and casting on site the superstructure is generally long enough to allow a relatively severe storm to occur before the superstructure is completed [Oumeraci;1994].

The design pressure distributions to determine the dimensions of concrete walls, are known from the design of the Sakata Port Breakwater. With these pressure distributions and the plastic analysis with the aid of yield lines, the distribution of the forces (moments and shear forces) is known and the corresponding concrete thicknesses can be calculated, see **Appendix M**.

In this study the concrete quality B35 and reinforcement steel FeB500 are used. To get a more economically attractive caisson, the calculation has to be optimised for concrete thickness and reinforcement. When it is preferred to use less reinforcement, a higher concrete quality can be used and larger concrete dimensions.

9.7 References and Literature

Funakoshi, H., Ohno, M., Takahashi, S., Oikawa, K.(1993); *Present Situation of Wave Energy Conversion Systems*; Civil Engineering in Japan, Vol.32, pp. 108-134

Goda, Y.(1994); *Dynamic response of upright breakwaters to impulsive breaking forces*; Coastal Engineering, Vol.22, pp. 135- 158

Mulder, H.(1984); *Interaction Water Motion and Closing Elements*; The Closure of Tidal Basins; Delft University Press, the Netherlands, pp. 343-354

Nakada, H., Suzuki, M., Takahashi, S., Shikamori, M.(1992); *Development test of wave power extracting caisson breakwater*; Civil Engineering in Japan, Vol.31, pp.146-164

Oumeraci, H.(1994); *Review and analysis of vertical breakwater failures - lessons learned*; Coastal Engineering, 22, pp. 3-29

Vos, Ch.,J., Jager, H.C.(1995); *Uitvoeringstechnologie van betonconstructies* (in Dutch); Delft University of Technology, the Netherlands

Vos, Ch.,J., Jager, H.C.(1995); *Construction technology of concrete structures, Lecture notes on special subjects*; Delft University of Technology, the Netherlands

10 Conclusions and Recommendations

10.1 Conclusions

Wave Energy Conversion, State of the Art and Prospects

Since the awareness that the conventional energy sources will run short, the use of various renewable energy sources has been investigated. Quite some countries are interested in wave energy conversion.

In several countries some full-scale wave energy converting pilot plants have been tested. Some of these are still operating. In Norway a tapered channel (TAPCHAN) is constructed. The waves are converted by a rising channel into potential energy and subsequently by a turbine into electricity. Some plants of 1.5 MW will be constructed in the near future. Most of the other full-scale pilot plants are oscillating water column devices, shore mounted (Isle of Islay at the West of Scotland, Japan, Norway) or in combination with a breakwater (India, Japan). In the oscillating water column devices, a volume of air is trapped within a structure. The air pressure varies corresponding to the oscillating water level and is used to drive a turbine. Although the success of the pilot plants, until now no commercial wave energy converting power plants (of some MWs or GWs) have been constructed.

The present state of wave energy conversion has reached the point at which it is possible to construct a breakwater with wave energy converting devices. It is concluded that these breakwaters have to be designed mainly for harbour protection. Simultaneously, they have to be used as pilot plants for larger power plants offshore. Besides, these wave power converting breakwaters can be successfully employed in many places throughout the world, like isolated islands with a low electricity demand or with high actual electricity costs.

For very large wave power plants, it is expected that they will consist of a number of point absorbers, installed some kilometres offshore. The advantage of these point absorbers is that they can capture wave energy from a larger width than the width of the structure. For the theoretical as well as the structural design aspects of this type of large power plants, more research has to be performed.

Combination of a Breakwater with Wave Energy Converting Devices

Potential energy converting devices (see Section 4.2) have a low efficiency and require relatively large structures. For these reasons they are not suitable for combination with breakwaters.

Flap type devices (see Section 4.3) have the drawback of moving parts and vulnerable linkages. When the wave power value is limited and the dimensions of the flap can be restricted, a hanging flap located at a quarter-wave length in front of a reflecting back wall has some prospects. The structure has to be designed carefully to avoid damage.

The oscillating water column devices (see Section 4.4) are most suitable for combination with a breakwater. These devices have a good performance, while they are able to convert large wave power values and they are not sensitive to damage. (Except of the turbine, they have no moving parts.)

Two types of oscillating water column (= OWC) devices can be discerned: (1) devices with a single air chamber above a column and consequently one particular resonance frequency or (2) devices with in front of the chamber a 'harbour' such that the devices become multi-resonant. In Japan, Sakata Port, a wave power converting caisson with only an air chamber has been constructed. The British inventors expect that a breakwater with 'harbour' type devices has the best prospects. These devices are placed at intervals in the breakwater and operate as point absorbers.

The design of a breakwater with 'harbour' type devices placed at intervals, is much more complicated than designing a breakwater with only air chambers placed side by side. Several theories (mainly numerical methods) exist to model the hydrodynamic characteristics of 'harbour' type devices.

Most theories show roughly the same results, namely varying the dimensions of the oscillating water column or the 'harbour' changes the natural periods of the device and thus the resonance frequency.

The influence of (1) the ratio 'harbour' length to chamber length, (2) the width of the device and (3) the immersion depth of the front wall is clearly explained in the Sections 5.4.3 - 5.4.5.

By comparing the results of the different theories and several designs of 'harbour' type devices, general applicable design rules have been derived. With these rules, the dimensions of a 'harbour' type device can be determined without the help of complicated numerical methods.

Design of a Wave Power Converting Breakwater for the Port of Bilbao

With the derived design rules, a wave power converting breakwater has been designed for the Port of Bilbao, North Spain. This 2280 m long breakwater consists of 38 caissons. In the middle of each caisson a 'harbour' type OWC device is situated.

The stability of the caissons has been calculated by the theory of Goda, with some modifications. Takahashi et al. have introduced a new impulsive pressure coefficient. However, this coefficient is not very important if the recommendation $d/h > 0.6$ is fulfilled (water depth above the rubble mound berm in front of the caisson larger than 0.6 times the water depth). For the sections with device, the impulsive pressure is assumed to be zero. For sloping top caissons, the theory of Goda is also modified by Takahashi et al. This last modification has been used for the sections without device.

The stability of a total caisson is calculated by the average stability of the caisson sections, proportional to the part of the caisson that is occupied by the device.

When the caissons have a sloping top and a length of 39 m, a width of 60 m and a crest height of + 17 C.D., they are sufficiently stable against sliding and overturning. Also the average maximum and minimum rubble mound stresses are not exceeded.

The width of a device is 13.75 m, the length of the 'harbour' and chamber is respectively 12.5 m and 9 m. The thickness of the immersed front wall is 1.5 m, consequently the total length of a device is 23 m. In each device a tandem type Wells turbine of 1 MW is installed. This means that the total installed capacity of the breakwater is 38 MW.

During winter periods the operating performance of the devices is considerably better than during summer periods. Yearly, about 80 GWh of electricity is generated (2.2 GWh per device). This means that the annual load factor is about 26%. This value agrees with the annual load factor of other proposed wave energy converting devices [Hagerman;1992].

This study shows that it is possible to make a design of a wave power converting breakwater, by using the design recommendations as derived in Chapter 5. Even for locations with very rough sea conditions, like Bilbao, this type of breakwater is feasible.

At present a wave power converting breakwater with an installed capacity of 38 MW would be the largest wave energy converting power plant of the world. The construction of such a breakwater, followed by operation with a good performance, will result into more confidence in wave energy conversion.

For Spain, the costs of the generated electricity are probably too high, but for locations with relatively high electricity costs and no large electricity demand, this type of breakwater can be successfully employed as commercial power plant.

In this study, the proposed layout of the new rubble mound breakwater for the Port of Bilbao has been used. If an other layout of the breakwater had been selected, with more normally incident waves, then the quantity of the total generated electricity is expected to be larger. However, if the wave conditions in the ultimate limit state (U.L.S.) are also normally incident, then the caissons are attacked more severely and have to be consequently larger (larger weight, larger bottom plate).

In general, wave power converting breakwaters cannot be selected instead of conventional power plants, because in most locations the wave power varies too much, resulting in periods with very low or even without electricity generation. However, with these wave power converting breakwaters, the consumption of conventional energy sources can be reduced.

10.2 Recommendations

For large wave energy converting power plants, research for installing a number of point absorbers at a distance of some kilometres offshore has to be continued.

If smaller power plants are desired, for instance at small islands, wave power converting breakwaters are ideal wave energy converters, because they can also be used for harbour protection.

To optimise the economic aspects of wave power converting breakwaters, two types of breakwater have to be compared. These are the one with OWC devices side by side (like that of Sakata Port) and that with 'harbour' type OWC devices placed at intervals (like the breakwater in this study). Until now, considerable research has been performed only for the electricity generation. However, this research should be combined with the constructional aspects (stability and strength of the caissons, construction costs of more complicated caissons etc.). By investigating these two aspects simultaneously, the economically superior type of breakwater can be selected more reliable.

If relatively small breakwaters are required (small water depth, low wave power) the use of flap type devices has to be investigated more detailed. It is suggested to pay attention to the use of a frame instead of a caisson.

For the layout of a wave power converting breakwater, not only the harbour aspects (good direction for entering ships, quantity of transmitted waves into the harbour through the entrance, etc.) but also the wave power conversion aspects have to be considered (normally incident waves are converted at the highest efficiency).

To create more confidence in wave energy conversion and to promote further research, a wave power converting breakwater for an appropriate location has to be constructed soon. For selection of a location, the wave length, height and direction and their corresponding probability of occurrence have to be known. Also the tidal variation has to be taken into account.

For pre-feasibility studies, the dimensions of wave energy converters can be determined by design rules. However, for an optimal design, computer programs are required that can calculate the generated electricity for every wave condition. The most accurate method is using a number of spectra of wave length, height and direction. When the overall efficiency of a system is calculated by the program for each wave condition, then the electricity generation corresponding to that condition is known. When this procedure is repeated for a full set of annual spectra, the total generated electricity can be calculated for a typical year.

More attention has to be paid to the varying characteristics of wave energy. It is preferred to search for methods which can store the converted wave power. For instance, a combination of wave energy conversion with pumping water into a reservoir can be investigated. In that way, wave energy can be converted as potential energy and can be used when electricity is required.

Wave Energy Conversion

*** Theory of Wave Energy Conversion**

*** Wave Energy Converters, the State of the Art**

*** Design of a Wave Power Converting Breakwater for the
Port of Bilbao, North Spain**

MSc. Thesis by Herald Vervoorn
March 1997

Appendixes

Delft University of Technology
Faculty of Civil Engineering
Hydraulic and Geotechnical Engineering Division
Hydraulic Engineering Group

Contents

Appendix A Linear Wave Theory

Introduction.....	A-1
Velocity Potential.....	A-1
Velocity of the Water Particles.....	A-2
Dispersion Relation.....	A-2
Wave Pressure.....	A-3
Wave Energy and Power.....	A-3
Shoaling Factor.....	A-4

Appendix B Theory of Oscillating Bodies

Introduction.....	B-1
Spring-and-damper System.....	B-1
Two-dimensional devices and the capture efficiency.....	B-3
Three-dimensional devices and the capture width.....	B-6
Interaction between oscillating bodies.....	B-6
Summary of the two-dimensional theory.....	B-8
References.....	B-10

Appendix C Theory of Several Converters

Two-dimensional capture efficiency.....	C-1
References.....	C-8

Appendix D Theory of Oscillating Bodies

The Two plate machine.....	D-1
The Triplate machine.....	D-2
References.....	D-4

Appendix E Theory of the Pendulor

Theory.....	E-1
Experiments.....	E-3
References.....	E-3

Appendix F Theory of Oscillating Water Column Devices

Introduction.....	F-1
Basic assumptions.....	F-1
Wave energy extraction.....	F-3
Three-dimensional pressure distributions.....	F-4
Turbine characteristic and resonance conditions.....	F-6
Comparison with a rigid plate model.....	F-8
Air compressibility.....	F-8
Oscillating water column with a reflecting wall.....	F-9
Non-linear air turbine.....	F-9
Phase control.....	F-10
References.....	F-10

Appendix G Theory of the 'Harbour' Type OWC	
Part I Theory of Malmo and Reitan.....	G-1
Part II Theory of Count and Evans.....	G-4
Approximate Method.....	G-4
Numerical Method.....	G-6
Comparison of Results of the Approximate Method and Numerical Method...	G-6
Part III Conclusions.....	G-10
References.....	G-10
Appendix H Theory of a 'Harbour' Type OWC in a Reflecting Wall	
Part I Single Device in a Reflecting Wall placed in a Channel.....	H-1
Part II Single Device in a Reflecting Wall placed in an infinite Sea.....	H-6
Part III Finite Row of Devices in a Reflecting Wall (Malmo and Reitan).....	H-9
Part IV Finite Row of Devices in a Reflecting Wall (McIver and Evans).....	H-12
Part V Conclusions.....	H-15
References.....	H-16
Appendix I Theory of Goda and Modifications	
Part I Theory of Goda.....	I-1
Design wave conditions.....	I-1
Wave pressure, buoyancy and uplift pressure.....	I-2
Stability of the caisson.....	I-4
Stability of the rubble mound foundation.....	I-4
Part II Modified Theory of Goda.....	I-4
References.....	I-6
Appendix J Maximum Wave Height Calculation	
Deep water wave height.....	J-1
Design wave height of each segments of the breakwater.....	J-1
Appendix K Drawings of the Final Design	
Drawing 1, Overview Drawing	
Drawing 2, Cross Section A-A	
Drawing 3, Cross Section B-B	
Drawing 4, Cross Section C-C	
Drawing 5, Cross Section D-D	
Drawing 6, 3-D View Total Caisson	
Drawing 7, 3-D View, Cross Section of the Device	
Appendix L Stability and Rubble Mound Stress of the Final Design	
Wave Conditions.....	L-1
Modification factors.....	L-1
Used symbols.....	L-1
Weight and buoyancy.....	L-2
Averaged safety factors and rubble mound stresses.....	L-2
Results.....	L-3
Wave Conditions.....	L-3
Stability at C.D.....	L-4
Stability at +2.5 m C.D.....	L-8
Stability at +5 m C.D.....	L-12
Averaged Safety Factors and Rubble mound Stresses.....	L-16
Appendix M Calculation of Concrete Dimensions	

Appendix A Linear Wave Theory

Introduction

A travelling wave is assumed to be sinusoidal with a wave height H and wave length λ . Related to certain co-ordinates, the wave has a period T and velocity c . The relation $L = c \cdot T$ is valid. The wave is shown in Figure A.1.

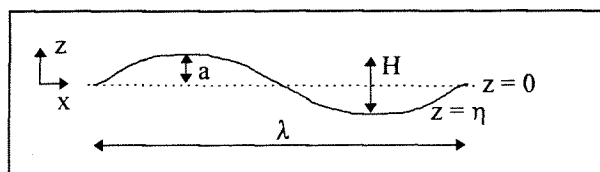


Figure A.1 Sinusoidal wave

The surface level of the wave is defined as:

$$\eta(x,t) = 1/2H \cdot \sin\left(\frac{2\pi t}{T} - \frac{2\pi x}{\lambda}\right) \quad (\text{A.1})$$

The following definition will be used:

$$\begin{aligned} a &= \text{wave amplitude [m]} \\ &= 0.5 H \\ \omega &= \text{wave frequency [s}^{-1}\text{]} \\ &= 2\pi/T \\ k &= \text{wave number [m}^{-1}\text{]} \\ &= 2\pi/L \end{aligned}$$

Equation A.1 can be rewritten:

$$\eta(x,t) = a \cdot \sin(\omega t - kx) \quad (\text{A.2})$$

For the wave velocity follows:

$$c = \omega/k \quad (\text{A.3})$$

Velocity Potential

In linear wave theory the water particles have a velocity potential ϕ , with the following conditions:

$$\frac{\delta^2 \phi}{\delta x^2} + \frac{\delta^2 \phi}{\delta z^2} = 0 \quad (\text{A.4})$$

$$\frac{\delta \phi}{\delta z} = 0 \quad \text{at the bottom} \quad (\text{A.5})$$

$$\frac{\delta \phi}{\delta z} = \frac{\delta \eta}{\delta t} \quad \text{at the surface} \quad (\text{A.6})$$

With the expression of the surface (A.2) and the conditions above, it follows:

$$\phi(x,z,t) = \frac{\omega a}{k} \frac{\cosh k(h+z)}{\sinh kh} \cos(\omega t - kx) \quad (\text{A.7})$$

Velocity of the Water Particles

By differentiating of ϕ the velocity of the water particles can be obtained:

$$u = \frac{\delta \phi}{\delta x} = \omega a \frac{\cosh k(h+z)}{\sinh kh} \sin(\omega t - kx) \quad (\text{A.8a})$$

$$= u_{\text{amplitude}} \cdot \sin(\omega t - kx) \quad (\text{A.8b})$$

$$w = \frac{\delta \phi}{\delta z} = \omega a \frac{\sinh k(h+z)}{\sinh kh} \cos(\omega t - kx) \quad (\text{A.9a})$$

$$= w_{\text{amplitude}} \cdot \cos(\omega t - kx) \quad (\text{A.9b})$$

In deep water the velocity amplitudes are:

$$u_{\text{amplitude}} = w_{\text{amplitude}} = \omega a e^{kz} \quad (\text{A.10})$$

In shallow water the velocity amplitudes are:

$$u_{\text{amplitude}} = \omega a / kh \quad (\text{A.11})$$

$$w_{\text{amplitude}} = \omega a \cdot (1+z/h) \quad (\text{A.12})$$

Dispersion Relation

For free oscillating waves, there exist a relation between the wave frequency and the wave number, this is the so-called dispersion relation:

$$\omega^2 = gk \tanh kh \quad (\text{A.13})$$

In terms of wave length the relation can be rewritten:

$$\lambda = \frac{gT^2}{2\pi} \tanh \frac{2\pi h}{\lambda} \quad (\text{A.14})$$

$$\lambda = \lambda_0 \cdot \tanh \frac{2\pi h}{\lambda} \quad (\text{A.15})$$

with $\lambda_0 =$ deep water wave length [m]

The wave velocity ($c = \omega/k$) can be rewritten by using the dispersion relation:

$$c^2 = \omega^2/k^2 = \frac{g}{k} \tanh kh \quad (\text{A.16})$$

$$\text{or } c = \left(\frac{g\lambda}{2\pi} \tanh \frac{2\pi h}{\lambda} \right)^{1/2} \quad (\text{A.16})$$

$$c = \frac{gT}{2\pi} \tanh \frac{2\pi h}{cT} \quad (\text{A.17})$$

$$= c_0 \cdot \tanh kh \quad (\text{A.18})$$

In deep water the wave velocity is:

$$c = c_0 = \frac{gT}{2\pi} \quad (\text{A.19})$$

In shallow water the wave velocity is:

$$c = (gh)^{1/2} \quad (\text{A.20})$$

Wave Pressure

The varying wave pressure below a wave can be represented by Bernoulli's equation:

$$p = -\rho gz - \rho \frac{\partial \phi}{\partial t} - \frac{1}{2} \rho v^2 \quad (\text{A.21})$$

with p = pressure [N/m² = Pa]
 ρ = density of water [kg/m³]
 g = gravitational acceleration [m/s²]
 v = water particle velocity [m/s]

The part $1/2\rho v^2$ can be neglected for a linear wave, so the pressure becomes:

$$p = -\rho gz + \frac{\rho g H}{2} \frac{\cosh k(z+h)}{\cosh kh} \sin(\omega t - kx) \quad (\text{A.22})$$

Wave Energy and Power

Wave energy consists of potential energy and kinetic energy:

$$E_p = E_k = 1/4 \rho g a^2 \quad (\text{A.23})$$

with E_p = potential energy per square metre of surface [J/m²]
 E_k = kinetic energy per square metre of surface [J/m²]

The total energy per square metre of surface is:

$$E = \frac{\rho \cdot g \cdot a^2}{2} = \frac{\rho \cdot g \cdot H^2}{8} \quad (\text{A.24})$$

with E = total energy per square metre of surface [J/m²]

The total energy per metre wave crest is:

$$E_T = \frac{\rho \cdot g \cdot H^2 \cdot \lambda}{8} = \frac{\rho \cdot g \cdot a^2 \cdot \lambda}{2} \quad (\text{A.25})$$

with E_T = total energy per metre of crest width [J/m]
 λ = wave length [m]

The mean energy transported in the wave propagation direction per time per width of the crest is called the wave power or energy flux:

$$P = (1/2 \rho g a^2) \left(\frac{1}{2} + \frac{kh}{\sinh(2kh)} \right) (\omega/k) \quad (\text{A.26})$$

$$= E \cdot n \cdot c \quad (\text{A.27})$$

with P = wave power or energy flux [W/m]

$$n = \frac{1}{2} + \frac{kh}{\sinh(2kh)} \quad [-] \quad (\text{A.28})$$

The factor n is an indication of water depth, the value varies between 0.5-1.0 for respectively deep to shallow water.

In general, waves are travelling in a group of waves. The velocity of this group of waves is:

$$c_g = n \cdot c \quad (\text{A.29})$$

= group velocity [m/s]

Shoaling Factor

The wave height and length of waves travelling in varying water depth is influenced by this variation. The influence of a varying water depth can be derived by using the assumption that the wave power does not change. Two water locations, 0 means a deep water location.

Wave power constant:

$$1/8 \rho g H_0^2 n_0 c_0 = 1/8 \rho g H_1^2 n_1 c_1$$

in deep water $n_0 = 1/2$

$$1/2 H_0^2 c_0 = H_1^2 n_1 c_1$$

rewritten:

$$\frac{H_1}{H_0} = \frac{c_0}{c_1} \frac{1}{2n_1} = K_{sh} \quad (\text{A.30})$$

$$K_{sh} = \frac{1}{\tanh kh \left(1 + \frac{2kh}{\sinh 2kh} \right)} \quad (\text{A.31})$$

with K_{sh} = shoaling factor

Appendix B Theory of Oscillating Bodies

Introduction

The motion of a floating body depends on the amplitude and period ω (or angular frequency) of the incident waves, when assumed that the incoming waves are regular. The waves produce a periodic disturbing force of the form $F \cdot \cos(\omega t)$. In this way, the theory of the well known spring-and-damper system can be derived, which is described in various books about mechanics. The force $F \cdot \cos(\omega t)$ can be written as $\text{Re}\{F \cdot \exp(i\omega t)\}$, which indicates the real part of $F \cdot \exp(i\omega t)$. This exponential form is more easily manipulated than the form $F \cdot \cos(\omega t)$ [Shaw; 1982].

Evans described the oscillation of a damped two-dimensional body in regular waves [Evans; 1976, 1979, 1985]. McCormick has also given a description of this oscillation [McCormick; 1976, 1981]. In 'Wave Energy, a design challenge' some parts of the theory are written [Shaw; 1982].

In this appendix, the mentioned literature is used and the theory has been written again. The symbols in the equations are selected as much as possible equal to the common used symbols. Most are the same as the symbols used by Evans, sometimes for clearness they are changed or a subscript is added. All parameters are provided with their accompanying unit, that generally is omitted in the existing literature.

Spring-and-damper system

The oscillating body is accelerated and decelerated under the action of three forces. The waves produce (1) the wave exciting force. The motion of the body is controlled by (2) a restoring force, produced by changing buoyancy and proportional to the displacement and by (3) a damping force, caused by friction, energy extraction and radiation. This last force is generally assumed to be linearly related to the velocity of motion of the body. In this way the classical equation for forced, damped oscillation of a *two-dimensional* body can be obtained [Evans; 1976] [Count;1982].

It is worth noting, that this equation is purely conventional and only applies to simple harmonic motions at the fundamental frequency ω . The correct description of the motion of a floating body as a function of time involves a convolution integral describing the continuing influence of previous body motions on its present motion.

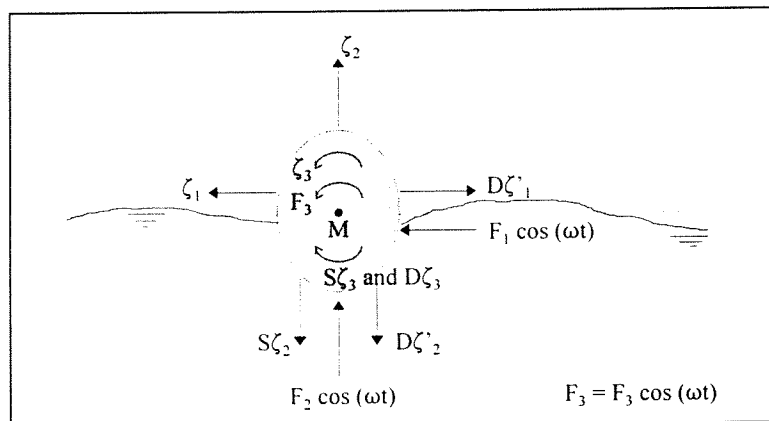


Figure B.1 Forces acting on an oscillating body

The equation of motion is:

$$M\zeta''_i + D\zeta'_i + S\zeta_i = F_i \quad (B.1)$$

applied force damping force restoring force mass x acceleration

$$\text{or } M\zeta''_i + D\zeta'_i + S\zeta_i = F_i \cos(\omega t) = \text{Re}\{F_i \exp(i\omega t)\} \quad (B.2)$$

with	M	= $i \times i$ matrix of inertia of the body (including the 'added inertia') [kg] or [kg·m ²]
	ζ_1	= horizontal displacement of the body (sway) [m]
	ζ_2	= vertical displacement of the body (heave) [m]
	ζ_3	= angular displacement about the point of rotation (roll) [rad]
	' , ''	= time derivatives
	F_i	= wave exciting force or moment [N] or [Nm]
	F_1	= horizontal force [N]
	F_2	= vertical force [N]
	F_3	= moment about the point of rotation [Nm]
	i	= imaginary constant ($i^2 = -1$) [-]
	ω	= circular frequency [s ⁻¹]
	t	= time [s]
	D	= matrix of damping coefficient [Ns/m] or [Nms/rad]
	S	= matrix of spring coefficient (for heave and roll motions including a restoring force coefficient caused by the change in buoyancy) [N/m] or [Nm/rad]
		= $\rho g A$
with	ρ	= density of water [kg/m ³]
	g	= gravitational acceleration [m/s ²]
	A	= horizontal cross section [m ²]

The mass (of the displaced water) and the moment of inertia of a floating body must be augmented by a mass of water which is influenced by the motions of the body. This so-called 'added mass' can be predicted by hydrodynamic theory and is related to the shape and dimensions of the body [Evans; 1979].

In the case of the natural, undamped oscillation for which $D = F_i = 0$, the natural frequency (or resonant angular frequency) of a body can be derived. It is normally adequate to assume that the damped natural frequency ω_d is equal to the natural angular frequency ω_0 [Shaw; 1982].

$$\omega_d = \sqrt{\frac{S}{M} - \frac{D^2}{4M^2}} \approx \omega_0 = \sqrt{\frac{S}{M}} \quad (\text{B.3})$$

with	ω_d	= damped natural frequency [s ⁻¹]
	ω_0	= natural angular frequency [s ⁻¹]

Equation (B.2) can be solved and the displacement of the body, ζ_i , is given in the equations (B.4) and (B.5). The phase angle α is used by McCormick [McCormick; 1981].

$$\zeta_i = \frac{|F_i| \exp[i(\omega t + \epsilon)]}{\sqrt{(S - M\omega^2)^2 + D^2\omega^2}} \quad (\text{B.4})$$

$$= \frac{|F_i| \exp[i(\omega t + \epsilon)]}{\sqrt{[1 - (\omega/\omega_0)^2]^2 S^2 + D^2\omega^2}} \quad (\text{B.5})$$

with	ϵ	= $(\theta - \alpha)$ [rad]
	θ	= phase angle that depends on the wave force [rad]
	α	= phase angle between motion and wave [rad]

$$= \tan^{-1} \left\{ \frac{D\omega}{S - M\omega^2} \right\} = \tan^{-1} \left\{ \frac{D\omega}{M(\omega_b^2 - \omega^2)} \right\} \quad (\text{B.6})$$

For convenience, McCormick introduced the damping ratio Δ , defined as the ratio of the actual damping coefficient D to the critical damping coefficient when $\omega_d = 0$ and $D = 2\sqrt{MS}$, from (B.3). He gives several plots of this damping factor and the phase angle α .

$$\zeta_i = \frac{|F_i| \exp[i(\omega t + \varepsilon)]}{S \sqrt{[1 - (\omega/\omega_b)^2]^2 + (2\Delta \omega/\omega_b)^2}} \quad (\text{B.7})$$

with Δ = damping ratio [-]

$$= \frac{D}{2\sqrt{MS}} = \frac{D}{2M\sqrt{S/M}} = \frac{D}{2M\omega_b} \quad (\text{B.8})$$

ε = $(\theta - \alpha)$ [rad]

θ = phase angle that depends on the wave force [rad]

α = phase angle between motion and wave [rad]

$$= \tan^{-1} \left\{ \frac{2\omega/\omega_b \Delta}{1 - \omega^2/\omega_b^2} \right\} \quad (\text{B.9})$$

From the general equations (B.1), (B.2) and (B.4), equations can be derived for a vertically or horizontally oscillating body, for a rolling body or for a combination of these motions. For a wave contouring raft, an equation can also be derived. Describing the wave energy absorbing phenomenon by this linear wave theory, has shown a very good agreement with several experiments.

Two-dimensional devices and the capture efficiency

In the two-dimensional case all forces are per unit width of the device. This means that also the damping and restoring coefficients must be given per unit width of the device.

The damping coefficient D depends upon friction, energy extraction and radiation. The friction component D_f represents a loss of power, but is frequently relatively insignificant.

The energy extraction (or applied) damping coefficient D_e is such that the work producing force is $D_e \zeta'_i$ and the instantaneous work rate or power caused by this force is $(D_e \zeta'_i) \zeta'_i$, which is obviously significant. This applied coefficient depends on the power loading and can be controlled by the designer of the device.

Radiation damping coefficient D_r , is related to surface waves which are produced when a body is caused to oscillate at the surface of the fluid. These waves are produced by the alternating displacement volume of the body and also by friction and surface tension. This coefficient can be estimated from the geometry of the body, the dimensionless angular frequency and in case of an array of devices, from the spacing and alignment of the array to the wave crest.

Thus, the damping consists of:

$$D = D_e + D_f + D_r = D_e + D_L \quad (\text{B.10})$$

The power per unit length captured by a body, P_{cap} , is the mean rate at which work is being done:

$$P_{cap} = \frac{\omega}{2\pi} \int_0^{2\pi/\omega} D_e \zeta'_i \zeta'_i dt \quad (B.11)$$

$$= \frac{1}{2} \omega^2 D_e |\xi_i|^2 \quad (B.12)$$

$$= \frac{1}{2} \frac{\omega^2 D_e |F_i|^2}{(S - M\omega^2)^2 + D^2 \omega^2} \quad (B.13)$$

with P_{cap} = power per unit length captured by a body [W/m]
 ζ_i = $\text{Re} \{ \xi_i \exp(i\omega t) \}$ [m] or [rad]

Since $P_{cap} = P_{cap}(D_e, \omega)$, the maximum power $P_{cap,max}$ is obtained when:

$$(I) \frac{\partial P_{cap}}{\partial D_e} = 0 \quad \text{and} \quad (II) \frac{\partial P_{cap}}{\partial \omega} = 0$$

These requirements furnish two design criteria:

$$(I) D_e = D_L \quad \text{and} \quad (II) \omega^2 = S/M$$

Physically, this implies that for the maximum efficiency the energy extraction rate must equal the rate of radiation damping and that the floating body must be kept in resonance.

The corresponding maximum power is:

$$P_{cap,max} = \frac{|F_i|^2}{8D_L} \quad (B.14)$$

The efficiency can be calculated by comparing the captured wave power to the power of incoming waves. Newman has derived for F_i and D_L the following relations [Newman; 1962]:

$$F_i = \rho g A A_i^+ \quad (B.15)$$

with A_i^+ A_i^- = complex wave amplitudes of the waves generated respectively in upstream and downstream directions due to forced motion of the body, the incident wave is assumed to come from the upstream direction [m]

The relation for D_L is:

$$D_L = \frac{1}{2} \rho \omega \left(A_i^{+2} + A_i^{-2} \right) \quad (B.16 a)$$

$$= \frac{1}{2} \rho \omega |A_i^+|^2 (1-\delta)^{-1} \quad (B.16 b)$$

$$\text{with } \delta = \frac{A_i^{-2}}{A_i^{+2} + A_i^{-2}} \quad [-]$$

The equations (B.15) and (B.16 a) can be combined in the more well known relation of Newman [Newman; 1976]:

$$F_i^2 / D_L = 8 \cdot P_w \cdot \gamma \quad (\text{B.17})$$

with P_w = mean wave power of incident waves [W/m]

$$\gamma = \frac{A_i^{+2}}{A_i^{+2} + A_i^{-2}} [-] \quad (\text{B.18})$$

Substituting (B.15) and (B.16 a) in (B.14) gives:

$$P_{\text{cap,max}} = P_w \cdot \frac{|A_i^+|^2}{|A_i^+|^2 + |A_i^-|^2} \quad (\text{B.19})$$

The maximum efficiency is:

$$E_{\text{max}} = \frac{P_{\text{cap,max}}}{P_w} = \frac{|A_i^+|^2}{|A_i^+|^2 + |A_i^-|^2} = 1 - \delta = \gamma \quad (\text{B.20})$$

Consequently, a highly efficient device is one for which the amplitude of waves downstream, produced by the forced oscillation of the body in the absence of the incident waves, must be as small as possible, compared to the amplitude of the waves produced upstream. For a symmetrical body follows $A_i^+ = A_i^-$, thus $P_{\text{cap,max}} = 1/2 \cdot P_w$. For an asymmetrical body, the efficiency can be improved when it generates little wave motion downstream compared to upstream. The maximum efficiency occurs when $A_i^- = 0$ and thus $E_{\text{max}} = 1$.

An other method to calculate the capture efficiency is to compare the captured wave power to the incoming wave power. The mean power of the incoming waves is (see also Appendix A):

$$\begin{aligned} P_w &= 1/2 \cdot \rho \cdot g \cdot A^2 \cdot c_g & (\text{B.21}) \\ &= \rho \cdot g^2 \cdot A^2 / 4\omega & \text{in deep water} \\ &= \rho \cdot g^2 \cdot A^2 / 2\omega & \text{in shallow water} \end{aligned}$$

The proportion of captured wave power (in deep water) or capture efficiency E is (using (B.12)):

$$E = \frac{P_{\text{cap}}}{P_w} \quad (\text{B.22 a})$$

$$= \frac{2\omega^3}{\rho g^2} D_e \left| \frac{\xi_i}{A} \right|^2 \quad (\text{B.22 b})$$

$$= \frac{2\omega^3 D_e \rho |A_i^+|^2}{(S - M\omega^2)^2 + \omega^2 (D_e + D_L)^2} \quad (\text{B.22 c})$$

$$= \frac{4\omega^2 D_e D_L (1 - \delta)}{(S - M\omega^2)^2 + \omega^2 (D_e + D_L)^2} \quad (\text{B.22 d})$$

From this last form of the formula of efficiency (B.22 d), can also be seen that maximum efficiency occurs when $S = M\omega^2$ and $D_e = D_L$, giving $E_{\max} = 1 - \delta$.

Another possibility when maximum efficiency can be reached, is the case when a body can oscillate in more than one direction simultaneously.

Three-dimensional devices and the capture width

When oscillating bodies are tested in three-dimensional waves, capture efficiencies higher than 100% can be obtained. This is caused by the wave focusing, that results from the interaction between the incident waves and the radiated waves at or near the condition of resonance. In section 3.3.2 this phenomenon is called point absorbing.

Newman [Newman; 1976] has given the relation between the exciting force F_i and the damping coefficient D_L for oscillating bodies with a vertical axis of symmetry:

$$2\pi F_i^2 = 8D_L \lambda P_w \quad \text{for heaving bodies} \quad (\text{B.23})$$

$$2\pi F_i^2 = 16D_L \lambda P_w \quad \text{for swaying and rolling bodies} \quad (\text{B.24})$$

The capture width is defined as the width of a two-dimensional wave crest having the same mean power as the power that is captured by the device:

$$w_{\text{cap}} = \frac{P_{\text{cap}}}{P_w} \quad [\text{m}] \quad (\text{B.25})$$

In literature often the non-dimensionalised capture width is given, which is the capture width divided by the width of the device ($W_{\text{cap}} = w_{\text{cap}} / \text{width}$). This capture width ratio can be seen as the three-dimensional efficiency.

The maximum capture width appears when the device is performing optimally:

$$w_{\text{cap,max}} = \frac{P_{\text{cap,max}}}{P_w} \quad (\text{B.26})$$

Combining the equations (B.21), (B.22) and (B.14) gives:

$$w_{\text{cap,max}} = \lambda/2\pi \quad \text{for heaving bodies} \quad (\text{B.27})$$

$$w_{\text{cap,max}} = \lambda/\pi \quad \text{for swaying and rolling bodies} \quad (\text{B.28})$$

When the body is not axi-symmetrical, the theory for three-dimensional devices can be extended for waves of different angles of incidence,

Interaction between oscillating bodies

In the case that some devices are placed in a row, there will exist some interaction between these devices. When the devices are assumed to be identical and oscillating in one and the same mode some relations can be derived [Evans; 1979] [Thomas and Evans; 1981]. In this case vertically oscillating bodies are considered.

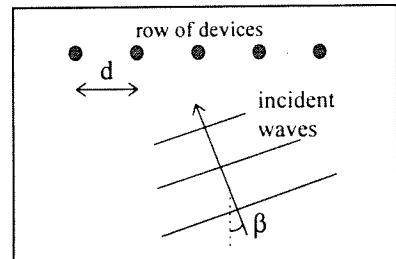


Figure B.2 Plan of a row of devices

$$\begin{aligned} P_{\text{cap,max}} &= \frac{|F_i|^2}{8D_L} \\ &= P_w \cdot \frac{\lambda}{2\pi} \cdot L \cdot J^{-1} \cdot L \end{aligned} \quad (\text{B.29})$$

with $P_{\text{cap,max}}$ = maximum captured wave power [W]
 $L = \exp\{-i \cdot k \cdot d \cdot \sin(\beta)\}$ [-] (B.30)

\bar{L} = conjugated L [-]
 $\lambda/2\pi$ = capture width [m]
 $J = J_0 \cdot (k \cdot d)$ [-] (B.31)

with J_0 = zero-order Bessel function of the first kind
 k = wave number [m^{-1}]
 d = spacing [m]

Hence, the maximum capture width is:

$$W_{\text{cap,max}} = \frac{P_{\text{cap,max}}}{P_w} \quad (\text{B.32})$$

$$= \frac{\lambda}{2\pi} \cdot N \cdot q(\beta) \quad (\text{B.33})$$

with $q(\beta) = \frac{1}{N} \cdot \bar{L} \cdot J^{-1} \cdot L$ [-] (B.34)

N = number of devices in the reflecting wall [-]

The factor $q(\beta)$ represents the mean gain factor for each device of the row of N devices, compared to the capture width of a single device. This factor depends among other things on the angle of incidence.

An illustration of the q -factor is given in Figure B.3 [Thomas and Evans; 1981]. The variation of it with the non-dimensional spacing kd is shown for an optimally tuned system of two, three, five and ten equally spaced heaving bodies. The heavy solid line corresponds to an array of an infinite number of devices [Thomas and Evans; 1981].

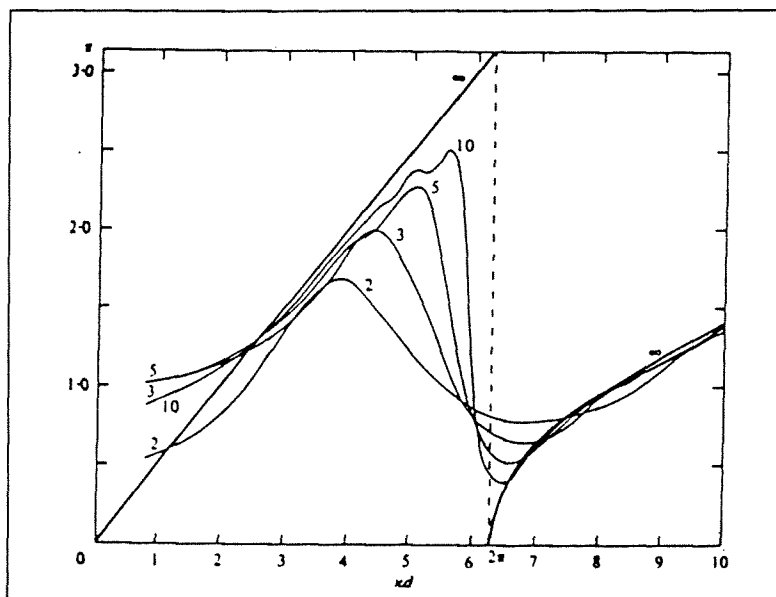


Figure B.3 Variation of the q factor with kd for several systems of heaving bodies

Summary of the two-dimensional theory

After some years of development of the theory of oscillating bodies and oscillating pressure distributions (this last is used for oscillating water column devices, see Appendix F), Evans came to a kind of summary of the theory [Evans; 1985]. The equation of motion (B.1) for oscillating bodies, can be rewritten in the next form:

$$-i\omega M \cdot U = F_e + F_w + i\omega^{-1} S \cdot U \quad (B.35)$$

with M = inertia of the body [kg] or [kg·m²]
 F_e = energy extracting force [N] or [Nm]
 F_w = wave exciting force [N] or [Nm]
 S = linearised hydrostatic restoring force [N/m] or [Nm/rad]
 U = velocity [m/s] or [rad/s]
 $-i\omega U$ = maximum acceleration [m/s²] or [rad/s²]
 $i\omega^{-1} U$ = maximum displacement [m] or [rad]

The wave force is conveniently separated into a term F (when the body is in rest) and a term $+i\omega MU - UB$ (when the body is oscillating in absence of incident waves (= radiation)). For this two-dimensional case all forces are per unit width of the device. Equation (B.35) can be written as:

$$Z \cdot U = F_e + F \quad (B.36)$$

$$\text{with } F_e = -\Lambda \cdot U \quad (B.37)$$

$$Z = B - i\omega(M + M_a - S\omega^{-2}) \quad (B.38)$$

with Λ = power take-off coefficient (opposing the motion of the body) [Ns/m] or [Nms/rad]
 B = added radiation-damping (called D_L in this Appendix B) [Ns/m] or [Nms/rad]
 M = inertia [kg] or [kg·m²]
 M_a = added inertia [kg] or [kg·m²]

The captured power is the mean rate of working of the waves over a cycle (B.12):

$$P_{\text{cap}} = 1/2 \cdot \text{Re } F_w U = -1/2 \cdot \text{Re } F_e U \quad (B.39)$$

From (B.37) follows that:

$$P_{\text{cap}} = 1/4 (\Lambda + \Lambda) U^2 \quad (B.40)$$

$$= \frac{F^2}{8B} \left\{ 1 - \frac{\Lambda - Z^2}{\Lambda + Z^2} \right\} \quad (B.41)$$

The maximum captured power is (B.14), when $\Lambda = \bar{Z}$:

$$P_{\text{cap,max}} = \frac{F^2}{8B} \quad (\text{B.42})$$

Although in many practical cases Λ is real and positive, $\Lambda = Z$:

$$P_{\text{cap,max}} = \frac{F^2}{4(Z + B)} \quad (\text{B.43})$$

For the maximum efficiency follows (using B.17, B.18, B.19):

$$E_{\text{max}} = \frac{2\gamma B}{Z + B} \quad (\text{B.44})$$

If a predominant wave frequency ω_0 is chosen at which the device will be tuned (thus fixing $\Lambda = \Lambda_0 = Z(\omega_0)$), the efficiency at any other frequency can be determined from:

$$E = \frac{2\gamma B}{Z + B} \left\{ 1 - \frac{(\Lambda_0 - Z)^2}{\Lambda_0 + Z^2} \right\} \quad (\text{B.45})$$

By using this last equation (B.45), the 2-D efficiency of different devices has been calculated [Evans; 1985]. Two examples are given in the next figures, one of the Salter's duck (rolling mode, see section 3.3.4) and one of an oscillating water column device (heaving mode, see section 3.3.4).

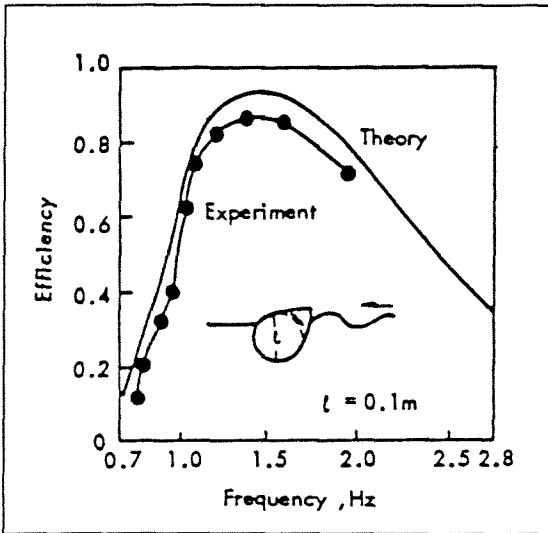


Figure B.4 Efficiency of the Salter's duck

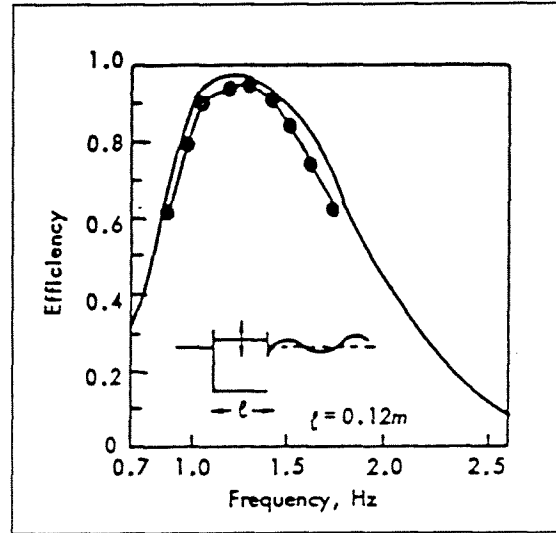


Figure B.5 Efficiency of an oscillating water column device

References

- Count, B.M.(1982); *On the hydrodynamic characteristics of wave energy absorption*; Proceedings of The 2nd International Symposium on Wave Energy Utilization, The Norwegian Institute of Technology, Trondheim, Norway
- Evans, D.V.(1976); *A theory for wave-power absorption by oscillating bodies*; Journal of Fluid Mechanics, Vol. 77, part I, pp. 1-25
- Evans, D.V.(1979); *Some analytic results for two and three dimensional wave-energy absorbers*; Power from Sea Waves; Conference on Power from Sea Waves, University of Edinburgh, England
- Evans, D.V.(1985); *The Hydrodynamic Efficiency of Wave-Energy Devices*; Hydrodynamics of Ocean Wave-Energy Utilization; Iutam Symposium Lisbon, Portugal
- McCormick, M.E.(1976); *A modified linear analysis of a wave-energy conversion buoy*; Ocean Engineering Volume 3 pp. 133-144
- McCormick, M.E.(1981); *Ocean Wave Energy Conversion*; U.S. Naval Academy, Annapolis, Maryland, USA
- Newman, J.N.(1962); *The exciting forces on fixed bodies in waves*; Journal of Ship Research, 6, 10-17
- Newman, J.N.(1976); *The interaction of stationary vessels with regular waves*; Proceedings 11th Symposium Naval Hydrodynamics, London pp. 492-501
- Shaw, R. (1982); *Wave Energy, a design challenge*; University of Liverpool, England
- Thomas, G.P.; Evans, D.V.(1981); *Arrays of three-dimensional wave-energy absorbers*; Journal of Fluid Mechanics, Vol.108, pp. 67-88

Appendix C Theory of Several Converters

In this appendix the derivation of the two-dimensional capture efficiency of the basic types of energy converters is given. Most of the theory is derived from 'Ocean Wave Energy Conversion' [McCormick;1981]. However, also the knowledge of other authors has been used for some devices. The symbols used in the equations, are mostly the same as in the corresponding literature and Appendix B. In this appendix also the units of the parameters are given.

Two-dimensional capture efficiency

1. Heaving and Pitching Bodies

The theory of oscillating bodies has been derived in the previous **Appendix B**. Maximum theoretical 2-D capture efficiency varies from 50% for symmetrical bodies, to 100% for asymmetrical bodies or oscillating bodies in more than one direction.

2. Oscillating Water Column Devices or Cavity Resonators

The first derived theory for OWC devices is based on replacing the free surface by a weightless piston and requires the determination of the added mass and damping of the piston. The calculated two-dimensional capture efficiency reaches 50% for symmetric devices to 100% for devices with a reflecting vertical wall behind the air chamber.

3. Pressure Devices

McCormick has calculated the efficiency of some sea bed based devices [McCormick;1981]. The theory is based on the theory of the pressure beneath a wave [Battjes;1993]. The change in water level affects the hydrostatic pressure, the motion of the water particles affects the dynamic pressure. The varying pressure can be represented by Bernoulli's Equation:

$$p = -\rho gz - \rho \frac{\partial \varphi}{\partial t} - \frac{1}{2} \rho v^2 \quad (C.1)$$

with p = pressure [N/m² = Pa]
 ρ = density of water [kg/m³]
 g = gravitational acceleration [m/s²]
 z = vertical co-ordinate, water level $z = 0$ [m]
 v = water particle velocity [m/s]
 φ = velocity potential [m²/s]

$$= \frac{gH}{2\omega} \frac{\cosh k(z+h)}{\cosh kh} \sin(\omega t - kx) \quad (C.2)$$

$$= \frac{\omega H}{2k} \frac{\cosh k(z+h)}{\sinh kh} \cos(\omega t - kx) \quad (C.3)$$

with H = wave height [m]

The part $1/2\rho v^2$ can be neglected for a linear wave, so the pressure becomes:

$$p = -\rho gz + \frac{\rho g H}{2} \frac{\cosh k(z+h)}{\cosh kh} \sin(\omega t - kx) \quad (C.4)$$

By using this last equation a 2-D efficiency of some devices is calculated of about 5%.

4. Surging-Wave Energy Converters

A possible surging-wave energy converter and its theory is described by McCormick [McCormick;1981]. The converter is shown in figure C.1.

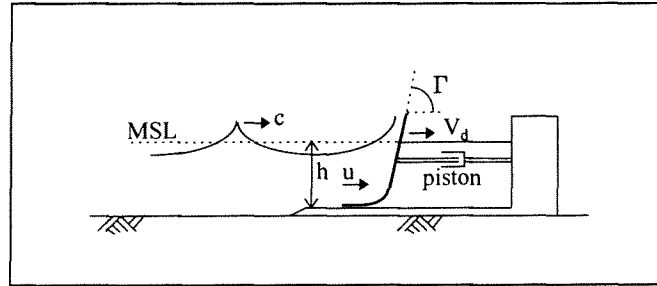


Figure C.1 Surging-wave converter, schematically

The horizontal particle velocity in shallow water [m/s] is derived in **Appendix A**:

$$u = \frac{H}{2} \sqrt{\frac{g}{h}} \cos(kx - \omega t) \quad (C.5)$$

The horizontal particle velocity does not vary with vertical position. This is approximately the situation when a swell nears the surface zone on a very gradual beach. When the wave breaks, the condition is described by $u_{\text{crest}} = c$. Where c is the velocity of the wave in shallow water [m/s]:

$$c = \sqrt{\frac{g}{h}} \quad (C.6)$$

The deflector is designed to absorb some of the momentum of the surge, while turning the flow upward at an angle Γ to the horizontal direction. From basic fluid mechanics the force on the deflector is:

$$F_d = \rho A_d u(u - V_d) \{1 - \cos(\Gamma)\} \quad (C.7)$$

with

$$\begin{aligned} F_d &= \text{force on the deflector [N]} \\ V_d &= \text{velocity of the deflector [m/s]} \\ \Gamma &= \text{angle of the deflector to the horizontal direction [deg]} \\ A_d &= \text{vertical flow area of the surge [m}^2\text{]} \\ &= (h + \eta) \cdot B_d \end{aligned} \quad (C.8)$$

with

$$\begin{aligned} B_d &= \text{width of the deflector [m]} \\ \eta &= \text{surface profile (sinusoidal assumed) [m]} \\ &= H/2 \cdot \cos(kx - \omega t) \end{aligned} \quad (C.9)$$

In equation (C.7) can be seen that the maximum power occurs when:

$$(I) V_d = u/2 \quad \text{and} \quad (II) \Gamma = 180^\circ$$

However, in practise $\Gamma = 180^\circ$ is impossible, the practical maximum power occurs when $\Gamma = 90^\circ$. In the ideal situation the deflector exactly follows the waves. When the crest strikes the deflector, the velocity of the deflector is maximum towards the shore. The deflector then begins to decelerate until the wave node ($\eta = 0$) arrives, at which time the deflector stops. Then the deflector accelerates seawards and attains a relative maximum velocity as the wave trough arrives, deceleration in the seaward direction occurs until the next node arrives at which time the deflector stops and then begins its landward motion again. Thus, the velocity of the deflector is:

$$V_d = V_0 \cos(\omega t) \quad (C.10)$$

The maximum force on the deflector with $V_d = u/2$, obtained from combining (C.5), (C.7), (C.8), (C.9) and (C.10) is:

$$F_d = \rho \left[h + \frac{H}{2} \cos(\omega t) \right] B_d \cdot \frac{H}{2} \sqrt{\frac{g}{h}} \cos(\omega t) \left[\frac{H}{2} \sqrt{\frac{g}{h}} - V_0 \right] \cos(\omega t) \cdot [1 - \cos(\Gamma)] \quad (C.11)$$

The maximum power captured by the deflector [W] is:

$$\begin{aligned} P_{cap} &= F_d \cdot V_d \\ &= \rho \left[h + \frac{H}{2} \cos(\omega t) \right] B_d \cdot \frac{H}{2} \sqrt{\frac{g}{h}} V_0 \cdot \left[\frac{H}{2} \sqrt{\frac{g}{h}} - V_0 \right] \cdot [1 - \cos(\Gamma)] \cdot \cos^3(\omega t) \end{aligned} \quad (C.12)$$

When this maximum captured power of the deflector (with angle $\Gamma = 90^\circ$) is compared to the wave power of shallow water, it can be seen that the maximum 2-D capture efficiency is about 8%. For average power this value will be even less.

5. Particle Motion Converters

Water Wheel

The water wheel is a type of particle motion converter and is shown schematically in Figure C.2.

Consider the case when the wheel is fully submerged. The horizontal gradient of the velocity, illustrated in the figure is not significant over the diameter of the wheel, assuming the diameter is much less than the wave length. Thus, the dynamic pressure acting on the blades will vary slightly over the diameter, resulting in little energy transfer to the wheel.

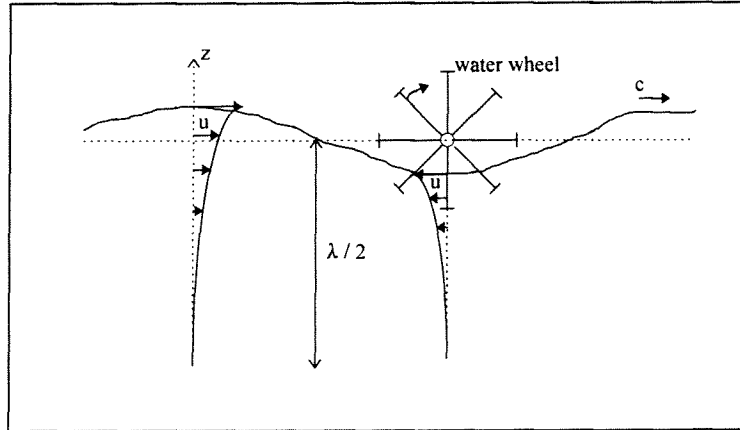


Figure C.2 Water wheel, schematically

It can be seen that the optimum design for this system operating in deep water, is that for which the axis of rotation is just above the crest of the wave. In this case, wave power is converted when a crest passes, or over one-half of the wave period. The average rotational velocity will be:

$$\omega_p = \frac{\omega}{2} = \frac{\pi}{T} \quad (C.13)$$

with ω_p = average rotational velocity [rad/s]
 T = wave period [s]

The product of the resisting torque of the generator and the rotational velocity ω_p results in the power captured by the device:

$$\begin{aligned} P_{cap} &= T_p \cdot \omega_p \\ &= \frac{T_p \pi}{T} \end{aligned} \quad (C.14)$$

with T_p = resisting torque of the generator [Nms/rad]

From equation (C.13) it is evident that the rotational velocity decreases as the wave period increases. Equation (C.14) shows that the lower the rotational velocity, the lower the captured power will be. This indicates, that this device will operate well only in relatively short waves. Waves with long periods have in general high wave heights, consequently the wave power of these waves is greater than for the shorter-period waves. It is for this reason that the water wheel is not efficient to capture wave power.

Compliant Flap

An other particle motion converter is the compliant flap, shown in Figure C.3. The theory is described by Parks [Parks;1979]. The flap operation is schematically shown in Figure C.4.

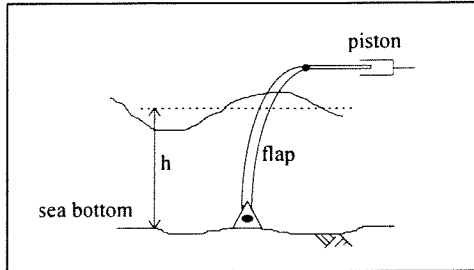


Figure C.3 Compliant flap

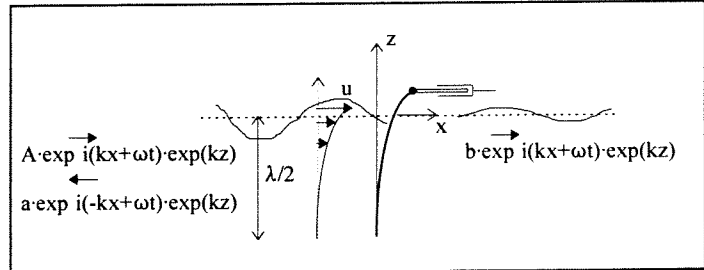


Figure C.4 Flap operation

A, a, b are the velocity potential complex amplitudes of the incoming, reflected and transmitted waves. The flap has a displacement R. The local flap velocity R' for deep water is given:

$$R' = - \frac{\partial \Phi}{\partial x} \text{ at } x = 0^+ \quad (\text{C.15 a})$$

$$= - \frac{\partial \Phi}{\partial x} \text{ at } x = 0^- \quad (\text{C.15 b})$$

$$R' = - ikA \cdot \exp(i\omega t) \cdot \exp(kz) + ika \cdot \exp(i\omega t) \cdot \exp(kz) \quad \text{at } x = 0^- \quad (\text{C.16 a})$$

$$= - ikb \cdot \exp(i\omega t) \cdot \exp(kz) \quad \text{at } x = 0^+ \quad (\text{C.16 b})$$

From the last two equations the following expression can be obtained:

$$R' = i\omega R_0 \cdot \exp(i\omega t) \cdot \exp(kz) \quad (\text{C.17})$$

with $R' = \text{flap velocity [m/s]}$

$$\omega R_0 = -kA + ka \text{ [m/s]}$$

$$= -kb$$

$$R_0 = \text{amplitude of flap displacement [m]}$$

The wave power is captured from the dynamic pressure (for deep water) on the flap:

$$p = - \rho \frac{\partial \Phi}{\partial t} \quad (\text{C.18})$$

When the flap is assumed to have no mass and an infinite length (in practise longer than $\lambda/2$), the equation of motion of the flap reduces to a force balance equation and the captured power can be calculated by the virtual work principle:

$$P_{\text{cap}} = \int_{-\infty}^0 \rho \left\{ \frac{\partial \Phi}{\partial t} \text{ (at } x = 0^+) - \frac{\partial \Phi}{\partial t} \text{ (at } x = 0^-) \right\} \exp(kz) dz \quad (\text{C.19})$$

$$P_{\text{cap}} = -D_e \cdot R' \text{ [W/m]} \quad (\text{C.20})$$

$$= -D_e \cdot i\omega R_0 \cdot \exp(i\omega t) \quad (\text{C.21})$$

with D_e = energy extracting coefficient [Ns/m]

Combining the equations (C.19) and (C.21) gives:

$$\frac{\rho i \omega (A + a - b)}{2k} = -D_e \cdot i\omega R_0 \quad (\text{C.22})$$

The capture efficiency is the ratio between captured wave energy and reflected or transmitted energy:

$$E = 1 - \left| \frac{a}{A} \right|^2 - \left| \frac{b}{A} \right|^2 \quad (\text{C.23})$$

$$= 1 - \frac{s^2}{(1+s)^2} - \frac{1}{(1+s)^2} = \frac{2s}{(1+s)^2} \quad (\text{C.24})$$

with $s = k^2 \cdot D_e / (\rho \omega)$ [-]

The optimal damper coefficient is given by $s = 1$ or $D_e = \rho \omega / k^2$, when $E = 1/2$. In practice the maximum efficiency will be lower because of non ideally loading of the piston. Fixing D_e at $\rho \omega_0 / k_0^2$, the efficiency at other frequencies can be given in the next form:

$$E = \frac{2 \left(\frac{\omega}{\omega_0} \right)^3}{\left(1 + \left(\frac{\omega}{\omega_0} \right)^3 \right)^2} \quad (\text{C.25})$$

$$= \frac{2 \left(\frac{\lambda_0}{\lambda} \right)^{3/2}}{\left(1 + \left(\frac{\lambda_0}{\lambda} \right)^{3/2} \right)^2} \quad (\text{C.26})$$

The capture efficiency as a function of λ/λ_0 is plotted in figure C.5.

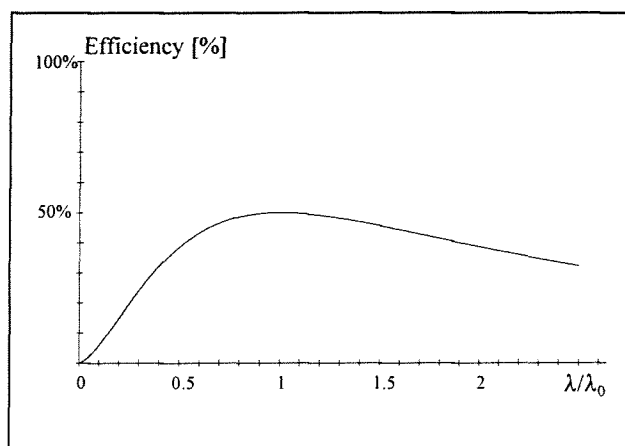


Figure C.5 Efficiency of the compliant flap

6. Salter's Duck

Theory for the Salter's Duck is based on the spring-and-damper theory of **Appendix B**. The duck is asymmetrical, so theoretically a maximum two-dimensional efficiency of 100% can be attained. By scale models using sinusoidal waves, an efficiency of 90% was measured.

7. Cockerell's Raft

The energy conversion of contouring rafts depends on the relative angular motions of raft pairs. These angular motions can be described similar to the spring-damper system of **Appendix B**. A set of equations of the next form can be obtained [McCormick;1981] [Shaw;1982]:

$$I_i \theta_i'' + D (\theta_i' - \theta_j') + FL_i/2 = M_i \quad (C.27)$$

- with
- I_i = mass moment of raft i (including the 'added mass moment') [$\text{kg}\cdot\text{m}^2$]
 - D = damping coefficient [Nms/rad]
 - $\theta_{i,j}$ = angular deflection of raft i and j [rad]
 - F = vertical reaction force between raft i and j [N]
 - L_i = length of raft i [m]
 - M_i = wave induced moment about the centre of raft i [Nm]

The time averaged (for sinusoidal waves) captured power is:

$$P_{\text{cap}} = \frac{1}{2} D_e \omega^2 (\theta_i' - \theta_j')^2 \quad (C.28)$$

- with
- D_e = energy extraction coefficient [Nms/rad]
 - ω = angular frequency [s^{-1}]

The maximum two-dimensional theoretical efficiency is 100%, models using sinusoidal waves showed about 80%.

8. Russell's Rectifier

McCormick [McCormick;1981] gave a theory for calculating the efficiency of the Rectifier. The energy available to the turbine is the potential energy of the water column that passes the turbine. If the turbine flow area is A , the potential energy at any instant is:

$$E_R^i = \frac{\rho g \Delta_R^2 A}{2} \quad (C.29)$$

with E_R^i = potential energy at any instant [J]
 ρ = density of water [kg/m³]
 g = gravitational acceleration [m/s²]
 A = turbine flow area [m²]
 Δ_R = hydraulic head [m]

$$= \delta_u(t) + \frac{H}{2} - \delta_l(t) \quad (C.30)$$

with δ_u = level of the inflow reservoir above the SWL [m]
 δ_l = level of the outflow reservoir above $z = -H/2$ [m]
 H = wave height [m]

The idealised operating sequence of the Russell's Rectifier can be divided into four periods of $\pi/2$. The wave profile, the water level of the inflow and outflow reservoir and the hydraulic head are shown in the next figure.

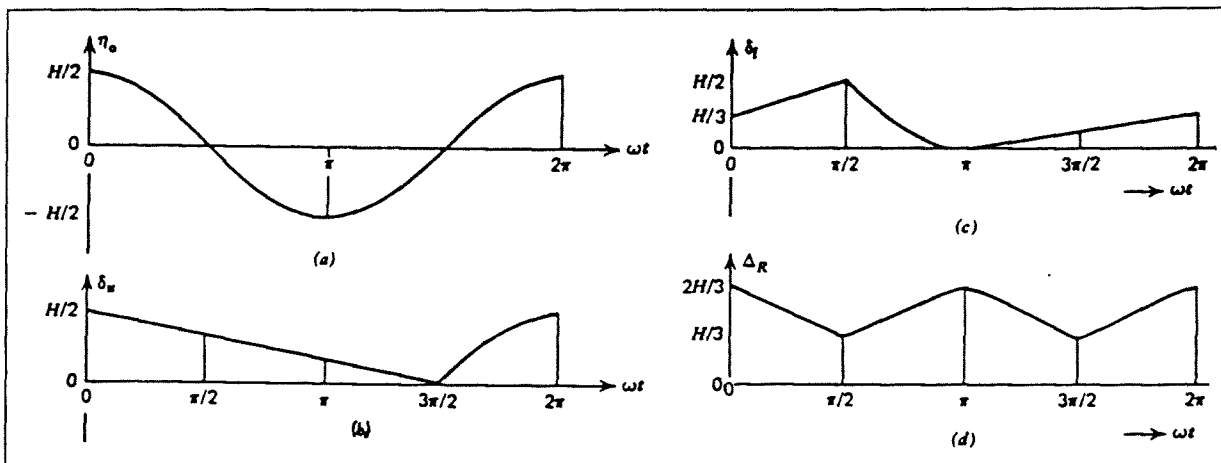


Figure C.6 Idealised operating of the Rectifier: (a) wave profile at the valves; (b) water level of the inflow reservoir; (c) water level of the outflow reservoir; (d) hydraulic head

Integrating the potential energy over one wave period gives:

$$E_R = 0.123 \cdot \rho g H^2 A \quad (C.31)$$

There is a practical limit for the flow area A , which is determined by the width of the outflow basin B . This limit is shown in Figure C.7.

The maximum outflow area is then:

$$A_{\max} = \frac{\pi B^2}{4} \quad (C.32)$$

From experiments the optimum length L of the reservoirs turned out to be $1/5$ of the wave length [Simeons; 1980]:

$$L_{\text{opt}} = 0.2 \lambda \quad (C.33)$$

with L_{opt} = optimal length of the inflow reservoir
 λ = wave length

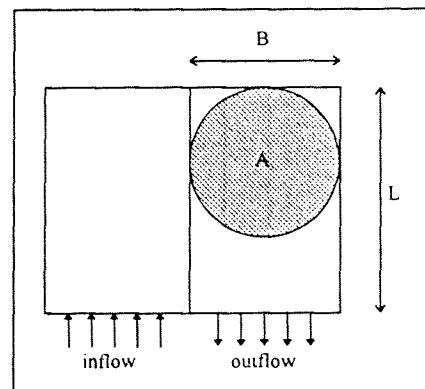


Figure C.7 Limit of the flow area A

McCormick says that this optimum length is an indication for harbour resonance [McCormick;1981]. When this resonance occurs the height of the standing wave in the inflow basin is twice that of the wave ($H_{opt} = 2H$). Cranfield proposed a design of the Rectifier at a location in deep water conditions [Cranfield;1979]. With the dimensions of this design McCormick calculated a maximum capture efficiency of about 20% in deep water.

From general hydrodynamic theory is known that harbour resonance with an ideal standing wave occurs for $L = 0.25 \lambda$. It is possible that also $L = 0.2 \lambda$ is an indication of resonance of the device, because also other devices have a resonance length of 0.2λ (see Appendix G and H).

However, Shaw says that the length must not equal 0.25λ , to avoid valve closure due to wave reflections from the rear face of the device [Shaw;1982]. When the height in the inflow basin becomes lower than the assumed $2H$, then the efficiency becomes quadratic lower (C.31).

These contradictions show that the calculation of the efficiency using $H_{opt} = 2H$ is not very reliable. The theory of McCormick but shows a method of determining the efficiency and gives only an indication of its value. This indication seems to be quite well, because estimations of other authors show an efficiency of the same magnitude [Grove-Palmer;1982].

9. Wave Focusing Techniques

The capture efficiency of the point absorbing devices is explained in **Appendix B**. The theory of the devices which make use of the refraction of waves can is not given in this appendix. The amount of wave power can be derived by using the theory for refraction of waves (Snel's Law). The theory for wave energy conversion depends on which principle of conversion is used.

References

- Battjes, J.A. (1993); *Short Waves (in Dutch)*; Delft University of Technology, The Netherlands
- Cranfield, J. (1979); *Interest in wave power growing*; Ocean Industry, February, pp. 67-76
- Grove-Palmer, C. (1982); *Wave energy in the United Kingdom- A review of the programme June 1975-March 1982*; Proceedings of The 2nd International Symposium on Wave Energy Utilization, The Norwegian Institute of Technology, Trondheim, Norway
- McCormick, M.E. (1981); *Ocean Wave Energy Conversion*; U.S. Naval Academy, Annapolis, Maryland, USA
- Parks, P.C. (1979); *Wedges, plates and waves - Some simple mathematical models of wave power machines*; Conference on Power from Sea Waves, University of Edinburgh, England
- Shaw, R. (1982); *Wave Energy, a design challenge*; University of Liverpool, England
- Simeons, C. (1980); *Hydro Power, The Use of Water as an Alternative Source of Energy*; Pergamon Press

Appendix D Theory of the Two Plate and the Triplate Machine

A mathematical analysis is described for as well the Two plate as the Triplate machine by Farley [Farley et al;1978] and Parks [Parks;1979]. The plates can be considered mass-less, infinite in depth and they can sway to and fro following the exponential profile of the waves, $\exp(kz)$. The value of $-z$ is the depth below the surface. The pump is replaced by an ideal load with force proportional to the velocity.

The Two plate machine

The operation of the Two plate machine is shown schematically in Figure D.1.

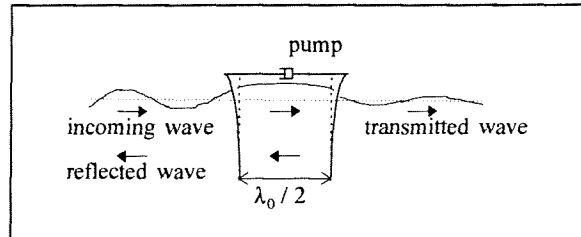


Figure D.1 Operation of the Two plate machine

An analysis similar to that of the single flap, given in **Appendix C**, leads to the following theoretical expression for the efficiency. For the maximum efficiency of 50% is required that $\lambda = \lambda_0$ and the optimum damper constant is $D_e = \rho\omega/4k^2$. The efficiency with this optimal damper constant is:

$$E = \frac{2\left(\frac{\lambda_0}{\lambda}\right)^{3/2} (1 - \cos 2\alpha)}{\left\{\left(\frac{\lambda_0}{\lambda}\right)^3 + 2\left(\frac{\lambda_0}{\lambda}\right)^{3/2}\right\} (1 - \cos 2\alpha) + 2} \quad (D.1)$$

with λ = wave length [m]
 λ_0 = design wave length [m]
 $\alpha = \frac{\pi\lambda_0}{2\lambda}$ [-]

This efficiency is plotted as a function of λ / λ_0 in Figure D.2. The theory shows a maximum capture efficiency of 50% at the design wavelength.

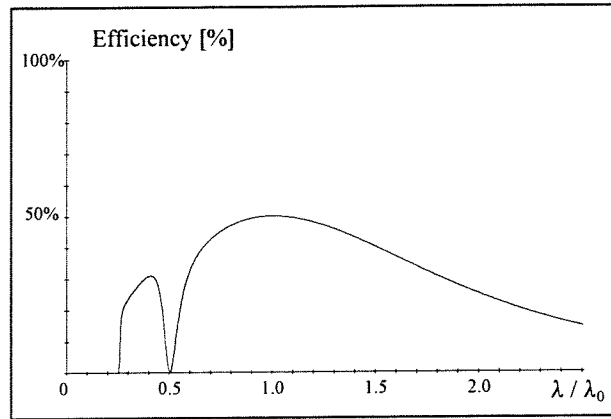


Figure D.2 Efficiency of the Two plate machine

By comparing this figure to Figure C.5 (Appendix C) of the efficiency of the single compliant flap, it can be concluded that the performance of the Two plate machine is even worse. The efficiency of the single flap has no falls at wave lengths shorter than the design wave and it has higher values for the wave lengths longer than the design wave length.

The Triplate machine

The three plates can be considered mass-less, infinite in depth and they can sway to and fro following an exponential profile $\exp(kz)$ where $-z$ is the depth below the surface. This enables the various boundary conditions to be matched exactly. In linear wave theory the velocity potential Φ is taken as:

$$\Phi = A_1 \exp \{kz + i(\omega t - kx)\} + A_2 \exp \{kz + i(\omega t + kx)\} \quad (D.2)$$

with A_1 = transmitted complex wave amplitude [m]
 A_2 = reflected complex wave amplitude [m]

The amplitudes of the different places in the Triplate machine are indicated in the next table:

Table D.1 Amplitudes in the Triplate machine

	A_1 , transmitted wave	A_2 , reflected wave
Open sea in front of the device	1	R_1
Between plates 1 and 2	T_2	R_2
Between plates 2 and 3	T_3	R_3
Open sea behind the device	T_4	0

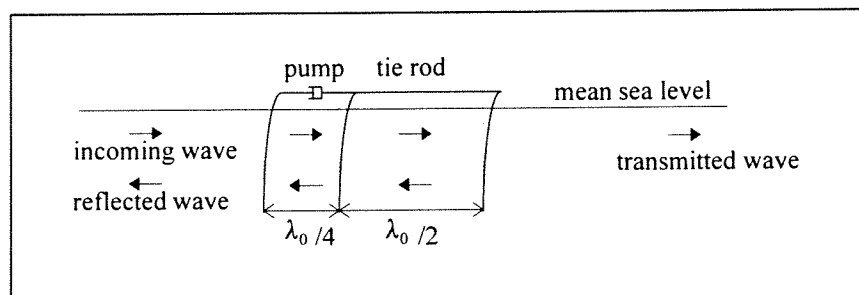


Figure D.3 Operation of the Triplate machine

Given an incoming wave with unit amplitude, it is desired to calculate the reflected and the transmitted amplitudes R_1 and T_4 . The efficiency can be calculated by:

$$E = 1 - |R_1|^2 - |T_4|^2 \quad (D.3)$$

The horizontal displacements of the three plates are given by:

$$P_i \cdot \exp(kz + i\omega t) \quad (D.4)$$

with P_i = horizontal displacement of plate i [m]
 $i = 1, 2, 3$

Since the second and third plate are bolted together, it follows:

$$P_2 = P_3 \quad (D.5)$$

A viscous damper is connected between the top of the first two plates, producing a force F_{1-2} on each plate with appropriate sign:

$$F_{1-2} = D_e (P_1 - P_2) i\omega \exp(i\omega t) \quad (D.6)$$

The tie rod force, F_{2-3} between plates 2 and 3 is taken as a compression:

$$F_{2-3} = F \cdot \exp(i\omega t) \quad (D.7)$$

There are three equations for each plate:

- the boundary condition that $-\partial\Phi / \partial x$ on each side of the plate equals its horizontal velocity
- the equation of motion of the plate, which is in this model a force balance equation since the plates are considered to have no mass

These equations can be solved and the efficiency can be calculated. For 100% efficiency it is required that $\lambda = \lambda_0$ and the damper constant must be optimal, $D_e = \rho\omega/2k^2$. The efficiency with this optimal damper constant is:

$$E = \frac{2\left(\frac{\lambda_0}{\lambda}\right)^{3/2} \{(\cos\alpha - \cos 2\alpha)(3\sin^2\alpha - 1) + 2\sin^2\alpha \cos^2\alpha\}}{\left\{\left(\frac{\lambda_0}{\lambda}\right)^{3/2} (\cos\alpha - \cos 2\alpha) - \cos 2\alpha\right\}^2 + \sin^2\alpha \cos^2\alpha \left\{\left(\frac{\lambda_0}{\lambda}\right)^{3/2} + 2\right\}^2} \quad (D.8)$$

with λ = wave length [m]
 λ_0 = design wave length [m]
 $\alpha = \frac{\pi\lambda_0}{2\lambda}$ [-]

This efficiency is plotted as a function of λ/λ_0 in Figure D.4. The theory shows a maximum capture efficiency of 100% at the design wavelength. The machine gives a reasonable broad response covering a factor of about two in wave length.

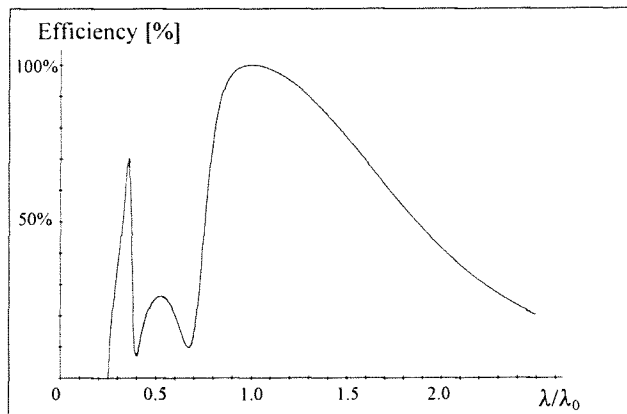


Figure D.4 Efficiency of the Triplate machine

Wave motion diminishes with depth, see **Appendix A**. For the Triplate machine with a finite depth D of the plates, it is assumed that a fraction $\exp(-2kD)$ of the power passes under the system. To intercept most of the power without excessive expense $D = \lambda/2\pi = 1/k$ is a reasonable choice. Consequently, the theoretical efficiency is reduced by a factor of about 0.86, because of this limited depth of the plates. Due to non-ideally loading of the pumps, there exists a reduction of the overall efficiency by a factor 0.64. Adding hydraulic and friction losses, one can expect an overall power conversion efficiency of the Triplate machine of about 50%. Measured efficiencies of model tests agree well with the theory.

References

Farley, F.J.M.; Parks, P.C.; Altmann, H. (1978); *A wave power machine using free floating vertical plates*; Wave and Tidal Energy, International Symposium on Wave and Tidal Energy, BHRA, University of Kent, Canterbury, England

Parks, P.C. (1979); *Wedges, plates and waves - Some simple mathematical models of wave power machines*; Conference on Power from Sea Waves, University of Edinburgh, England

Appendix E Theory of the Pendulor

Watabe et al. describe the theory to calculate the efficiency of the pendulor, which has been derived by Asano [Watabe et al.;1986]. However, their description is not easy to understand, because the theory is given in broad outlines and in unusual arrangement. In this appendix the theory has been rewritten, in analogy to Appendix B. The used symbols are given the accompanying units.

Theory

The load F_c which acts on the hydraulic cylinder is proportional to the angular velocity θ' of the pendulor and the cylinder has elastic deform x_c in proportion to the load F_c . The wave condition is sinusoidal regular. With these assumptions the theory of the pendulor and its efficiency have been derived.

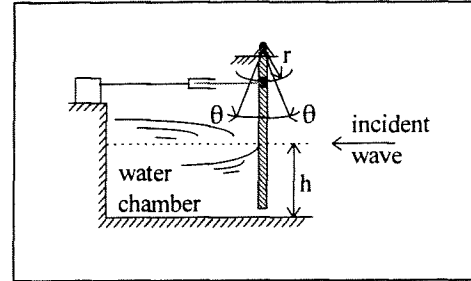


Figure E.1 Pendulor, schemetically

On the conditions described above, the motion of the pendulor becomes a sinusoidal oscillation, analogous to the spring-and-damper system of Appendix B, the equation of motion is expressed in equation (E.1):

$$\Sigma I \theta'' + (D_0 + D) \theta' + (S_0 + S) \theta = M \cos(\omega t) \quad (E.1)$$

with ΣI = equivalent moment of inertia of the pendulor with added water [$\text{kg}\cdot\text{m}^2$]
 θ = swing angle [rad]
 $'$ = time derivatives
 D_0 = load coefficient of the pendulor by hydraulic cylinder [Nms/rad]
 D = damping coefficient due to radiation waves generated by the pendulor [Nms/rad]
 S_0 = restoring coefficient of the pendulor [Nm/rad]
 S = restoring coefficient due to the water elevation behind the pendulor [Nm/rad]
 ω_0 = natural circular frequency of the pendulor [s^{-1}]

$$= S_0 (S_0 + S) / \Sigma I \quad (E.2)$$

M = amplitude of wave exciting moment [Nm]

$$= \frac{\rho B Y_0 \omega^2 H}{k^3 \sinh(kh)} \quad (E.3)$$

with ρ = density of water [kg/m^3]
 B = width of the pendulor [m]
 ω = circular frequency of incident waves [s^{-1}]
 H = wave height [m]
 k = wave number [m^{-1}]
 $= 2\pi / \text{wave length}$

$$Y_0 = k_0 h \cdot \sinh(k_0 h) \cdot \cosh(k_0 h) - 1 [-] \quad (E.4)$$

with h = supporting height of the pendulor from the water surface [m]

The equation (E.1) can be solved and the equation for θ follows:

$$\theta = \frac{M \cos(\omega t)}{\sqrt{(\sum I)^2 (\omega_0^2 - \omega^2)^2 + (D_0 + D)^2 \omega^2}} \quad (\text{E.5})$$

Now the power P_{cap} , captured by the cylinder, is the mean rate at which work is being done (with $M = F_c \cdot r = D_0 \cdot \theta^2$)

$$P_{\text{cap}} = \frac{\omega}{2\pi} \int_0^{2\pi/\omega} F_c r \theta' dt \quad (\text{E.6})$$

$$= \frac{\omega}{2\pi} \int_0^{2\pi/\omega} D_0 \theta' \theta' dt \quad (\text{E.7})$$

$$= \frac{1}{2} \omega^2 D_0 \theta^2 \quad (\text{E.8})$$

$$= \frac{\omega^2 D_0 M^2}{2(\sum I)^2 (\omega_0^2 - \omega^2)^2 + (D_0 + D)^2 \omega^2} \quad (\text{E.9})$$

The overall efficiency is formed by the product of two parts, namely the capture efficiency of the pendulum and the efficiency of the power take-off by the cylinder. The overall efficiency of the device can be calculated with the next equation:

$$E = \frac{\text{Power captured by the device}}{\text{Incoming wave power to the pendulum } P_w} = E_{\text{pendulum}} \cdot E_{\text{cylinder}} \quad (\text{E.10})$$

E_{pendulum} = capture efficiency

$$= \frac{P_{\text{cap}}}{P_w} \quad (\text{E.11})$$

with P_{cap} = power absorbed by the cylinder [W/m], from equation (E.6)
 M = amplitude of wave exciting moment [Nm], from (E.3)
 P_w = wave power per width of the pendulum [W/m]

$$= \frac{\rho g B H^2 \omega}{8k} \left\{ \frac{1}{2} + \frac{kh}{\sinh(2kh)} \right\} \quad (\text{E.12})$$

Using these equations, it follows for the capture efficiency of the pendulor:

$$E_{\text{pendulor}} = \frac{D_0}{\Sigma(I)^2(\omega_0^2 - \omega^2)^2 + \omega^2(D_0 + D)^2} \cdot \frac{8\rho B\omega^3 Y_0^2}{k^4 X_0} \quad (\text{E.13})$$

$$\text{with } X_0 = \sinh(kh) \cosh(kh) + kh \quad [-] \quad (\text{E.14})$$

The efficiency of the cylinder is:

$$E_{\text{cylinder}} = 1 - \frac{M\omega \theta' k_e r^2}{1 + (M\omega \theta' k_e r^2)^2} \quad (\text{E.15})$$

$$\begin{aligned} \text{with } M &= F_c \cdot r \\ &= D_0 \cdot \theta' \\ k_e &= \text{spring constant of the cylinder [N/m]} \\ &= F_c / x_c \\ r &= \text{length between a supporting centre of the pendulor and the centre of the cylinder-} \\ &\quad \text{connecting pin on the pendulor [m]} \end{aligned}$$

For maximum efficiency exist three design criteria:

$$(I) D = D_0, (II) \omega = \omega_0 \text{ and } (III) k_e = \infty$$

Physically, this implies that for the maximum efficiency the energy extraction rate must equal the rate of radiation damping, that the pendulor must be kept in resonance and the stiffness of the cylinder must be as high as possible. At this operation the angle $\theta_{E=1}$ of the pendulor becomes:

$$\theta_{E=1} = \frac{M}{\omega D} = 0.5 \theta_0 \quad (\text{E.16})$$

$$\theta_0 = \text{amplitude of pendulor when } \omega_0 = \omega \text{ and } D_0 = 0$$

Experiments

The efficiency of the pendulor has been checked in a model test [Watabe et al.;1986]. It was demonstrated that the maximum efficiency E , is about 80% of the incident waves, using a two dimensional model driven by a sinusoidal regular wave.

Also a 5 kW prototype has been investigated at a coastal site, during a period of almost 20 months. The maximum ratio of power extraction was above 50%. During severe sea conditions the output was 18 ~ 35 kW, while the mean incoming wave power was estimated at 55 kW and the pendulor system was sufficiently durable against this condition. However, during a next severe storm the pendulor was deformed and after that the pressure plate had been lost [Watabe et al.;1986] [Seymour;1992].

References

Seymour, R.J.(1982); *Ocean Energy Recovery, The state of the Art*; Scripps Institution of Oceanography, University of California at San Diego; Offshore Technology Research Center, Texas A&M University, USA

Watabe, T.; Kondo, H. Yano, K.(1986); *Studies on a pendulor-type wave energy converter*; Water for Energy; 3rd International Symposium on Wave, Tidal, OTEC, and Small Scale Hydro Energy, BHRA, Brighton, England

Appendix F Theory of Oscillating Water Column Devices

Introduction

The first theory of the oscillating water column devices consisted of describing the device by a simple spring-and-damper system, as explained in Appendix B. Evans has developed a new hydrodynamic method [Evans;1982]. The potential flow theory is used and it is supposed that the pressure in the air chamber is proportional to the vertical velocity of the water column. This method correctly allows for the applied surface pressure and the consequent spatial variation of the internal free surface. The results, which are based on the classical linear wave theory, show the close analogies which exist with the theory of oscillating bodies. The devices are not called oscillating water column any more, but oscillating surface-pressure distributions. Later on, also other authors used this hydrodynamic theory instead of the spring-and-damper theory.

Evans describes the theory for the general case of wave-power absorption by two- and three-dimensional systems of oscillating surface-pressure distributions, including scattering due to submerged structures [Evans;1982]. However, the theory is only applied to structures of which the fixed immersed part is of shallow draught, so that the scattered potential can be neglected. It is assumed that the air in the capture chamber is incompressible and that the turbine characteristic is linear.

Sarmiento and Falcão extended the theory by introducing air compressibility and a reflecting wall behind the chamber (however, the other immersed parts of the structure are also ignored for scattering) [Sarmiento, Falcão;1985]. They also checked the influence of finite water depth, the influence of a non-linear turbine and of a turbine characteristic that exhibits a phase difference between pressure and flow rate (phase control). These authors published in 1990 another paper about phase control [Sarmiento et al.;1990].

This appendix starts by following mainly the theory of Evans [Evans;1982]. Subsequently, it will be extended with air compressibility and some other results of Sarmiento et al. [Sarmiento et al.;1985,1990]. The used symbols for the various parameters are mostly the same as used by Evans. However, some are chosen equal to the symbols used in Appendix B or for clearness subscripts are added. In this way is tried to give a comprehensible survey of the theory of oscillating surface-pressure distributions, which is a method of describing the operation of oscillating water column devices.

Basic assumptions

A fixed structure is considered, open at the bottom end and closed at the other end. It intersects the free surface, trapping a volume of air. (This volume of air can be represented in a series of sections each having its own internal free surface and its own turbine, as proposed by Evans (1982). In this appendix just a single internal free surface with one turbine is considered.) The effect of the incoming waves is to cause the internal free surface to oscillate at the same frequency as the incident waves, driving the air volume back and forth through the turbine. If the air compressibility is small, than the air pressure at the turbine is, by approximation, the same as the uniformly distributed pressure just above the corresponding free surface. The power (which is total mean rate of work) is the time averaged product of this pressure and the volume which flows through the turbine. This is the same as the product of the spatial average of the internal velocity of each internal free surface and its area. It is assumed, that the turbine has linear characteristics, so that the pressure drop across the turbine is proportional to the volume flow through it.

Cartesian co-ordinates are taken: x, y horizontal and z vertically upwards, with $z = 0$ the undisturbed free surface. S_I is the internal free surface and S_F the external free surface. $P_I(t)$ is the simple harmonic pressure on S_I . Under these assumptions a velocity potential $\Phi(x,y,z,t)$ can be given. The capture chamber has a length a .

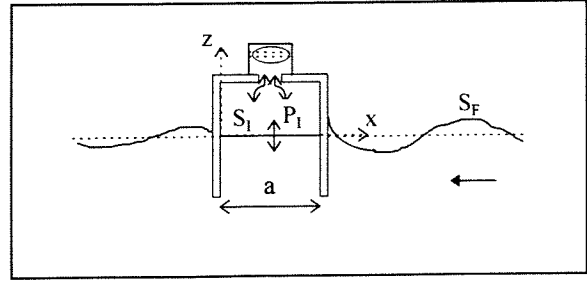


Figure F.1 O.W.C. device with coordinates

According to the assumptions of the linear wave theory, the velocity potential $\Phi(x,y,z,t)$ must satisfy Laplace's equation and boundary conditions:

$$\nabla^2 \Phi = 0 \quad \text{in the fluid} \quad (\text{F.1})$$

$$g\eta + \frac{\partial \Phi}{\partial t} = \begin{cases} -P_I(t) & \text{on } S_I \\ \rho & \\ 0 & \text{on } S_F \end{cases} \quad (\text{F.2})$$

with Φ = velocity potential [m^2/s]
 g = gravitational acceleration [m/s^2]
 η = surface elevation [m]
 t = time [s]
 ρ = water density [kg/m^3]
 S_I = internal surface [m^2]
 S_F = external surface [m^2]
 $P_I(t)$ = simple harmonic pressure on S_I [Pa/s]

The surface elevation is $\eta(x,y,z,t)$:

$$\frac{\partial \eta}{\partial t} = \frac{\partial}{\partial z} \Phi(x, y, 0, t) \quad (\text{F.3})$$

$$\frac{\partial \Phi}{\partial n} = 0 \quad \text{on rigid boundaries, } S_B \quad (\text{F.4})$$

with n = unit normal vector in the fluid

The effect of the structure is partially to scatter the incident waves so that, at large distances, in addition to the incident wave potential, there exist a wave field travelling outwards away from the structure. Other terms used for scattering are: diffraction, transmission and reflection. The motion of the oscillating water column it self causes a radiation potential, which behaves like outgoing waves at large distances.

The velocity potential of the incoming wave is:

$$\Phi_0(x,y,z,t) = \frac{gA}{\omega} e^{kz} \cos\{kx(\cos\beta) + ky(\sin\beta) - \omega t\} \quad (\text{F.5})$$

with Φ_0 = velocity potential of incoming wave [m^2/s]
 A = wave amplitude [m]
 ω = angular frequency [s^{-1}]
 k = wave number [m^{-1}]
 β = angle between wave train and positive x -axis [deg] or [rad]

Equations (F.2) and (F.3) can be combined to give:

$$\frac{\partial \Phi}{\partial z} - k\Phi = \frac{1}{\rho g} \frac{dP_1}{dz} \quad (F.6)$$

It is convenient to write:

$$\Phi = \Phi_d + \Phi_r \quad (F.7)$$

with Φ = velocity potential [m²/s]
 Φ_d = velocity potential of incident and scattered wave [m²/s]
 Φ_r = velocity potential of radiation wave [m²/s]

Wave energy extraction

For calculating the energy extraction, the volume flow through the turbine has to be known. The volume flow rate across S_1 becomes:

$$\int_{S_1} \frac{\partial \Phi}{\partial z} dS = \int_{S_1} \frac{\partial \Phi_d}{\partial z} dS + \int_{S_1} \frac{\partial \Phi_r}{\partial z} dS \quad (F.8)$$

$$Q(t) = Q_d(t) + Q_r(t) \quad (F.9)$$

The captured power is the total rate of working of the pressure force across S_1 :

$$P^T(t) \cdot \{Q_d(t) + Q_r(t)\} \quad (F.10)$$

with $P^T(t)$ = simple harmonic pressure on S_1 [Pa/s]
 $Q_d(t)$ = diffraction and incident volume flow rate of air through the turbine due to the incident and scattered wave [m³/s / s]
 $Q_r(t)$ = radiation volume flow rate of air through the turbine due to the oscillating pressure in the chamber [m³/s / s]

It is assumed that the incident wave field is monochromatic, with angular frequency ω . It follows that the volume flow rate Q_d is a simple time-harmonic function of time. Also the turbine characteristics are assumed to be linear, so the whole problem becomes linear and the following result can be written:

$$\{\Phi, \Phi_d, \Phi_r, P, Q_d, Q_r\} = \text{Re}\{\phi, \phi_d, \phi_r, p, q_d, q_r\} \cdot e^{-i\omega t} \quad (F.11)$$

The velocity potentials ϕ, ϕ_d, ϕ_r and amplitudes p, q_d, q_r are time-independent quantities and in general complex. Here, and whenever a physical quantity is equated to a complex expression, only the real part has to be taken, in accordance with the usual convention.

The next arbitrary but convenient decomposition can be made:

$$Q_r = -AP' - BP \quad (F.12)$$

In terms of time-independent quantities (F.12) can be written:

$$q_r = -Z \cdot p \quad (F.13)$$

with $Z = B - i\omega A$ (F.14)

= complex admittance [m³s⁻¹ / Pa]

$i^2 = -1$ [-]

A = hydrodynamic coefficient [m³ / Pa]

B = damping coefficient [m³s⁻¹ / Pa]

The complex admittance Z , is the time-independent volume flux of air measured downwards across the water surface of the OWC due to a unit amplitude simple harmonic pressure on the surface. B and A are real quantities that depend on the geometry and frequency. The damping coefficient B is associated with the energy radiation by the pressure fluctuation in the chamber and is positive. Only

for systems with a vertical axis or plane of symmetry, B can take zero-values for discrete values of ω . The hydrodynamic coefficient A can in general take negative, zero or positive values depending on the geometry and frequency [Sarmento et al.;1990].

The captured power of the device can be calculated by averaging the mean rate of working of the pressure over a period:

$$P_{\text{cap}} = \frac{1}{2} \text{Re} \{ \bar{p} \cdot (q_d + q_r) \} \quad (\text{F.15})$$

with P_{cap} = captured wave power [W]

\bar{p} = conjugate transpose of the pressure [Pa]

Using $Z = B - i\omega A$ (F.14) the captured power of equation (F.15) becomes:

$$P_{\text{cap}} = \frac{1}{2} \text{Re} \{ \bar{p} \cdot q_d \} - \frac{1}{2} \bar{p} \cdot B \cdot p \quad (\text{F.16})$$

When $B \neq 0$, the last expression (F.16) can be rewritten in the form:

$$P_{\text{cap}} = \frac{q_d^2}{8B} - p - \frac{q_d^2}{2B} \frac{B}{2} \quad (\text{F.17})$$

It follows that the maximum power $P_{\text{cap,max}}$ occurs, when the pressure amplitude p is:

$$p = \frac{q_d}{2B} \quad (\text{F.18})$$

$$P_{\text{cap,max}} = \frac{q_d^2}{8B} \quad (\text{F.19})$$

The last two results are identical with the corresponding expressions obtained for an oscillating body in a regular wave train. The roles of pressure and incident wave-produced volume flux are then replaced by velocity and incident wave exciting force on the body, see **Appendix B** equation (B.40) and (B.42).

Three-dimensional pressure distributions

By analogy to the theory of an oscillating body, the maximum capture width of an axi-symmetric oscillating surface-pressure distribution (or oscillating water column) which oscillates at resonance frequency ($P_{\text{cap,max}} = q_d^2 / 8B$), can be calculated:

$$w_{\text{cap,max}} = \frac{P_{\text{cap,max}}}{P_w} = \frac{\lambda}{2\pi} = \frac{1}{k} \quad (\text{F.20})$$

with $w_{\text{cap,max}}$ = maximum capture width [m]

$P_{\text{cap,max}}$ = maximum captured power [W]

P_w = mean wave power of incident wave [W/m]

For non axi-symmetric pressure distributions, further progress can be made. The relation between B and q_d for non axi-symmetric devices is dependent on the angle of incidence β :

$$B = \frac{1}{8\lambda P_w} \int_0^{2\pi} q_d(\theta)^2 d\theta \quad (\text{F.21})$$

with $\beta = \pi + \theta$

From the last equations can be derived:

$$k \cdot w_{\text{cap,max}} = q_d(\beta)^2 / \int_0^{2\pi} q_d(\theta)^2 d\theta \quad (\text{F.22})$$

Evans [Evans;1982] considered a rectangular pressure distribution with a length a ($x = a$) and a width $2b$ ($y = \pm b$). The volume flow rate equals:

$$q_d(\beta) = \int_{S_1} \{\partial \Phi_0 / \partial z\}_{z=0} dS \quad (\text{F.23})$$

$$= 4 \cdot g \cdot A \cdot \omega^{-1} \cdot k^{-1} \cdot f(\beta) \quad (\text{F.24})$$

with $\Phi_0 = gA\omega^{-1} \cdot \exp(ikx \cdot \cos\beta +iky \cdot \sin\beta +kz)$ (F.25)

$$f(\beta) = \sin(ka \cdot \cos\beta) \cdot \sin(kb \cdot \sin\beta) / \sin\beta \cdot \cos\beta \quad (\text{F.26})$$

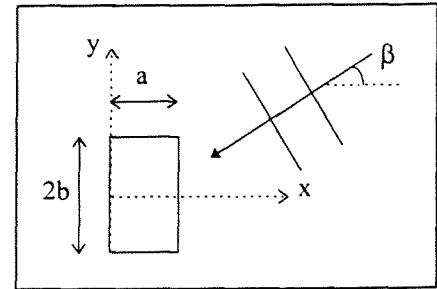


Figure F.2 Waves approaching the rectangular device

These expressions make it possible to estimate the influence of the shape and situation of a single rectangular pressure distribution on the maximum power and capture width. From equation (F.25) the following two relations can be derived, showing the relative effectiveness of a pressure surface in head ($\beta = 0^\circ$) and beam seas ($\beta = 90^\circ$).

$$w_{\text{cap,max}}(\beta_1) / w_{\text{cap,max}}(\beta_2) = |f(\beta_1)|^2 / |f(\beta_2)|^2 \quad (\text{F.27})$$

$$w_{\text{cap,max}}(1/2\pi) / w_{\text{cap,max}}(0) = a^2 \cdot \sin^2 kb / b^2 \cdot \sin^2 ka \quad (\text{F.28})$$

Results based on the computation of these equations are shown in the next two figures. Figure F.3 shows the variation of the maximum capture width ratio, $W_{\text{cap,max}} = w_{\text{cap,max}} / 2b$, with the angle of incidence β , for waves approaching a rectangular device, for different values of the dimensionless wave number ka and $b/a = 2$.

In Figure F.4 the variation of the maximum capture width ratio in beam seas, $w_{\text{cap,max}}(0^\circ) / 2b$, with aspect ratio b/a is shown for different values of ka .

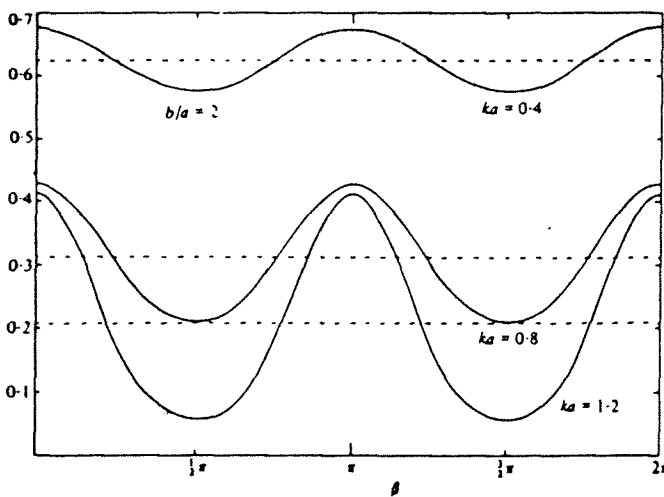


Figure F.3 Variation of maximum capture width ratio, with angle of incidence

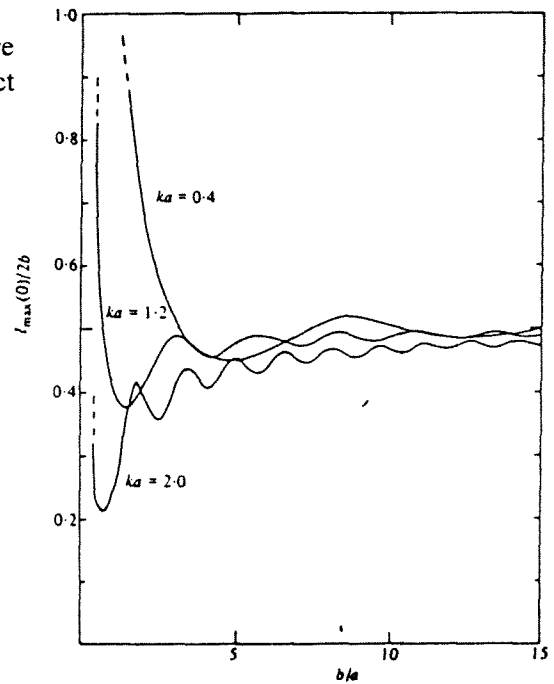


Figure F.4 Variation of maximum capture width ratio, with aspect ratio b/a

As might be expected the fluctuations of $w_{\text{cap,max}} / 2b$ with β are larger for larger ka since the rectangular shape has more influence on the shorter waves. For instance, an axi-symmetric pressure distribution has a maximum capture width of about 5/8 of a diameter in waves of about 8 times the diameter ($ka = 0.4$). For a rectangular distribution of the same width but half the length ($b/a = 2$) in beam seas the increase in capture width is only about 10%. For waves of 4 times the diameter ($ka = 0.8$) the capture width increases from 3/10 of the diameter of the axi-symmetric device to over 2/5 of the width of the rectangular device. In Figure F.4 the capture width ratio approaches 0.5 as $b/a \rightarrow \infty$, being the result for the maximum two-dimensional efficiency.

Turbine characteristic and resonance conditions

When the turbine has linear characteristics, then the pressure drop across the turbine is proportional to the volume flow through it. In practise it may be easier to control the flow through the turbines than the pressure drop across. The next linear relation is assumed:

$$q_r + q_d = + \Lambda \cdot p \quad (\text{F.29})$$

with Λ = complex turbine characteristic (sign in front of Λ is taken positive, while the pressure force and volume flux are both measured vertically upwards) [$\text{m}^3\text{s}^{-1}/\text{Pa}$]

In combination with $q_r = -Z \cdot p$ (F.13) this gives:

$$q_d = (\Lambda + Z) \cdot p \quad (\text{F.30})$$

The mean captured wave power can be rewritten in the form:

$$P_{\text{cap}} = \frac{q_d^2}{8B} \left\{ 1 - \frac{\Lambda - \bar{Z}^2}{\Lambda + Z^2} \right\} \quad (\text{F.31})$$

Knowing that the maximum power occurs when the pressure amplitude $p = q_d / 2B$, it follows that for maximum power the turbine characteristic must be equal to the complex conjugate of the admittance Z .

$$\Lambda = Z \quad (\text{F.32})$$

In the beginning of the development of the OWC devices [Evans;1982] it was assumed that in practise Λ would be real and positive. This can be written as $\Lambda = Z$ or $\Lambda = (B^2 + \omega^2 A^2)^{1/2}$. In that case the maximum power $P'_{\text{cap,max}}$ becomes:

$$P'_{\text{cap,max}} = \frac{q_d^2}{4(Z + B)} \quad (\text{F.33})$$

Another common expression is the ratio between $P'_{\text{cap,max}}$ (the maximum power absorption at optimal damping with a real positive turbine characteristic) and $P_{\text{cap,max}}$ (the maximum power at optimal impedance matching (F.19))

$$\frac{P'_{\text{cap,max}}}{P_{\text{cap,max}}} = 4B\Lambda \{ (\Lambda+B)^2 + \omega^2 A^2 \}^{-1} \quad (\text{F.34})$$

The maximum two-dimensional efficiency for $\Lambda = Z$, can be derived by using the results of Newman of equation (B.17) of Appendix B. For oscillating pressure distributions this equation becomes: $q_d^2 / B = 8 \cdot P_w \cdot \gamma$ with $\gamma = \{A_i^+{}^2\} / \{A_i^+{}^2 + A_i^-{}^2\}$.

$$E_{\max} = \frac{2\gamma B}{Z + B} \quad (\text{F.35})$$

$$= \frac{1}{1 + (1 + \omega^2 A^2 / B^2)^{1/2}} \text{ for a symmetric pressure distribution} \quad (\text{F.36})$$

Falcão and Sarmento (1980) have shown that $A(ka) = 0$ for $ka = 1.3$ and thus the maximum efficiency of 0.5 for a symmetric device is achieved [Evans;1982]. The value $ka = 1.3$ corresponds to a capture chamber length of about one-fifth of the wave length.

As another example, Evans showed an axi-symmetric oscillating pressure distribution over a disk with radius a , on the free surface of deep water [Evans;1982]. Figure F.5 shows the variation of $k \cdot w_{\text{cap,max}}$ and Figure F.6 shows the non-dimensionalised (with respect to the disk diameter) maximum capture width ratio.

The maximum value of $k \cdot w_{\text{cap,max}}$ occurs at the first zero of $A(ka)$, this is at $ka = 1.96$ corresponding to a disk diameter of about six-tenth of the wave length. The value of $k \cdot w_{\text{cap,max}}$ is reduced to zero for the first zero of $B(ka)$, when $ka = 3.83$.

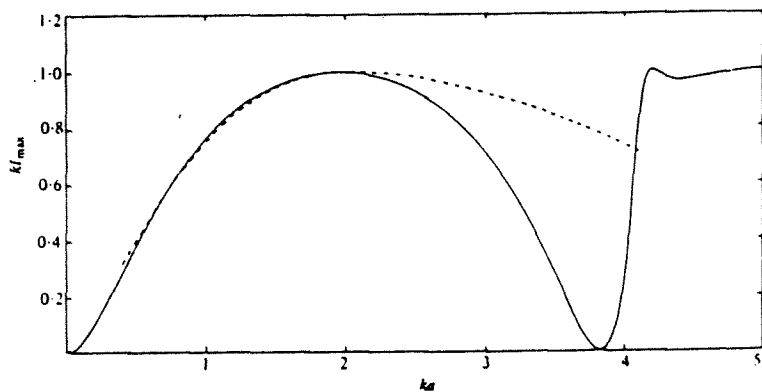


Figure F.5 Variation of $k \cdot w_{\text{cap,max}}$ with dimensionless wave number ka

The effect of the term $A(ka)$ is to give an absolute maximum to the capture width ratio of about 0.4 in the range of interest at $ka = 0.7$ (a wavelength to diameter ratio of about 5). In Figure F.6 also the maximum capture width ratio for resonance frequencies $(2ka)^{-1}$ is shown, the only point of contact with $w_{\text{cap,max}} / 2a$ occurs when $A(ka)$ is zero.

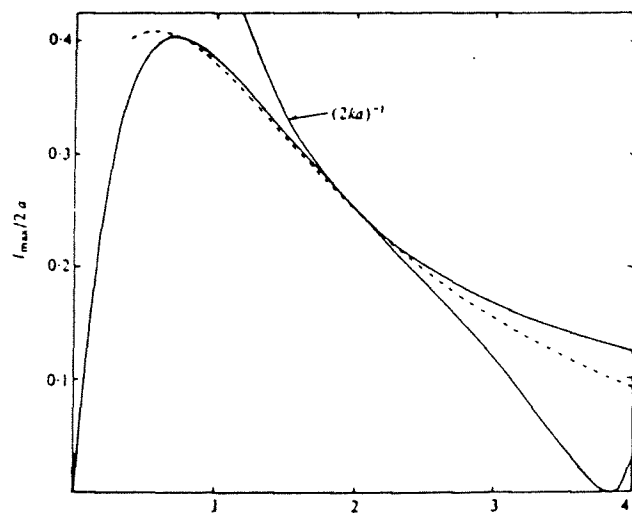


Figure F.6 Variation of dimensionless capture width with, dimensionless wave number ka

Comparison with a rigid plate model

In Figure F.5 and F.6 the dotted lines come from modelling the pressure distribution by a rigid surface plate. The plate is assumed to lie on the free surface and its mass is ignored compared to its added mass.

In Figure F.5 can be seen that, in the range $0 < ka < 4$, which encompasses the range of practical interest for wave energy devices, the major difference between the two methods occurs for $ka > 2$, where the pressure distribution values begin to fall. At the value of $ka = 3.83$ when $B(ka)$ has its first zero, $k \cdot w_{\text{cap,max}}$ reaches zero for the pressure distribution, but for the rigid surface plate, $B(ka)$ is never zero and no such fall in $k \cdot w_{\text{cap,max}}$ occurs. The same is true for the capture width ratios in Figure F.6. In fact over the range from 1.5 to 4 of the diameter / wavelength ratio (ka), the differences in the two capture ratios are small.

Air compressibility

Sarmento and Falcão showed that the air compressibility can effect significantly the performance of full-scale devices [Sarmento, Falcão;1985]. Linearizing the springlike air-compressibility effect can provide a satisfactory approximation to what is obtained by using the non-linear isentropic pressure-density relation. Malmo and Reitan have also described the air compressibility [Malmo, Reitan;1985]. Under operating conditions the volume of the air through a turbine, fulfilling the linearity condition is:

$$Q(t) = \frac{dV}{dt} = \Lambda \cdot P(t) \quad (\text{F.37})$$

with Q = air flow rate through the turbine [m^3/s /s]
 $= Q_r + Q_d$ (F.9)

V = volume flow through the turbine [m^3/s]

Λ = complex turbine characteristic [$\text{m}^3 \cdot \text{s}^{-1}/\text{Pa}$]

$P(t)$ = excess chamber pressure [Pa/s]
 $= P_c(t) - p_0$

$P_c(t), p_0$ = respectively, pressure of air in the chamber and outside [Pa/s],[Pa]

The adiabatic pressure law is:

$$\frac{p_c}{p_0} = \left(\frac{\rho_c}{\rho_0} \right)^\gamma \quad \text{or} \quad \frac{\rho_c}{\rho_0} = \left(\frac{p_c}{p_0} \right)^{1/\gamma} \quad (\text{F.38})$$

γ = specific heat ratio [-] = 1.4
 $= c_p / c_v$

c_p, c_v = respectively, specific heat of air at constant pressure and at constant volume
 $[\text{J}/\text{kg}/\text{K}]$

ρ_c = air density inside the chamber [kg/m^3]

ρ_0 = outside air density [kg/m^3]

When it is assumed that variations in air density are relatively small, the pressure law (F.38) can be linearized:

$$\rho_c = \rho_0 + \frac{\rho_0 \cdot P(t)}{\gamma p_0} \quad (\text{F.39})$$

Under these conditions the volume flow rate of air through the turbine can be written as:

$$Q_{c.a.}(t) = Q(t) + \frac{V_c}{\gamma p_0} \frac{dP_c}{dt} \quad (F.40)$$

$$= \Lambda \cdot P(t) + \frac{V_c}{\gamma p_0} \frac{dP_c}{dt} \quad (F.41)$$

with $Q_{c.a.}(t)$ = compressible air flow rate through the turbine [$m^3/s/s$]
 $Q(t)$ = air flow rate through the turbine without compressibility influence [$m^3/s/s$]
 V_c = volume of air in the chamber [m^3]

In the case of linear wave theory, with $P(t) = p \cdot \exp(-i\omega t)$, equation (F.41) becomes (note that Sarmento, Falcão and Malmo, Reitan use $\exp(i\omega t)$, instead of $\exp(-i\omega t)$, used by Evans):

$$Q_{c.a.}(t) = \Lambda_{c.a.} \cdot P(t) \quad (F.42)$$

with $\Lambda_{c.a.}$ = effective turbine characteristic (with compressible air) [$m^3 s^{-1}/Pa$]

$$= \Lambda + i\omega \frac{V_c}{\gamma p_0} \quad (F.43)$$

In many later articles this last equation is written as the effective turbine characteristic $\Lambda_{c.a.}$ is called Λ . In the remaining part of this report the next notation will be used, namely:

$$\Lambda = C_t, \text{ when air is assumed incompressible} \quad (F.44)$$

$$\Lambda = C_t + i\omega \frac{V_c}{\gamma p_0}, \text{ when air is assumed compressible} \quad (F.45)$$

In this approximation, the air compressibility has the effect of replacing the actual and possibly already complex turbine characteristic C_t by an effective turbine constant Λ of equation (F.45). For the specific heat ratio γ , it seems to be appropriate to use the adiabatic value 1.4 [Malmo et al.;1985].

Oscillating water column with a reflecting wall

Sarmento and Falcão have shown also an example of an oscillating pressure distribution with a reflecting wall, submerged vertically from the surface to the bottom at $x = 0$, as shown in Figure F.7 [Sarmento et al.;1985]. Maximum theoretical efficiency (100%), in deep water and with incompressible air, occurs for $a/\lambda = 0.206$ (chamber length / wave length). With an optimal fixed turbine constant, the efficiency remains above 60% if $0.16 < a/\lambda < 0.38$.

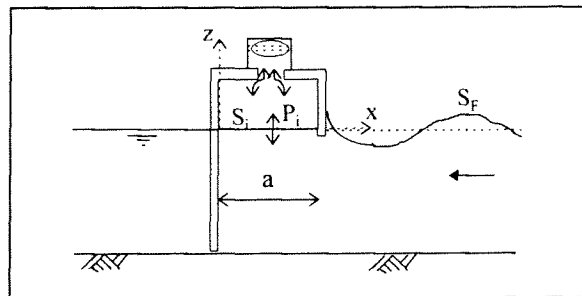


Figure F.7 OWC device with a reflecting wall

Non-linear air turbine

Sarmento and Falcão made also some numerical calculations, using a non-linear turbine characteristic [Sarmento et al.;1985]. It turned out that the maximum efficiency is close to unity and occurs at a ratio a/λ which does not differ significantly from the resonance value 0.206. However, unlike the linear case, the efficiency is dependent as well on the length as on the height of the incident wave. Consequently, the non-linear power take-off system has to be tuned to the wavelength and to the wave height. It can be concluded that a non-linear turbine has no benefits, compared to the linear turbine.

Phase control

From the equations (F.18) and (F.19) can be seen that for maximum power absorption the pressure should be in phase with the incident and scattered flow rate q_d . This condition is given by $\Lambda = \bar{Z}$ (F.32). In this case, the flow through the turbine is given by (F.37):

$$Q(t) = \bar{Z} \cdot p \cdot \exp(-i\omega t) \quad (\text{F.46})$$

When the air is compressible, this equation can be written:

$$Q(t) = \left\{ B - i\omega \left(A + \frac{V_c}{\gamma p_0} \right) \right\} \cdot p \cdot \exp(-i\omega t) \quad (\text{F.47})$$

$$= D \cdot P \cdot \exp(-i\omega t) \quad (\text{F.48})$$

This last equation indicates that the turbine should be able to maintain a phase difference $\theta = \arg D$, between flow rate and pressure, which is non-zero, except if $A = -V_c / (\gamma p_0)$. This last condition occurs for particular combinations of geometry and frequency [Sarmiento et al.;1990]. Operating the turbine with a phase difference is called phase control.

Phase control can be a method of considerably increasing the amount of energy extracted from the waves. A possibility of implementing it, consists in using a self-rectifying turbine of variable geometry. Phase control can also drastically reduce the size of as well the device chamber as the turbine [Sarmiento et al.;1990] [Hunter;1991].

In real sea conditions, phase control requires the prediction of the incident waves, for which no fully satisfactory solution seems yet to have been found [Sarmiento et al.;1990].

References

- Evans, D.V.(1982); *Wave-power absorption by systems of oscillating surface pressure distributions*; Journal of Fluid Mechanics, Vol. 114, pp. 481-499
- Hunter, R.(1991); *Future possibilities for the NEL Oscillating Water Column wave energy converter*; Wave Energy, IMechE, Institution of Mechanical Engineers, Seminar, England
- Malmo, O.; Reitan, A.(1985); *Wave-power absorption by an oscillating water column in a channel*; Journal of Fluid Mechanics, Vol. 158, pp. 153-175
- Sarmiento, A.J.N.A.; Falcão, A.F. de O.(1985); *Wave generation by an oscillating surface-pressure and its application in wave-energy extraction*; Journal of Fluid Mechanics, Vol. 150, pp. 467-485
- Sarmiento, A.J.N.A.; Gato, L.M.C; Falcão, A.F. de O.(1990); *Turbine-controlled wave energy absorption by oscillating water column devices*; Vol. 17, No. 5, pp. 481-497

Appendix G Theory of the Harbour Type OWC

In this appendix the theory of the 'harbour' type oscillating water column is given. This device has been developed in Norway. Later on, also the British investors became involved with the derivation of the theory for this device. In Part I, the method of Malmo and Reitan is handled, in Part II the method of Count and Evans. The theory has been rewritten, using symbols in analogy to Appendix B and F. The units of the symbols used in the equations, are also added.

Part I Theory of Malmo and Reitan

Malmo and Reitan describe an approximate theory of the operation of the 'harbour' type device, based on the results of spring-and-damper system [Malmo, Reitan; 1985]. They assume a vertically oscillating water column, excited by waves and damped by radiation, hydrodynamic resistance and power take-off by a turbine.

The Norwegian Hydrotechnical Laboratory (NHL) has been working with the development of the oscillating water column device since 1978. The wish was to keep the dimensions of the device small compared to the wave length, however by small devices, the natural bandwidth of the resonance frequency tends to be narrow. For broadening this bandwidth, a 'harbour' in front of the 'chamber' is introduced. The 'harbour' is formed by a pair of walls protruding from the front of the OWC, thereby partly enclosing a rectangular basin. In this basin the phenomenon of 'harbour' resonance occurs [Ambli et al.;1982] [Malmo, Reitan; 1985].

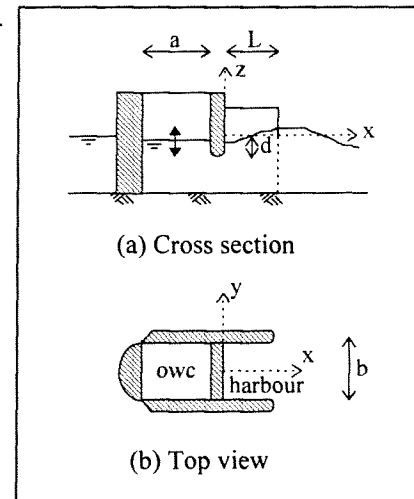


Figure G.1 Kvaerner MOWC

The equation describing the motion of the water column can be written in the next form (in analogy to Appendix B, equation B.36):

$$F = (Z + \Lambda) \cdot z' \quad (G.1)$$

with $F =$ exciting force [N]
 $Z =$ complex admittance [Ns/m]
 $= B + i\omega A$ (G.2)

$\Lambda =$ power take-off coefficient [Ns/m]
 $z' =$ velocity of the water column [m/s]

with $B =$ radiation coefficient [Ns/m]
 $A =$ hydrodynamic resistance coefficient [Ns²/m]
 $= M + M_a - S/\omega^2$ (G.3)

with $M =$ mass of the water column [kg]
 $M_a =$ mass of the 'harbour' (added mass) [kg]
 $S =$ spring constant due to gravity [N/m]

In the theory of Malmo and Reitan, the effective turbine characteristic is assumed to be real and linear with the velocity of the column, so that $\Lambda = C_t$ (no phase control, air incompressible) [Malmo, Reitan; 1985]. In agreement with the theory of oscillating bodies of Appendix B the equation of motion can be written:

$$F = (M + M_a) \cdot z'' + (C_t + B) \cdot z' + S \cdot z \quad (G.4)$$

with $C_t =$ real turbine characteristic

M_a , B and F are not easy to determine, several detailed methods, as well numerical as analytical, exist to calculate them [Malmo, Reitan; 1985].

If the OWC, the 'harbour' and the boundary conditions outside the 'harbour' are studied separately, the maximum performance at complete impedance matching ($\Lambda = \bar{Z}$), only depends on the radiation coefficient at the virtual boundary of the 'harbour'. The dynamics of the 'harbour' and the 'chamber' do not enter the problem, until it is considered how impedance matching can practically be achieved.

In figure G.2 the calculated radiation coefficient B for a single device is shown for different 'harbour' lengths. The model has the next dimensions: length of the 'chamber' $a = 0.57$ m, depth of the immersion of the front wall $d = 0.25$ m and a water depth $h = 0.75$ m.

The radiation resistance is significantly increased by the introduction of the 'harbour'. When B increases, there will be also a corresponding increase in the excitation force F . Local maxima in F and B occur for:

$$L + L' = \lambda/4 (1 + 2n) \quad (G.5)$$

with L = 'harbour' length [m]
 L' = added length depending on λ [m]
 λ = wave length [m]
 $n = 0, 1, 2, \dots$

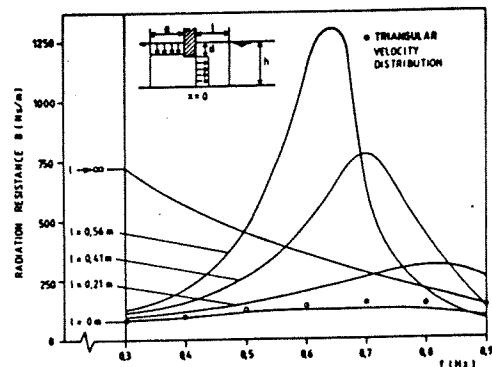


Figure G.2 Radiation coefficient for different 'harbour' lengths

This is the well known criterion for 'harbour' resonance. Resonance occurs when the total hydrodynamic resistance is zero, thus when (G.3) is zero:

$$A = M + M_a - S/\omega^2 = 0 \quad (G.6)$$

For any constant S and M there is just a single resonant frequency in the extremal cases when $L = 0$ and $L = \infty$. The introduction of the 'harbour' changes the added mass term. As a first estimate the 'harbour' length should be chosen in the next way [Malmo, Reitan; 1985]:

$$\lambda_{\min} / 4 < L + L' < \lambda_{\min} / 3 \quad (G.7)$$

with λ_{\min} = wave length of the shortest waves from which energy has to be captured [m]

Figure G.3 illustrates how L , S and M can be selected to optimise the performance of a wave energy absorber in a given wave spectrum. For the case that $L = 0.56$ m and $M = 330$ kg, there will be just a single resonant frequency. For the case $L = 0.56$ m and $M = 165$ kg resonance occurs at three frequencies, thus giving a much broader bandwidth. By changing the geometry of the OWC it is possible to match the system parameters S and M to the added mass determined by L and the reflection coefficient r at the 'harbour' mouth. There are two possibilities, a close match in a smaller frequency range or an approximate match in a wider range.

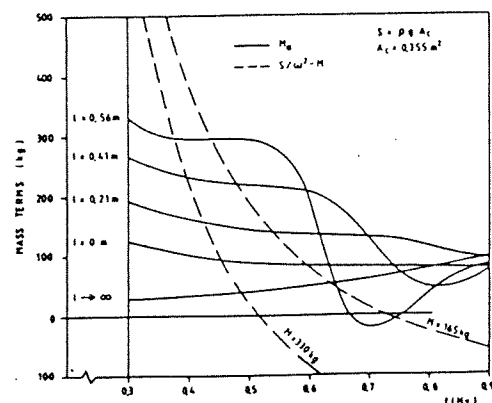


Figure G.3 Mass terms for different 'harbour' lengths

The capture width ratio between the performance at optimal damping for a real turbine characteristic $W'_{cap,max}$ and the performance at complete optimal damping $W_{cap,max}$ is shown in the next figure (see also equation (F.34)). Three cases are shown, the two-dimensional absorber ($L = \infty, M = 330$ kg), no 'harbour' ($L = 0, M = 330$ kg) and a 'harbour' of $L = 0.56$ m ($M = 165$ kg).

The introduction of the 'harbour' of $L = 0.56$ m causes a significant broadening of the frequency response of the device. This is not only because of the multiple resonances of the system, but also the increase of the radiation coefficient B , relative to the resistance term ωA at the lowest 'harbour' resonant frequency is important in providing a better phase matching.

In the 2-D case ($l \rightarrow \infty$), the resonance has a broader response than in the no 'harbour' case, because the radiation resistance is larger.

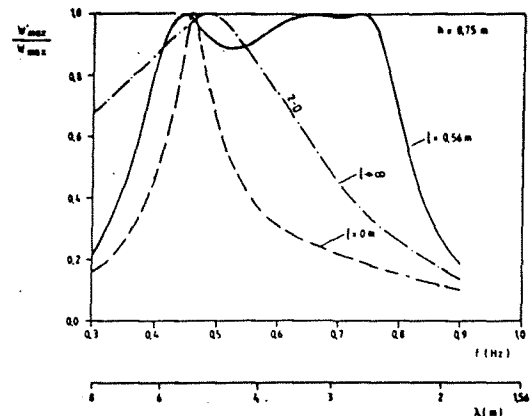


Figure G.4 Variation of ratio W'_{max} / W_{max} with frequency

When the turbine characteristic is real and positive and the air incompressible (see also Appendix F, $\Lambda = Z$), the optimal value has the next expression:

$$C_{t,opt} = (B^2 + \omega^2 A^2)^{1/2} \quad (G.8)$$

A local minimum of $C_{t,opt}$ exists at the primary resonance for all devices. For the device with a 'harbour' length of 0.56 m occurs a local maximum at 'harbour' resonance ($f \approx 0.65$ Hz, see Figure G.2). This device has a local minimum of $C_{t,opt}$ at $f \approx 0.76$ Hz, where the rapidly decreasing B (see Figure G.2) is balanced by the increase of ωA .

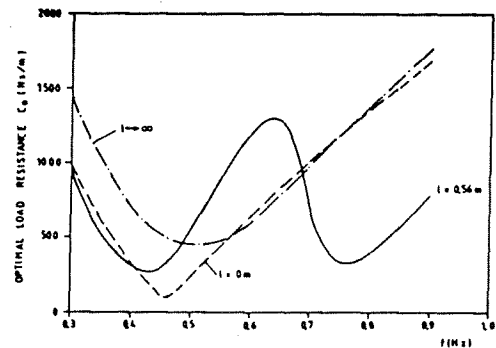


Figure G.5 Variation of optimal turbine characteristic $C_{t,opt}$

In a real sea state, waves have different frequencies. In practise, it is difficult to have the turbine characteristic optimal at every frequency simultaneously. Because of this fact, the turbine characteristic will have a fixed value C_t .

In Figure G.6 the relative performance for two fixed values of C_t is compared to the performance when the real turbine characteristic is $C_{t,opt}$. The reduction in captured power due to non-optimal damping is not dramatic. The reduction in the range $f = 0.5 - 0.7$ Hz for $C = 270$ Ns / m, is related to the 'harbour' resonance. In this frequency range the damping is much lower than optimal.

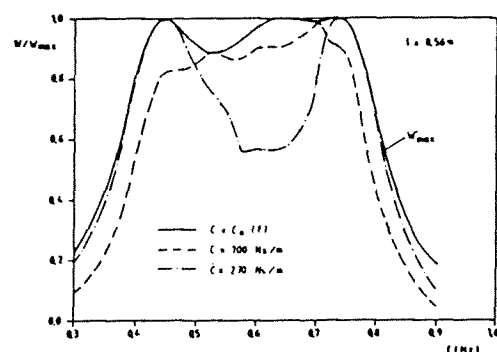


Figure G.6 Capture width ratio W/W_{max} for two fixed turbine constants and one optimal turbine constant

For a real sea state with a given wave spectrum, there exist an optimal value of C_1 . The determination of this value is influenced by hydrodynamic losses, desired amplitude of the OWC, the efficiency of the turbine and generator and the extra costs of the turbine (in general, the larger the turbine constant, the more expensive the turbine).

Part II Theory of Count and Evans

Approximate Method

Another approximate theory for the 'harbour' type device is given by Count and Evans [Evans;1982] [Count,Evans;1984] [Evans; 1985]. They show that it is possible to obtain results for the three-dimensional device, using solely information about the two-dimensional performance of the device. This theory is based on the results of the spring-and-damper system (Appendix B). A typical device is shown in Figure G.7. The width of the device is $2a$, the length of respectively the 'harbour' and the 'chamber' (or OWC) are L and d .

An obliquely incident wave in open sea, gives rise to a plane wave formed by the side-walls, there being no local effect felt at the 'chamber'. In this case, the OWC responds in open sea the same as to a plane wave in a narrow tank.

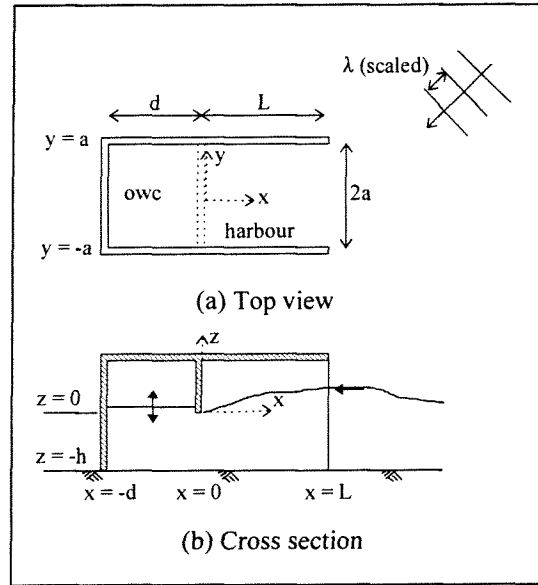


Figure.7 (a) Top view; (b) cross section of the 'harbour' type OWC

The wave is reflected as a wave of (complex) amplitude $A \cdot r$, which in turn is reflected from the open end as a wave of amplitude $A \cdot r \cdot R$, back down towards the device. Here, r and R are reflection coefficients, corresponding respectively to the device and the open end. This process, when repeated indefinitely, gives rise ultimately to a wave of amplitude $A/(1-rR)$ travelling towards the 'chamber' and $Ar/(1-rR)$ travelling away.

Since the incident power at the mouth of the 'harbour' is proportional to the wave amplitude $|A|^2$ per unit 'harbour' width, it follows that the capture width ratio based on 'harbour' width is just [Evans;1982]:

$$w_{\text{cap}}/2a = P / P_w \quad (\text{G.9})$$

$$= \frac{1 - r^2}{1 - rR^2} \quad (\text{G.10})$$

When the device has a two-dimensional capture efficiency of 100%, then r would be zero and $w_{\text{cap}}/2a$ equals 1. However it is possible to improve upon this, since it is possible to write $w_{\text{cap}}/2a$ in the next form:

$$w_{\text{cap}}/2a = \frac{1}{1 - R^2} \left(1 - \frac{r - R^2}{1 - rR^2} \right) \quad (\text{G.11})$$

It follows that the maximum capture width ratio is reached when $r = R$:

$$(w_{\text{cap}}/2a)_{\text{max}} = \frac{1}{1 - R^2} \quad (\text{G.12})$$

The reflection coefficient R for radiation into an infinite domain or open sea, is known from hydrodynamics [Count,Evans;1984]:

$$R = e^{-ka} \cdot e^{2ik(L+L')} \quad (G.13)$$

$$\text{with } L'/a = \pi^{-1} \left(1 - \gamma + \log \frac{2\pi}{ka} \right) - (ka)^{-1} \sum_{n=1}^{\infty} \left\{ \sin^{-1} \left(\frac{ka}{n\pi} \right) - \frac{ka}{n\pi} \right\} \quad (G.14)$$

with L' = added length [m]
 γ = Euler's constant [-]
= 0.5772..

This gives for the maximum capture width:

$$(w_{\text{cap}}/2a)_{\text{max}} = \frac{1}{1 - e^{-2ka}} \quad (G.15)$$

For radiation into an infinite channel, bounded by parallel walls, Count and Evans give two other equations for the reflection coefficient R and the added length L' [Count,Evans;1984].

Another form of the capture width ratio is based on the equation of mean power absorption of an oscillating body (B.41) and several relations between three- and two-dimensional parameters. In this way, an expression for the capture width ratio is obtained, entirely in terms of the impedance Z for the effectively two-dimensional problem with $L = \infty$, the complex reflection coefficients r , R and the power take-off parameter Λ [Count,Evans;1984]. The superscript h means that the parameters are valid for three-dimensionality, when the device is considered as a 'harbour' with an OWC.

$$w_{\text{cap}}/2a = \frac{1}{1 - R^2} \left(1 - \frac{\Lambda - \bar{Z}^h{}^2}{\Lambda + Z^h{}^2} \right) \quad (G.16)$$

$$= \frac{\Lambda + Z^2 - \Lambda - Z^2}{(\Lambda + Z) - rR(\Lambda - Z)^2} \quad (G.17)$$

with Λ = power take-off characteristic [Ns/m]
 Z^h = complex three-dimensional admittance [Ns/m]
= $(Z + rR Z) / (1 - rR)$ (G.18)

r = reflection coefficient of the device [-]
= $r_0 (\Lambda - Z) / (\Lambda + Z)$ [Evans;1982] (G.19)

with r_0 = reflection coefficient at $x = -d$, when no wave power is absorbed [-]

The complex impedance Z (and thus Z^h) is time-independent and for a given geometry of a device it can be known. In the spring-and-damper system, the free surface is assumed to be a rigid plate (with $Z = B - i\omega A$), $\text{Re}(Z)$ is just B , the radiation damping coefficient, while $\text{Im}(Z)$ is just $-A\omega$, related to the mass, added mass and buoyancy-restoring terms.

Other used relations are:

$$\text{Re}(Z^h) = B^h \quad (G.20)$$

= radiation damping of the device [Ns/m]

$$= B(1 - R^2) / 1 - rR^2 \quad (G.21)$$

$$F^h = \text{exciting force on the 'harbour' entrance [N]} \\ = F / (1 - rR) \quad (G.22)$$

F = exciting force on the OWC [N]

Modification to the capture width ratio for obliquely incident waves, making an angle θ with the side walls is straightforward and only affects F^h and not Z^h . Thus an obliquely incident wave of amplitude A will be guided by the side walls towards the absorbing front face as a wave of amplitude A' . This last amplitude A' depends on the angle of incidence θ before multiple reflections take place. Thus (G.22) needs to be modified by the term A'/A on the right hand side, also $(w_{cap}/2a)$ of (G.16) and (G.17) requires the multiplication factor $|A'/A|^2$ on the right hand side. The expression for this factor $|A'/A|^2$ is [Evans;1982]:

$$|A'/A|^2 = e^{-ka(1-\cos\theta)} \cdot \sin(ka \cdot \sin\theta) \cdot (ka \cdot \sin\theta)^{-1} \quad (G.23)$$

with A = amplitude of incoming wave [m]
 A' = amplitude of wave in the 'harbour' [m]
 k = wave number [m^{-1}]
 a = half of the width of the device [m]
 θ = angle of incidence [rad]

From **Appendix B** (B.27) and (B.28) the results for the capture width of oscillating devices are known. The maximum capture width of an axi-symmetric vertically oscillating (heaving) device is:

$$(w_{cap}/2a)_{max} = (2ka)^{-1}$$

For a horizontally oscillating device (swaying or rolling) w_{max} the maximum capture width is:

$$(w_{cap}/2a)_{max} = (ka)^{-1} \cos^2\theta$$

In Figure G.8 the maximum capture width of a 'harbour' type device for various angles of incidence in comparison to the result $(2ka)^{-1}$ for a heaving axi-symmetric device.

It is clear, that the device has the highest capture width in beam seas ($\theta = 0$). The shorter the waves (higher ka), the greater the influence of the angle of incidence on the capture width.

Numerical Method

Count and Evans made a numerical solution, which involves solving for the flow inside the 'harbour' and matching this with another solution valid outside [Count,Evans;1984]. These two solutions are matched across the connecting region, which is the 'harbour' mouth. The advantage of this approach is allowing the predominantly two-dimensional flow within the 'harbour' matching with a fully three-dimensional solution outside.

Comparison of Results of the Approximate of Evans and the Numerical Method

In order to calculate the values of Z^h and F^h of respectively (G.18) and (G.22), it is necessary to determine Z and \tilde{r} for the device in a semi-finite channel (the two-dimensional case). The scattering problem for the simple idealised considered here (see Figure G.7) is easy to solve, since the solution

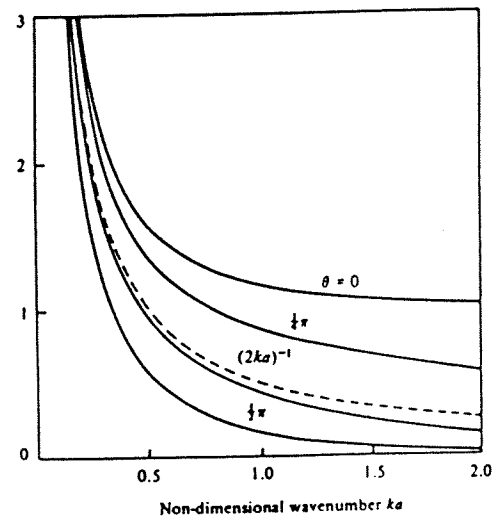


Figure G.8 Maximum capture width of the 'harbour' device

is a standing wave of amplitude $2A$, corresponding to the complete reflection of the incident wave at the fixed front face. In that case $|r_0| = 1$.

However, the solution of the radiation problem is more complicated and is a special case of the Havelock's (1929) wavemaker theory [Count,Evans;1984]. The $\arg r_0$ can be determined from solving a radiation problem alone, since it is proportional to the complex wave amplitude radiated down the 'harbour' due to an unit oscillatory pressure on the surface of the OWC. The power take-off characteristic Λ (turbine), relates the air flow across the surface to the pressure drop across the turbine. $\Lambda = 0$ corresponds to shutting of the flow completely, while $\Lambda^{-1} = 0$ corresponds to widening the orifice of the turbine so that the pressure drop is zero. In either case no net work is done and from (G.19) can be seen that $|r| = |r_0| = 1$. With R given by (G.13) Z^h and F^h of respectively (G.18) and (G.22) can be computed [Evans;1982].

The well known expression of $Z = B - i\omega A$, can be rewritten in:

$$Z = B - i\omega \left(M + M_a - \frac{S}{\omega^2} \right) \quad (G.24)$$

with Z = complex admittance [Ns/m]
 B = radiation damping coefficient [Ns/m]
 M = mass of the oscillating water column [kg]
 $= 2 \cdot a \cdot d \cdot h \cdot \rho$
 M_a = added mass (frequency dependent) [kg]
 S = linearized hydrostatic restoring force [N/m]
 ω = angular frequency

It is convenient to non-dimensionalise the added-mass and damping coefficients M and B by writing:

$$\mu = \frac{M_a^h}{M} \quad (G.25)$$

$$\lambda = \frac{B^h}{M\omega} \quad (G.26)$$

with μ = non-dimensionalised added mass [-]
 λ = non-dimensionalised damping [-]
 M_a^h = added mass [kg]
 M = mass of the oscillating water column [kg]
 B^h = added damping coefficient [Ns/m]

The exciting force can also be non-dimensionalised, using the increase in hydrostatic force of the oscillating water column due to an increase A in water elevation. This ensures that $\xi = 1$ at zero frequency.

$$\xi = \frac{F^h}{2 \cdot a \cdot \rho \cdot g \cdot d \cdot A} \quad (G.27)$$

with ξ = non-dimensionalised exciting force [-]
 F^h = exciting force [N]
 $2 \cdot a$ = width of the device [m]
 ρ = density of water [kg/m³]
 g = gravitational acceleration [m/s²]
 d = length of the OWC [m]
 A = increase in water elevation [m]

Results shown are shown in the next figure. The variation of μ , λ , ξ and $\arg F^h$ with the dimensionless wave number ka for different harbour lengths is given. The dimensions of the model-sized device are $d = 1.2$ m, $h = 1.3$ m and $a = 1$ m. The different harbour lengths are characterised by L/d . The case $L/d = 0$ corresponds to the absence of projecting sidewalls. The results of a numerical method are also shown in this figure, which are in fair agreement [Count,Evans;1984]

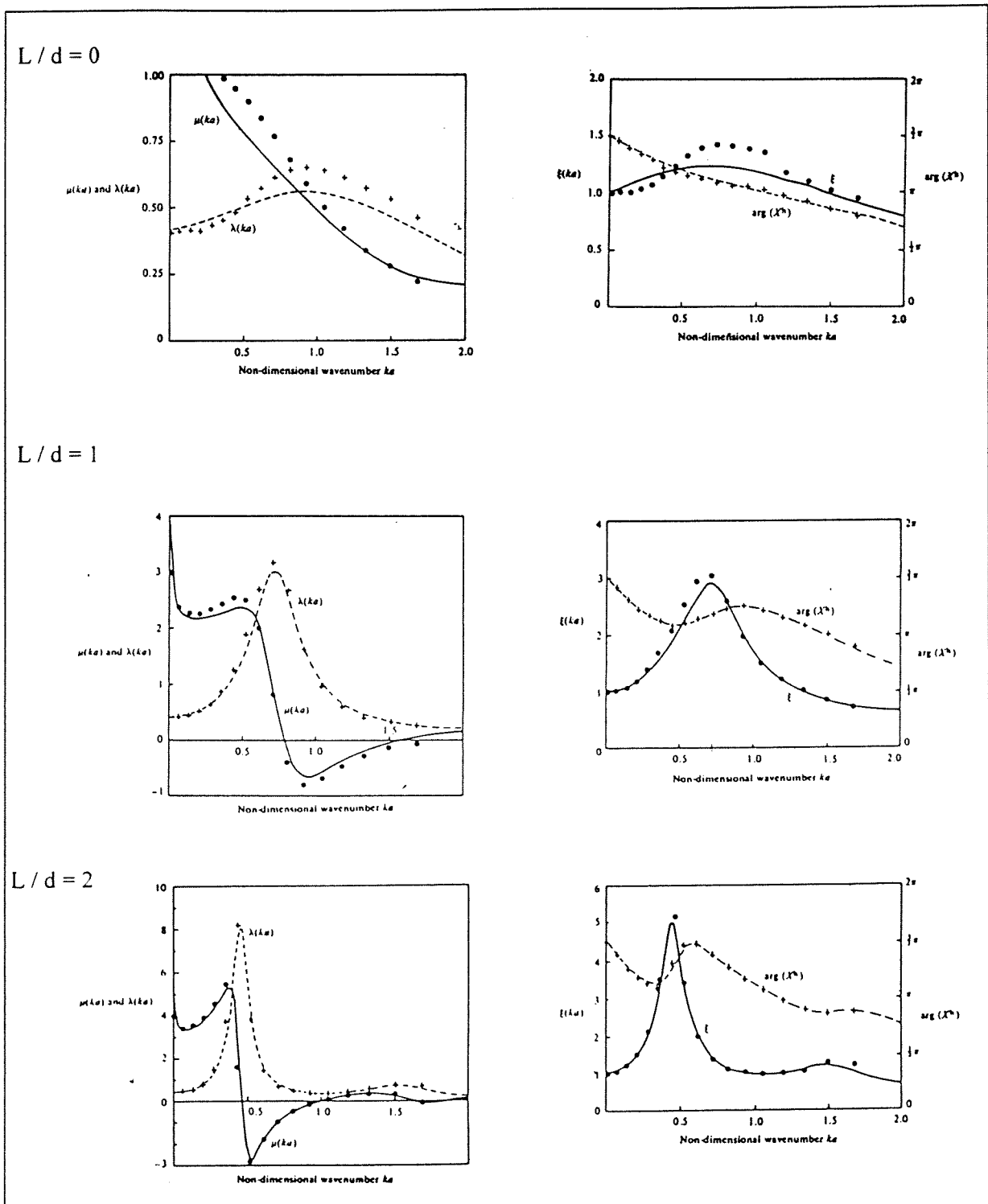


Figure G.9 Variation of μ , λ , ξ and $\arg F^h$ with the dimensionless wave number ka for $L/d = 0, 1, 2$. Solid and dashed lines approximate theory and \bullet , $+$ numerical results

It is clear that the approximate theory is in agreement with the numerical results over the entire frequency range of interest. The effect of increasing the 'harbour' length is to produce a narrower, more peaked damping coefficient λ as a function of frequency, while the added mass coefficient μ displays more rapid variations and an increasing number of zeros.

Note also that the behaviour of λ and μ is in agreement with the results of Malmo and Reitan for radiation resistance and added mass given in Figure G.2 and G.3.

A realistic device has a natural resonance when $S \neq 0$. S can be determined in the next way:

$$S = 2 \cdot a \cdot \rho \cdot g \cdot d \quad (G.28)$$

$$= M \cdot g / h \text{ [N/m]} \quad (G.29)$$

with $2a, d, h$ = width, length and height of the oscillating water column [m]

This value of S provides a first resonant frequency at the lowest ω . This can be seen from $Z = B - i\omega(M + M_a - S/\omega^2)$ satisfying:

$$\omega^2 \cdot h / g = (1 + \mu)^{-1} \quad (G.30)$$

with μ = non-dimensionalised added mass [-]

As can be seen from (G.16), maximum capture width is obtained at complete matching if $\Lambda = Z^h$, when the power take-off is real and positive. In this case $\text{Im } Z^h = 0$ and (G.30) is satisfied. The optimal capture width is then:

$$(w_{\text{cap}}/2a)'_{\text{max}} = \frac{(1 - e^{-2ka})^{-1} \cdot 2B^h}{(Z^h + B^h)} \quad (G.31)$$

This expression is shown in Figure G.10 as a function of ka for different values of L/d . Also the upper limit $(1 - e^{-2ka})^{-1}$ is shown. The addition of side walls increases the peak performance and shifts it to the lower end of the frequency range. When the 'harbour' becomes longer, more peaks approach the upper limit. Both of these effects can be explained in terms of modifications of μ and λ as L/d increases. It is of interest to note that the curve of $L/d = 1$ is close to the upper limit of performance over a wide range of frequency. This is achieved by using a linear real turbine characteristic, optimal chosen at every frequency (called $C_{t,\text{opt}}$ in Part I), but avoiding the need for sophisticated control mechanism involving the complex values of Λ (phase control).

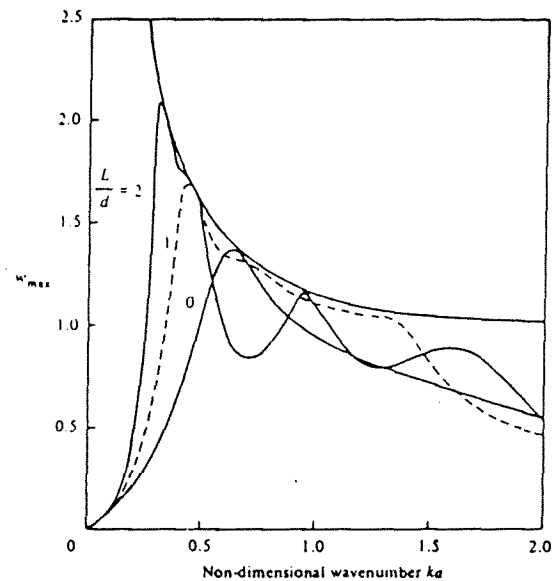


Figure G.10 Capture width ratios, using an optimised real damping constant

Part III Conclusions

The results of the theory of Malmo, Reitan (Part I) and Count, Evans (Part II) agree quite well. However, it must be noted that the first theory is of a two-dimensional device, while the second is of a three-dimensional device. The behaviour of the non-dimensionalised added mass and added radiation coefficient μ and λ shown in Figure G.9 is the same as the behaviour of the added mass and radiation of Figure G.3 and G.2.

The resonance frequency of the 'harbour' type device of which the 'chamber' length equals the 'harbour' length, can be compared for the two theories. The low resonance frequency belongs to the device resonance, the high resonance belongs to the 'harbour' resonance. In Figure G.4 the resonance frequencies are $f = 0.45$ Hz and 0.75 Hz, which means a wave length of 5.4 m and 2.6 m. In Figure G.10 the resonance frequencies are $ka = 0.47$ and 1.33, which means a wave length of 13.4 m and 4.7 m. Resonance frequencies of the 'harbour' type device with $L/d = 1$ are:

	device resonance: L/λ	'harbour' resonance: L/λ
Part I Malmo,Reitan	0.20	0.20
Part II Count,Evans	0.18	0.25

All resonance frequencies can be seen as a quarter-wave resonance. The differences between the theories can be caused by the differences in geometry of the two considered devices. The device of Part I has an immersion depth of the front wall, which is zero in Part II, see Figure G.1, G.7.

A linear optimal turbine characteristic $C_{t,opt}$ (frequency dependent) gives a broad resonance frequency range, in this way no phase control is needed, however a variable geometry of turbine is required (Figure G.6; G.10).

When a fixed turbine constant is used, the reduction of the captured wave power is not dramatic (Figure G.6). For a real sea state with a given wave spectrum, there exist an optimal value of C_t . The determination of this value is influenced by hydrodynamic losses, desired amplitude of the OWC, the efficiency of the turbine and generator and the extra costs of the turbine (in general, the larger the turbine constant, the more expensive the turbine).

It is shown that the addition of side walls to an OWC can improve the performance markedly. The peak performance is increased and shifted to the lower wave frequencies. This last result is appreciated, because waves with longer periods have in general more energy (Figure G.10). When the 'harbour' length equals the OWC length ($L/d = 1$), then the performance is close to the upper limit of complete impedance matching over a broad bandwidth (Figure G.4; G.10).

References

- Ambli, N.; Bønke, K.; Malmo, O.(1982); *The Kværner multiresonant OWC*; Proceedings of The 2nd International Symposium on Wave Energy Utilization, The Norwegian Institute of Technology, Trondheim, Norway
- Count, B.M.; Evans, D.V.(1984); *The influence of projecting sidewalls on the hydrodynamic performance of wave-energy devices*; Journal of Fluid Mechanics, Vol. 145, pp. 361-376
- Evans, D.V.(1982); *Wave-power absorption within a resonant harbour*; Proceedings of The 2nd International Symposium on Wave Energy Utilization, The Norwegian Institute of Technology, Trondheim, Norway
- Evans, D.V.(1985); *The Hydrodynamic Efficiency of Wave-Energy Devices*; Hydrodynamics of Ocean Wave-Energy Utilization, Iutam Symposium Lisbon, Portugal
- Malmo, O.; Reitan, A.(1985); *Development of the Kvaerner Multiresonant OWC*, Hydrodynamics of Ocean Wave-Energy Utilization, Iutam Symposium Lisbon, Portugal

Appendix H Theory of a Harbour Type OWC in a Reflecting Wall

In this Appendix the theory of a 'harbour' type OWC in a reflecting wall is described. In Part I, a single device symmetrically placed in a channel or equivalently an infinite row of identical and equidistant devices is considered. The waves approaching the device are normally incident. The next investigation is a single device placed in an infinitely wide wall and an infinite sea with waves of different angles of incidence, given in Part II. The intermediate case of a finite row of devices in an infinitely reflecting wall is handled in Part III and IV. Part I to III originate from articles of Malmo and Reitan, Part IV comes from an article of McIver and Evans. In Part V conclusions are drawn.

Part I Single Device in a Reflecting Wall placed in a Channel

Introduction

Malmo and Reitan derived an oscillating pressure theory for the 'harbour' type device in a reflecting wall. A single device symmetrically placed in a channel or equivalently an infinite row of identical and equidistant devices was concerned. The waves approaching the device are harmonic and normally incident [Malmo, Reitan;1985].

The idealised system considered, is shown in Figure H.1. The air chamber has a length a , width b and height H above the water surface. The 'harbour' has a length l , width b and is separated from the air chamber by a thin barrier of depth d . The device is placed symmetrically in a channel of width c . The regions at the sides of the 'harbour' are (1) open, (2) an absorbing beach or (3) a reflecting wall. The water has a depth of h .

Three important parameters have to be known to calculate the wave power absorption:

- (1) the volume flux through the surface of the chamber when it is open (without roof and turbine)
- (2) admittance of the system, which is a measure of the volume flux through the chamber surface caused by an imposed harmonic chamber pressure
- (3) the turbine characteristic, the volume flux of air divided by the driving pressure

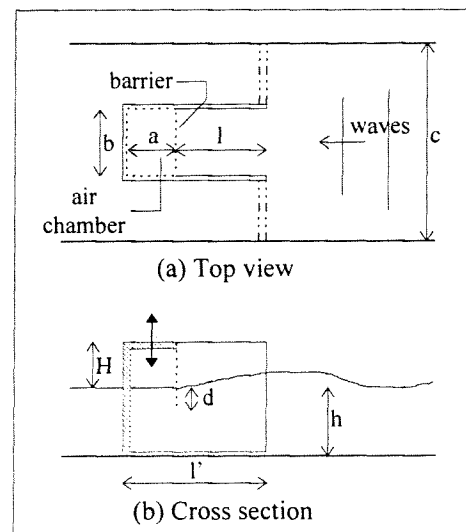


Figure H.1 'Harbour' type device in a channel

Theory

It is convenient to work with the mean wave amplitude in the chamber rather than the corresponding volume fluxes. An incoming wave with amplitude η_0 , produces a wave in the chamber with amplitude η_c . The next ratio can be given:

$$\xi_c = \eta_c / \eta_0 \quad (\text{H.1})$$

$$= \xi_0 \cdot \Lambda (\Lambda + Z)^{-1} \quad (\text{H.2})$$

with

$$\begin{aligned} \xi_c &= \text{wave amplitude ratio [-]} \\ \eta_c &= \text{amplitude of chamber wave [m]} \\ \eta_0 &= \text{amplitude of incoming wave (1/2 wave height) [m]} \\ \xi_0 &= \text{the value of } \xi_c \text{ when the chamber is open [-]} \\ Z &= \text{admittance of the device } (Z = B + i\omega A, \text{ see Appendix F) [m}^3\text{s}^{-1}\text{/Pa]} \\ \Lambda &= \text{effective turbine characteristic (compressible air) [m}^3\text{s}^{-1}\text{/Pa]} \\ &= C_t + i\omega V_c / \gamma p_0 \end{aligned} \quad (\text{H.3})$$

with C_t = turbine characteristic [$\text{m}^3 \text{s}^{-1} / \text{Pa}$]
 γ = specific heat ratio [-]
 p_0 = atmospheric pressure [Pa]
 V_c = chamber volume [m^3]
= $A_c \cdot H$
 A_c = surface area of the chamber [m^2]
= $a \cdot b$
 H = chamber height [m]

Another used parameter is the pressure ratio π_c , which is the pressure divided by the wave amplitude:

$$\pi_c = p_c / \eta_0 \quad (\text{H.4})$$

$$= i \cdot \omega \cdot A_c \cdot \xi_0 \cdot (\Lambda + Z)^{-1} \quad (\text{H.5})$$

with π_c = pressure ratio [Pa/m]
 p_c = pressure in the chamber [Pa]
 ω = angular frequency [s^{-1}]

This pressure ratio has in a closed chamber, with $C_t = 0$ the value π_1 :

$$\pi_1 = i \cdot \omega \cdot A_c \cdot \xi_0 \cdot (Z + i\omega V_c / \gamma p_0)^{-1} \quad (\text{H.6})$$

An infinitely large air chamber is equivalent to an open chamber of finite size, with $C_t \rightarrow \infty$, in both cases $\xi_c \rightarrow \xi_0$ and $\pi_c \rightarrow 0$

The power captured by the system can be written as P_{cap} :

$$P_{\text{cap}} = \frac{1}{4} \cdot A_c \cdot |\eta_0|^2 \{ (i\omega \xi_c) \cdot \pi_c + (i\omega \xi_c) \cdot \overline{\pi_c} \} \quad (\text{H.7})$$

$$= \frac{1}{2} \cdot |\eta_0|^2 \cdot \text{Re}(\Lambda) |\pi_c|^2 \quad (\text{H.8})$$

From this equation can be seen that π_c and thus ξ_0 (H.5) are important measures for wave power absorption performance. Another useful measure is the already introduced capture width ratio $W = w_{\text{cap}} / b$ and $E = w_{\text{cap}} / c$:

$$W = w_{\text{cap}} / b \quad (\text{H.9a})$$

$$= P_{\text{cap}} / (P_w \cdot b) \quad (\text{H.9b})$$

$$E = w_{\text{cap}} / c \quad (\text{H.10a})$$

$$= P_{\text{cap}} / (P_w \cdot c) \quad (\text{H.10b})$$

with w_{cap} = capture width [m]
 b = width of the device [m]
 c = width of the channel [m]
 P = power captured by the device [W]
 P_w = wave power per unit width [W/m]

$$= |\eta_0|^2 \cdot \frac{g^2 \rho}{4\omega} \left\{ 1 + \frac{2kh}{\sinh(2kh)} \right\} \tanh(kh) \quad (\text{H.13a})$$

$$= |\eta_0|^2 \cdot \frac{g^2 \rho}{4\omega} \cdot f(kh) \quad (\text{H.13b})$$

The maximum capture with ratio occurs when $\Lambda = Z$, implying a phase lag between the flux through the turbine and the driving pressure. For this performance phase control is required.

$$W_{\text{max}} = \frac{1}{(2g^2 \rho)} \left(\frac{A_c^2 \omega^3}{b} \frac{\xi_0^2}{B} \right) \cdot f(kh)^{-1} \quad (\text{H.14})$$

with g = gravitational acceleration [m/s^2]
 ρ = density of water [kg/m^3]
 B = radiation resistance, real part of the admittance [$m^3 s^{-1}/Pa$]

When the turbine characteristic is real, no such phase lag exists ($\Lambda = Z$). The maximum capture width ratio is in that case is W'_{max} . The ratio between the maximum capture width, without and with phase control is:

$$\frac{W'_{max}}{W_{max}} = 4BC_{t,opt} \left\{ (C_{t,opt} + B)^2 + \omega^2 \{A + V_c / (\gamma p_0)\}^2 \right\}^{-1} \quad (H.15)$$

with A = hydrodynamic resistance, imaginary part of the admittance [m^3/Pa]
 B = real part of the admittance [$m^3 s^{-1}/Pa$]
 $C_{t,opt}$ = optimal turbine characteristic, frequency dependent [$m^3 s^{-1}/Pa$]
 $= [B^2 + \omega^2 \{(A + V_c / (\gamma p_0))\}^2]^{1/2}$ (H.16)

W_{max} and W'_{max} coincide at frequencies for which $A + V_c / (\gamma p_0) = 0$

Method of matching the velocity potentials

To calculate the parameter ξ_0 , the wave amplitude in the open chamber has to be known. The system is subjected to incident waves, travelling to the open end of the 'harbour' and from there to the chamber. On their way the amplitude of the waves will be changed.

The velocity potential in the various regions of the system can be expressed in terms of vertical and horizontal eigenmodes, consistent with the boundary conditions on the solid walls and on the surface and the bottom of the water. The following regions can be discerned, namely (1) the region in front of the device (incident wave), (2) the regions beside each side (3) the region back of the device (in the case when the side regions are accessible) (4) the internal region of the device called the 'harbour' and (5) the chamber. The various amplitudes in the regions are interrelated by the matching conditions for the velocity potential and its derivative with respect to x at the boundaries of the various regions.

Results

Influence of different side regions

As a first result Figure H.2 is shown. A comparison is made of the different conditions of the side regions of a device with an open chamber (ξ_0). In the case of a reflecting wall the device has its best performance. When the side regions are open or consist of an absorbing beach the highest value of ξ_0 is almost the same as in the case of the wall, but the peak is much narrower. When the sides are open the influence of waves travelling from behind ($x = -$) and towards the device ($x = +$) is also shown. It can be seen that, when waves travel to the closed end of the device, the value of ξ_0 is smallest. The main peak can roughly be interpreted as a quarter-wave resonance of the total length of the device $l' = l + a$.

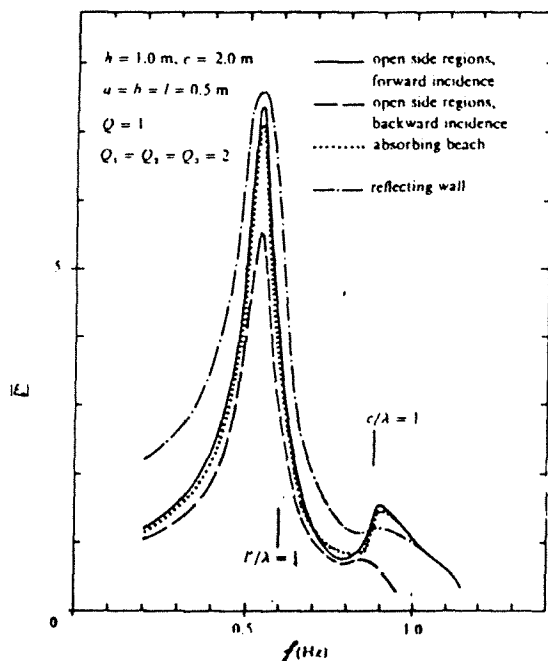


Figure H.2 Average chamber wave amplification, versus frequency

Quarter-wave resonance of the 'harbour'

When the chamber is closed, the pressure ratio $|\pi_1|$ gives an indication of the performance. The model has the same geometry as in the case of figure H.2. The quarter-wave resonance in the 'harbour' manifests itself as a pressure resonance in the chamber. In this case the frequency where $l = \frac{1}{4} \lambda$ coincides with that where $c = \lambda$. Other results show that pressure resonance is mainly caused by the quarter-wave resonance of the 'harbour' when $l = (2n-1) \cdot \frac{1}{4} \lambda$.

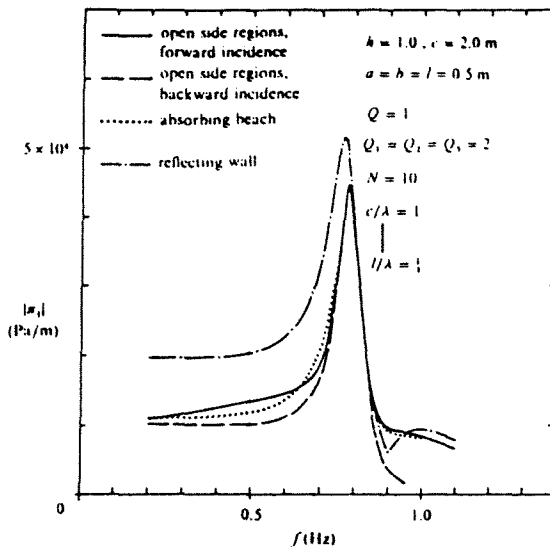


Figure H.3 Closed-chamber pressure ratio versus frequency

Wave length equals channel width

The efficiency E_{\max} (complete impedance matching of Z , complex turbine characteristic) is shown in Figure H.3. The maximum efficiency for the reflecting wall is 100%, the efficiencies of the other configurations are lower. It is noteworthy, to know that $c = 2$ m and $b = 0.5$ m. When the efficiency E_{\max} is higher than 50%, the capture width is still higher than the device width.

An abrupt change in performance exists at the frequency, when the wave length equals the channel width $\lambda = c$. This means that for an infinite row of absorbers with a distance between them of $c = \lambda$ the efficiency will decrease.

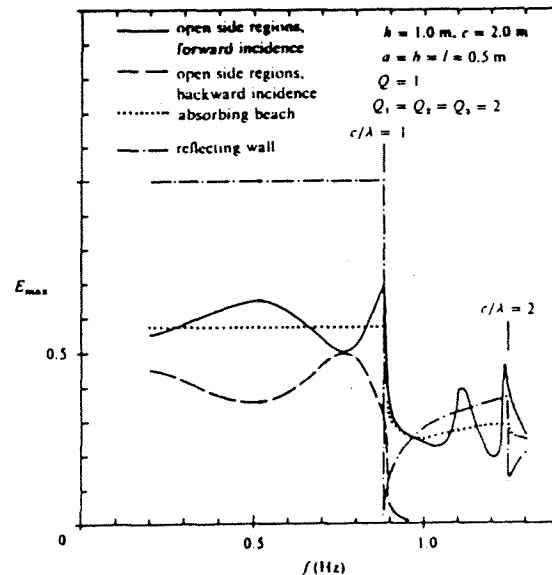


Figure H.4 Variation of E_{\max} for different configurations of the device

Influence of harbour length and width

The efficiency E' (when the turbine characteristic is real) depends on the separate lengths of the chamber and the 'harbour'. These lengths influence the imaginary part of the admittance, B . Figure H.5 shows the variation of E' of a device in a reflecting wall. Four examples are given. Three devices with different 'harbour' lengths (0, 0.5, and 1.0 m) and an optimal real turbine characteristic, giving E'_{\max} and one device with a 'harbour' length of 0.5 m and a fixed turbine constant.

In Figure H.6 the influence on E'_{\max} of the width b of a device without 'harbour' is given. The channel width in this example is 1.0 m.

Note that Figure H.5 shows the same as Figure G.10. The longer the 'harbour' length, the higher the efficiency and the peak performance is shifted to the lower wave frequencies. However, the increase in efficiency in Figure H.5 is limited by the channel width.

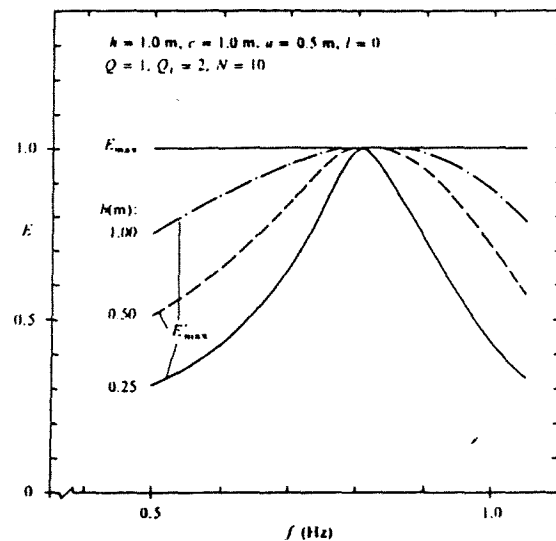
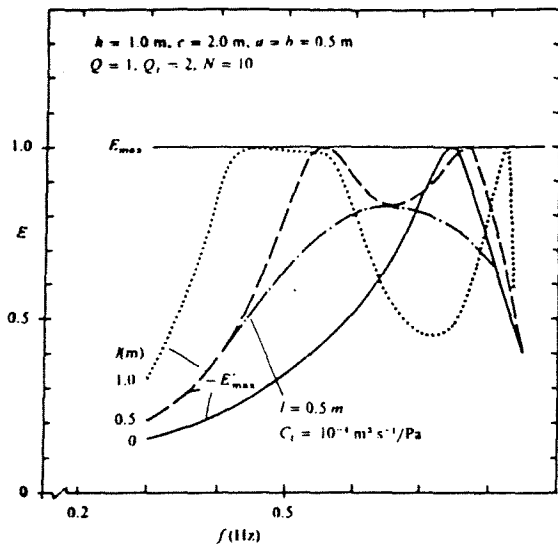


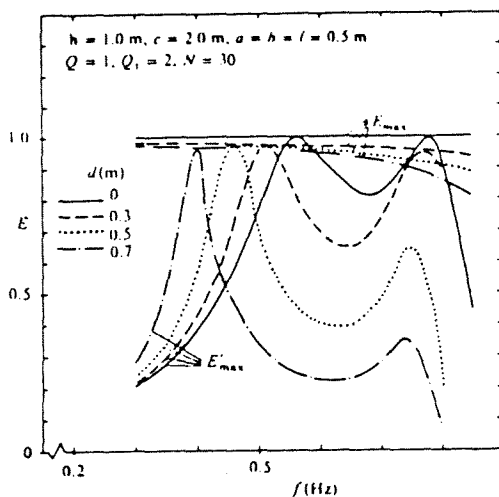
Figure H.5 Variation of E' for different 'harbour' lengths, versus frequency

Figure H.6 Variation of E' for different widths of the device, versus frequency

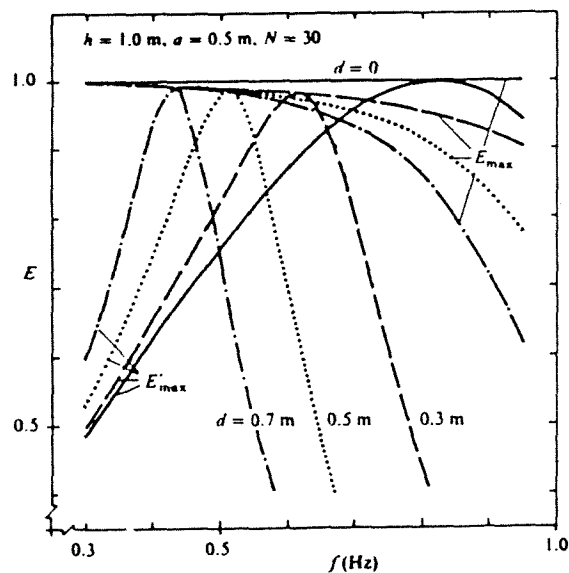
Influence of barrier depth

All the results up to here are derived for a device of which the depth of the barrier between the harbour and the chamber is zero. However, in practise the barrier should remain submerged during the operation of power absorption, thus the depth depends on the expected wave heights. The influence of the depth d of this barrier is shown in the next Figures H.7 a, b and c.

E'_{\max} depends more weakly on the barrier depth than might be expected from the behaviour of $|\xi_0|$. This is because the real part of the admittance depends in a similar way on d . However, when the air flux is in phase with the driving pressure (turbine characteristic is real) the value of E'_{\max} depends quite strongly on d . Generally speaking, an increase in barrier depth makes the E'_{\max} curve narrower and pushes the peak towards lower frequencies.

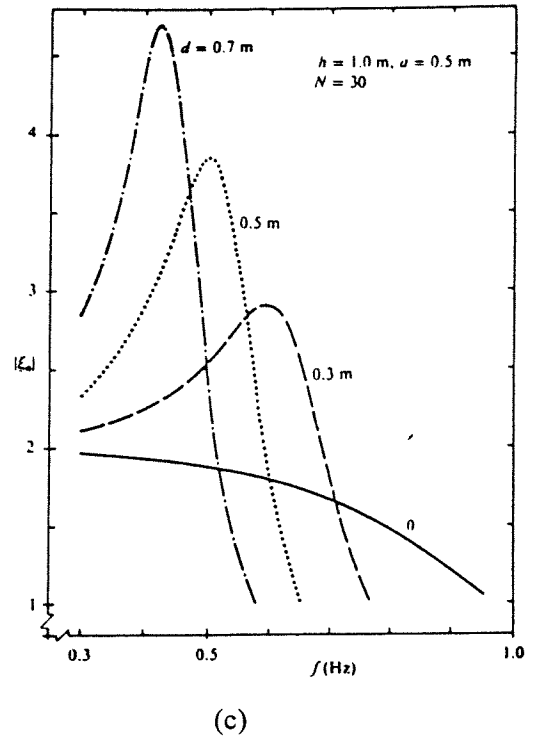


(a)



(b)

Figure H.7 Influence of the depth of the barrier versus frequency;
 (a) variation of E ;
 (b) variation of E for $b = c$;
 (c) variation of ratio ξ_0



Part II Single Device in a Reflecting Wall placed in an Infinite Sea

Introduction

The next investigation was a single device placed in an infinitely wide wall and an infinite sea with waves of different angles of incidence [Malmo,Reitan;1986,a]. The geometry of the device is the same as in Part I.

In the same manner as in Part I, the velocity potentials are expanded in terms of transverse and vertical modes satisfying the boundary conditions.

The same parameters as in Part I are investigated, namely ξ_0 , the ratio between the average wave amplitude in the open chamber and the amplitude of the incoming wave, the admittance Z and the capture width ratio between the capture width and the width of the device $w_{cap} / b = P_{cap} / (P_w \cdot b)$.

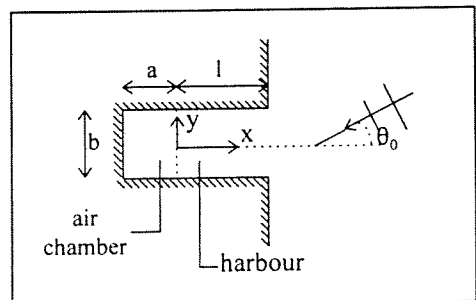


Figure H.8 Harbour type device in a reflecting wall

Results

The quarter-wave resonance

An interesting result is the pressure ratio π_1 of the device in open sea, shown in Figure H.9. This result can be compared with Figure H.3 for the case that the device is placed in a channel. When the device is placed in open sea the pressure resonances are quite far from the quarter-wave and three-quarter-wave frequencies. This is due partly to the radiation term B of the admittance and partly to the number of vertical modes.

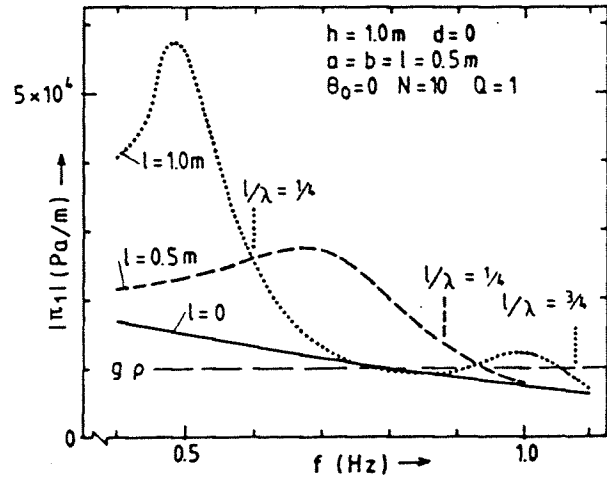


Figure H.9 Pressure ratio π_1 versus frequency for various 'harbour' lengths

Number of transverse modes

The contribution of $q \neq 0$ transverse modes is considered. When the angle of incidence is not zero, inside of the device the wave pattern will be complicated by anti-symmetric transverse modes. Only at frequencies above $b / \lambda = 1$ these complications have reasonable influence on the performance. Consequently, from the practical point of view, the $q \neq 0$ transverse modes complications can be disregarded, since the width of the absorber will be much less than the wave length of the peak of the incoming wave spectrum.

Influence of harbour length

By comparing W_{\max} and W'_{\max} for different 'harbour' lengths can be seen how a suitable size of the harbour serves to bring W'_{\max} close to W_{\max} over a sizeable range of frequencies. In Figure H.10 this is shown for 'harbour' lengths of $l = 0$ and $l = 0.5$ m and finite widths b .

Turbine constant

As explained in Part I, for W'_{\max} the turbine characteristic has to be optimised for every wave frequency. This frequency dependence of $C_{t,\text{opt}}$ is shown in Figure H.11 for $C_{t,\text{opt}}^{-1}$. See also Figure G.5 of Appendix G.

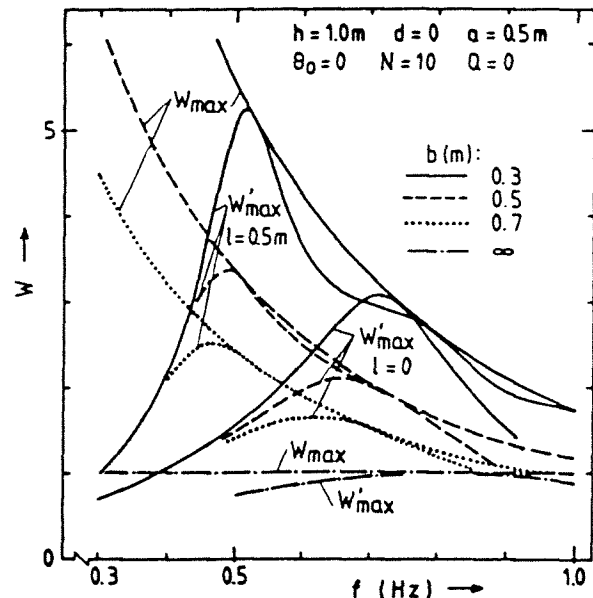


Figure H.10 Capture width ratio versus frequency for various chamber widths and two 'harbour' lengths

Influence of turbine characteristic

In Figure H.12 the capture width ratio of a system without 'harbour' for several chamber lengths is shown. It can be seen that the peaks of the system with constant C_t coincides with the peaks of W'_{max} . Only the bandwidth of the system with constant C_t is somewhat smaller, in particular at the lower-frequency side. It can be concluded that, when the turbine constant is chosen frequency independent at a fixed value C_t the captured power will not be drastically reduced.

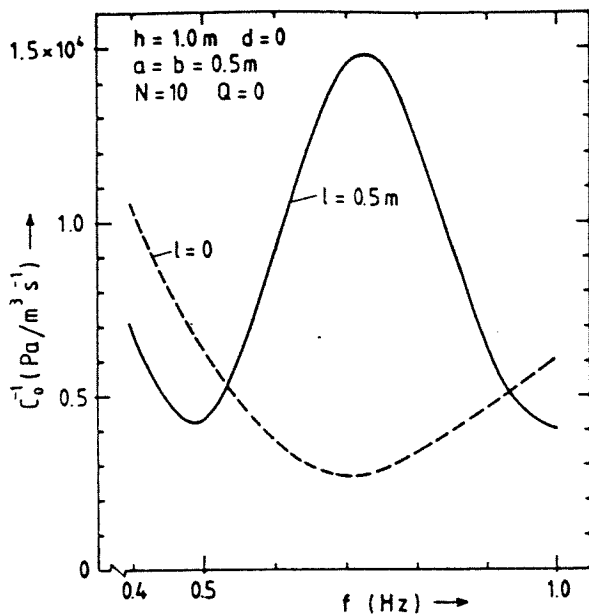


Figure H.11 Inverse turbine characteristic, versus frequency for two 'harbour' lengths

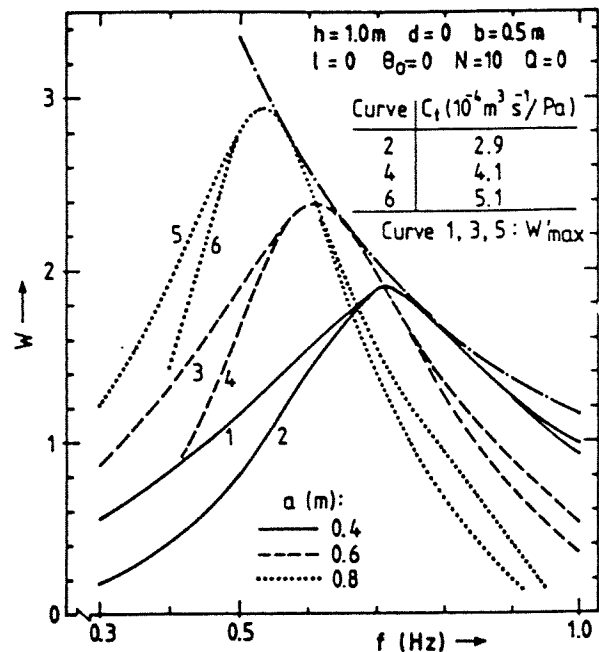


Figure H.12 Capture width ratios, versus frequency for various chamber lengths

Part of the device occupied by the 'harbour'

When a device has a certain chamber length the performance can be influenced by adding a 'harbour'. However, the added 'harbour' does not only broaden the response curve, but also increases the costs of the system (in general the larger the device, the higher the costs).

The influence of the fraction of the device which is occupied by the 'harbour' is a good method of illustrating the possibilities for cost savings by equipping a device with a 'harbour'. This is done by varying the 'harbour' length and keeping the total length constant ($a+l = 1 \text{ m}$), which is the ratio $l / (a+l)$ in Figure H.13. This figure shows that, when a longer 'harbour' is build, a smaller turbine is possible (lower C_t value).

It is concluded that, when construction costs depend on the total length of the device, major savings in turbine costs can be reached if a longer 'harbour' is used instead of a longer chamber.

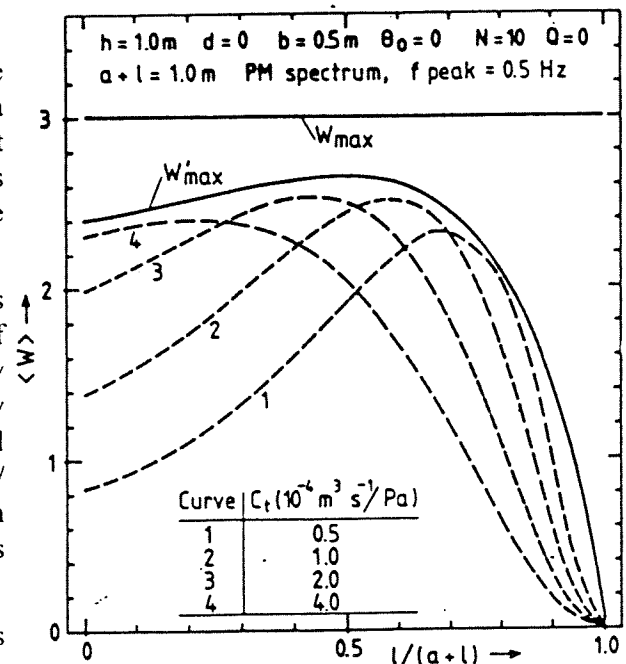


Figure H.13 Average capture width ratios versus the ratio 'harbour' length to total length of the device

Part III Finite Row of Devices in a reflecting wall (Malmo and Reitan)

Introduction

Finally, the case of a finite row of devices in an infinitely reflecting wall is handled. Malmo and Reitan have made an extension of their theory [Malmo,Reitan;1986,b]. It is known, from the theory of oscillating bodies, that by placing the devices in a row one can increase as well as decrease the power absorbed by each of the devices.

A system of various devices which need not to be identical is considered. The device of number s has a width of b_s , 'harbour' length of l_s and a chamber length of a_s . The centre line of the harbour is located at a distance c_s from a chosen axis of reference. The total number of devices is S .

Theory

The theory of a system of several 'harbour' type OWC's in a row can be formulated in much the same way as that of the single device. The volume flux or amplitude ratio and the pressure ratio have to be defined as matrices. The admittance and turbine characteristic must also be written in the form of a matrix.

In this system of S devices the average wave amplification and average pressure ratio follows by:

$$\langle |\xi_0| \rangle = S^{-1} \sum_{s=1}^S \xi_{0,s} \quad (\text{H.17})$$

with $\langle |\xi_0| \rangle$ = average wave amplification [-]

$|\xi_{0,s}|$ = wave amplification of device s [-]

$$\langle |\pi_1| \rangle = S^{-1} \sum_{s=1}^S \pi_{1,s} \quad (\text{H.18})$$

with $\langle |\pi_1| \rangle$ = average pressure ratio [Pa/m]

$|\pi_{1,s}|$ = pressure ratio of device s [Pa/m]

The average capture width of S devices is the total captured power divided by the incoming wave power and the number S :

$$w_{\text{cap}} = P_{\text{cap}} / (P_w \cdot S) \quad (\text{H.19})$$

The corresponding capture width ratio is this capture width divided by the average width of the devices:

$$W_{\text{cap}} = w_{\text{cap}} / \langle b \rangle \quad (\text{H.20})$$

$$= P_{\text{cap}} / (P_w \cdot \sum_{s=1}^S b_s) \quad (\text{H.21})$$

with W_{cap} = capture width to device width ratio [-]

$\langle b \rangle$ = average device width [m]

P_{cap} = captured wave power [W]

P_w = incoming wave power [W/m]

b_s = width of device s [m]

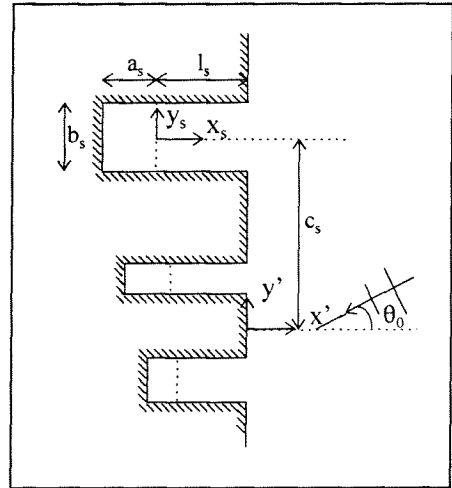


Figure H.14 Devices in an infinite reflecting wall in an infinite sea

A new parameter is introduced, the power amplification factor:

$$I_p = W_{S, \text{cap}, \text{max}} / W_{1, \text{cap}, \text{max}} \quad (\text{H.22})$$

with $W_{S, \text{cap}, \text{max}}$ = maximum capture width ratio of S devices [-]

$W_{1, \text{cap}, \text{max}}$ = maximum capture width ratio of a single device [-]

When the capture with ratio of S devices is optimised by admittance matching $\Lambda = \bar{Z}$ the turbine matrix Λ requires a coupling between the turbines of the various devices and in general a phase lag between the chamber pressure and air flow in each device (phase control).

In the case that the devices are identical the admittance matrix is the same and when there is no mutual influence of the admittance, the optimum real turbine constant is the same as in the case of the single device $C_{t, \text{opt}} = [B^2 + \omega^2(A + V_c / (\gamma p_0))^2]^{1/2}$.

In practise the turbines may be not coupled and will have the same real value C_t . However, for the system of more than one device it seems impossible to find an explicit expression for the common real value of C_t which optimises the absorbed power. Numerical methods are needed to find the optimal value of C_t .

Results

The numerical examples which are considered have identical devices and are equidistant. For that case follows: $a_s = a$, $b_s = b$, $l_s = l$ and $c_{s+1} - c_s = c$.

Wave amplification and pressure ratio

As in the other parts the wave amplification and pressure ratio are shown in Figure H.15 and H.16. The influence of the number S of devices is noticeable particularly in the pressure curve, showing that the 'harbour' resonance becomes more prominent as S increases. The peak of the amplitude ratio (device resonance) only shifts over a small distance to the lower frequencies.

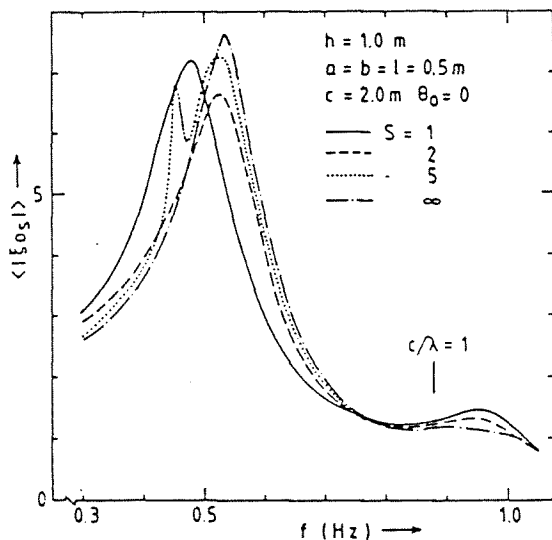


Figure H.15 Average wave amplification versus frequency

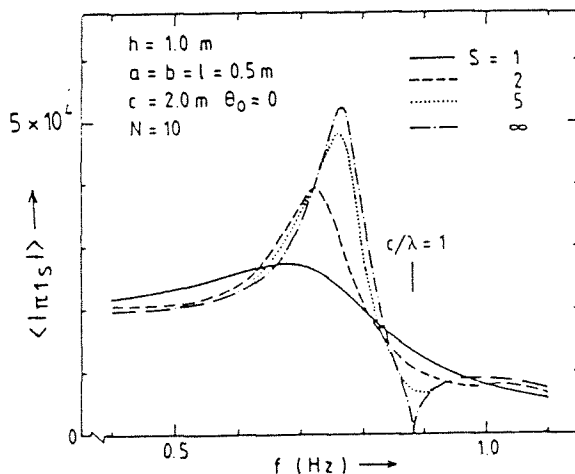


Figure H.16 Average pressure ratio versus frequency

Capture width ratio and power amplification

The optimum average capture width ratio is shown in figure H.17. It can be seen that over a major part of the frequency considered here, a device in a row has on the average the ability to capture more power than a single device. In this case the power amplification I_p is larger than unity. This effect is quite noticeable even for a system of two devices. In Figure H.18 the frequency is kept constant and

the power amplification factor I_p is shown as a function of c/λ . It is clear that, when the number of devices increases, the behaviour of I_p changes from the fairly smooth oscillations at $S = 2$ to the saw-tooth variation of $S = \infty$.

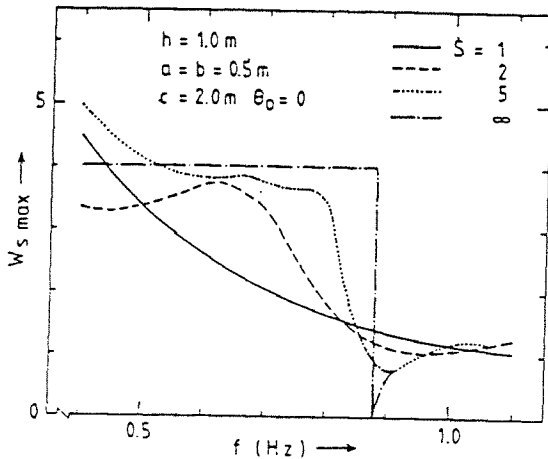


Figure H.17 Optimum capture width ratio versus frequency

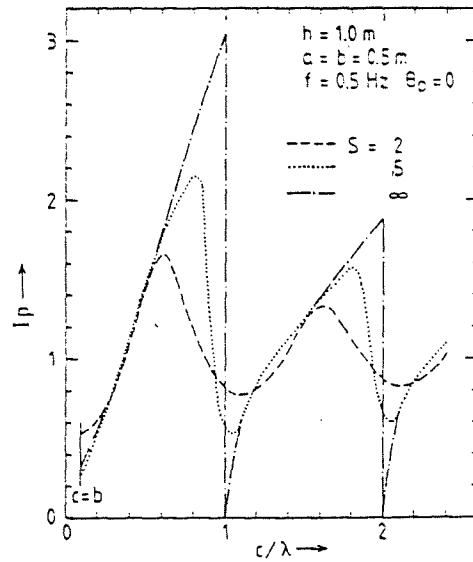


Figure H.18 Power amplification versus the ratio c/λ

From Figure H.18 can be concluded that the spacing must be chosen not too close to the maximum power amplification, because it decreases very fast at the right side of this maximum, on particular for systems of a lot of devices. In practise the spacing must be chosen dependent on the local wave spectrum with the power amplification value higher than $I_p = 1$.

Capture width ratio

The capture width ratios of a system consisting of two devices are calculated at complete matching ($W_{2,max}$) and when the turbine characteristics are real, frequency dependent, ($W'_{2,max}$). This is shown for a fixed frequency ($f = 0.5$ Hz or $\lambda = 5.2$ m) and a varying distance c between the devices. Since for devices with a certain geometry (width b , chamber length a) the resulting $W'_{2,max}$ also depends on the 'harbour' length l , it is possible to show the usefulness of adding a harbour. Figure H.19 illustrates that choosing the 'harbour' length wisely the curve of $W'_{2,max}$ follows the theoretical optimum of $W_{2,max}$. Although, the 'harbour' length for which this is achieved is frequency dependent, the effectiveness of the harbour survives to a large extent also in a realistic wave spectrum.

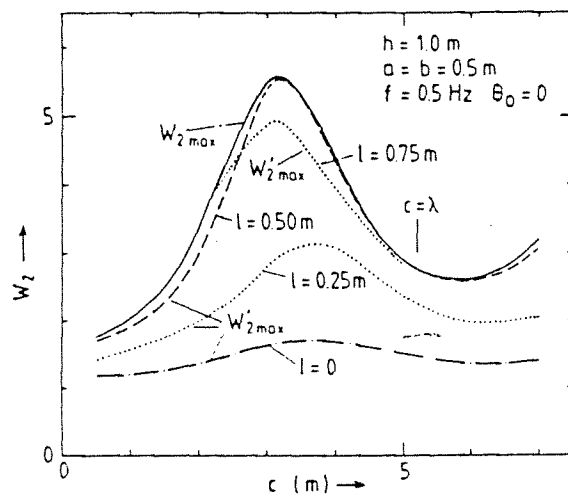


Figure H.19 Optimum capture width ratios for two devices versus distance between them

Part IV Finite Row of Devices in a Reflecting Wall (McIver and Evans)

Introduction

McIver and Evans have also investigated the case of a number of devices in a reflecting wall. They also use the method of matching the velocity potentials. However, they do not use the theory of an oscillating pressure distribution, instead of this, they represent the oscillating water column by a rigid body oscillating in the x-direction (oscillating on the boundary between the chamber and the 'harbour'). In this way the power absorption can be calculated by the theory of oscillating bodies (Appendix B and G) [McIver, Evans; 1988].

The geometry of the device is the same as in the other three parts. The width of the 'harbour' and chamber is called $2a$. The length of the 'harbour' is l and the length of the chamber is a . All devices are identical and equally spaced by a distance d .

Results

The results are mainly the same as in the other parts. Because of the fact that the device is modelled as an oscillating body in the horizontal direction below the front wall, some values differ slightly to the results of Part III.

Influence of harbour length

Figure H.20. shows the capture width ratio of the device for different 'harbour' lengths with an optimal real load damping. The maximum capture width of a device operating in the sway mode is $\lambda / 2\pi$, this is shown as $(ka)^{-1}$ (compare to equation G.15 and Figure G.10).

The figure shows that adding a 'harbour', shifts the peak capture width ratios to longer wave lengths, thereby opening up the possibility of building smaller chambers. For $l/a = 2$ the curve has a high maximum but a small band width. Reducing the length of the 'harbour' produces an increase in bandwidth, but at the expensive of a reduced peak performance.

In Figure G.10 of **Appendix G**, the upper limit $(1 - e^{-2ka})^{-1}$ of the same device in open sea, is shown. It can be seen that, when the device is placed in a reflecting wall the upper limit is $(ka)^{-1}$, which indicates that the device in the wall has a somewhat better performance.

Spacing

A more interesting factor which is investigated is the spacing between the devices. This has been done in a similar way as in the oscillating body theory with the point absorber results.

$$w_{\text{cap. max}} = \frac{P_{\text{cap. max}}}{P_w} \quad (\text{H.23})$$

$$= \frac{2}{k} \cdot N \cdot q(\beta) \quad (\text{H.24})$$

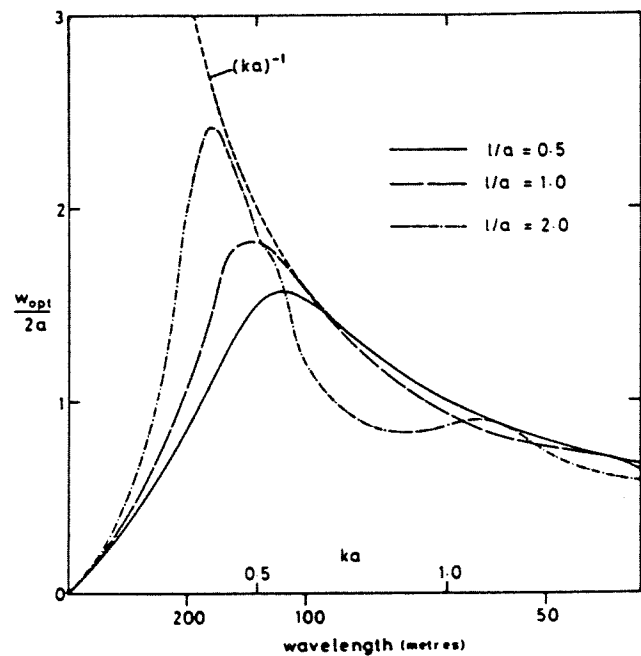


Figure H.20 Optimum capture width of a single device ($a = h = 10 \text{ m}$)

The quantity $2/k (= \lambda/\pi)$ is just the maximum capture length of the device. The factor $q(\beta)$ represents the mean gain factor for each device of the row of N devices, compared with the capture width of a single device. This factor depends among other things on the angle of incidence.

$$q(\beta) = \frac{1}{N} \cdot \bar{L} \cdot J^{-1} \cdot L \quad (\text{H.25})$$

with N = number of devices in the reflecting wall [-] (H.26)

L = $\exp\{-i \cdot k \cdot d \cdot \sin(\beta)\}$ [-]

\bar{L} = conjugated L [-]

J = $J_0 \cdot (k \cdot d)$ [-] (H.27)

J_0 = zero-order Bessel function of the first kind

It is noteworthy, that in this approximation the capture width and also the maximum absorbed power, depend on the position of the devices (spacing), the angle of incidence and the frequency of the incident waves. This means that there is no dependence on the chamber or 'harbour' characteristics.

For the case that the angle of incidence is normal to the wall, the q -factor is shown in Figure H.21. The oscillatory behaviour is clear. In this case, the spacing is selected in that way that the first maximum in q corresponds to a wave length of about 150 m. With the spacing determined in this way the q -factor is given for systems of two, three and four devices.

The values of d/L ($N = 2, 3, 4$; $d/L = 0.61, 0.71, 0.77$) agree well with the values of Figure H.18 of the power amplification. For two, five and infinite devices the values of d/λ , at which the power amplification is maximal, are 0.6, 0.8 and 1.

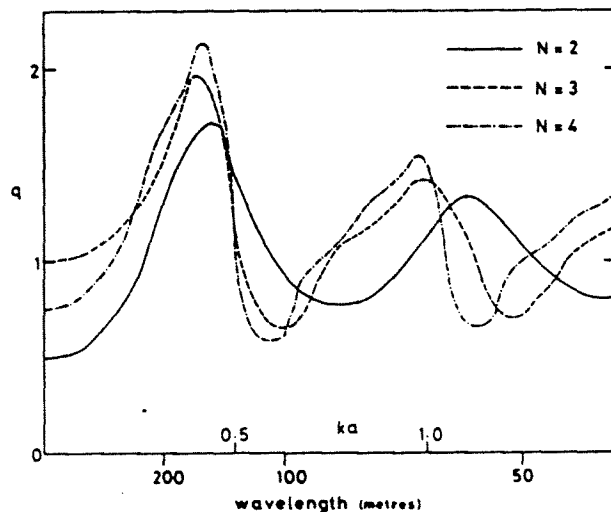


Figure H.21 The q -factor for a system of 2, 3 and 4 devices ($d/a = 9.148$, $d/a = 10.596$, $d/a = 11.475$, $a = h = 10\text{m}$)

As known from the other results (Fig. G.6 and H.12), when the damping is real and fixed (no phase difference, frequency independent) the capture width can be close to the optimum capture width of real damping $C_{t,opt}$ (frequency dependent). This can be achieved when the value of the real constant is chosen roughly the same as the value which is required when the device operates at peak performance at optimal damping.

In Figure H.22 the capture width is shown for a system of a single device, two and four devices. The damping is real constant and the spacing is optimal chosen for a wave length of 150 m.

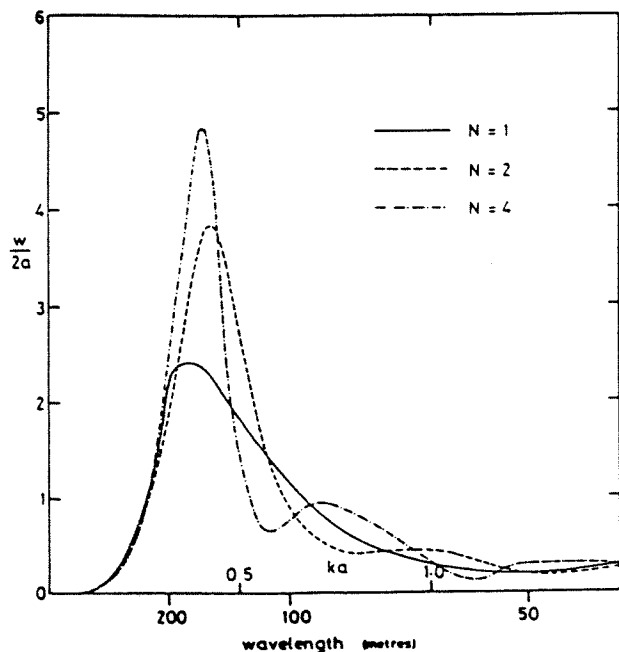


Figure H.22 Capture width for a system of 1, 2 and 4 devices ($a = h = 10$ m)

Angle of incidence

Finally, the effect of the angle of wave incidence on the system performance is considered. Results are given in Figure H.23 and H.24 for a system of two and four devices. The spacing is selected to give the best performance in beam seas ($\beta = 0$). This means that the curves for oblique incidence are probably not the best obtainable. There is a fall-off in the capture width for obliquely incident waves, but a substantial amount of power is still available to the devices.

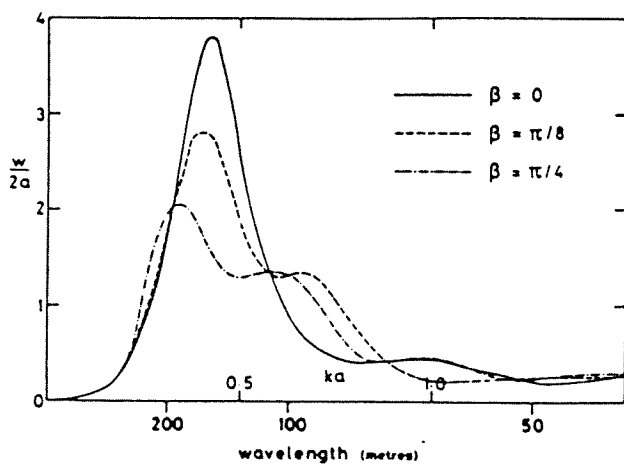


Figure H.23 Capture width for a system of two devices for various angles β ($l/a = 2$, $a = h = 10$ m)

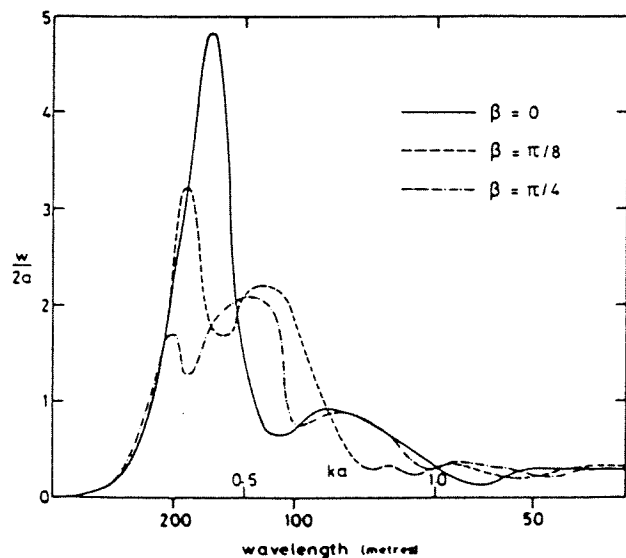


Figure H.24 Capture width for a system of four devices for various angles β ($l/a = 2$, $a = h = 10$ m)

From the results of comparison the performance of various number of devices can be concluded that there are clear advantages in building devices together rather than singly.

Part V Conclusions

The performance of the 'harbour' type OWC in a reflecting wall has a better performance than in open sea. When the device is placed in an absorbing beach, the peak performance at device resonance is not much lower, however, the peak is much narrower, see Figure H.2. Also the peak performance at 'harbour' resonance has for a device in a reflecting wall higher values over a broader frequency range, see Figure H.3. Figure H.4 shows the differences of efficiency of the various devices show. The device in an absorbing beach has a lower value of about 40%.

The influence of the depth of the front barrier is shown in Figure 7 a, b and c. Generally speaking, an increase in barrier depth makes the E'_{\max} curve (real optimal turbine characteristic) narrower and pushes the peak towards lower frequencies.

Figure H.12 shows that by using a fixed turbine constant, only the bandwidth of the performance is somewhat smaller, in particular at the lower-frequency side. It can be concluded that, when the turbine constant is chosen frequency independent at a fixed value C_t , the captured power will not be drastically reduced.

When construction costs depend on the total length of the device, major savings in turbine costs may be achieved if one invests in a 'harbour' rather than in a longer chamber. This is shown by Figure H.13.

Part III and IV show that placing more devices in a reflecting wall at a well selected distance from each other, can increase the captured power considerably, see Figure H.17, H.18 and H.22. Even when the waves are not normally incident, the captured power can be increased by placing more devices in a row, see Figure H.23 and H.24.

The spacing between the devices must be selected carefully. McIver and Evans say that this spacing can be chosen without reference to the characteristic of the device [McIver, Evans;1988]. However, Malmo and Reitan show that for instance the length of the 'harbour' affects slightly the spacing, see Figure H.19. This figure shows that the spacing for a system of two devices must be $0.6 - 0.7 \lambda$, dependent on the 'harbour' length.

The selection of the appropriate spacing depends strongly on the number of devices, see Figure H.18 and H.21. Figure H.18 shows that the spacing must be chosen not too close to the maximum power amplification, because it decreases very fast at the right side of this maximum, in particular for systems of a lot of devices. In practice the spacing must be chosen dependent on the local wave spectrum with the power amplification value higher than $I_p = 1$. This means a value of somewhere between $0.6 - 0.8 \lambda$.

The influence of the angle of incidence on the appropriate spacing has not been investigated in the used literature [Malmo,Reitan;1986,b] [McIver,Evans;1988]. Consequently, when in practice the waves are obliquely incidence, further investigation for the appropriate spacing is required.

References

Malmo, O.; Reitan, A.(1985); *Wave-power absorption by an oscillating water column in a channel*; Journal of Fluid Mechanics, Vol. 158, pp. 153-175

Malmo, O., Reitan, A.(1986,a); *Wave-power absorption by an oscillating water column in a reflecting wall*; Applied Ocean Research, Vol. 8, No. 1, pp. 42-48

Malmo, O., Reitan, A.(1986,b); *Wave-power absorption by a finite row of oscillating water columns in a reflecting wall*; Applied Ocean Research, Vol. 8, No. 2, pp. 105-109

McIver, P., Evans, D.V.(1988); *An approximate theory for the performance of a number of wave-energy devices set into a reflecting wall*; Applied Ocean Research, Vol. 10, No. 2, pp. 58-65

Appendix I Theory of Goda and Modifications

The complete theory of Goda is described in 'Random Seas and the Design of Maritime Structures' [Goda; 1985]. Some reviews are given in other literature [Goda, 1992] [Tanimoto et al.;1994a,b]. The theory of Goda is described in Part I.

In 1992, Takahashi et al. proposed a new impulsive pressure coefficient for the Goda theory, this is described in Part II. [Takahashi et al.;1994]

Part I Theory of Goda

Design wave conditions

A caisson breakwater has to be designed against the largest force of a single wave expected during its life time. This largest force depends on the wave height, period and direction of the incident waves.

Wave height

The largest force will be reached by the highest wave H_{\max} in a train of random waves corresponding to the design condition on the average. The highest wave can be determined by the following formulas:

$$H_{\max} = 1.8 \cdot H_{1/3} \quad : h/L_0 \geq 0.2 \quad (I.1 a)$$

$$= \min \{(\beta_0^* \cdot H_0 + \beta_1^* \cdot h), \beta_{\max}^* \cdot H_0, 1.8 \cdot H_{\text{sig}}\} \quad : h/L_0 < 0.2 \quad (I.1 b)$$

$$H_{\text{sig}} = K_s \cdot H_0 \quad : h/L_0 \geq 0.2 \quad (I.2 a)$$

$$= \min \{(\beta_0 \cdot H_0 + \beta_1 \cdot h), \beta_{\max} \cdot H_0, K_s \cdot H_0\} \quad : h/L_0 < 0.2 \quad (I.2 b)$$

with $\min a, b$ = minimum value of a ,b

H_{sig} = significant wave height, $H_{1/3}$ [m]

H_{\max} = maximum wave height, $H_{1/250}$ [m]

H_0 = deep water wave height [m]

K_s = shoaling coefficient [-]

$$\beta_0 = 0.028 (H_0/L_0)^{-0.38} \exp[20 \tan^{1.5} \theta] \quad (I.3 a)$$

$$\beta_1 = 0.52 \exp[4.2 \tan \theta] \quad (I.3 b)$$

$$\beta_{\max} = \max \{0.92, 0.32 (H_0/L_0)^{-0.29} \exp[2.4 \tan \theta]\} \quad (I.3 c)$$

$$\beta_0^* = 0.052 (H_0/L_0)^{-0.38} \exp[20 \tan^{1.5} \theta] \quad (I.4 a)$$

$$\beta_1^* = 0.63 \exp[3.8 \tan \theta] \quad (I.4 b)$$

$$\beta_{\max}^* = \max \{1.65, 0.53 (H_0/L_0)^{-0.29} \exp[2.4 \tan \theta]\} \quad (I.4 c)$$

with θ = inclination of sea bottom

L_0 = deep water wave length [m]

The shoaling coefficient K_s can be calculated by a figure based on the theory of Shuto [Shuto;1974]. The shoaling factor derived by the linear wave theory, see **Appendix A**, can also be used because this factor gives the same values as the figure. In this study the shoaling factor of the linear wave theory is used.

The selection of the fixed relation $H_{\max} = 1.8 \cdot H_{1/3}$ when the waves are not breaking (outside the surf zone), was based on three subjects. (1) Based on the Raleigh distribution of wave heights, the wave height $H_{1/250}$ is about 1.8 to 2.0 times larger than the wave height $H_{1/3}$. A fixed ratio was preferred, because a variable relation would cause some confusion in design procedures. (2) A possible deviation of the relation $H_{\max} = 1.8 \cdot H_{1/3}$ to $2.0 \cdot H_{1/3}$ corresponds to an increase of 11% and can be covered within the margin of the safety factors, which are usually taken as 1.2. (3) Prototype caisson breakwaters showed sufficient safety against sliding and overturning. Based on these considerations, a value of 1.8 is recommended and this is also used in this study.

For the calculation of the maximum wave height H_{max} of breaking waves (within the surf zone), the water depth at a distance of $5 \cdot H_{1/3}$ seaward of the breakwater has to be used. At this distance h_b , the breaking waves cause the highest wave force in the breakwater. For a breakwater at a steep sea bottom, this shift to the sea site, produces a considerable increase of the wave force and consequently the required weight of the breakwater will be increased.

Figure I.1 shows the significant and maximum wave height as a function of the water depth for two deep water wave conditions.

Wave period

The period of the highest wave H_{max} is taken the same as the significant wave period of the significant design wave height i.e.:

$$T_{max} = T_{1/3} \quad [I.5]$$

This relation is valid for the mean period T_{max} of irregular waves. Although, this relation can have quite large variation for individual wave records, the use of it is recommended for the sake of simplicity.

Wave direction

Obliquely incident waves cause a lower wave pressure on the breakwater than normally incident waves, especially when waves are breaking. The angle of incidence β is measured as that between the direction of wave approach and a line normal to the breakwater. It is recommended to rotate the wave direction by 15° towards the most dangerous direction, i.e. to the normally incident wave direction.

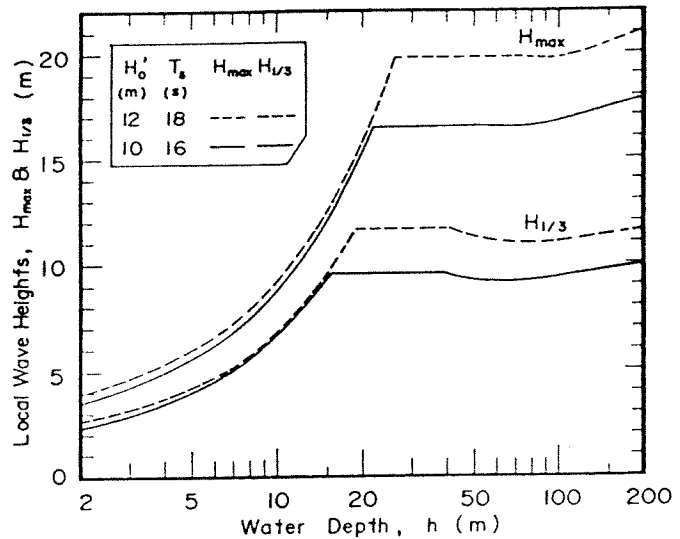


Figure I.1 Significant and maximum wave height as a function of the water depth

Wave pressure, buoyancy and uplift pressure

Elevation of the wave pressure

The exact elevation of a wave crest along a vertical wall is difficult to assess, because it varies considerably from 1.0 to 2.0 times the wave height, depending on the wave steepness and the relative water depth. In order to provide a consistent wave pressure calculation method, the elevation is determined by the following equation:

$$\eta^* = 0.75 \cdot (1 + \cos\beta) \cdot \lambda_1 \cdot H_{max} \quad (I.6)$$

with η^* = elevation of the wave pressure [m]

β = angle of incidence

λ_1 = modification factor for the type of caisson breakwater in general: $\lambda_1 = 1$

For normally incident waves this equation gives $\eta^* = 1.5 \cdot H_{max}$.

The distribution of the wave pressure is shown in Figure I.2. The pressure has the highest value p_1 at the design water level and decreases linearly towards the elevation η^* to a value p_4 and to the sea bottom to a value p_2 . These pressures can be calculated by the following equations:

$$p_1 = 0.5 \cdot (1 + \cos\beta) \cdot (\lambda_1 \cdot \alpha_1 + \lambda_2 \cdot \alpha_2 \cos^2\beta) \cdot \rho \cdot g \cdot H_{\max} \quad [\text{N/m}^2] \quad (\text{I.7})$$

$$p_2 = p_1 / \cosh(kh) \quad [\text{N/m}^2] \quad (\text{I.8})$$

$$p_3 = \alpha_3 \cdot p_1 \quad [\text{N/m}^2] \quad (\text{I.9})$$

$$p_4 = \alpha_4 \cdot p_1 \quad [\text{N/m}^2] \quad (\text{I.10})$$

$$p_u = 0.5 \cdot (1 + \cos\beta) \cdot \lambda_3 \cdot \alpha_1 \cdot \alpha_3 \cdot \rho \cdot g \cdot H_{\max} \quad [\text{N/m}^2] \quad (\text{I.11})$$

with $\alpha_1 = 0.6 + 0.5 \cdot (2kh / \sinh(2kh))^2 \quad (\text{I.12})$

$$\alpha_2 = \min \{ ((h_b - d) / 3h_b) \cdot (H_{\max} / d)^2, 2d / H_{\max} \} \quad (\text{I.13})$$

$$\alpha_3 = 1 - (h' - h) \cdot (1 - 1 / \cosh(kh)) \quad (\text{I.14})$$

$$\alpha_4 = 1 - h_c^* / \eta^* \quad (\text{I.15})$$

$\lambda_1, \lambda_2 =$ modification factor for the type of caisson breakwater in general: $\lambda_1 = 1, \lambda_2 = 1$

with $h_c^* = \min \{ \eta^*, h_c \} \quad (\text{I.16})$

and $k =$ wave number $[\text{m}^{-1}]$

$g =$ gravitational acceleration $[\text{m/s}^2]$

$\rho =$ density of water $[\text{kg/m}^3]$

$h_b =$ water depth at a distance of five times the significant wave height

$h, h_c, h', d :$ see Figure I.2

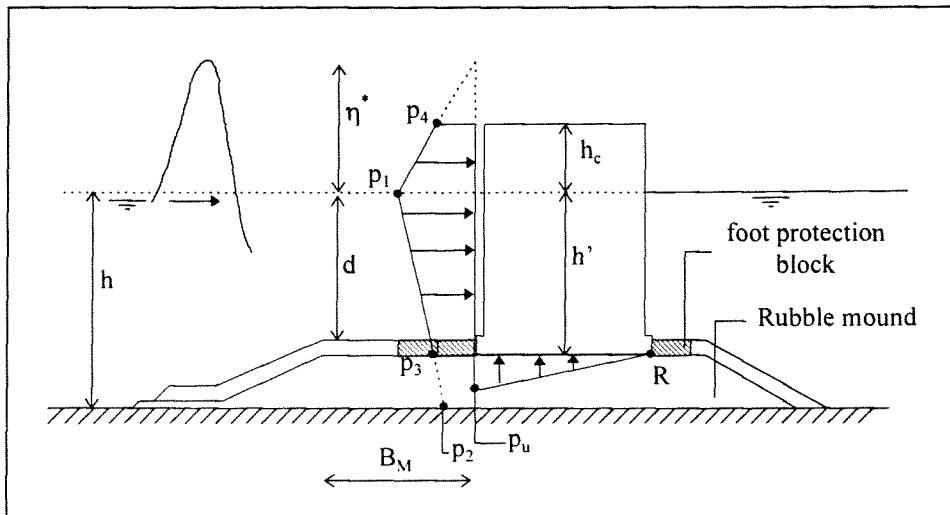


Figure I.2 Wave pressure distribution by the theory of Goda

The coefficient α_1 represents the effect of wave period on the wave pressure. It takes the minimum value of 0.6 for deep water waves and the maximum value 1.1 for waves in very shallow water. The coefficient α_2 is introduced to express the increase of wave pressure by the presence of the rubble mound foundation. Both coefficients have been empirically determined. The coefficient α_3 is derived by the linear pressure distribution.

The effect of the wave direction on the wave pressure is incorporated in η^* and in p_1 with the factor $0.5 \cdot (1 + \cos\beta)$ and a modification to the term with α_2 with the factor $\cos^2\beta$.

For ordinary types of caissons, the modification factors λ_1, λ_2 and λ_3 have a value of 1.0. When other types of caissons are used, these modification factors have to be determined. The factor λ_1 represents the reduction or increase of the slowly varying wave pressure component, while the factor λ_2 represents the change of the breaking pressure component (dynamic or impulsive pressure). The factor λ_3 represents the changes of the uplift pressure.

Stability of the caisson

The caisson has to be stable against sliding (horizontal displacement) and overturning (rotational displacement around the back toe). For both failure conditions the safety factor can be determined. As a value for the safety factor, 1.2 is recommended.

Sliding:

$$\text{S.F.} = \mu \cdot (W_0 - F_u) / F_{H,\text{tot}} \quad (1.17)$$

with μ = friction coefficient between caisson and rubble mound [-]
= usually taken as 0.6

W_0 = submerged weight of the caisson (weight of the caisson - buoyancy) [N]

F_u = wave uplift force [N]

$F_{H,\text{tot}}$ = total horizontal wave force [N]

Overturning:

$$\text{S.F.} = (M_{W_0} - M_{F_u}) / M_{F_{H,\text{tot}}} \quad (1.18)$$

with M_{W_0} = moment of submerged weight of the caisson around R (back toe) [Nm]

M_{F_u} = moment of wave uplift force around R [Nm]

$M_{F_{H,\text{tot}}}$ = total moment of horizontal wave force around R [Nm]

Stability of the Rubble Mound Foundation

The bearing capacity of the rubble mound foundation has also to be checked. It is mentioned that the maximum stress of the rubble mound, has been taken usually as 400-500 kN/m² [Tanimoto et al.;1994] This maximum stress occurs in general at the toe at the back side of the caisson. As a maximum value 600 kN/m² is mentioned [Hou et al.;1994]. In Japan in 1989, a new calculation method for the bearing capacity of a caisson breakwater on a rubble mound foundation was included in the Technical Standards. This calculation uses the simplified Bishop method of circular slip failure analysis [Kobayashi et al.;1987].

Part II Modified Theory of Goda

In 1992, a new impulsive pressure coefficient α^* has been proposed by Takahashi et al. [Takahashi et al.;1994]. The effect of the impulsive pressure indicated by the pressure coefficient α_2 in the Goda theory does not accurately estimate the effective pressure (equivalent static pressure) due to impulsive pressure. The length and height of the berm in front of the caisson have a strong influence on this impulsive pressure.

The pressure p_1 is replaced by:

$$p_1 = 0.5 \cdot (1 + \cos\beta) \cdot (\lambda_1 \cdot \alpha_1 + \lambda_2 \cdot \alpha^* \cos^2\beta) \cdot \rho \cdot g \cdot H_{\text{max}} \quad [\text{N/m}^2] \quad (1.19)$$

with α^* = max { α_2 , α_1 } (1.20)

α_2 : described in Part I

The impulsive pressure coefficient α_1 is expressed by:

$$\alpha_1 = \alpha_{10} \cdot \alpha_{11} \quad (1.21)$$

with $\alpha_{10} = H / d$: $H \leq 2d$

$$= 2 \quad : H > 2d \quad (1.22)$$

$$\begin{aligned} \alpha_{11} &= \cos \delta_2 / \cosh \delta_1 && : \delta_2 \leq 0 \\ &= 1 / \{ \cosh \delta_1 (\cosh \delta_2)^{1/2} \} && : \delta_2 > 0 \end{aligned} \quad (1.23)$$

with H = wave height ($= H_{\max}$)

$$\begin{aligned} \delta_1 &= 20 \delta_{11} && : \delta_{11} \leq 0 \\ &= 15 \delta_{11} && : \delta_{11} > 0 \end{aligned} \quad (1.24)$$

$$\begin{aligned} \delta_2 &= 4.9 \delta_{22} && : \delta_{22} \leq 0 \\ &= 3 \delta_{22} && : \delta_{22} > 0 \end{aligned} \quad (1.25)$$

with $\delta_{11} = 0.93(B_M/L - 0.12) + 0.36\{(h-d)/h - 0.6\}$ (1.26)

$\delta_{22} = -0.36(B_M/L - 0.12) + 0.93\{(h-d)/h - 0.6\}$ (1.27)

with L = wave length

B_M = length of the berm in front of the caisson

h, d : see Figure I.2

Figure I.3 shows the values of coefficient α_{11} . The coefficient $\alpha_1 (= \alpha_{10} \cdot \alpha_{11})$ reaches a maximum of 2 at $B_M / L = 0.12$, $d/h = 0.4$ and $H / d = 2$. When $d/h \geq 0.7$, α_1 is always nearly zero and lower than α_2 . In that case α_2 has to be taken, see equation I.20.

It should be noted that the impulsive pressure decreases significantly when the angle of incidence is not zero (i.e. for obliquely incident waves). It is mentioned that the impulsive pressure can be neglected when the incident angle is about 30 degrees. See for an illustration of the influence of the angle of incidence Figure I.4.

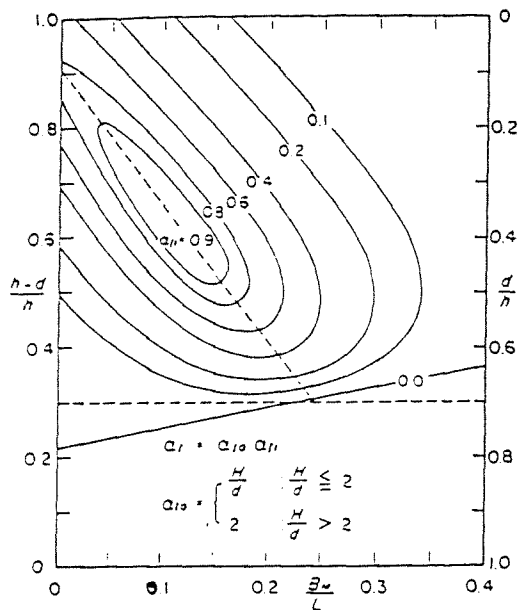


Figure I.3 Coefficient α_{11} for the calculation of α_{11}

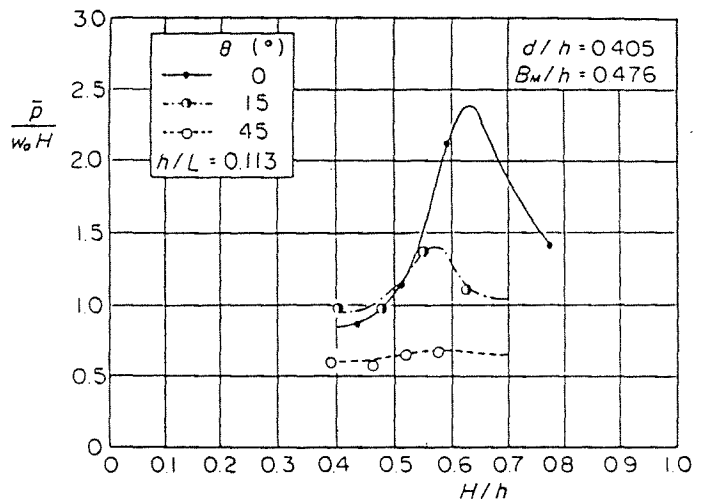


Figure I.4 Influence of the angle of incidence on impulsive pressure α_{11}

It is recommended that the water depth d , above the rubble mound berm has to be at least more than $0.6 \cdot$ the water depth h ($d/h > 0.6$) [Takahashi et al.;1994.

To show the influence of the modified pressure coefficient on the average pressure intensity, the next two figures are shown. For the broken lines, α_2 is used, for the dense lines, α_1 is used.

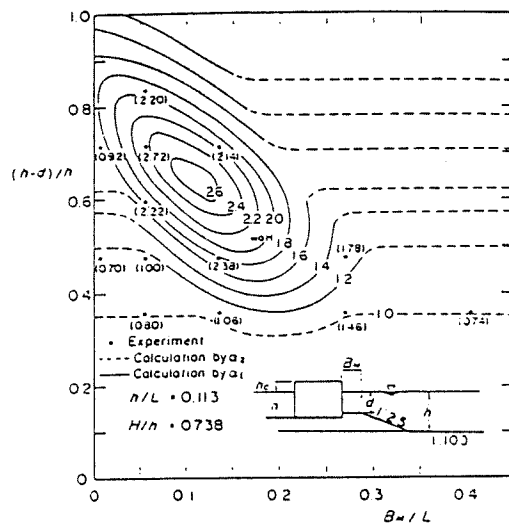


Figure I.5 Comparison of pressure intensity,
 $h/L = 0.113$, $H/h = 0.738$

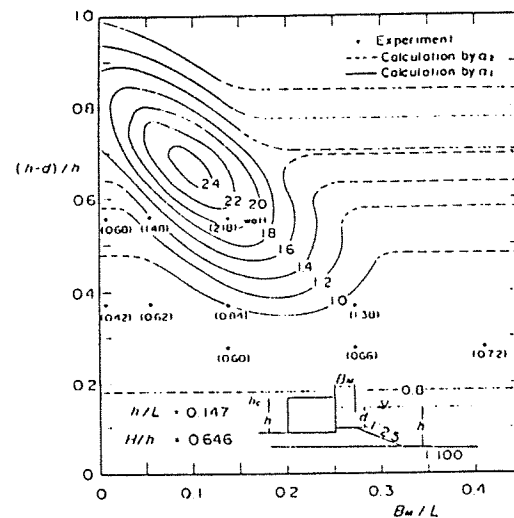


Figure I.6 Comparison of pressure intensity,
 $h/L = 0.147$, $H/h = 0.646$

References

- Goda, Y.(1975); *Random Seas and the Design of Maritime Structures*; University of Tokyo Press
- Goda, Y.(1992); *The Design of Upright Breakwaters*; Proc. of the Short Course on Design and Reliability of Coastal Structures, attached to the 23rd Int. Conf. On Coastal Engineering, pp. 547-568
- Hou, H.S., Chen, C.C., Hu, T.M., (1994); *Study of Deep Water Breakwater Design Factors*; Hydro-Port '94; Proceedings of the Int. Conf. On Hydro-Technical Engineering for Port and Harbor Construction, pp. 721-733
- Kobayashi, M., Terashi, M., Takahashi, K.(1987); *Bearing capacity of a rubble mound supporting a gravity structure*; Rept. Port and Harbour Res. Inst., Vol.26, No.5, pp. 215-252
- Takahashi S., Tanimoto, K., Shimosako, K.(1994); *Dynamic Response and Sliding of Breakwater Caisson Against Impulsive Breaking Wave Forces*; Proc. of the Int. Workshop on Wave Barriers in Deepwaters, Yokosuka, Japan, pp. 362-401
- Tanimoto, K., Takahashi, S. (1994 a); *Design and construction of caisson breakwaters - the Japanese experience*; Coastal Engineering, 22, pp.57-77
- Tanimoto, K., Takahashi, S. (1994 b); *Japanese Experience on Composite Breakwaters*; Proc. of Int. Workshop on Wave Barriers in Deepwaters, pp. 1-25

Appendix J Maximum Wave Height Calculation

Deep water wave height

Estimation of the significant deep water wave height, with a return period of 500 years is executed for a wave steepness of 2.0 - 4.0 %. The deep water wave length and the shoaling factor are calculated by the next equations:

$$L_0 = \frac{gT_z^2}{2\pi} \quad (J.1)$$

with L_0 = deep water wave length [m]
 g = gravitational acceleration [m/s^2] = 9.81 m/s^2
 T_z = mean wave period [s]
 $= T_p / 1.2$
with T_p = peak period [s]

$$K_S = \frac{1}{\tanh kh \left(1 + \frac{2kh}{\sinh 2kh}\right)} \quad (J.2)$$

with K_S = shoaling factor [-]
 k = wave number [m^{-1}]
 h = water depth [m] = 34 m

Table J.1 Calculation of deep water wave height

H [m]	S_p [%]	T_p [s]	L_0 [m]	h [m]	L [m]	k [m^{-1}]	kh [-]	K_S [-]	H_0 [m]
11.80	2.00	19.44	409.72	34.00	270.02	0.02	0.79	0.95	12.41
11.80	2.50	17.39	327.78	34.00	235.66	0.03	0.91	0.93	12.69
11.80	3.00	15.87	273.15	34.00	209.99	0.03	1.02	0.92	12.84
11.80	3.50	14.69	234.13	34.00	189.58	0.03	1.13	0.91	12.91
11.80	4.00	13.75	204.86	34.00	172.93	0.04	1.24	0.91	12.92

Design wave height of each segment of the breakwater

With the formulas of Goda for breaking waves, see Appendix I, the maximum wave height for each segment can be calculated. The coefficients of the formulas are given in the Table J.2. The inclination of the bottom θ , is set at zero.

Table J.2 Coefficients of the breaking formulas of Goda

H_0	L_0	β_0	β_1	$\beta_{\max,1}$	$\beta_{\max,2}$	β_{\max}	β^*_0	β^*_1	$\beta^*_{\max,1}$	$\beta^*_{\max,2}$	β^*_{\max}
12.41	410	0.11	0.52	0.92	0.88	0.92	0.20	0.63	1.65	1.46	1.65
12.69	328	0.10	0.52	0.92	0.82	0.92	0.18	0.63	1.65	1.36	1.65
12.84	273	0.09	0.52	0.92	0.78	0.92	0.17	0.63	1.65	1.29	1.65
12.91	234	0.08	0.52	0.92	0.74	0.92	0.16	0.63	1.65	1.23	1.65
12.92	205	0.08	0.52	0.92	0.71	0.92	0.15	0.63	1.65	1.18	1.65

The shoaling factor in the formulas of Goda of Appendix I, for the determination of H_{sig} and H_{\max} is replaced by the propagation factor K_a and the direction factor K_d of Table 6.6. The determination of the maximum wave height is shown in the next table, for high water + 5.0 m C.D. The wave steepness is 2.0 - 4.0 %.

Table J.3 Wave height and length at a water level of +5.0 m C.D., for each segment of the breakwater

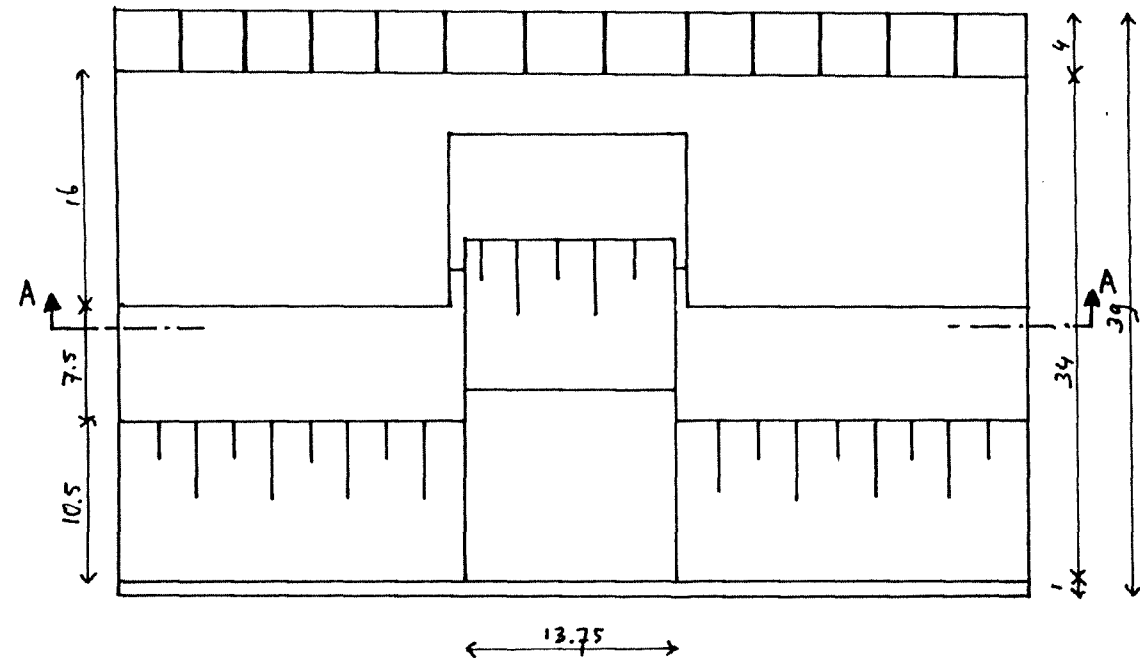
Segment	h [m]	H _{sig} [m]	H _{sig} [m]	H _{sig} [m]	H _{sig} [m]	H _{max} [m]	H _{max} [m]	H _{max} [m]	H _{max} [m]	L [m]
A	27	15.35	11.42	10.00	10.0	19.45	20.48	18.00	18.0	245
	27	15.26	11.68	10.00	10.0	19.28	20.94	18.00	18.0	215
	27	15.19	11.82	10.00	10.0	19.14	21.19	18.00	18.0	193
	27	15.13	11.88	10.00	10.0	19.03	21.31	18.00	18.0	175
	27	15.07	11.89	10.00	10.0	18.93	21.32	18.00	18.0	161
B	30	16.91	11.42	10.00	10.0	21.34	20.48	18.00	18.0	257
	30	16.82	11.68	10.00	10.0	21.17	20.94	18.00	18.0	225
	30	16.75	11.82	10.00	10.0	21.03	21.19	18.00	18.0	201
	30	16.69	11.88	10.00	10.0	20.92	21.31	18.00	18.0	182
	30	16.63	11.89	10.00	10.0	20.82	21.32	18.00	18.0	166
C	31	17.43	11.42	9.80	9.8	21.97	20.48	17.64	17.6	260
	31	17.34	11.68	9.80	9.8	21.80	20.94	17.64	17.6	228
	31	17.27	11.82	9.80	9.8	21.66	21.19	17.64	17.6	203
	31	17.21	11.88	9.80	9.8	21.55	21.31	17.64	17.6	184
	31	17.15	11.89	9.80	9.8	21.45	21.32	17.64	17.6	168
D	31	17.43	11.42	11.70	11.4	21.97	20.48	21.06	20.5	260
	31	17.34	11.68	11.70	11.7	21.80	20.94	21.06	20.9	228
	31	17.27	11.82	11.70	11.7	21.66	21.19	21.06	21.1	203
	31	17.21	11.88	11.70	11.7	21.55	21.31	21.06	21.1	184
	31	17.15	11.89	11.70	11.7	21.45	21.32	21.06	21.1	168
E	30	16.91	11.42	12.30	11.4	21.34	20.48	22.14	20.5	257
	30	16.82	11.68	12.30	11.7	21.17	20.94	22.14	20.9	225
	30	16.75	11.82	12.30	11.8	21.03	21.19	22.14	21.0	201
	30	16.69	11.88	12.30	11.9	20.92	21.31	22.14	20.9	182
	30	16.63	11.89	12.30	11.9	20.82	21.32	22.14	20.8	166
F	28	15.87	11.42	12.90	11.4	20.08	20.48	23.22	20.1	249
	28	15.78	11.68	12.90	11.7	19.91	20.94	23.22	19.9	218
	28	15.71	11.82	12.90	11.8	19.77	21.19	23.22	19.8	196
	28	15.65	11.88	12.90	11.9	19.66	21.31	23.22	19.7	177
	28	15.59	11.89	12.90	11.9	19.56	21.32	23.22	19.6	163
G	26	14.83	11.42	12.90	11.4	18.82	20.48	23.22	18.8	241
	26	14.74	11.68	12.90	11.7	18.65	20.94	23.22	18.7	212
	26	14.67	11.82	12.90	11.8	18.51	21.19	23.22	18.5	190
	26	14.61	11.88	12.90	11.9	18.40	21.31	23.22	18.4	173
	26	14.55	11.89	12.90	11.9	18.30	21.32	23.22	18.3	159

The maximum wave heights with a return period of 500 years are also determined for a water level of + 2.5 m C.D. and at Chart Datum. The maximum wave heights H_{sig} and H_{max} and the corresponding wave length are shown in Table J.4.

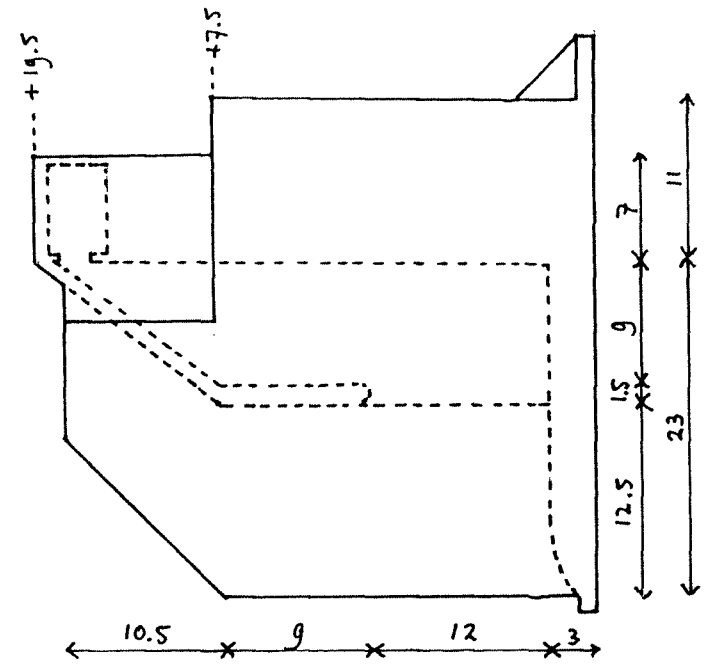
Table J.4 Wave height and length at a water level of 2.5 m + C.D. and C.D. for each segment

Segment	+ 2.5 m C.D.				C.D.			
	h [m]	H _{sig} [m]	H _{max} [m]	L [m]	h [m]	H _{sig} [m]	H _{max} [m]	L [m]
A	24.5	10.0	17.9	236	22	10.0	16.3	225
	24.5	10.0	17.7	207	22	10.0	16.1	198
	24.5	10.0	17.6	186	22	10.0	16	178
	24.5	10.0	17.5	169	22	10.0	15.9	162
	24.5	10.0	17.4	155	22	10.0	15.8	149
B	27.5	10.0	18.0	247	25	10.0	18	237
	27.5	10.0	18.0	217	25	10.0	18	209
	27.5	10.0	18.0	194	25	10.0	17.9	187
	27.5	10.0	18.0	176	25	10.0	17.8	170
	27.5	10.0	18.0	162	25	10.0	17.7	156
C	28.5	9.8	17.6	251	26	9.8	17.6	241
	28.5	9.8	17.6	220	26	9.8	17.6	212
	28.5	9.8	17.6	197	26	9.8	17.6	190
	28.5	9.8	17.6	179	26	9.8	17.6	173
	28.5	9.8	17.6	164	26	9.8	17.6	159
D	28.5	11.4	20.4	251	26	11.4	18.8	241
	28.5	11.7	20.2	220	26	11.7	18.7	212
	28.5	11.7	20.1	197	26	11.7	18.5	190
	28.5	11.7	20.0	179	26	11.7	18.4	173
	28.5	11.7	19.9	164	26	11.7	18.3	159
E	27.5	11.4	19.8	247	25	11.4	18.2	237
	27.5	11.7	19.6	217	25	11.7	18.0	209
	27.5	11.8	19.5	194	25	11.8	17.9	187
	27.5	11.9	19.3	176	25	11.9	17.8	170
	27.5	11.9	19.2	162	25	11.9	17.7	156
F	25.5	11.4	18.5	239	23	11.4	16.9	229
	25.5	11.7	18.3	210	23	11.7	16.8	202
	25.5	11.8	18.2	189	23	11.8	16.6	181
	25.5	11.9	18.1	171	23	11.9	16.5	165
	25.5	11.9	18.0	157	23	11.9	16.4	152
G	23.5	11.4	17.2	231	21	11.4	18.8	220
	23.5	11.7	17.1	203	21	11.7	18.7	194
	23.5	11.8	16.9	183	21	11.8	18.5	175
	23.5	11.9	16.8	166	21	11.9	18.4	159
	23.5	11.9	16.7	153	21	11.9	18.3	147

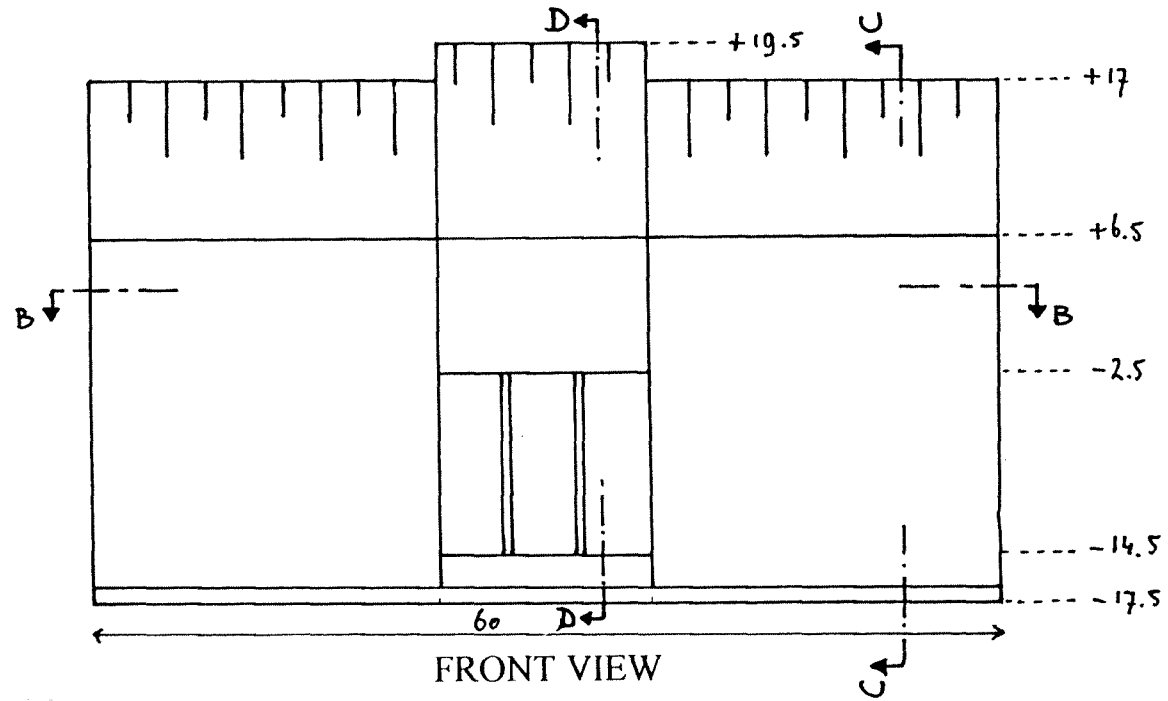
Appendix K Drawings of the Final Design



TOP VIEW

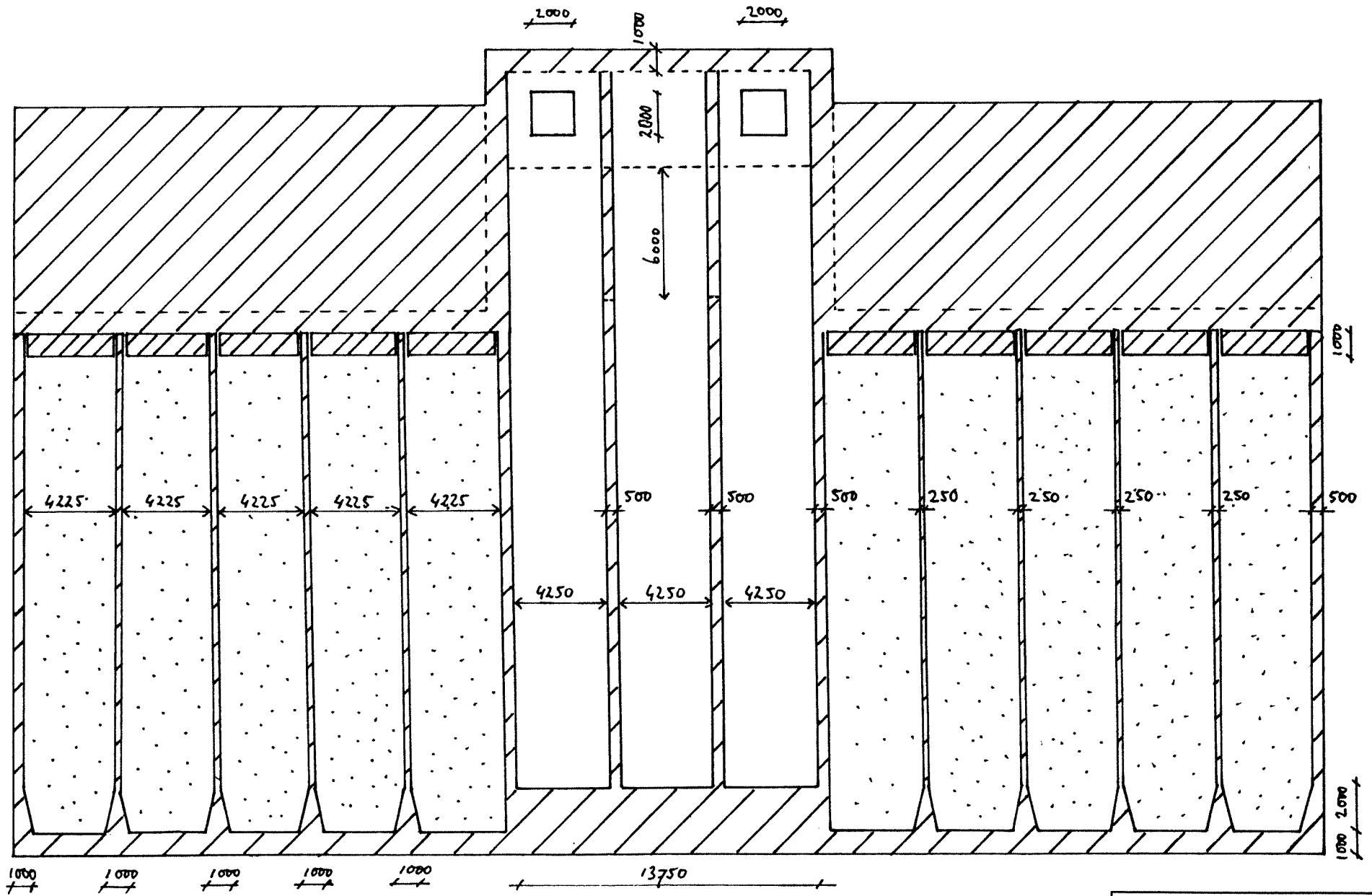


SIDE VIEW

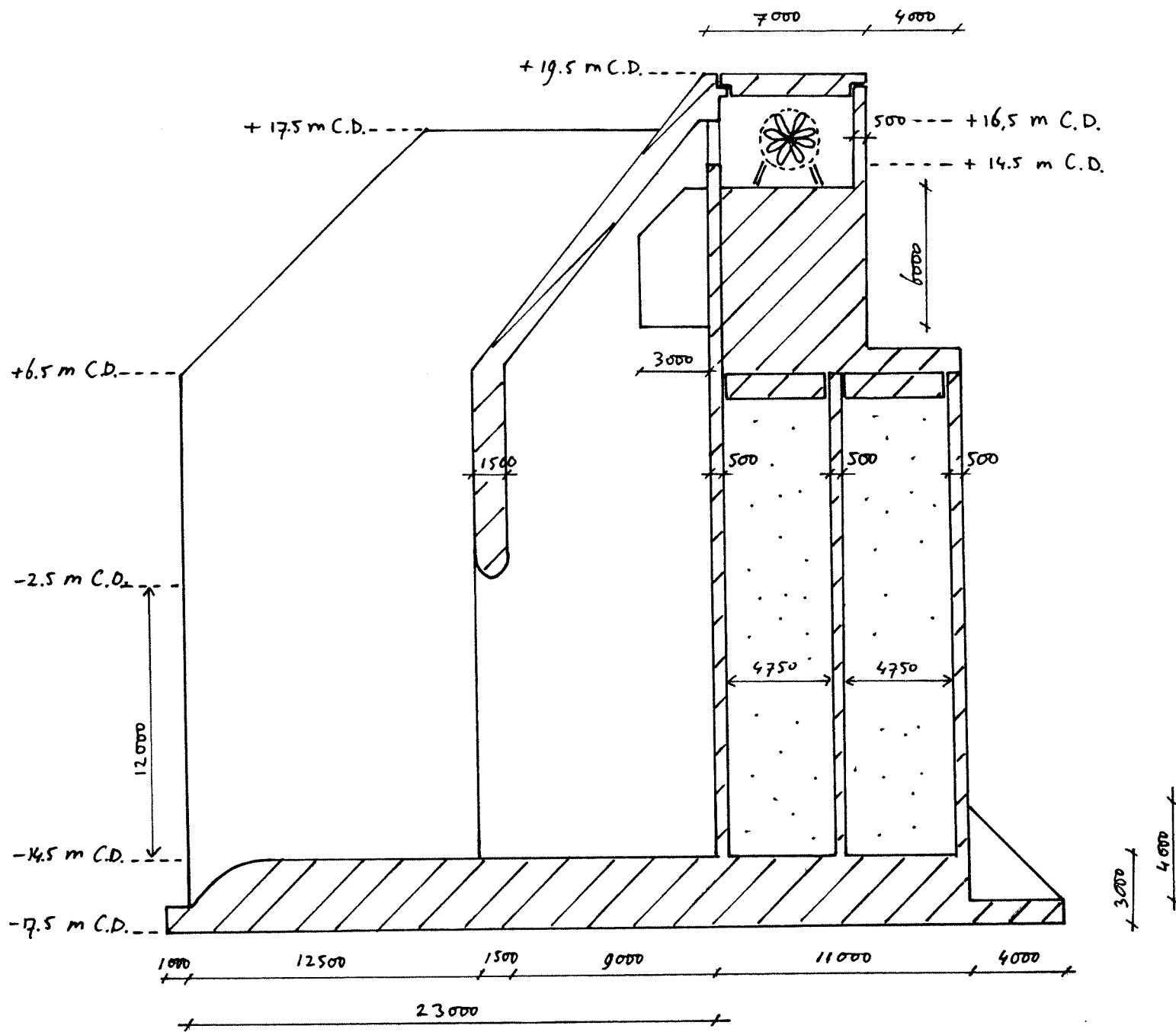


FRONT VIEW

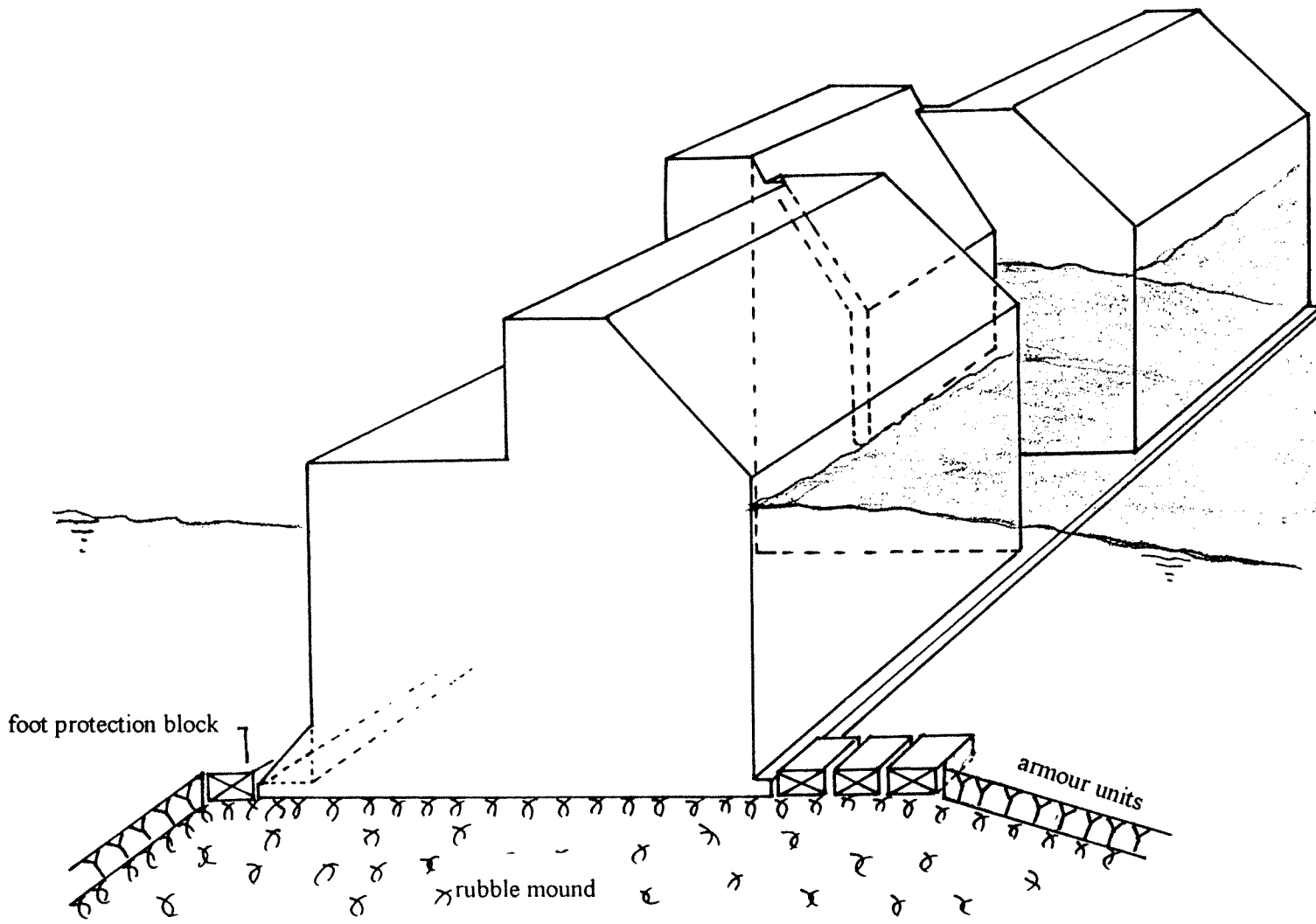
Overview Drawing
Scale 1:500, A4
Dimensions in [m]
Levels related to C.D.
Appendix K, Drawing 1



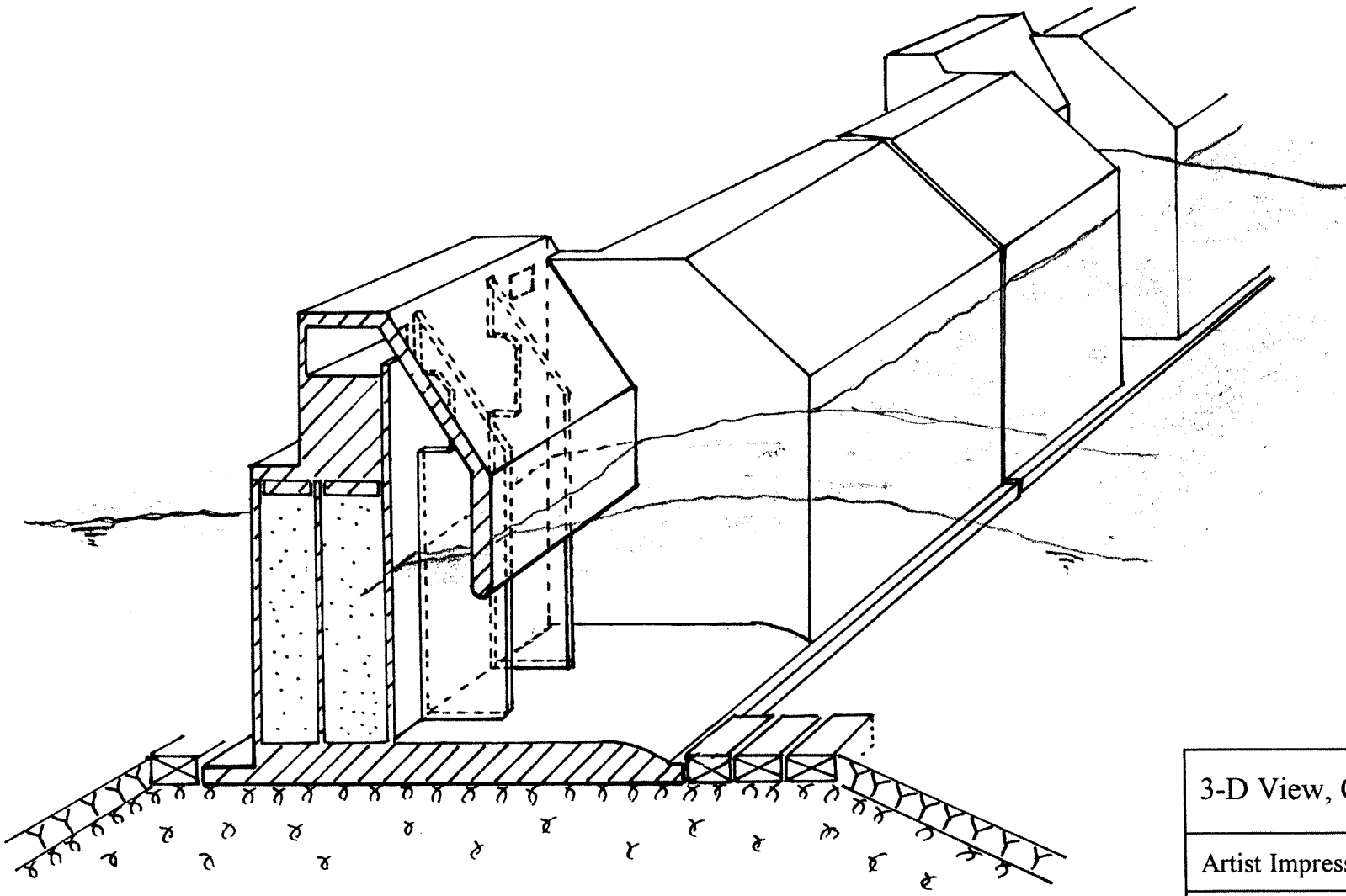
Cross Section A-A
Scale 1:250, A4
Dimensions in [mm]
Appendix K, Drawing 2



Cross Section D-D
Scale 1:250, A4
Dimensions in [mm]
Appendix K, Drawing 5



3-D View of the total caisson
Artist Impression
H.A. Vervoorn
Appendix K, Drawing 6



3-D View, Cross section of the device

Artist Impression

H.A. Vervoorn

Appendix K, Drawing 7

Appendix L Stability and Rubble Mound Stress of the Final Design

In this appendix the results of the stability calculations of the caissons with devices are represented (segments C, D, E, F, and G). The stability is calculated for two sections of the caisson, namely a section with and without wave energy device. The calculations are executed for a water level at C.D., at + 2.5 and + 5 m C.D. in combination with five wave conditions. The last table shows the average safety factors and rubble mound stresses of a complete caisson for all segments and water levels.

Wave Conditions

- Wave Steepness : 2.0, 2.5, 3.0, 3.5, 4.0 %
 Wave Height : H_{max} derived in **Appendix J**
 Wave Length : L , corresponding to the wave steepness and the depth of the segment, derived in **Appendix J**
 Angle of incidence : β , for sections without device, corresponding to the segments, for sections with a device the waves are assumed to be normally incident

	sections without device	sections with device
angle of incidence β [°]	corresponding to the segment	0

Modification factors

The modification factors are derived in Section 7.5. The used factors are shown in the following table.

modification factor	sections without device	sections with device
λ_1	1	1
λ_2	1	0
λ_{SL}	not used	not used
λ_V	function of H_{max} / L and d_c	1

The Goda theory with the symbols of **Appendix I** has been used. The new proposed impulsive pressure coefficient of Takahashi et al. is used in this study. The influence is not very important because the recommendations $d/h > 0.6$ is fulfilled in all conditions.

In this study, an extra parameter p_3 has been used, which is the wave pressure at the beginning of the sloping top.

Used symbols

- F_1 = total wave force on the slope [kN]
 F_{H+} = horizontal wave force above sea level at the vertical wall [kN]
 F_{H-} = horizontal wave force below sea level at the vertical wall [kN]
 F_{SH} = horizontal wave force on the slope [kN]
 F_{SV} = vertical wave force on the slope [kN]
 F_{Htot} = total horizontal wave force [kN]
 F_U = uplift wave force [kN]
 $M_{FU/R}$ = moment of the uplift wave force around back toe, R [kNm]
 $M_{FH/R}$ = moment of the total horizontal wave force around back toe, R [kNm]
 $M_{FV/R}$ = moment of the vertical wave force on the slope around back toe, R [kNm]
 $M_{W/R}$ = moment of the weight of the caisson around back toe, R [kNm]

- $M_{W/T}$ = moment of the weight of the caisson around the centre of the bottom plate, T [kNm]
 $S.F._{SL}$ = safety factor against sliding [-]
 $S.F._{O.T.}$ = safety factor against overturning [-]
 σ_{max} = maximum rubble mound pressure under the back toe of the caisson [kN/m²]
 σ_{min} = minimum rubble mound pressure under the front toe of the caisson [kN/m²]
 h_c = crest height [m]
 h_s = slope height [m]
 h = water depth in front of the caisson [m]
 h' = depth of the caisson below water level
 d = water depth above berm [m]
 d_c = distance between water level and lowest point of the sloping top [m]

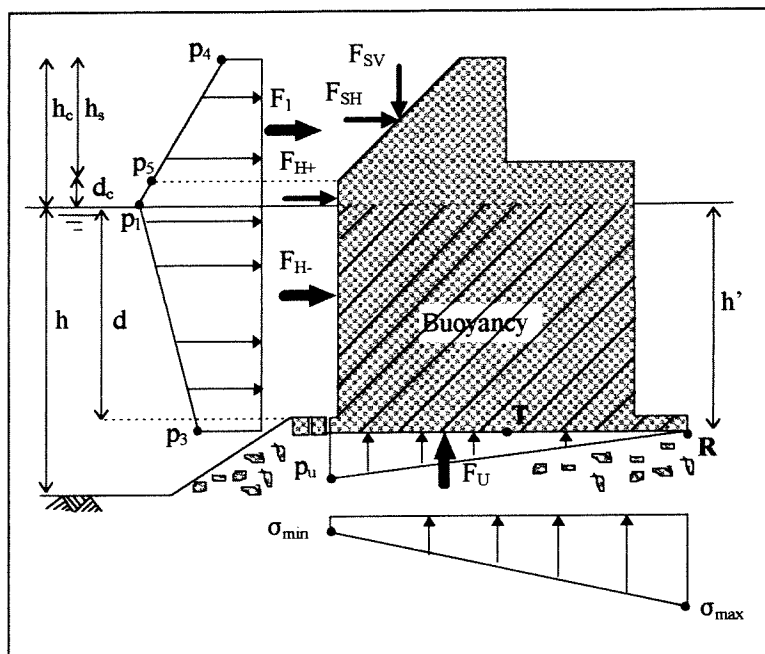


Figure L.1 Used symbols in the stability calculations

Weight and buoyancy

The weight and buoyancy per m width of the caisson, which have been used in the calculations are shown in the following table.

	C.D.		+ 2.5 m C.D.		+ 5 m C.D.	
	section without device	section with device	section without device	section with device	section without device	section with device
Weight [kN/m]	19162	9006	19162	9006	19162	9006
Buoyancy [kN/m]	6012	2667	6871	2927	7730	3274

Averaged safety factors and rubble mound stresses

For calculation of the averaged safety factors and rubble mound stresses, it is assumed that the wave forces are equally distributed over the total bottom plate. In that case, the safety factors and rubble mound stresses of the sections without device contribute for $(60-13.75)/60$ and the safety factors and rubble mound stresses of the sections with device contribute for $13.75/60$.

The following table gives the wave conditions for all segments. The modification factor λ_v is also given, which is valid for the sections without device:

Seg- ment	S [%]	β [°]	C.D.						+ 2.5 m C.D.						+ 5 m C.D.					
			h [m]	H_{max} [m]	L [m]	H_{max}/L [-]	λ_v [-]	h [m]	H_{max} [m]	L [m]	H_{max}/L [-]	λ_v [-]	h [m]	H_{max} [m]	L [m]	H_{max}/L [-]	λ_v [-]			
C	2.0	7.5	26	17.6	241	0.073	1.0	28.5	17.6	251	0.070	0.92	31	17.6	260	0.068	0.83			
	2.5	7.5	26	17.6	212	0.083	1.0	28.5	17.6	220	0.080	0.9	31	17.6	228	0.077	0.8			
	3.0	7.5	26	17.6	190	0.093	1.0	28.5	17.6	197	0.089	0.88	31	17.6	203	0.087	0.8			
	3.5	7.5	26	17.6	173	0.102	1.0	28.5	17.6	179	0.098	0.85	31	17.6	184	0.096	0.8			
	4.0	7.5	26	17.6	159	0.111	1.0	28.5	17.6	164	0.107	0.83	31	17.6	168	0.105	0.8			
D	2.0	30	26	18.8	241	0.078	1.0	28.5	20.4	251	0.081	0.87	31	20.5	260	0.079	0.8			
	2.5	30	26	18.7	212	0.088	1.0	28.5	20.2	220	0.092	0.84	31	20.9	228	0.092	0.8			
	3.0	30	26	18.5	190	0.097	1.0	28.5	20.1	197	0.102	0.81	31	21.1	203	0.104	0.8			
	3.5	30	26	18.4	173	0.106	1.0	28.5	20	179	0.112	0.8	31	21.1	184	0.115	0.8			
	4.0	30	26	18.3	159	0.115	1.0	28.5	19.9	164	0.121	0.8	31	21.1	168	0.126	0.8			
E	2.0	30	25	18.2	237	0.077	1.0	27.5	19.8	247	0.080	0.87	30	20.5	257	0.080	0.8			
	2.5	30	25	18	209	0.086	1.0	27.5	19.6	217	0.090	0.85	30	20.9	225	0.093	0.8			
	3.0	30	25	17.9	187	0.096	1.0	27.5	19.5	194	0.101	0.82	30	21.0	201	0.104	0.8			
	3.5	30	25	17.8	170	0.105	1.0	27.5	19.3	176	0.110	0.8	30	20.9	182	0.115	0.8			
	4.0	30	25	17.7	156	0.113	1.0	27.5	19.2	162	0.119	0.8	30	20.8	166	0.125	0.8			
F	2.0	35	23	16.9	229	0.074	1.0	25.5	18.5	239	0.077	0.9	28	20.1	249	0.081	0.8			
	2.5	35	23	16.8	202	0.083	1.0	25.5	18.3	210	0.087	0.87	28	19.9	218	0.091	0.8			
	3.0	35	23	16.6	181	0.092	1.0	25.5	18.2	189	0.096	0.85	28	19.8	196	0.101	0.8			
	3.5	35	23	16.5	165	0.100	1.0	25.5	18.1	171	0.106	0.83	28	19.7	177	0.111	0.8			
	4.0	35	23	16.4	152	0.108	1.0	25.5	18	157	0.115	0.81	28	19.6	163	0.120	0.8			
G	2.0	35	21	18.8	220	0.085	1.0	23.5	17.2	231	0.074	0.92	26	18.8	241	0.078	0.8			
	2.5	35	21	18.7	194	0.096	1.0	23.5	17.1	203	0.084	0.9	26	18.7	212	0.088	0.8			
	3.0	35	21	18.5	175	0.106	1.0	23.5	16.9	183	0.092	0.88	26	18.5	190	0.097	0.8			
	3.5	35	21	18.4	159	0.116	1.0	23.5	16.8	166	0.101	0.86	26	18.4	173	0.106	0.8			
	4.0	35	21	18.3	147	0.124	1.0	23.5	16.7	153	0.109	0.84	26	18.3	159	0.115	0.8			

The following two tables show the results of the modified Goda theory of a section without device, at a water level of C.D. The used modification factors are $\lambda_1 = 1$, $\lambda_2 = 1$ and λ_v as a function of H_{max}/L and d_c .

Segment	h [m]	H _{max} [m]	L [m]	H _{max} /L [-]	β [°]	η [m]	λ _v [-]	α ₁ [-]	α ₂ [-]	α ₂ [-]	α ₁ [-]	α ₂ [-]	α ₃ [-]	α ₄ [-]	P ₁ [N/m ²]	P ₃ [N/m ²]	P ₄ [N/m ²]	P ₅ [N/m ²]	P _u [N/m ²]
C	26	17.6	241	0.073	7.5	26.3	1.0	0.880	0.155	1.818	0.158	0.870	0.353	183434	159644	64806	138076	135653	
	26	17.6	212	0.083	7.5	26.3	1.0	0.839	0.155	1.818	0.185	0.840	0.353	180820	151886	63883	136109	124831	
	26	17.6	190	0.093	7.5	26.3	1.0	0.803	0.155	1.818	0.215	0.810	0.353	179496	145413	63415	135112	115131	
	26	17.6	173	0.102	7.5	26.3	1.0	0.771	0.155	1.818	0.247	0.782	0.353	179522	140334	63424	135132	106724	
	26	17.6	159	0.111	7.5	26.3	1.0	0.743	0.155	1.818	0.283	0.754	0.353	180899	136403	63911	136168	99240	
D	26	18.8	241	0.078	30	26.3	1.0	0.880	0.177	1.702	0.166	0.870	0.354	179538	156253	63535	135184	135776	
	26	18.7	212	0.088	30	26.2	1.0	0.839	0.175	1.711	0.193	0.840	0.350	173420	145670	60771	130349	124280	
	26	18.5	190	0.097	30	25.9	1.0	0.803	0.171	1.730	0.222	0.810	0.343	168999	136909	58035	126572	113396	
	26	18.4	173	0.106	30	25.8	1.0	0.771	0.170	1.739	0.254	0.782	0.340	166801	130390	56685	124698	104548	
	26	18.3	159	0.115	30	25.6	1.0	0.743	0.168	1.749	0.290	0.754	0.336	165761	124988	55733	123692	96688	
E	25	18.2	237	0.077	30	25.5	1.0	0.887	0.155	1.758	0.130	0.870	0.333	172188	149825	57266	128247	132439	
	25	18	209	0.086	30	25.2	1.0	0.847	0.152	1.778	0.151	0.840	0.325	163136	137055	53046	121043	120816	
	25	17.9	187	0.096	30	25.1	1.0	0.810	0.150	1.788	0.175	0.809	0.321	158955	128666	51087	117712	110702	
	25	17.8	170	0.105	30	24.9	1.0	0.778	0.149	1.798	0.202	0.780	0.318	156004	121693	49544	115298	101879	
	25	17.7	156	0.113	30	24.8	1.0	0.750	0.147	1.808	0.232	0.751	0.314	154110	115775	48349	113672	93992	
F	23	16.9	229	0.074	35	23.1	1.0	0.902	0.113	1.893	0.067	0.870	0.263	151842	132122	39892	109037	121858	
	23	16.8	202	0.083	35	22.9	1.0	0.863	0.112	1.905	0.078	0.840	0.258	144892	121659	37430	103804	111929	
	23	16.6	181	0.092	35	22.6	1.0	0.827	0.109	1.928	0.090	0.809	0.249	137423	111124	34273	97983	102084	
	23	16.5	165	0.100	35	22.5	1.0	0.796	0.108	1.939	0.104	0.779	0.245	131738	102657	32256	93701	94102	
	23	16.4	152	0.108	35	22.4	1.0	0.769	0.107	1.951	0.119	0.751	0.240	127916	96039	30731	90757	86993	
G	21	18.8	220	0.085	35	25.7	1.0	0.916	0.110	1.702	0.009	0.870	0.337	170993	148716	57665	127662	137667	
	21	18.7	194	0.096	35	25.5	1.0	0.879	0.108	1.711	0.010	0.839	0.334	163606	137187	54593	121925	126703	
	21	18.5	175	0.106	35	25.2	1.0	0.846	0.106	1.730	0.012	0.809	0.326	156017	126170	50937	115839	116380	
	21	18.4	159	0.116	35	25.1	1.0	0.815	0.105	1.739	0.013	0.777	0.323	149653	116336	48312	110905	107077	
	21	18.3	147	0.124	35	25.0	1.0	0.788	0.104	1.749	0.014	0.749	0.319	144257	108072	46036	106702	99294	

with: $h' = 17.5$ m; $d = 16$ m; $h_c = 17$ m; $h_s = 10.5$ m; $d_c = 6.5$

Segment	F ₁ [kN]	F _{H+} [kN]	F _{H-} [kN]	F _{SH} [kN]	F _{SV} [kN]	F _{Htot} [kN]	F _U [kN]	M _{FUR} [kNm]	M _{FHR} [kNm]	M _{FVR} [kNm]	M _{WR} [kNm]	M _{WT} [kNm]	S.F. _{SL} [-]	S.F. _{O.T.} [-]	σ _{max} [kN/m ²]	σ _{min} [kN/m ²]
C	1065	1045	3002	533	533	4579	2645	68810	63971	-17442	-294223	-37802	1.45	3.80	480	194
	1050	1030	2911	525	525	4466	2434	63321	62779	-17193	-294223	-37802	1.51	3.95	471	204
	1042	1022	2843	521	521	4387	2245	58400	62045	-17067	-294223	-37802	1.56	4.08	463	211
	1042	1023	2799	521	521	4343	2081	54136	61794	-17070	-294223	-37802	1.60	4.16	458	216
	1050	1030	2776	525	525	4332	1935	50340	62012	-17201	-294223	-37802	1.63	4.21	455	220
	1043	1023	2938	522	522	4483	2648	68873	62627	-17084	-294223	-37802	1.48	3.87	476	199
D	1003	987	2792	502	502	4281	2423	63041	60144	-16430	-294223	-37802	1.57	4.12	461	213
	969	961	2677	485	485	4122	2211	57521	58194	-15870	-294223	-37802	1.66	4.34	449	225
	952	947	2600	476	476	4024	2039	53032	57116	-15593	-294223	-37802	1.73	4.50	441	234
	942	941	2544	471	471	3956	1885	49045	56445	-15425	-294223	-37802	1.78	4.62	434	240
	974	976	2818	487	487	4281	2583	67180	59572	-15948	-294223	-37802	1.55	4.08	464	211
	914	924	2627	457	457	4007	2356	61285	56029	-14966	-294223	-37802	1.68	4.42	446	229
E	886	899	2517	443	443	3859	2159	56154	54264	-14511	-294223	-37802	1.78	4.65	434	240
	865	882	2430	433	433	3744	1987	51678	52943	-14171	-294223	-37802	1.86	4.85	425	249
	851	870	2361	425	425	3657	1833	47678	51994	-13929	-294223	-37802	1.93	5.01	418	256
	782	848	2485	391	391	3723	2376	61813	51120	-12803	-294223	-37802	1.80	4.80	430	244
	741	808	2332	371	371	3511	2183	56776	48469	-12142	-294223	-37802	1.94	5.15	416	259
	694	765	2175	347	347	3287	1991	51783	45589	-11370	-294223	-37802	2.10	5.57	401	274
G	661	733	2051	331	331	3114	1835	47734	43425	-10828	-294223	-37802	2.24	5.93	389	285
	638	711	1960	319	319	2989	1696	44128	41901	-10444	-294223	-37802	2.36	6.22	380	294
	973	971	2797	486	486	4255	2685	69832	59262	-15932	-294223	-37802	1.54	4.06	465	209
	927	928	2632	463	463	4023	2471	64271	56363	-15175	-294223	-37802	1.66	4.35	450	225
	876	884	2469	438	438	3790	2269	59034	53361	-14338	-294223	-37802	1.79	4.68	434	240
	836	847	2327	418	418	3592	2088	54315	50872	-13688	-294223	-37802	1.92	4.99	420	254
	802	816	2208	401	401	3424	1936	50367	48758	-13131	-294223	-37802	2.03	5.27	409	265

In the following two tables the results of the modified Goda theory of a section with device, at a water level of C.D. are shown in the following two tables. The used modification factors are $\lambda_1 = 1$, $\lambda_2 = 0$ and $\lambda_v = 1$. The wave conditions are the same as for the sections without device, however the angle of incidence $\beta = 0^\circ$.

Segment	η [m]	α_1 [-]	α_3 [-]	α_4 [-]	p_1 [N/m ²]	p_3 [N/m ²]	p_4 [N/m ²]	p_5 [N/m ²]	p_u [N/m ²]
C	26.4	0.880	0.870	0.261	156538	136236	40913	97849	136236
	26.4	0.839	0.840	0.261	149249	125367	39008	93294	125367
	26.4	0.803	0.810	0.261	142726	115625	37303	89216	115625
	26.4	0.771	0.782	0.261	137112	107182	35836	85707	107182
	26.4	0.743	0.754	0.261	132178	99666	34547	82623	99666
	28.2	0.880	0.870	0.309	167211	145525	51586	128669	145525
D	28.1	0.839	0.840	0.305	158577	133203	48336	121830	133203
	27.8	0.803	0.810	0.297	150025	121538	44602	114884	121538
	27.6	0.771	0.782	0.293	143344	112054	42068	109586	112054
	27.5	0.743	0.754	0.290	137435	103630	39804	104892	103630
	27.3	0.887	0.870	0.286	163135	141948	46610	124294	141948
	27.0	0.847	0.840	0.278	154132	129491	42814	117026	129491
E	26.9	0.810	0.809	0.274	146582	118650	40126	111096	118650
	26.7	0.778	0.780	0.270	139980	109193	37747	105902	109193
	26.6	0.750	0.751	0.266	134098	100741	35608	101268	100741
	25.4	0.902	0.870	0.231	153968	133972	35531	114489	133972
	25.2	0.863	0.840	0.226	146556	123057	33150	108754	123057
	24.9	0.827	0.809	0.217	138794	112233	30100	102563	112233
F	24.8	0.796	0.779	0.212	132765	103458	28162	97898	103458
	24.6	0.769	0.751	0.207	127387	95641	26409	93728	95641
	28.2	0.916	0.870	0.309	174025	151353	53689	133913	151353
	28.1	0.879	0.839	0.305	166125	139300	50637	127629	139300
	27.8	0.846	0.809	0.297	158218	127950	47038	121158	127950
	27.6	0.815	0.777	0.293	151437	117722	44443	115772	117722
G	27.5	0.788	0.749	0.290	145717	109165	42202	111212	109165

with: $h' = 17.5$ m; $d = 16$ m; $h_c = 19.5$ m; $h_s = 13$ m

Seg- ment	F ₁ [kN]	F _{H+} [kN]	F _{H-} [kN]	F _{SH} [kN]	F _{SV} [kN]	F _{H,tot} [kN]	F _U [kN]	M _{FUR} [kNm]	M _{FHR} [kNm]	M _{FVR} [kNm]	M _{WR} [kNm]	M _{WT} [kNm]	S.F.sL [-]	S.F.o.T. [-]	σ _{max} [kN/m ²]	σ _{min} [kN/m ²]
C	902	827	2562	604	424	3993	2657	69106	58312	-8266	-71696	37697	0.62	0.19	609	-284
	860	788	2403	576	404	3767	2445	63593	55365	-7882	-71696	37697	0.68	0.29	592	-267
	822	754	2261	551	387	3565	2255	58651	52727	-7537	-71696	37697	0.75	0.39	577	-252
	790	724	2138	529	371	3391	2090	54368	50454	-7241	-71696	37697	0.82	0.49	564	-239
	762	698	2029	510	358	3237	1943	50556	48452	-6980	-71696	37697	0.88	0.58	552	-227
	1172	962	2736	785	551	4483	2838	73818	68256	-10738	-71696	37697	0.54	0.13	653	-328
D	1106	911	2553	741	520	4205	2597	67567	64368	-10137	-71696	37697	0.61	0.22	632	-307
	1037	861	2376	695	487	3932	2370	61650	60441	-9501	-71696	37697	0.68	0.32	610	-285
	986	822	2235	660	463	3717	2185	56840	57431	-9034	-71696	37697	0.75	0.42	594	-269
	941	788	2109	630	442	3527	2021	52567	54763	-8620	-71696	37697	0.81	0.51	579	-254
	1111	934	2669	744	522	4348	2768	72004	65844	-10181	-71696	37697	0.56	0.15	642	-317
	1039	881	2482	696	488	4059	2525	65685	61728	-9522	-71696	37697	0.64	0.25	619	-294
E	983	837	2321	659	462	3817	2314	60186	58355	-9009	-71696	37697	0.71	0.35	601	-276
	934	799	2180	626	439	3605	2129	55389	55402	-8558	-71696	37697	0.77	0.45	584	-259
	890	765	2055	596	418	3416	1964	51101	52765	-8154	-71696	37697	0.84	0.54	570	-245
	975	872	2519	653	458	4045	2612	67958	60446	-8937	-71696	37697	0.62	0.21	617	-292
	922	830	2359	618	434	3807	2400	62421	57173	-8454	-71696	37697	0.69	0.31	598	-273
	862	784	2196	578	405	3559	2189	56931	53665	-7903	-71696	37697	0.77	0.42	579	-254
F	819	750	2067	549	385	3366	2017	52479	51008	-7510	-71696	37697	0.84	0.52	564	-239
	781	719	1951	523	367	3193	1865	48514	48633	-7157	-71696	37697	0.91	0.62	551	-226
	1219	1001	2847	817	573	4665	2951	76774	71032	-11176	-71696	37697	0.51	0.09	667	-342
	1159	955	2672	776	545	4404	2716	70660	67419	-10620	-71696	37697	0.57	0.17	647	-322
	1093	908	2504	732	514	4144	2495	64903	63730	-10020	-71696	37697	0.63	0.26	627	-302
	1041	868	2355	698	489	3921	2296	59715	60640	-9544	-71696	37697	0.69	0.35	609	-284
997	835	2230	668	469	3733	2129	55374	58026	-9139	-71696	37697	0.75	0.44	595	-270	

The following two tables show the results of the modified Goda theory of a section without device, at a water level of + 2.5 m C.D. The used modification factors are $\lambda_1 = 1$, $\lambda_2 = 1$ and λ_v as a function of H_{max}/L and d_c .

Segment	h [m]	H _{max} [m]	L [m]	H _{max} /L [-]	β [°]	η [m]	λ _v [-]	α ₁ [-]	α ₂ [-]	α ₁ [-]	α ₂ [-]	α ₁ [-]	α ₂ [-]	α ₃ [-]	α ₄ [-]	P ₁ [N/m ²]	P ₃ [N/m ²]	P ₄ [N/m ²]	P ₅ [N/m ²]	P _u [N/m ²]
C	28.5	17.6	251	0.070	7.5	26.3	0.92	0.864	0.106	2.102	0.114	0.106	0.853	0.448	171460	146219	76882	145369	130506	
	28.5	17.6	220	0.080	7.5	26.3	0.90	0.821	0.106	2.102	0.133	0.120	0.818	0.448	166283	136032	74561	140980	118935	
	28.5	17.6	197	0.089	7.5	26.3	0.88	0.784	0.106	2.102	0.153	0.139	0.785	0.448	162971	127895	73076	138172	108919	
	28.5	17.6	179	0.098	7.5	26.3	0.85	0.752	0.106	2.102	0.176	0.160	0.753	0.448	160949	121176	72169	136458	100243	
	28.5	17.6	164	0.107	7.5	26.3	0.83	0.724	0.106	2.102	0.203	0.184	0.722	0.448	160168	115571	71819	135796	92517	
D	28.5	20.4	251	0.081	30	28.6	0.87	0.864	0.142	1.814	0.091	0.142	0.853	0.492	186723	159235	91891	160562	141741	
	28.5	20.2	220	0.092	30	28.3	0.84	0.821	0.139	1.832	0.107	0.139	0.818	0.487	176268	144201	85859	151327	127908	
	28.5	20.1	197	0.102	30	28.1	0.81	0.784	0.138	1.841	0.125	0.147	0.785	0.485	169427	132962	82095	145336	116556	
	28.5	20	179	0.112	30	28.0	0.80	0.752	0.137	1.850	0.144	0.168	0.753	0.482	165574	124658	79801	141913	106738	
	28.5	19.9	164	0.121	30	27.9	0.80	0.724	0.135	1.859	0.166	0.193	0.722	0.479	162931	117565	78103	139530	98019	
E	27.5	19.8	247	0.080	30	27.7	0.87	0.870	0.125	1.869	0.074	0.125	0.852	0.477	179975	153394	85800	153995	138483	
	27.5	19.6	217	0.090	30	27.4	0.85	0.828	0.122	1.888	0.087	0.122	0.818	0.471	170036	139065	80154	145241	125187	
	27.5	19.5	194	0.101	30	27.3	0.82	0.791	0.121	1.897	0.102	0.121	0.784	0.469	162063	126994	75956	138309	113899	
	27.5	19.3	176	0.110	30	27.0	0.80	0.758	0.119	1.917	0.120	0.130	0.751	0.463	155704	116872	72118	132646	103534	
	27.5	19.2	162	0.119	30	26.9	0.80	0.731	0.118	1.927	0.138	0.148	0.720	0.460	152494	109846	70205	129793	95359	
F	25.5	18.5	239	0.077	35	25.2	0.90	0.884	0.092	2.000	0.041	0.092	0.852	0.426	160681	136845	68375	135217	127954	
	25.5	18.3	210	0.087	35	25.0	0.87	0.843	0.090	2.022	0.048	0.090	0.816	0.419	151808	123949	63646	127487	115699	
	25.5	18.2	189	0.096	35	24.8	0.85	0.807	0.089	2.033	0.056	0.089	0.783	0.416	144985	113591	60323	121629	105803	
	25.5	18.1	171	0.106	35	24.7	0.83	0.774	0.088	2.044	0.065	0.088	0.748	0.413	138467	103643	57164	116039	96325	
	25.5	18	157	0.115	35	24.6	0.81	0.745	0.087	2.056	0.076	0.087	0.716	0.410	132935	95187	54447	111283	88301	
G	23.5	17.2	231	0.074	35	23.5	0.92	0.898	0.061	2.151	0.012	0.061	0.852	0.382	148442	126401	56722	123140	120864	
	23.5	17.1	203	0.084	35	23.3	0.90	0.858	0.061	2.164	0.014	0.061	0.816	0.378	141242	115212	53460	117026	109999	
	23.5	16.9	183	0.092	35	23.1	0.88	0.824	0.059	2.189	0.017	0.059	0.782	0.371	134148	104954	49788	110876	100128	
	23.5	16.8	166	0.101	35	22.9	0.86	0.791	0.058	2.202	0.019	0.058	0.747	0.367	128209	95807	47104	105835	91279	
	23.5	16.7	153	0.109	35	22.8	0.84	0.764	0.058	2.216	0.021	0.058	0.715	0.364	123176	88095	44788	101552	83838	

with: $h' = 20$ m; $d = 18.5$ m; $h_c = 14.5$ m; $h_s = 10.5$ m; $d_c = 4.0$

Segment	F ₁ [kN]	F _{H+} [kN]	F _{H-} [kN]	F _{SH} [kN]	F _{SV} [kN]	F _{It,tot} [kN]	F _U [kN]	M _{FV/R} [kNm]	M _{FH/R} [kNm]	M _{FV/R} [kNm]	M _{W/R} [kNm]	M _{W/T} [kNm]	S.F.sL [-]	S.F.o.T. [-]	σ _{max} [kN/m ²]	σ _{min} [kN/m ²]
C	1167	583	2923	583	583	4089	2545	66200	63576	-19107	-276187	-36514	1.52	3.60	457	174
	1132	553	2721	566	566	3840	2319	60330	61271	-18530	-276187	-36514	1.65	3.83	443	188
	1109	530	2560	555	555	3644	2124	55250	59688	-18161	-276187	-36514	1.77	4.01	432	198
	1095	506	2398	548	548	3451	1955	50848	58605	-17935	-276187	-36514	1.89	4.15	424	207
	1090	491	2289	545	545	3325	1804	46929	57985	-17848	-276187	-36514	1.99	4.26	418	213
D	1325	604	3010	663	663	4277	2764	71899	70138	-21703	-276187	-36514	1.43	3.22	484	146
	1245	550	2692	623	623	3865	2494	64882	65704	-20391	-276187	-36514	1.62	3.53	462	169
	1194	510	2449	597	597	3556	2273	59124	62729	-19552	-276187	-36514	1.79	3.77	446	185
	1164	492	2322	582	582	3396	2081	54143	60903	-19060	-276187	-36514	1.91	3.96	434	196
	1143	484	2244	571	571	3299	1911	49720	59543	-18710	-276187	-36514	1.99	4.12	425	205
E	1259	581	2900	629	629	4111	2700	70246	67291	-20615	276187	-36514	1.49	3.37	473	157
	1183	536	2627	592	592	3755	2441	63501	63084	-19377	276187	-36514	1.67	3.68	452	179
	1125	493	2370	562	562	3425	2221	57776	59706	-18420	276187	-36514	1.86	3.97	434	196
	1075	461	2181	538	538	3179	2019	52518	56925	-17603	276187	-36514	2.04	4.24	419	211
	1050	452	2099	525	525	3075	1860	48371	55396	-17194	276187	-36514	2.14	4.42	410	220
F	1069	533	2678	534	534	3745	2495	64905	59161	-17503	-276187	-36514	1.66	3.87	441	190
	1003	486	2399	502	502	3387	2256	58689	55433	-16431	-276187	-36514	1.87	4.22	421	209
	955	453	2198	478	478	3129	2063	53669	52570	-15642	-276187	-36514	2.05	4.53	406	224
	909	422	2010	455	455	2887	1878	48861	49834	-14890	-276187	-36514	2.26	4.86	392	238
	870	396	1848	435	435	2678	1722	44791	47507	-14248	-276187	-36514	2.47	5.17	380	250
G	944	500	2529	472	472	3500	2357	61309	53942	-15462	-276187	-36514	1.78	4.27	420	211
	895	465	2308	448	448	3220	2145	55797	50931	-14656	-276187	-36514	1.97	4.61	404	227
	843	431	2104	422	422	2957	1952	50790	47965	-13812	-276187	-36514	2.18	4.99	388	242
	803	403	1927	401	401	2731	1780	46302	45488	-13148	-276187	-36514	2.40	5.34	375	255
	768	378	1775	384	384	2536	1635	42527	43387	-12581	-276187	-36514	2.61	5.68	364	266

In the following two tables, the results of the modified Goda theory of a section with device, at a water level of + 2.5 m C.D. are shown. The used modification factors are $\lambda_1 = 1$, $\lambda_2 = 0$ and $\lambda_3 = 1$. The wave conditions are the same as for the sections without device, however the angle of incidence $\beta = 0^\circ$.

Segment	η [m]	α_1 [-]	α_3 [-]	α_4 [-]	p_1 [N/m ²]	p_3 [N/m ²]	p_4 [N/m ²]	p_5 [N/m ²]	p_u [N/m ²]
C	26.4	0.864	0.853	0.356	153692	131066	54724	103458	131066
	26.4	0.821	0.818	0.356	146008	119446	51988	98286	119446
	26.4	0.784	0.785	0.356	139387	109387	49630	93828	109387
	26.4	0.752	0.753	0.356	133717	100673	47611	90012	100673
	26.4	0.724	0.722	0.356	128768	92914	45849	86681	92914
D	30.6	0.864	0.853	0.444	178143	151918	79175	154857	151918
	30.3	0.821	0.818	0.439	167578	137091	73557	145455	137091
	30.2	0.784	0.785	0.436	159186	124925	69429	138067	124925
	30.0	0.752	0.753	0.433	151951	114401	65846	131691	114401
	29.9	0.724	0.722	0.430	145596	105056	62677	126085	105056
E	29.7	0.870	0.852	0.428	174146	148426	74466	150692	148426
	29.4	0.828	0.818	0.422	164056	134175	69194	141736	134175
	29.3	0.791	0.784	0.419	155788	122077	65244	134484	122077
	29.0	0.758	0.751	0.413	147837	110967	61024	127411	110967
	28.8	0.731	0.720	0.410	141888	102206	58135	122181	102206
F	27.8	0.884	0.852	0.387	165177	140675	63988	141368	140675
	27.5	0.843	0.816	0.381	155790	127201	59308	133089	127201
	27.3	0.807	0.783	0.377	148470	116321	56016	126716	116321
	27.2	0.774	0.748	0.374	141484	105901	52894	120639	105901
	27.0	0.745	0.716	0.370	135579	97080	50214	115493	97080
G	25.8	0.898	0.852	0.341	156050	132879	53226	131856	132879
	25.7	0.858	0.816	0.337	148258	120935	49997	125138	120935
	25.4	0.824	0.782	0.329	140702	110082	46346	118501	110082
	25.2	0.791	0.747	0.325	134293	100354	43698	112976	100354
	25.1	0.764	0.715	0.321	128878	92173	41416	108299	92173

with: $h' = 20$ m; $d = 18.5$ m; $h_c = 17$ m; $h_s = 13.0$ m; $d_c = 4.0$

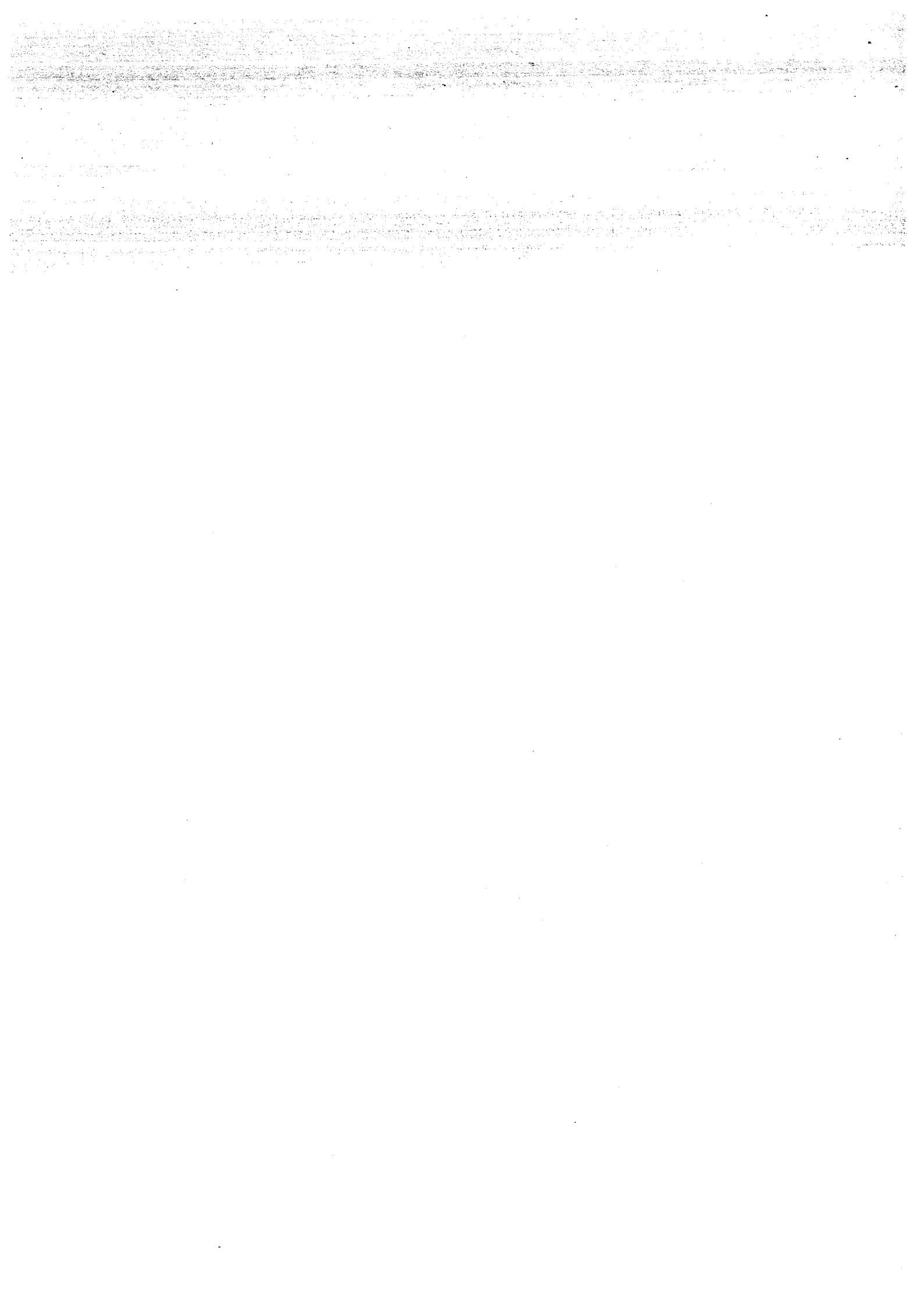
Segment	F ₁ [kN]	F _{H+} [kN]	F _{H-} [kN]	F _{SH} [kN]	F _{SV} [kN]	F _{H,rot} [kN]	F _T [kN]	M _{FUR} [kNm]	M _{FHR} [kNm]	M _{FVR} [kNm]	M _{WR} [kNm]	M _{WT} [kNm]	S.F.sl. [-]	S.F.o.T. [-]	σ _{max} [kN/m ²]	σ _{min} [kN/m ²]
C	1028	514	2848	689	483	4051	2556	66484	61486	-9423	-69056	34919	0.59	0.20	601	-291
	977	489	2655	654	459	3798	2329	60589	58073	-8952	-69056	34919	0.66	0.30	581	-272
	932	466	2488	625	438	3579	2133	55487	55129	-8546	-69056	34919	0.73	0.40	565	-255
	895	447	2344	599	420	3391	1963	51067	52602	-8199	-69056	34919	0.79	0.50	550	-241
	861	431	2217	577	405	3225	1812	47131	50386	-7895	-69056	34919	0.86	0.59	538	-228
D	1521	666	3301	1019	715	4986	2962	77061	79584	-13942	-69056	34919	0.46	0.07	682	-373
	1424	626	3047	954	669	4627	2673	69540	74314	-13047	-69056	34919	0.52	0.17	654	-345
	1349	595	2841	904	634	4339	2436	63369	70161	-12361	-69056	34919	0.59	0.26	632	-322
	1284	567	2664	860	603	4091	2231	58031	66573	-11768	-69056	34919	0.65	0.34	612	-303
	1227	543	2507	822	577	3872	2049	53290	63412	-11245	-69056	34919	0.71	0.43	595	-286
E	1464	650	3226	981	688	4856	2894	75290	77280	-13413	-69056	34919	0.47	0.09	672	-362
	1371	612	2982	919	644	4512	2616	68061	72257	-12566	-69056	34919	0.54	0.19	645	-335
	1298	581	2779	870	610	4229	2380	61924	68179	-11898	-69056	34919	0.61	0.28	622	-313
	1225	550	2588	821	576	3959	2164	56288	64218	-11226	-69056	34919	0.67	0.37	601	-292
	1172	528	2441	785	551	3754	1993	51844	61271	-10742	-69056	34919	0.73	0.46	585	-276
F	1335	613	3059	894	627	4566	2743	71358	72132	-12234	-69056	34919	0.52	0.14	647	-338
	1251	578	2830	838	588	4246	2480	64523	67484	-11462	-69056	34919	0.59	0.24	622	-313
	1188	550	2648	796	558	3994	2268	59004	63898	-10886	-69056	34919	0.65	0.33	603	-293
	1128	524	2474	756	530	3754	2065	53718	60475	-10338	-69056	34919	0.72	0.42	584	-275
	1077	502	2327	722	506	3550	1893	49244	57575	-9872	-69056	34919	0.79	0.52	568	-259
G	1203	576	2889	806	565	4271	2591	67404	66882	-11026	-69056	34919	0.56	0.19	623	-313
	1138	547	2692	763	535	4001	2358	61345	63088	-10433	-69056	34919	0.63	0.29	602	-292
	1072	518	2508	718	504	3744	2147	55840	59366	-9820	-69056	34919	0.70	0.39	582	-272
	1018	495	2346	682	479	3523	1957	50905	56254	-9334	-69056	34919	0.78	0.49	565	-255
	973	474	2211	652	457	3337	1797	46755	53618	-8919	-69056	34919	0.84	0.58	550	-241

The following two tables show the results of the modified Goda theory of a section without device, at a water level of + 5 m C.D. The used modification factors are $\lambda_1 = 1$, $\lambda_2 = 1$ and λ_v as a function of H_{max}/L .

Segment	h [m]	H _{max} [m]	L [m]	H _{max} /L [-]	β [°]	η [m]	λ _v [-]	α ₁ [-]	α ₂ [-]	α ₂ [-]	α ₁ [-]	α ₁ [-]	α ₁ [-]	α ₃ [-]	α ₄ [-]	p ₁ [N/m ²]	p ₃ [N/m ²]	p ₄ [N/m ²]	p ₅ [N/m ²]	P _u [N/m ²]
C	28.5	17.6	260	0.068	7.5	26.3	0.83	0.849	0.076	2.386	0.071	0.076	0.076	0.835	0.544	163395	136451	88805	154071	125473
	28.5	17.6	228	0.077	7.5	26.3	0.80	0.805	0.076	2.386	0.083	0.083	0.083	0.797	0.544	156890	125079	85270	147938	113607
	28.5	17.6	203	0.087	7.5	26.3	0.80	0.766	0.076	2.386	0.096	0.096	0.096	0.759	0.544	152285	115602	82767	143595	102923
	28.5	17.6	184	0.096	7.5	26.3	0.80	0.734	0.076	2.386	0.110	0.110	0.110	0.724	0.544	149138	107933	81057	140627	94031
	28.5	17.6	168	0.105	7.5	26.3	0.80	0.706	0.076	2.386	0.127	0.127	0.127	0.689	0.544	147178	101367	79991	138780	86121
D	28.5	20.5	260	0.079	30	28.7	0.80	0.849	0.102	2.049	0.076	0.102	0.102	0.835	0.582	178836	149346	104036	169486	136943
	28.5	20.9	228	0.092	30	29.2	0.80	0.805	0.107	2.010	0.088	0.107	0.107	0.797	0.590	174301	138960	102793	165362	126412
	28.5	21.1	203	0.104	30	29.5	0.80	0.766	0.109	1.991	0.102	0.109	0.109	0.759	0.594	168503	127914	100029	159944	115620
	28.5	21.1	184	0.115	30	29.5	0.80	0.734	0.109	1.991	0.116	0.116	0.116	0.724	0.594	163267	118159	96920	154974	105630
	28.5	21.1	168	0.126	30	29.5	0.80	0.706	0.109	1.991	0.133	0.133	0.133	0.689	0.594	160285	110395	95150	152143	96745
E	27.5	20.5	257	0.080	30	28.7	0.80	0.855	0.095	2.049	0.058	0.095	0.095	0.835	0.582	179125	149635	104203	169759	138096
	27.5	20.9	225	0.093	30	29.2	0.80	0.811	0.099	2.010	0.066	0.099	0.099	0.797	0.590	174498	139018	102909	165549	127357
	27.5	21.0	201	0.104	30	29.4	0.80	0.773	0.100	2.000	0.076	0.100	0.100	0.759	0.592	167946	127504	99373	159375	116231
	27.5	20.9	182	0.115	30	29.2	0.80	0.741	0.099	2.010	0.087	0.099	0.099	0.723	0.590	160578	116079	94700	152344	105498
	27.5	20.8	166	0.125	30	29.1	0.80	0.712	0.098	2.019	0.099	0.099	0.099	0.687	0.588	154281	105961	90682	146331	95923
F	25.5	20.1	249	0.081	35	27.4	0.80	0.867	0.076	2.090	0.026	0.076	0.076	0.834	0.562	169683	141533	95433	160402	133640
	25.5	19.9	218	0.091	35	27.2	0.80	0.824	0.075	2.111	0.030	0.075	0.075	0.794	0.558	159869	127009	89211	151037	119713
	25.5	19.8	196	0.101	35	27.0	0.80	0.788	0.074	2.121	0.034	0.074	0.074	0.758	0.556	152450	115575	84731	143985	108718
	25.5	19.7	177	0.111	35	26.9	0.80	0.754	0.073	2.132	0.039	0.073	0.073	0.720	0.554	145430	104650	80501	137314	98239
	25.5	19.6	163	0.120	35	26.7	0.80	0.728	0.073	2.143	0.044	0.073	0.073	0.686	0.551	139854	95945	77096	132009	89925
G	23.5	18.8	241	0.078	35	25.7	0.80	0.880	0.051	2.234	0.005	0.051	0.051	0.833	0.532	158047	131693	84107	148805	126730
	23.5	18.7	212	0.088	35	25.5	0.80	0.839	0.051	2.246	0.005	0.051	0.051	0.794	0.530	150100	119219	79502	141275	114563
	23.5	18.5	190	0.097	35	25.2	0.80	0.803	0.050	2.270	0.006	0.050	0.050	0.756	0.525	142135	107435	74561	133688	103145
	23.5	18.4	173	0.106	35	25.1	0.80	0.771	0.049	2.283	0.007	0.049	0.049	0.719	0.522	135967	97807	70974	127843	93790
	23.5	18.3	159	0.115	35	25.0	0.80	0.743	0.049	2.295	0.007	0.049	0.049	0.684	0.519	130502	89230	67780	122661	85474

with: $h' = 22.5$ m; $d = 21.0$ m; $h_c = 12.0$ m; $h_s = 10.5$ m; $d_c = 1.5$

Segment	F ₁ [kN]	F _{H+} [kN]	F _{H-} [kN]	F _{SH} [kN]	F _{SV} [kN]	F _{H,lot} [kN]	F _U [kN]	M _{FUR} [kNm]	M _{FUR} [kNm]	M _{FVR} [kNm]	M _{WR} [kNm]	M _{WT} [kNm]	S.F.SL [-]	S.F.O.T. [-]	σ _{max} [kN/m ²]	σ _{min} [kN/m ²]
C	1275	198	2800	638	638	3635	2447	63264	-20880	-258151	-35226	-35226	1.59	3.40	433	153
	1224	183	2538	612	612	3333	2215	60243	-20049	-258151	-35226	-35226	1.77	3.66	417	170
	1188	178	2411	594	594	3183	2007	57984	-19460	-258151	-35226	-35226	1.89	3.89	403	183
	1164	174	2314	582	582	3069	1834	47697	-19058	-258151	-35226	-35226	1.99	4.07	393	193
	1149	172	2237	574	574	2983	1679	43685	-18807	-258151	-35226	-35226	2.08	4.23	385	201
	1436	209	2954	718	718	3881	2670	69465	-23514	-258151	-35226	-35226	1.47	3.04	461	126
	1408	204	2819	704	704	3727	2465	64123	-23053	-258151	-35226	-35226	1.56	3.21	447	139
	1365	197	2668	682	682	3547	2255	58648	-22349	-258151	-35226	-35226	1.67	3.42	432	154
	1322	191	2533	661	661	3385	2060	53581	-21655	-258151	-35226	-35226	1.78	3.63	419	168
	1298	187	2436	649	649	3273	1887	49074	-21259	-258151	-35226	-35226	1.87	3.79	408	178
E	1438	209	2959	719	719	3887	2693	70050	-23552	-258151	-35226	-35226	1.46	3.03	462	125
	1409	204	2822	705	705	3730	2483	64602	-23079	-258151	-35226	-35226	1.55	3.20	448	138
	1358	196	2659	679	679	3535	2267	58959	-22244	-258151	-35226	-35226	1.67	3.42	432	154
	1297	188	2490	648	648	3326	2057	53514	-21238	-258151	-35226	-35226	1.81	3.68	415	171
	1244	180	2342	622	622	3145	1870	48657	-20376	-258151	-35226	-35226	1.94	3.94	400	186
	1343	198	2801	672	672	3671	2606	67789	-21994	-258151	-35226	-35226	1.55	3.22	446	140
	1261	187	2582	631	631	3399	2334	60725	-20654	-258151	-35226	-35226	1.72	3.54	424	162
	1201	178	2412	600	600	3190	2120	55147	-19662	-258151	-35226	-35226	1.86	3.83	407	180
	1144	170	2251	572	572	2992	1916	49832	-18725	-258151	-35226	-35226	2.02	4.13	390	196
	1098	163	2122	549	549	2834	1754	45615	-17976	-258151	-35226	-35226	2.17	4.39	377	209
G	1223	184	2608	611	611	3403	2471	64284	-20023	-258151	-35226	-35226	1.69	3.51	426	160
	1159	175	2424	580	580	3178	2234	58113	-18980	-258151	-35226	-35226	1.85	3.81	408	179
	1093	165	2246	547	547	2958	2011	52320	-17903	-258151	-35226	-35226	2.02	4.16	390	197
	1044	158	2104	522	522	2784	1829	47575	-17092	-258151	-35226	-35226	2.18	4.46	375	211
	1000	152	1978	500	500	2629	1667	43357	-16372	-258151	-35226	-35226	2.34	4.76	362	224



Seg- ment	F ₁ [kN]	F _{H+} [kN]	F _{H-} [kN]	F _{SH} [kN]	F _{SV} [kN]	F _{H,tot} [kN]	F _U [kN]	M _{FUR} [kNm]	M _{FHR} [kNm]	M _{FVR} [kNm]	M _{WR} [kNm]	M _{WT} [kNm]	S.F. _{SL} [-]	S.F. _{o.T.} [-]	σ _{max} [kN/m ²]	σ _{min} [kN/m ²]
C	1367	220	3115	916	643	4251	2457	63920	69141	12530	66416	32140	0.55	0.22	610	-316
	1297	209	2894	869	609	3971	2225	57875	65118	11884	66416	32140	0.62	0.31	588	-294
	1234	198	2695	827	580	3720	2016	52432	61518	11307	66416	32140	0.69	0.41	568	-274
	1182	190	2530	792	556	3513	1841	47902	58561	10836	66416	32140	0.76	0.50	552	-258
	1138	183	2386	762	535	3331	1687	43873	55988	10428	66416	32140	0.82	0.59	538	-244
	1690	257	3628	1133	794	5018	2862	74452	82560	15493	66416	32140	0.44	0.09	673	-379
D	1646	249	3436	1103	773	4787	2642	68727	79514	15081	66416	32140	0.48	0.16	655	-361
	1586	239	3231	1062	745	4532	2416	62859	75958	14533	66416	32140	0.54	0.24	635	-341
	1520	229	3034	1018	714	4281	2208	57428	72322	13927	66416	32140	0.59	0.32	616	-322
	1462	220	2860	980	687	4061	2022	52598	69157	13404	66416	32140	0.65	0.39	598	-304
	1704	259	3658	1142	801	5059	2886	75079	83233	15618	66416	32140	0.43	0.08	676	-382
	1659	251	3463	1112	780	4826	2662	69241	80157	15205	66416	32140	0.48	0.15	658	-364
E	1591	240	3248	1066	748	4554	2429	63192	76300	14585	66416	32140	0.53	0.23	637	-343
	1515	229	3032	1015	712	4276	2205	57357	72202	13881	66416	32140	0.59	0.32	615	-321
	1447	219	2841	970	680	4029	2005	52151	68591	13262	66416	32140	0.66	0.40	596	-302
	1682	258	3635	1127	791	5019	2865	74528	82484	15418	66416	32140	0.44	0.09	673	-379
	1576	242	3344	1056	741	4643	2566	66762	76901	14448	66416	32140	0.50	0.18	643	-349
	1498	231	3118	1003	704	4352	2331	60630	72643	13725	66416	32140	0.57	0.27	620	-326
F	1423	219	2904	953	669	4076	2106	54786	68612	13041	66416	32140	0.63	0.36	598	-304
	1364	211	2733	914	641	3858	1928	50150	65415	12498	66416	32140	0.69	0.44	581	-287
	1557	244	3449	1043	732	4736	2717	70675	77461	14271	66416	32140	0.47	0.13	649	-355
	1474	232	3201	987	693	4420	2456	63890	72875	13505	66416	32140	0.54	0.22	624	-330
	1388	219	2964	930	652	4112	2211	57522	68333	12722	66416	32140	0.61	0.32	600	-306
	1323	209	2773	887	622	3868	2011	52305	64787	12128	66416	32140	0.67	0.41	581	-287
G	1266	201	2603	848	595	3652	1832	47667	61644	11603	66416	32140	0.74	0.49	564	-270

The averaged safety factors and rubble mound stresses are given in this last table.

Segment	C.D.						+ 2.5 m C.D.						+ 5 m C.D.					
	S.F. _{SL} [-]	S.F. _{O.T.} [-]	σ_{max} [kN/m ²]	σ_{min} [kN/m ²]	S.F. _{SL} [-]	S.F. _{O.T.} [-]	σ_{max} [kN/m ²]	σ_{min} [kN/m ²]	S.F. _{SL} [-]	S.F. _{O.T.} [-]	σ_{max} [kN/m ²]	σ_{min} [kN/m ²]	S.F. _{SL} [-]	S.F. _{O.T.} [-]	σ_{max} [kN/m ²]	σ_{min} [kN/m ²]		
C	1.26	2.97	510	84	1.30	2.82	490	67	1.35	2.67	474	46	1.35	2.67	474	46		
	1.32	3.11	499	96	1.42	3.02	474	82	1.51	2.89	456	63	1.51	2.89	456	63		
	1.38	3.23	489	105	1.53	3.18	462	94	1.61	3.09	441	78	1.61	3.09	441	78		
	1.42	3.32	482	112	1.64	3.31	453	104	1.71	3.26	429	90	1.71	3.26	429	90		
	1.46	3.38	477	117	1.73	3.42	445	112	1.79	3.39	420	99	1.79	3.39	420	99		
D	1.26	3.01	516	78	1.21	2.50	529	27	1.23	2.36	509	10	1.23	2.36	509	10		
	1.35	3.22	500	94	1.37	2.76	506	51	1.31	2.51	495	24	1.31	2.51	495	24		
	1.44	3.42	486	108	1.51	2.97	488	68	1.41	2.69	479	40	1.41	2.69	479	40		
	1.50	3.56	476	118	1.62	3.13	475	82	1.51	2.87	464	56	1.51	2.87	464	56		
	1.56	3.68	468	127	1.70	3.27	464	93	1.59	3.01	452	67	1.59	3.01	452	67		
E	1.32	3.18	505	90	1.26	2.62	518	38	1.22	2.35	511	8	1.22	2.35	511	8		
	1.44	3.47	485	109	1.41	2.88	496	61	1.31	2.50	496	23	1.31	2.50	496	23		
	1.53	3.67	472	122	1.57	3.12	477	79	1.41	2.69	479	40	1.41	2.69	479	40		
	1.61	3.84	462	133	1.73	3.35	461	96	1.53	2.91	461	59	1.53	2.91	461	59		
	1.68	3.99	453	142	1.82	3.51	450	107	1.65	3.13	445	74	1.65	3.13	445	74		
F	1.53	3.75	473	121	1.39	3.01	488	69	1.30	2.50	498	21	1.30	2.50	498	21		
	1.65	4.04	458	137	1.57	3.31	467	89	1.44	2.77	474	45	1.44	2.77	474	45		
	1.79	4.39	442	153	1.73	3.57	451	105	1.57	3.01	456	64	1.57	3.01	456	64		
	1.92	4.69	429	165	1.91	3.84	436	121	1.70	3.26	438	81	1.70	3.26	438	81		
	2.03	4.94	419	175	2.08	4.10	423	134	1.83	3.49	424	95	1.83	3.49	424	95		
G	1.31	3.15	511	83	1.50	3.34	466	91	1.41	2.73	477	42	1.41	2.73	477	42		
	1.41	3.39	495	100	1.67	3.62	449	108	1.55	2.99	457	62	1.55	2.99	457	62		
	1.53	3.67	478	116	1.84	3.93	433	124	1.70	3.28	438	81	1.70	3.28	438	81		
	1.64	3.92	464	131	2.03	4.23	419	138	1.84	3.53	422	97	1.84	3.53	422	97		
	1.74	4.16	452	143	2.21	4.51	407	150	1.97	3.78	409	111	1.97	3.78	409	111		

Appendix M Calculation of Concrete Dimensions

In this appendix, thicknesses of several parts of the caisson are determined. The used concrete is B35 and the reinforcement steel FeB500. With the plastic analysis with the aid of yield lines, the distribution of forces can be determined. With Table M.1 of the T.G.B. 1990, the reinforcement percentage ω_0 can be determined. The thickness of the concrete is determined for the maximum moment and shear force. For a practical design, the reinforcement has to be calculated in all directions.

Front wall caisson

maximum load:

$$\text{wave: } 1.0 \cdot \rho \cdot g \cdot H = 1.0 \cdot 1030 \cdot 9.81 \cdot 21 = 212190 \text{ N/m}^2$$

$$\text{hydrostatic: } \rho \cdot g \cdot h = 21.5 \cdot 1030 \cdot 9.81 = 227347 \text{ N/m}^2$$

$$\text{ballast sand: } \rho \cdot g \cdot h \cdot 0.5 = 2000 \cdot 9.81 \cdot 4.5 = 41690 \text{ N/m}^2$$

(neutral soil stress, $h < 4.25$)

force distribution:

$$\begin{aligned} F &= 0.5 \cdot 2.25 \cdot 4.5 \cdot 212190 = 1074 \text{ kN} \\ M_{yy,tot} &= 2.25/3 \cdot 1074 = 806 \text{ kNm} \\ &= \cdot \text{safety factor } 1.5 = 1209 \text{ kNm} \\ M_{yy,max} &= 3/2 \cdot 1209 \cdot 1/4.5 = 403 \text{ kNm} \\ M_{yy,field} &= 1/8 \cdot 403 = 50 \text{ kNm} \\ M_{yy,support} &= 7/8 \cdot 403 = 353 \text{ kNm} \\ M_{xx,max} &= 1/8 \cdot 212190 \cdot 4.5^2 = 537 \text{ kNm} \\ &= \cdot \text{safety factor } 1.5 = 806 \text{ kNm} \\ M_{xx,field} &= 1/3 \cdot 806 = 269 \text{ kNm} \\ M_{xx,support} &= 2/3 \cdot 806 = 537 \text{ kNm} \\ V_{yy,max} &= 3/2 \cdot 1074 \cdot 1/4.5 = 358 \text{ kN} \\ &= \cdot \text{safety factor } 1.5 = 537 \text{ kNm} \\ V_{xx,max} &= 1/2 \cdot 212190 \cdot 4.5 = 478 \text{ kNm} \\ &= \cdot \text{safety factor } 1.5 = 717 \text{ kNm} \end{aligned}$$

thickness: 0.5 m

maximum moment: 537 kNm

$$M/b \cdot d^2: 537 / (1.0 \cdot (0.8 \cdot 0.5)^2) = 3356$$

ω_0 : 0.85%

$$V_{concrete} = \tau_1 \cdot b \cdot d = 0.56 \cdot 10^{-3} \cdot 1.0 \cdot 0.4 = 224 \text{ kN}$$

For the shear force, reinforcement is required what has to withstand $717 - 224 = 493$ kN. This is $493 / (0.435 \cdot 0.4) = 2833 \text{ mm}^2/\text{m}$.

Front wall and roof of the air chamber

The maximum pressure distribution for these parts is the same as for the front wall of the caisson, namely $1.0 \cdot \rho \cdot g \cdot H$. The maximum spans will not be more than about 4.5 m. A thickness of 0.5 m will be sufficient, but to avoid a high reinforcement percentage in this sloping wall a thickness of 1.0 m is selected. The immersed front wall has a thickness of 1.5 m for wave power conversion reasons.

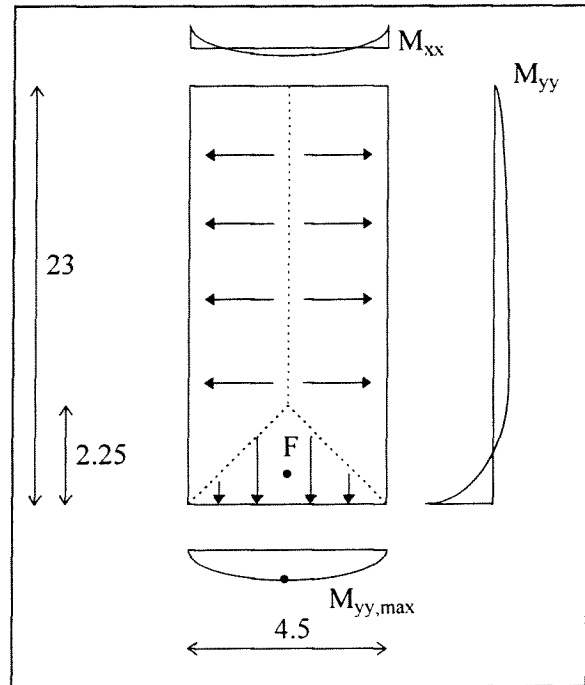


Figure M.1 Force distribution in the front wall

Chamber dividing walls

The maximum pressure distribution for these parts is $0.5 \cdot \rho \cdot g \cdot H$. The spans can be quite long. A thickness of 0.5 m is assumed to be sufficient.

Side walls and back wall of the chamber

The maximum pressure distribution for these walls is $1.0 \cdot \rho \cdot g \cdot H$. The maximum spans will not be more than about 4.5 m. A thickness of 0.5 m will be sufficient.

'Harbour' side walls

The pressure distribution of these parts is assumed to be between $0.5 \cdot \rho \cdot g \cdot H$ and $1.0 \cdot \rho \cdot g \cdot H$, because waves will not attack normally incident and no air pressure exists. These walls will have the same thickness as the chamber side walls, 0.5 m.

Inner cell walls

On both sides of the inner cell walls (in the width direction) ballast sand is placed. There does not exist a pressure difference. The walls have to be strong enough to support the top structure. A thickness of 0.25 m is sufficient.

Inner cell (shear) walls

The inner cell walls in the length direction act as shear walls. They receive the wave forces of the front wall and the sloping top. The thickness must be sufficient for the occurring moment and shear force. They also support the top structure.

Vertical wave force of the vertical wall per shear wall:

$$1.0 \cdot \rho \cdot g \cdot H \cdot 4.5 \cdot 23 = 21962 \text{ kN} \quad \text{moment: } 21962 \cdot (23/2) = 252563 \text{ kNm}$$

Vertical wave force of the sloping structure per shear wall:

$$0.5 \cdot (1.0 \cdot \rho \cdot g \cdot H \cdot 4.5 \cdot 10.5) = 5013 \text{ kN} \quad \text{moment: } 5013 \cdot (23 + 10.5/2) = 141617 \text{ kNm}$$

$$\text{wall thickness: } 0.25 \text{ m}$$

$$\text{maximum force: } 26975 \cdot 1.5 (\text{S.F.}) = 40463 \text{ kN}$$

$$\text{maximum moment: } 394180 \cdot 1.5 (\text{S.F.}) = 591284 \text{ kNm}$$

$$M/b \cdot d^2: \quad 591284 / (0.25 \cdot (0.8 \cdot 33)^2) = 3393$$

$$\omega_0: \quad 0.86\%$$

$$V_{\text{concrete}}: \tau_1 \cdot b \cdot d = 0.56 \cdot 10^3 \cdot 0.25 \cdot (0.8 \cdot 33) = 3696 \text{ kN}$$

For the shear force, reinforcement is required what has to withstand $40463 - 3696 = 36767 \text{ kN}$. This is $36767 / (0.435 \cdot 26.4) = 3202 \text{ mm}^2/\text{m}$.

Side walls caisson

No direct wave attack after placement. The largest loading is the water pressure at the lowest point below sea level. A thickness of 0.5 m is sufficient.

Back wall caisson

Reduced wave conditions, like the side walls the wall must be strong enough to withstand the water pressure at the lowest point. A thickness of 0.5 m is sufficient.

Bottom plate

The calculation of the bottom plate is more complex. The bottom is loaded by uplift pressure, hydrostatic pressure, rubble mound stress and the weight of the caisson. The bottom plate must be able to resist the most severe combination of these loadings. Two combinations have been investigated. The combination of a sea level at C.D. (low hydrostatic pressure) without waves, in that case no uplift pressure exists and a low rubble mound stress. And a combination of a sea level at +5 m C.D. and severe wave conditions.

The bottom plate of a section without device is calculated, because at the section with device the bottom plate has a thickness of 3 m, what will sufficient.

Weight: caisson $24 \cdot 2000 \cdot 9.81 = 471 \text{ kN/m}^2$
top structure $10.5 \cdot 2400 \cdot 9.81 = 247 \text{ kN/m}^2$

Combination no waves, sea level C.D.

Hydrostatic pressure: $1030 \cdot 9.81 \cdot 17.5 = 177 \text{ kN/m}^2$
Rubble mound stress: 337 kN/m^2

Combination waves, sea level + 5 m C.D.

Wave pressure at the sloping top: $1.0 \cdot 1030 \cdot 9.81 \cdot 21 = 106 \text{ kN/m}^2$
Wave uplift pressure: 140 kN/m^2
Hydrostatic pressure: $1030 \cdot 9.81 \cdot 22.5 = 227 \text{ kN/m}^2$
Rubble mound stress: $\sigma_{\min} = 10 \text{ kN/m}^2$
 $\sigma_{\max} = 510 \text{ kN/m}^2$

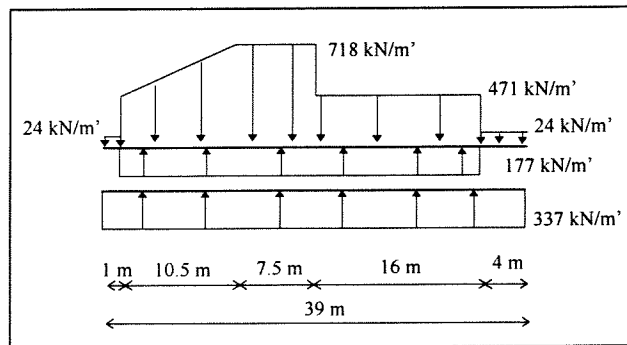


Figure M.2 Pressure on the bottom plate, no waves

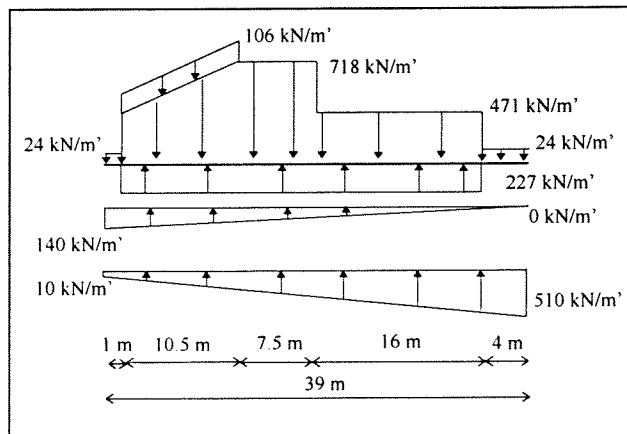


Figure M.3 Pressure on the bottom plate, with waves

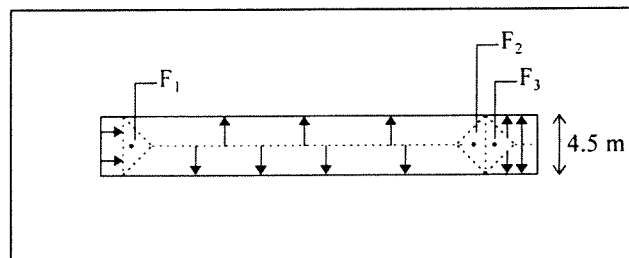


Figure M.4 Force distribution on the bottom plate

The largest moment M_{xx} occurs at 11.5 m from the left, when the caisson is attacked by waves. In this situation also the back toe has the most severe loading. The front toe has the highest loading when no waves exist.

Bottom plate at 11.5 m from the left

$$\begin{aligned}
 M_{xx,max} &= 1/8 \cdot 341 \cdot 4.5^2 &= 863 \text{ kNm} \\
 &= \cdot \text{safety factor } 1.5 &= 1295 \text{ kNm} \\
 M_{xx,field} &= 1/3 \cdot 806 &= 432 \text{ kNm} \\
 M_{xx,support} &= 2/3 \cdot 806 &= 863 \text{ kNm} \\
 V_{xx,max} &= 1/2 \cdot 341 \cdot 4.5 &= 767 \text{ kNm} \\
 &= \cdot \text{safety factor } 1.5 &= 1150 \text{ kNm}
 \end{aligned}$$

$$\begin{aligned}
 \text{thickness:} & & 1.0 \text{ m} \\
 M/b \cdot d^2: & & 863 / (1.0 \cdot (0.8 \cdot 1.0)^2) = 1348 \\
 \omega_0: & & 0.32\% \\
 V_{concrete} = \tau_1 \cdot b \cdot d &= & 0.56 \cdot 10^{-3} \cdot 1.0 \cdot 0.8 = 448 \text{ kN}
 \end{aligned}$$

For the shear force, reinforcement is required what has to withstand $1150 - 448 = 702 \text{ kN}$.
This is $702 / (0.435 \cdot 0.8) = 2017 \text{ mm}^2/\text{m}$.

$$\begin{aligned}
 F_1 &= 0.5 \cdot 2.25 \cdot 4.5 \cdot 301 &= 1524 \text{ kN} \\
 M_{yy,tot} &= 2.25/3 \cdot 1524 &= 1143 \text{ kNm} \\
 &= \cdot \text{safety factor } 1.5 &= 1715 \text{ kNm} \\
 M_{yy,max} &= 3/2 \cdot 1715 \cdot 1/4.5 &= 572 \text{ kNm} \\
 M_{yy,field} &= 1/8 \cdot 403 &= 72 \text{ kNm} \\
 M_{yy,support} &= 7/8 \cdot 403 &= 504 \text{ kNm} \\
 V_{yy,max} &= 3/2 \cdot 1524 \cdot 1/4.5 &= 508 \text{ kN} \\
 &= \cdot \text{safety factor } 1.5 &= 762 \text{ kN}
 \end{aligned}$$

$$\begin{aligned}
 M/b \cdot d^2: & & 572 / (1.0 \cdot (0.8 \cdot 1.0)^2) = 894 \\
 \omega_0: & & 0.21\% \\
 V_{concrete} = \tau_1 \cdot b \cdot d &= & 0.56 \cdot 10^{-3} \cdot 1.0 \cdot 0.8 = 448 \text{ kN}
 \end{aligned}$$

For the shear force, reinforcement is required what has to withstand $762 - 448 = 314 \text{ kN}$.
This is $314 / (0.435 \cdot 0.8) = 902 \text{ mm}^2/\text{m}$.

Back toe

$$\begin{aligned}
 F_3 &= 0.5 \cdot 2.25 \cdot 4.5 \cdot 460 &= 2329 \text{ kN} \\
 M_{yy,tot} &= 2.25/3 \cdot 2329 &= 1747 \text{ kNm} \\
 &= \cdot \text{safety factor } 1.5 &= 2620 \text{ kNm} \\
 M_{yy,max} &= 3/2 \cdot 2620 \cdot 1/4.5 &= 873 \text{ kNm} \\
 M_{yy,field} &= 1/8 \cdot 873 &= 109 \text{ kNm} \\
 M_{yy,support} &= 7/8 \cdot 873 &= 764 \text{ kNm} \\
 V_{yy,max} &= 3/2 \cdot 2329 \cdot 1/4.5 &= 776 \text{ kN} \\
 &= \cdot \text{safety factor } 1.5 &= 1165 \text{ kN} \\
 M_{xx,max} &= 1/8 \cdot 460 \cdot 4.5^2 &= 1164 \text{ kNm} \\
 &= \cdot \text{safety factor } 1.5 &= 1747 \text{ kNm} \\
 M_{xx,field} &= 1/3 \cdot 1747 &= 582 \text{ kNm} \\
 M_{xx,support} &= 2/3 \cdot 1747 &= 1164 \text{ kNm} \\
 V_{xx,max} &= 1/2 \cdot 460 \cdot 4.5 &= 1035 \text{ kNm} \\
 &= \cdot \text{safety factor } 1.5 &= 1553 \text{ kNm}
 \end{aligned}$$

thickness: 1.0 m
 maximum moment: 1164 kNm
 $M/b \cdot d^2: 1164 / (1.0 \cdot (0.8 \cdot 1.0)^2) = 1819$
 $\omega_0: 0.43\%$
 $V_{\text{concrete}} = \tau_1 \cdot b \cdot d = 0.56 \cdot 10^{-3} \cdot 1.0 \cdot 0.8 = 448 \text{ kN}$

For the shear force reinforcement is required what has to withstand $1553 - 448 = 1105 \text{ kN}$. This is $1105 / (0.435 \cdot 0.8) = 3175 \text{ mm}^2/\text{m}$.

Front toe

Maximum load when there are no waves and a sea level at C.D. The maximum load is 313 kN/m^2 . A thickness of 1.0 m will be sufficient.

Shear wall back toe

The back toe will be connected to the back wall by shear walls. The moment on these shear force and moment on these walls are:

$$2 \cdot \{0.5 \cdot 2.25 \cdot 460\} = 1035 \text{ kN} \quad \cdot 2.25/3 = 776 \text{ kNm}$$

$$2 \cdot \{1.75 \cdot 2.25 \cdot 460\} = 3623 \text{ kN} \quad \cdot (2.25 + 1.75/2) = 11320 \text{ kNm}$$

$$\text{total force: } 4658 \cdot 1.5 (\text{S.F.}) = 6987 \text{ kN}$$

$$\text{total moment: } 12069 \cdot 1.5 (\text{S.F.}) = 18144 \text{ kNm}$$

thickness: 0.5 m
 $M/b \cdot d^2: 18144 / (0.5 \cdot (0.8 \cdot 4.0)^2) = 3544$
 $\omega_0: 0.917\%$
 $V_{\text{concrete}} = \tau_1 \cdot b \cdot d = 0.56 \cdot 10^{-3} \cdot 0.25 \cdot (0.8 \cdot 4) = 448 \text{ kN}$

For the shear force, reinforcement is required what has to withstand $6987 - 448 = 6539 \text{ kN}$. This is $6539 / (0.435 \cdot 3.2) = 4698 \text{ mm}^2/\text{m}$.

Table M.1 Determination of reinforcement percentage ω_0 by M_u/bd^2 , from T.G.B. 1990 [Technische Grondslagen voor de Bouwvoorschriften (in Dutch); 1990]



B 35 FeB 500

GTB 1990 - 11.4.a

moment without normal stress
for rectangular cross section

$\frac{M_u}{b \cdot d^2}$	k_s	ω_0	k_x	k_z
100	0,434	0,02	0,006	0,998
200	0,433	0,05	0,013	0,995
300	0,432	0,07	0,019	0,993
400	0,431	0,09	0,026	0,990
500	0,430	0,12	0,032	0,987
600	0,428	0,14	0,039	0,985
700	0,427	0,16	0,045	0,982
800	0,426	0,19	0,052	0,980
900	0,425	0,21	0,058	0,977
1000	0,424	0,24	0,065	0,975
1100	0,423	0,26	0,072	0,972
1200	0,422	0,28	0,079	0,969
1300	0,421	0,31	0,085	0,967
1400	0,419	0,33	0,092	0,964
1500	0,418	0,36	0,099	0,961
1600	0,417	0,38	0,106	0,959
1700	0,416	0,41	0,113	0,956
1800	0,415	0,43	0,120	0,953
1900	0,414	0,46	0,127	0,951
2000	0,412	0,49	0,134	0,948
2100	0,411	0,51	0,141	0,945
2200	0,410	0,54	0,148	0,942
2300	0,409	0,56	0,155	0,940
2400	0,407	0,59	0,163	0,937
2500	0,406	0,62	0,170	0,934
2600	0,405	0,64	0,177	0,931
2700	0,404	0,67	0,185	0,928
2800	0,402	0,70	0,192	0,925
2900	0,401	0,72	0,200	0,922
3000	0,400	0,75	0,207	0,919
3100	0,399	0,78	0,215	0,916
3200	0,397	0,81	0,222	0,914
3300	0,396	0,83	0,230	0,911
3400	0,395	0,86	0,238	0,907
3500	0,393	0,89	0,246	0,904
3600	0,392	0,92	0,254	0,901
3700	0,391	0,95	0,262	0,898
3800	0,389	0,98	0,270	0,895
3900	0,388	1,01	0,278	0,892
4000	0,387	1,03	0,286	0,889
4100	0,385	1,06	0,294	0,886
4200	0,384	1,09	0,302	0,882
4300	0,382	1,12	0,311	0,879
4400	0,381	1,15	0,319	0,876
4500	0,380	1,19	0,327	0,873

4600	0,378	1,22	0,336	0,869
4700	0,377	1,25	0,345	0,866
4800	0,375	1,28	0,353	0,863
4900	0,374	1,31	0,362	0,859
5000	0,372	1,34	0,371	0,856
5100	0,371	1,38	0,380	0,852
5200	0,369	1,41	0,389	0,849
5300	0,368	1,44	0,398	0,845
5400	0,366	1,48	0,407	0,842
5500	0,365	1,51	0,417	0,838
5600	0,363	1,54	0,426	0,834
5700	0,361	1,58	0,436	0,831
5800	0,360	1,61	0,445	0,827
5900	0,358	1,65	0,455	0,823
6000	0,356	1,68	0,465	0,819
6100	0,355	1,72	0,475	0,815
6200	0,353	1,76	0,485	0,811
6300	0,351	1,79	0,495	0,807
6400	0,349	1,83	0,506	0,803
6500	0,348	1,87	0,516	0,799
6600	0,346	1,91	0,527	0,795
6673	0,344	1,94	0,535	0,792

$k_{x,max} = 0.335$
in the case of
re-distribution